Elevated Src Kinase Activity Accompanies Endocrine-Resistance in Breast Cancer and Promotes an Aggressive Cell Phenotype

A thesis presented for the degree of
Doctor of Philosophy at Cardiff University by

Liam David Morgan

July 2007

Tenovus Centre for Cancer Research
Welsh School of Pharmacy
Redwood Building
Cardiff University
King Edward VII Avenue
Cardiff, CF10 3XF

Tel: (029) 20875226

ProQuest LLC
789 East Eisenhower Parkway
P.O. Box 1346
Ann Arbor, MI 48106-1346

"Science is what you know, philosophy is what you don't know."

Bertrand Russell (1872-1970). British Philosopher.

Summary

Despite the effectiveness of tamoxifen in the treatment of oestrogen-receptor-positive breast cancer, a significant proportion of initially-responsive tumours will develop resistance. Using an *in vitro* cell-model (Tam-R), our laboratory has previously demonstrated that altered growth-factor signalling contributes to tamoxifen-resistant growth. Furthermore, preliminary studies have revealed that acquired tamoxifen-resistance is also accompanied by an aggressive cell-phenotype.

Src plays a key role in the regulation of cellular events such as proliferation, migration and invasion. Given that Src has been implicated in tumour progression and metastasis, the aims of this thesis were to further investigate the aggressive phenotype of tamoxifen-resistant breast cancer cells, together with the role of Src in such behaviour.

Characterisation of Tam-R cells revealed that these cells grew in loosely-packed colonies and displayed a more angular appearance, which is characteristic of cells undergoing an EMT-like process. Furthermore, Tam-R cells demonstrated increased growth and a significantly augmented motile and invasive phenotype compared to MCF7wt. Analysis of Src expression in these cell-lines revealed no change in mRNA or protein levels; however, a dramatic increase in basal Src activation (phosphorylation at Y419) was observed in Tam-R cells.

Inhibition of Src in Tam-R cells using AZM555130 restored cell-cell contacts, decreased cell-matrix attachment and suppressed migration and invasion in a dose-dependent manner. Furthermore, inhibition of Src was accompanied by decreased proliferation and a corresponding reduction in EGFR signalling. Conversely, over-expression of constitutively-active Src in MCF7wt cells resulted in elevated growth-factor signalling and FAK/paxillin activity, and promoted increased cell growth, migration and invasion. Importantly, these cells demonstrated insensitivity to the growth-inhibitory effects of tamoxifen, an effect reversed by co-treatment with AZM555130.

Together, these data suggest that Src plays a pivotal role in mediating the aggressive phenotype of tamoxifen-resistant breast cancer cells *in vitro*, and that targeting Src in such cancers may be of therapeutic advantage.

Publications and Presentations

Journal Articles (Abstracts can be found in appendix 4)

- Hiscox, S., Jordan, N.J., Morgan, L., Green, T.P. and Nicholson, R.I. (2007). Src Kinase Promotes Adhesion-Independent Activation of FAK and Enhances Cellular Migration in Tamoxifen-Resistant Breast Cancer Cells. *Clin Exp Metastasis* 24(3), pp. 157-167.
- Hiscox, S., Morgan, L., Green, T. and Nicholson, R.I. (2006). Src as a Therapeutic Target in Anti-Hormone/Anti-Growth-Factor Resistant Breast Cancer. *Endocr Relat Cancer* 13(S1), pp. S53-59.
- Hiscox, S., Morgan, L., Green, T.P., Barrow, D., Gee, J. and Nicholson, R.I. (2006). Elevated Src Activity Promotes Cellular Invasion and Motility in Tamoxifen Resistant Breast Cancer Cells. *Breast Cancer Res Treat* 97(3), pp. 263-274.
- Hiscox, S., Jiang, W.G., Obermeier, K., Taylor, K., Morgan, L., Burmi, R., *et al.* (2006). Tamoxifen Resistance in MCF7 Cells Promotes EMT-Like Behaviour and Involves Modulation of Beta-Catenin Phosphorylation. *Int J Cancer* 118(2), pp. 290-301.
- Hiscox, S., Morgan, L., Barrow, D., Dutkowski, C., Wakeling, A. and Nicholson, R.I. (2004). Tamoxifen Resistance in Breast Cancer Cells Is Accompanied by an Enhanced Motile and Invasive Phenotype: Inhibition by Gefitinib ('Iressa', Zd1839). *Clin Exp Metastasis* 21(3), pp. 201-212.

*Oral Presentations**

- Morgan, L., Hiscox, S. and Nicholson, R.I. (2006). Elevated Src Kinase Activity Accompanies Endocrine Resistance in Breast Cancer and Promotes an Aggressive Cell Phenotype. *Welsh School of Pharmacy Postgraduate Research Day.* Cardiff University, UK.
- Hiscox, S., Morgan, L., Green, T. and Nicholson, R.I. (2006). Src as a Therapeutic Target in Endocrine Resistant Breast Cancer. *2nd Tenovus/Astra Zeneca Annual Workshop.* Cardiff, UK.

*Poster Presentations**

- Morgan, L., Hiscox, S. and Nicholson, R.I. (2006). Elevated Src kinase activity accompanies endocrine-resistance in breast cancer and promotes an aggressive cell phenotype. *2nd Tenovus/Astra Zeneca Annual Work-shop.* Cardiff, UK.
- Morgan, L., Hiscox, S. and Nicholson, R.I. (2005). Elevated Src kinase activity accompanies endocrine-resistance in breast cancer and promotes an aggressive cell phenotype. *AACR Special Conference: Advances in Breast Cancer Research.* La Jolla, San Diego, CA.
- Morgan, L., Hiscox, S. and Nicholson, R.I. (2005). Elevated Src kinase activity promotes an aggressive tumour cell phenotype in endocrine-resistant breast cancer. *Welsh School of Pharmacy Postgraduate Research Day.* Cardiff University, UK.
- Hiscox, S., Morgan, L., Green, T. and Nicholson, R.I. (2004). Reduction of *in vitro* metastatic potential of tamoxifen-resistant breast cancer cells following inhibition of Src kinase activity by AZD0530. *EORTC-NCI-AACR.* Geneva, Switzerland.

* Presenter is underlined.

Acknowledgements

I would like to thank Professor Robert Nicholson for providing me with the opportunity and the means with which to conduct this research and also, the Tenovus Charity and the Welsh School of Pharmacy for funding my PhD placement. I am also grateful to Dr. Tim Green of AstraZeneca Pharmaceuticals Ltd. for the provision of their novel Src inhibitor, AZM555130.

I would also like to acknowledge the many members of the Tenovus group in Cardiff for their help over the last 4 years. Staff and students, past and present – you have all contributed in some way to the construction of this tapestry and for that I thank you. In particular, I would like to thank Carol Dutkowski and Richard McClelland for their proof-reading skills and Lynne Farrow for her help with statistics. I would especially like to thank Steve Hiscox for being such a supportive, generous and patient supervisor. I appreciate the fact that you were always around to answer my many questions and to make sure I kept my focus on the goal!

I would also like to thank my Mum and Dad for their amazing support and encouragement, not only for these past 4 years but for the whole of my life! You have always been there for me and I have you both to thank for everything I am today. I could not have done any of this without you.

Last, but certainly not least, I would like to thank Lucy for being with me throughout. You have been my rock, and your support and understanding through the difficult times have been unbelievable. You deserve this PhD every bit as much as I do! You have put your life on hold so that I can do this and for that I will be eternally grateful. I love you and look forward to spending the rest of my life with you xxxx

CARDIFF UNIVERSITY
PRIFYSGOL CAERDYDD

tenovus the cancer charity

AstraZeneca

Table of Contents:

Declaration and Statements i
Summary iii
Publications and Presentations iv
Acknowledgements vi
Table of Contents: vii
List of Figures xii
List of Tables xviii
Abbreviations xix
1 Introduction 2
1.1 Breast Cancer: Facts and Figures 2
1.1.1 Key Statistics 2
1.1.2 Risk Factors Associated with Breast Cancer 2
1.2 Therapeutic Options for the Treatment of Breast Cancer 4
1.3 Endocrine Therapy in the Treatment of ER-positive Breast Cancer 7
1.3.1 Oestrogen Receptor Signalling in Breast Cancer 8
1.3.2 Endocrine Therapies – Ovarian Ablation 14
1.3.3 Endocrine Therapies – Anti-oestrogens 16
1.3.4 Endocrine Therapies – Aromatase Inhibitors (AIs) 21
1.4 Tamoxifen Resistance in Breast Cancer 23
1.4.1 Acquired and de novo Resistance to Tamoxifen 23
1.4.2 Combating Tamoxifen Resistance in the Clinic 26
1.5 Src 27
1.5.1 The History of Src 27
1.5.2 The Structure of the Src Protein 28
1.5.3 Regulation of Src Kinase Activity 33
1.5.4 The Role of Src in Cancer 38
1.6 Aims 42
2 Materials and Methods 44

2.1 Materials 44
2.2 Cell Culture 48
2.2.1 Cell-lines 48
2.2.2 Cell Culture Techniques 48
2.2.3 Treatments 50
2.3 Gene Expression Analysis 50
2.3.1 RNA Extraction 50
2.3.2 RNA Quantitation 52
2.3.3 Reverse Transcription (RT) 52
2.3.4 Polymerase Chain Reaction (PCR) 53
2.3.5 Real-Time PCR (qPCR) 55
2.4 Analysis of Protein Expression/Activation 58
2.4.1 Cell Lysis 58
2.4.2 Protein Concentration Assay 59
2.4.3 SDS-PAGE Analysis 59
2.4.4 Western Blotting 61
2.4.5 Immunoprobing of Western Blots 63
2.5 Immunocytochemistry (ICC) 65
2.5.1 Fixation of Cells 65
2.5.2 Immunocytochemical Staining of Fixed Cells 66
2.6 Assessment of Cell Morphology 67
2.7 Growth Assays 67
2.7.1 MTT Cell Proliferation Assay 68
2.7.2 Cell Counting 68
2.8 Fluorescence Assisted Cell Sorting (FACS) 69
2.9 Cell Attachment Assays 70
2.10 Cell Migration Assays 71
2.11 Cell Invasion Assay 73
2.12 Expression of a constitutively-active Src Mutant in MCF7wt Cells 74
2.12.1 Plasmids 74
2.12.2 Transformation of Competent Bacteria 76
2.12.3 Plasmid Purification and Isolation 77

2.12.4 Plasmid Quantitation 78
2.12.5 Verification of Purified Plasmids 80
2.12.6 Transfection of MCF7wt cells with Mutated Src Gene Construct (Src Y529F) 83
2.12.7 Generation of Stably Transfected Src Y529F (MCF7-S) and pUSEamp Empty Vector (MCF7-EV) Cell-lines 84
2.13 Statistical Analysis 85
3 Acquired Tamoxifen Resistance in MCF7 Cells is Accompanied by Increased Aggressive Behaviour and Elevated Src Kinase Activity 87
3.1 Introduction and Aims 87
3.2 Results 89
3.2.1 Tam-R cells display an aggressive in vitro phenotype compared to MCF7wt cells 89
3.2.2 Analysis of Src expression and activation in Tam-R cells 96
3.2.3 Regulation of Src Kinase Activity in Tam-R Cells 109
3.3 Discussion 122
3.3.1 Characterisation of the tamoxifen-resistant cell-phenotype 122
3.3.2 Investigations into the mechanisms involved in regulating the aggressive cell-phenotype of Tam-R cells 124
3.3.3 Regulation of Src kinase activity in Tam-R cells 129
3.4 Chapter Summary 137
4 Src Kinase is Central to the Regulation of the Aggressive *in vitro* Phenotype of Tam-R Cells 139
4.1 Introduction and Aims 139
4.2 Results 140
4.2.1 AZM555130 decreases activation of Src kinase 140
4.2.2 Src inhibition in Tam-R cells alters cell morphology and decreases matrix-attachment, migration and invasion 148
4.2.3 Src inhibition with AZM555130 in MCF7wt and Tam-R cells decreases cell proliferation 158
4.3 Discussion 169

4.3.1 Characterisation of AZM555130 as a potent inhibitor of Src kinase activity 169
4.3.2 Src and the aggressive phenotype of tamoxifen resistant breast cancer cells in vitro 171
4.3.3 Increased Src activity in Tam-R cells enhances their growth through potentiation of EGFR signalling 176
4.4 Chapter Summary 180
5 Expression of Constitutively-Active Src in MCF7wt Cells Promotes an Aggressive Phenotype and Tamoxifen Insensitivity 182
5.1 Introduction and Aims 182
5.2 Results 183
5.2.1 Stable transfection of MCF7wt cells with Src Y529F. 183
5.2.2 Characterisation of the phenotype exhibited by the stable MCF7-S and MCF7-EV cell-lines. 190
5.2.3 Src: A potential mechanism of Tamoxifen-resistance? 217
5.3 Discussion 220
5.3.1 Stable expression of constitutively active Src in MCF7 breast cancer cells results in the acquisition of an aggressive cell-phenotype. 220
5.3.2 Src: A potential mechanism of Tamoxifen-resistance? 230
5.4 Chapter Summary 236
6 General Discussion and Conclusions 238
7 References 247
8 Appendices 269
8.1 Appendix 1 – Cell Culture 269
8.1.1 Cell Culture Medium Recipes 269
8.1.2 Charcoal Stripping Procedure 269
8.1.3 Trypsin/EDTA 270
8.1.4 Cryo-preservation of Cell-lines 270
8.1.5 Cell Seeding Densities 271
8.1.6 Constitution of Isoton® azide-free balanced electrolyte solution for use with Beckman Coulter™ Multisizer II 271

8.2 Appendix 2 – Buffers and Solutions 272
8.2.1 Reverse Transcription and PCR 272
8.2.2 SDS-PAGE/Western Blotting 273
8.2.3 Immunocytochemistry 276
8.3 Appendix 3 – Transfection Work 277
8.3.1 SOC Medium 277
8.3.2 Luria-Bertani (LB) Agar Plates 277
8.3.3 Luria-Bertani (LB) Broth 277
8.3.4 Src Y529F in pUSEamp(-) 278
8.3.5 pUSEamp(-) Vector 282
8.4 Appendix 4 - Abstracts of Published Journal Articles 286

List of Figures

Figure 1.1 Age-standardised incidence of and mortality from female breast cancer. 4

Figure 1.2 Structure of the oestrogen receptor (ER) protein. 9

Figure 1.3 'Classical' mechanism of ER signalling in breast cancer. 11

Figure 1.4 'Non-classical' mechanism of ER signalling in breast cancer 13

Figure 1.5 Non-genomic mechanisms of ER signalling in breast cancer. 15

Figure 1.6 Structure of the anti-oestrogens, tamoxifen and fulvestrant, in comparison with that of 17β-oestradiol (adapted from [50]) 18

Figure 1.7 Structural organisation of the non-receptor tyrosine kinase, Src. 29

Figure 1.8 Mechanisms of Src activation. 35

Figure 2.1 Optimisation of PCR thermocycling conditions for Src and β-actin .. 56

Figure 2.2 Assembly of Western blot transfer cassette 62

Figure 2.3 Schematic diagram of a Corning Standard Transwell® insert 72

Figure 2.4 Plasmid maps for SrcY529F gene construct in a pUSEamp expression vector and the pUSEamp empty vector 75

Figure 2.5 Monitoring of the plasmid purification process for Src Y529F and pUSEamp empty vector plasmids 79

Figure 2.6 Verification of the Src Y529F plasmid by restriction digestion and PCR 81

Figure 2.7 Verification of the pUSEamp Empty Vector plasmid by restriction digestion and PCR 82

Figure 3.1 Basal morphology of MCF7wt and Tam-R cell-lines 90

Figure 3.2 Growth rates of the MCF7wt and Tam-R cell-lines. 91

Figure 3.3 Basal migration of MCF7wt and Tam-R cell-lines 92

Figure 3.4 Basal invasion of MCF7wt and Tam-R cell-lines 94

Figure 3.5 Affinity of MCF7wt and Tam-R cells for uncoated and matrix-coated surfaces. 95

Figure 3.6 Basal Src mRNA levels in MCF7wt and Tam-R cells as measured by semi-quantitative RT-PCR. 97

Figure 3.7 Basal Src mRNA levels in MCF7wt and Tam-R cells as measured by quantitative 'real-time' qPCR. 98

Figure 3.8 Expression profile of Src in MCF7wt and Tam-R cell-lines using the Affymetrix HG-U133A cDNA array. 99

Figure 3.9 Basal levels of total and activated Src tyrosine kinase in MCF7wt and Tam-R cells as determined by Western blotting. 101

Figure 3.10 Levels and localisation of activated Src tyrosine kinase in basal MCF7wt and Tam-R cells as determined by immunocytochemistry. 102

Figure 3.11 Basal levels of total and phosphorylated (Y397 & Y861) FAK in MCF7wt and Tam-R cell-lines as determined by Western blotting. 103

Figure 3.12 Basal levels of total and phosphorylated (Y31) paxillin in MCF7wt and Tam-R cell-lines as determined by Western blotting. 105

Figure 3.13 Levels of total and phosphorylated (Y397 and Y861) FAK in MCF7wt and Tam-R cell-lines exposed to a fibronectin matrix for either 30 minutes or 5 days. 106

Figure 3.14 Induction of FAK phosphorylation (Y397 and Y861) in MCF7wt and Tam-R cells either in suspension or seeded onto a fibronectin matrix (30 minutes) 108

Figure 3.15 Rate of MCF7wt and Tam-R cell-attachment on uncoated and matrix-coated surfaces as measured using a cell attachment time-course assay. 110

Figure 3.16 MCF7wt and Tam-R cell-spreading on an uncoated plastic surface. 111

Figure 3.17 MCF7wt and Tam-R cell-spreading on a fibronectin-coated surface. 112

Figure 3.18 Basal levels of CSK and PTP1B in MCF7wt and Tam-R cells as determined by Western blotting. 114

Figure 3.19 Basal levels of Src tyrosine kinase phosphorylated at Y530 in MCF7wt and Tam-R cells as determined by Western blotting. 115

Figure 3.20 Basal levels of total and phosphorylated (Y845 and Y1068) EGFR in MCF7wt and Tam-R cell-lines as determined by Western blotting. 117

Figure 3.21 Src kinase activity in Tam-R cells following modulation of EGFR signalling as determined by Western blotting. 118

Figure 3.22 Effect of growth-factor treatment on Src activation in Tam-R cells as determined by Western blotting. 120

Figure 3.23 Effect of inhibition of various cell-signalling pathways on Src activation in Tam-R cells as determined by Western blotting. 121

Figure 4.1 Structure of AZM555130, one of a new series of 4-anilinoquinazoline based Src-family-kinase inhibitors developed by AstraZeneca. 141

Figure 4.2 Dose-dependent effect of AZM555130 Src-family-kinase inhibitor on Src activation in MCF7wt cells as determined by Western blotting. 142

Figure 4.3 Dose-dependent effect of AZM555130 Src-family-kinase inhibitor on Src activation in Tam-R cells as determined by Western blotting. 143

Figure 4.4 Effect of AZM555130 Src-family-kinase inhibitor (1 μM, 24 hrs) on Src activation in MCF7wt and Tam-R cells as determined by immunocytochemistry 145

Figure 4.5 Time-course experiment to demonstrate efficacy of AZM555130 (1μM) as an inhibitor of Src activation in MCF7wt cells. 146

Figure 4.6 Time-course experiment to demonstrate efficacy of AZM555130 (1μM) as an inhibitor of Src activation in Tam-R cells. 147

Figure 4.7 Dose-dependent effect of the proprietary Src-family-kinase inhibitor SU6656 on Src activation in Tam-R cells as determined by Western blotting. 149

Figure 4.8 Effect of Src inhibition using AZM555130 on the morphology of MCF7wt and Tam-R cells.....150

Figure 4.9 The effect of AZM555130 on migration of Tam-R cells *in vitro*.....152

Figure 4.10 The effect of AZM555130 on invasion of Tam-R cells *in vitro*.....153

Figure 4.11 Effect of Src inhibition using AZM555130 on the affinity of MCF7wt and Tam-R cells for uncoated and fibronectin-coated surfaces. .155

Figure 4.12 Effect of Src inhibition using AZM555130 on the rate of MCF7wt and Tam-R cell-attachment to uncoated and fibronectin-coated surfaces..156

Figure 4.13 Effect of Src inhibition using AZM555130 on FAK phosphorylation (pY397 and pY861) in MCF7wt and Tam-R cells. 157

Figure 4.14 Dose-dependent effect of AZM555130 Src-family-kinase inhibitor on cell growth in MCF7wt and Tam-R cells as determined by cell counting. 159

Figure 4.15 Effect of Src inhibition using AZM555130 on apoptosis in MCF7wt cells. 161

Figure 4.16 Effect of Src inhibition using AZM555130 on apoptosis in Tam-R cells. 162

Figure 4.17 Assessment of the inhibitory effects of AZM555130 on cell proliferation in MCF7wt cells using immunocytochemical staining for the Ki67 antigen.....163

Figure 4.18 Assessment of the inhibitory effects of AZM555130 on cell proliferation in Tam-R cells using immunocytochemical staining for the Ki67 antigen.....164

Figure 4.19 Effect of Src inhibition on EGFR activation in MCF7wt and Tam-R cells. 166

Figure 4.20 Effect of Src inhibition on ERK 1/2 activation in MCF7wt and Tam-R cells.....167

Figure 4.21 Effect of Src inhibition using AZM555130 on cell growth in MCF7wt and Tam-R cells following stimulation with TGFα. 168

Figure 5.1 Optimisation of the experimental conditions for the transfection of MCF7wt cells with a Src Y529F plasmid construct. 185

Figure 5.2 Verification of the experimental conditions selected for the transfection of MCF7wt cells with a Src Y529F plasmid construct. 186

Figure 5.3 Effects of G418 (Geneticin) on MCF7wt cell growth. 188

Figure 5.4 Effects of G418 (Geneticin) on MCF7wt cell growth (images). 189

Figure 5.5 Effects of G418 (Geneticin) on MCF7-S cell growth..... 191

Figure 5.6 Effects of G418 (Geneticin) on MCF7-S cell growth (images)..... 192

Figure 5.7 Effects of G418 (Geneticin) on MCF7-EV cell growth..... 193

Figure 5.8 Effects of G418 (Geneticin) on MCF7-EV cell growth (images)..... 194

Figure 5.9 Levels of total and activated Src tyrosine kinase in MCF7-S versus MCF7-EV cells as determined by Western blotting. 196

Figure 5.10 Dose-dependent effect of AZM555130 on Src activation in MCF7-S cells as determined by Western blotting. 198

Figure 5.11 Morphology of MCF7-S and MCF7-EV cells. 199

Figure 5.12 Localisation of activated Src tyrosine kinase in basal MCF7-S cells. 200

Figure 5.13 Effect of Src inhibition by AZM555130 on MCF7-S cell morphology. 201

Figure 5.14 Migratory capacity of MCF7-S cells versus MCF7-EV. 203

Figure 5.15 Invasive capacity of MCF7-S cells versus MCF7-EV..... 204

Figure 5.16 Affinity of MCF7-S and MCF7-EV cells for uncoated and matrix-coated surfaces as measured using a cell attachment assay. 205

Figure 5.17 Rate of MCF7-S and MCF7-EV cell-attachment to a fibronectin-coated surface as measured using a cell attachment time-course assay..... 207

Figure 5.18 MCF7-EV and MCF7-S cell-spreading on an uncoated plastic surface. 208

Figure 5.19 MCF7-EV and MCF7-S cell-spreading on a fibronectin-coated surface. 209

Figure 5.20 Levels of total and phosphorylated FAK in MCF7-S versus MCF7-EV cells as determined by Western blotting. 211

Figure 5.21 Levels of total and phosphorylated Paxillin in MCF7-S versus MCF7-EV cells as determined by Western blotting. 212

Figure 5.22 Dose-dependent effect of Src inhibition by AZM555130 on FAK phosphorylation in MCF7-S cells. 213

Figure 5.23 Dose-dependent effect of Src inhibition by AZM555130 on Paxillin phosphorylation in MCF7-S cells. 214

Figure 5.24 Basal growth rate of MCF7-S cells in comparison to growth of MCF7wt, MCF7-EV and Tam-R cell-lines. 215

Figure 5.25 Preliminary studies into the activation of erb-receptor signalling pathways in MCF7-S cells. 216

Figure 5.26 Dose-dependent effect of tamoxifen treatment on the growth of MCF7wt, MCF7-EV, MCF7-S and Tam-R cell-lines. 218

Figure 5.27 Dose-dependent effect of tamoxifen treatment on the growth of MCF7-S cells in the absence and presence of AZM555130 219

Figure 5.28 Dose-dependent effect of tamoxifen treatment on the growth of Tam-R cells in the absence and presence of AZM555130. 221

Figure 5.29 Proposed regulation of tamoxifen-resistant cell growth by Src. 233

List of Tables

Table 1.1 Staging of Invasive Breast Tumours* 5

Table 2.1 List of materials used in the study and their suppliers 44

Table 2.2 Treatments used in cell culture experiments 51

Table 2.3 Thermocycler program conditions for the reverse transcription of RNA 53

Table 2.4 Primer sequences used for the PCR amplification of Src and β-actin genes 54

Table 2.5 Thermocycler program conditions for PCR amplification of Src and β-actin 54

Table 2.6 Recipe for the Stacking Gel used in SDS-PAGE 59

Table 2.7 Recipe for the Resolving gel used in SDS-PAGE 60

Table 2.8 Antibodies used in the immunoprobing of Western blots 64

Table 2.9 Antibodies used in immunocytochemistry 66

Abbreviations

μ (as prefix)	micro-
A	amp
ADP	adenosine di-phosphate
AF	activator function
APS	ammonium persulphate
ATP	adenosine tri-phosphate
AZM	AZM555130
bp	base pair
BSA	bovine serum albumin
CAS	CRK associated substrate
cDNA	complementary DNA
CSK	c-terminal Src kinase
C-terminal	carboxy-terminal (*cf.* protein structure)
DAB	3,3'-diaminobenzidine
DAPI	4'6-diamidino-2-phenylindole-2HCl
DCCM	defined cell culture medium
DMSO	dimethyl sulphoxide
DNA	deoxyribonucleic acid
dNTP	deoxynucleotide tri-phosphate
DPX	di-butylpthalatexylene
DTT	di-thiothreitol
E_2	17β-oestradiol
ECM	extra-cellular matrix
EDTA	ethylene diamine tetraacetic acid
EGF	epidermal growth factor
EGFR	epidermal growth factor receptor

EGTA	ethylene glycol tetraacetic acid
EMT	epithelial-mesenchymal transition
ER	oestrogen receptor
ERE	oestrogen response element
ERICA	oestrogen receptor immunocytochemical assay
ERK	extracellular-signal regulated kinase
EtBr	ethidium bromide
EtOH	ethanol
FACS	fluorescence assisted cell sorting
FAK	focal adhesion kinase
FCS	foetal calf serum
FITC	fluorescein isothiocyanate
g (*cf.* centrifugal force)	gee *or* gravity
g (*cf.* weight)	gram
Gefitinib	4-(3-chloro-4-fluoroanilino)-7-methoxy-6-(3-morpholinopropoxy) quinazoline
HCl	hydrochloric acid
HER	human epidermal-growth-factor receptor
hr	hour
HRC	herceptin
HRG	heregulin
HRP	horse-radish peroxidase
HSP	heat shock protein
ICC	immuno-cytochemistry
IF	immunofluorescence
IgG	immunoglobulin g
IP	immunoprecipitation
Iressa™	*see Gefitinib*
K_2HPO_4	di-potassium hydrogen orthophosphate anhydrous

kDa	kilo Daltons
KH_2PO_4	potassium di-hydrogen orthophosphate
L	litre
LY	Lilley
M	molar
m (as prefix)	milli-
MAPK	mitogen-activated protein kinase
MCF	Michigan Cancer Foundation
MCF7-EV	MCF7wt cells transfected with pUSEamp vector
MCF7-S	MCF7wt cells transfected with Src Y529F plasmid
MCF7wt	wild-type MCF7 cell-line
MEK	MAP-kinase extra-cellular signal-regulated kinase
$MgCl_2$	magnesium chloride
min	minute
MMLV-RT	Molony-murine leukaemia virus reverse transcriptase
mRNA	messenger RNA
MTT	3-(4,5-dimethylthiazol-2-yl)-2,5-diphenyl-tetrazolium bromide
Na_2HPO_4	di-sodium hydrogen orthophosphate anhydrous
Na_2MoO_4	sodium molybdate
NaCl	sodium chloride
NaF	sodium fluoride
NaH_2PO_4	sodium di-hydrogen orthophosphate
NaOH	sodium hydroxide
$NaVO_4$	sodium orthovanadate
N-terminal	amino terminal (*cf.* protein structure)
OD	optical density
PAGE	polyacrylamide gel electrophoresis

PBS	phosphate-buffered saline
PCR	polymerase chain reaction
PD	Park Davies
PI3K	phosphatidylinositol-3-kinase
PMSF	phenylmethylsulfonyl fluoride
PTP1B	protein tyrosine phosphatase 1B
qPCR	quantitative (real-time) PCR
R+5%	RPMI 1640 (containing phenol-red pH indicator) supplemented with 5% (v/v) foetal calf serum, antibiotics (penicillin 100units/ml and streptomycin 100μg/ml) and an antifungal agent (amphotericin B 2.5μg/ml).
RH	random hexamers
RNA	ribonucleic acid
RNase	ribonuclease
rpm	revolutions per minute
RPMI	Roswell Park Memorial Institute
rRPMI	RPMI containing phenol-red pH indicator
RT-PCR	reverse transcription-polymerase chain reaction
SD	standard deviation
SDS	sodium-dodecyl-sulphate
sec	second (*cf.* time)
Ser *or* S	Serine
SERD	selective oestrogen receptor down-regulator
SERM	selective oestrogen receptor modulator
SFCS	charcoal-stripped foetal calf serum
SH	Src homology
TAE	tris-acetate-EDTA buffer
Tam	4-hydroxytamoxifen
Tam-R	tamoxifen-resistant MCF7 cell-line

Taq	*Thermus aquaticus*
TBS	tris-buffered saline
TBS-T	tris-buffered saline containing 0.05% v/v tween-20
TEMED	N,N,N',N'-tetramethylene-diamine
TESPA	3-aminopropyltriethoxysilane
TGFα	transforming growth factor alpha
Thr *or* T	Threonine
TKI	tyrosine kinase inhibitor
TPEN	N,N,N',N'-tetrakis(2-pyridylmethyl) ethylenediamine
Tris	tris(hydroxymethyl)aminomethane
TRITC	tetra-methyl rhodamine isothiocyanate
Tween-20	polyoxyethylene-sorbitan monolaurate
Tyr *or* Y	Tyrosine
U	restriction enzyme unit (defined as the amount of enzyme required to digest 1μg DNA in 1 hour at 37°C in a 50μl volume).
UV	ultra violet
V	volts
v/v	volume per volume
w/v	weight per volume
W+5%	Phenol-red-free RPMI 1640 supplemented with 5% (v/v) charcoal-stripped foetal calf serum, L-glutamine (200mM), antibiotics (penicillin 100units/ml and streptomycin 100μg/ml) and an antifungal agent (amphotericin B 2.5μg/ml).
wDCCM	white (phenol-red-free) DCCM
wRPMI	white (phenol-red-free) RPMI
ZD1839	*see Gefitinib*

Chapter One

Introduction

"While there are several chronic diseases more destructive to life than cancer, none is more feared."

Charles H. Mayo (1865-1939). US Physician.
Annals of Surgery, 83:357. 1926.

1 Introduction

1.1 Breast Cancer: Facts and Figures

1.1.1 Key Statistics

It is estimated that 4.4 million women alive in the world today have been diagnosed with breast cancer in the last 5 years [1]. The high prevalence of breast cancer is due to the current trend of increasing breast cancer incidence rates and decreasing mortality [1]. The worldwide incidence of breast cancer in 2002 was recorded as 1,151,298 (23% of all female cancers); while this disease claimed 410,712 lives in that same year (14% of all female cancer-related deaths) [1, 2]. Incidence of breast cancer is highest in the USA, where an estimated 180,510 new cases are expected in 2007 [3].

Breast cancer is also the most common form of female cancer in the UK, with a lifetime risk of contracting the disease at 1 in 9 [4]. Breast cancer accounts for over 30% of all female cancer diagnoses in the UK [4, 5], with an average of 44,100 new cases reported each year [6]. Of these, approximately 80% occur in post-menopausal women over the age of 50 [7]. However, despite a 5-year survival rate of 80% in women diagnosed with breast cancer between 2001 and 2003 [8], an average of 12,500 deaths are attributed to this disease each year in the UK (17% of all cancer related deaths in UK females) [6].

Together, these figures offer a striking realisation of the threat to public health posed by breast cancer, and thus highlight the need for research into methods to reduce both the incidence and mortality of breast cancer worldwide.

1.1.2 Risk Factors Associated with Breast Cancer

A large number of risk factors have been associated with the occurrence of breast cancer, although many are ill-defined and require additional research to further clarify their involvement. The single greatest risk factor in the development of breast cancer is age; the incidence of breast cancer in women has been shown to double for every 10 years until menopause is reached [9]. Thus, the risk of a woman in the UK developing breast cancer by the time she

is 30 years old is 1:1900, but by the time she is 50 years old the risk will have increased to 1:50 [6].

The life-time exposure of an individual to oestrogens, both endogenous and exogenous, is another major determinant of breast cancer risk. For example, age at onset of menstruation and menopause, age at first full-term pregnancy, parity, and whether off-spring are breast fed can all affect the probability of contracting this disease [6, 9]. Furthermore, small increases in risk are observed with the use of oral contraceptives [6, 9] and hormone-replacement therapy (HRT) [10]. The actual increase in risk depends on the type of oral contraceptive or HRT used and the duration for which it is taken; however, this risk will return to a baseline level after stopping use of these medications, although it can take 5-10 years for this to happen [2, 6, 9, 10].

Approximately 5-10% of breast cancers occur in women with a family history of the condition, suggesting the possible involvement of genetic factors [6, 9]. Thus far, at least 5 genes that might be responsible for inheritable predisposition to breast cancer have been identified, of which *BRCA1* is probably the most clinically important [11]. Approximately 56-80% of women carrying a mutated *BRCA1* gene will develop breast cancer; however, despite *BRCA1*-expressing cancers being associated with increased tumour stage/grade, increased proliferative index, and decreased oestrogen receptor (ER) and progesterone receptor (PgR) levels, the 5-year survival rate of these patients correlates favourably with that of sporadic tumours [12].

Breast cancer incidence varies throughout the world, with epidemiological studies demonstrating that breast cancer is more prevalent in Western populations, such as the UK and USA, than in Eastern countries, such as China and Japan [1, 9, 13]. Interestingly, following migration from a low-risk country to a high-risk country, migrants often acquire an increased risk of developing breast cancer during their lifetime, and will adopt the risk of the host country within 2-3 generations [1, 9]. This suggests that life-style (diet, alcohol consumption, weight), socio-economic status and environmental factors may also have an important role to play in the development of breast cancer [1, 6, 9].

1.2 Therapeutic Options for the Treatment of Breast Cancer

Despite a persistent increase in the incidence of breast cancer in the UK, mortality rates have decreased and are continuing to fall (figure 1.1) [7]. The five-year survival rate for women diagnosed between 1991 and 1995 was 73%; while for women diagnosed between 1996 to 1999 it was 78% [7]. The increase in 5-year survival is believed, in part, to be a result of earlier detection due to an intensive breast-screening program introduced in 1988 for women over the age of 50 [14-16]. The remainder of the increase is attributable to improvements in the number and efficacy of treatments currently available for breast cancer sufferers [1].

The method of breast cancer treatment used depends upon whether the tumour is non-invasive (confined to the lobes or ducts of the breast) or invasive (has spread to other parts of the breast and has the potential to spread to other parts of the body); the classification of a cancer into these categories is governed by the grade and stage of the tumour [17, 18]. The grade of a tumour is assigned following histological assessment of the appearance of the tumour cells, and

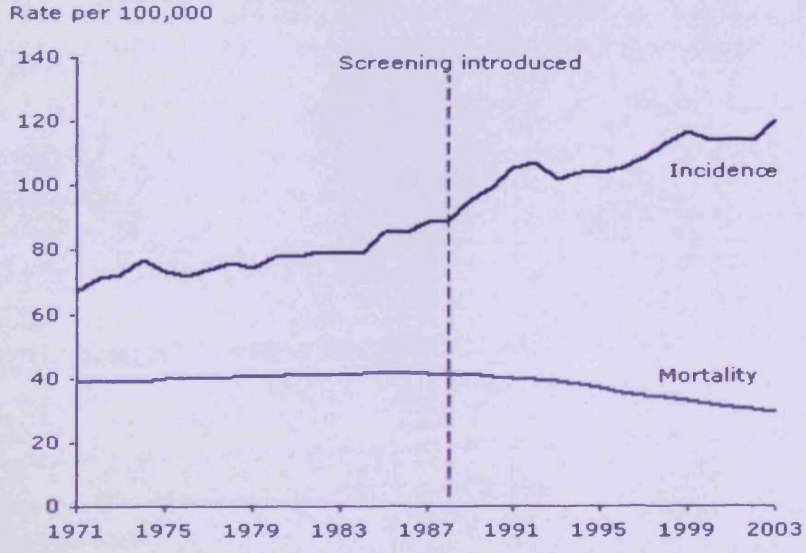

Figure 1.1 Age-standardised incidence of and mortality from female breast cancer.
England, 1971-2003. Figure obtained from Office of National Statistics [7].

gives an indication of the growth rate and metastatic potential of a cancer. Grade I tumours are slow-growing and demonstrate low metastatic potential, while grade III tumours are faster-growing and possess increased metastatic potential [18]. Invasive tumours are staged using the TNM (tumour, node, metastasis) system [19] which provides details of tumour size and degree of metastasis observed (summarised in table 1.1) [6, 18]. Non-invasive tumours are sometimes referred to as *Stage 0* [18].

Table 1.1 Staging of Invasive Breast Tumours*.

Tumour Stage	Characteristics
Stage I	Tumour size ≤ 2cm. No lymph node involvement. No evidence of spread beyond the breast.
Stage II	Tumour between 2cm and 5cm and/or; Involvement of lymph nodes in armpit. No evidence of spread beyond armpit.
Stage III	Tumour size ≥ 5cm. Involvement of lymph nodes in armpit. No evidence of spread beyond armpit.
Stage IV	Tumour of any size. Involvement of lymph nodes in armpit. Evidence of metastasis to distant sites.

* *Table adapted from Cancer Research UK News and Resources web site [6].*

The primary strategy used to treat most breast cancers is surgery followed by a course of radiotherapy to eliminate any stray cancer cells not removed during the operation. The type of operation carried out depends on how advanced the tumour is, and can range from a lumpectomy (removal of the lump and some surrounding breast tissue) to the more extreme modified radical mastectomy (removal of the breast and some muscle tissue from the chest wall). Where invasive carcinoma is involved, lymph nodes from the axilla are also often removed to help determine if the cancer has spread beyond the breast [17-19]; although it is now becoming increasingly popular to perform a sentinel node biopsy at the time of surgery to check for tumour spread as they are associated with a lower risk of lymphedema or sensory loss in the arm [20].

Approximately half of women who are treated with surgery and radiotherapy will eventually succumb to metastatic disease, suggesting that cancer spread may have already occurred by the time surgery is performed [19]. Thus, for high grade tumours, or if spread of the tumour is suspected due to lymph node involvement, additional treatment is given in the form of either chemotherapy or endocrine therapy to eliminate cancerous cells that may have travelled to other parts of the body via the circulatory system. This treatment regimen is known as adjuvant systemic therapy [17-19]. The use of chemotherapy or endocrine therapy in post-menopausal women as an adjuvant to surgery and radiotherapy has been shown to save an additional 12 lives for every 100 women treated; whereas the use of adjuvant chemotherapy in pre-menopausal women saves approximately 10 lives per 100 women treated [19].

The choice of adjuvant therapy used is most often dependent on the hormone-receptor status of the tumour [2]. As such, the testing of tumours for hormone receptor expression is now routine following surgery [18]. Patients with hormone-receptor-positive disease are typically offered some form of endocrine therapy to reduce the risk of disease recurrence. If possible, the use of endocrine therapy is preferable to chemotherapy as it has a high success rate, in addition to lower toxicity and less severe side-effects. In pre-menopausal women, endocrine therapy usually takes the form of either surgical or therapeutic ablation of ovarian function, as the ovaries are the primary source of oestrogen synthesis in these patients; often, this is in conjunction with the use of anti-oestrogens, such as tamoxifen [21]. In post-menopausal women, however, endocrine therapy usually involves the use of anti-oestrogens; although more recently, the newer aromatase-inhibitor compounds, such as anastrozole (Arimidex™), have been shown to be superior in this setting [21, 22]. Endocrine therapy will be discussed in more depth in the next section.

Patients with hormone-receptor negative tumours are commonly given chemotherapy to prevent the development of secondary disease. Chemotherapy involves the administration of a combination of cytotoxic drugs, usually every 3-4 weeks for a 4-6 month period (6 courses in total) [18]. The combination

of cytotoxic drugs selected for use is usually tailored for the best response in individual patients. Unfortunately, despite its efficacy as an anti-cancer treatment, chemotherapy can be accompanied by some serious side-effects, such as chronic fatigue, hair loss and even infertility [18]. Increasingly, chemotherapy is being used in combination with trastuzumab (Herceptin™), a monoclonal-antibody therapy, in the treatment of tumours that over-express the HER2/*neu* receptor regardless of hormone-receptor status or whether the patient has reached menopause [2, 17-19]. This is because over-expression of HER2/*neu* can often indicate decreased responsiveness to endocrine therapies [19, 23].

Chemotherapy or endocrine therapy may also be used prior to surgery in order to shrink the tumour [2, 18, 21]. This is known as neo-adjuvant therapy and is particularly important in fast growing tumours as it can minimise the degree of surgery required. Alternatively, these treatments may be offered as primary therapy to patients that cannot undergo surgery for a variety of reasons, including age or general ill-health [18, 21]. Furthermore, the use of tamoxifen as a cancer preventative agent has been investigated in patients at high risk of contracting breast cancer. Reports have revealed that tamoxifen, when given to healthy women at increased risk for breast cancer, reduced the occurrence of non-invasive tumours by 50% and decreased invasive tumours by 49% [24]. However, the benefits obtained from using tamoxifen as a chemo-preventative must outweigh the potentially serious side-effects of long-term tamoxifen use, such as increased risk of endometrial cancer and thromboembolic events, if this therapeutic regime is to be successful [2].

1.3 Endocrine Therapy in the Treatment of ER-positive Breast Cancer

The link between oestrogens and breast cancer was first established in 1896 when Sir George Thomas Beatson demonstrated shrinkage of some breast tumours following performance of a bilateral oophorectomy (surgical removal of the ovaries) [25]. Since then, the role of oestrogens and oestrogen receptor (ER) signalling in breast cancer has been well established, and modulation of

this signalling mechanism using endocrine therapy is now one of the most powerful tools in combating this disease.

Endocrine therapy may take a number of forms, including ovarian ablation, anti-oestrogens and aromatase inhibitor (AI) compounds [26]. The nature of each of these therapies will be discussed later in this section; but first one must consider the role of oestrogen receptor signalling in breast cancer in order to fully appreciate their mode of action.

1.3.1 Oestrogen Receptor Signalling in Breast Cancer

Endocrine therapy is not suitable for the treatment of all breast cancers as it requires the expression of functional hormone receptors, primarily the ER, in the cancerous cells [19]. Breast cancers can be classified as either hormone-dependent or hormone-independent, as determined by their oestrogen receptor status. Hormone-dependent tumours, which account for approximately 60-70% of all breast tumours, test positive for ER and are therefore presumed reliant on oestrogens for growth stimulation. Conversely, hormone-independent tumours are ER negative and so require alternative cell-signalling mechanisms for proliferation.

1.3.1.1 The Structure of the Oestrogen Receptor (ER)

There are two known forms of the ER protein: ERα, which was discovered over 40 years ago and is considered to be the 'classical' ER [27], and ERβ, which has been identified more recently and so is much less well characterised [28]. These two proteins, which are encoded by separate genes [29], share significant structural homology, particularly in the DNA and hormone binding domains [27]. However, differences in the N-terminal domains of these proteins suggest that they may have separate roles in oestrogen signalling, which are still under investigation [30]. As such, the importance of ERβ in breast cancer is ill-defined, and so for clarity this thesis will only discuss ERα (henceforth referred to as ER).

The structure of the ER protein has been comprehensively described in the literature (reviewed in [31]). Briefly, the ER is a 66kDa protein that possesses

a modular structure comprising 6 independent regions (see figure 1.2). The A/B region is found at the N-terminus of the ER protein and possesses an intrinsic transcription activator function (AF-1). The AF-1 domain is constitutively active and, thus, independent of ligand-binding; however, its activity may be enhanced following the activation of a number of cell signalling pathways, such as the Ras/MAPK pathway, which can then phosphorylate ER on serine residues at the N-terminus (S104, S106, S118 and S167) [32, 33]. Phosphorylation of S118 has been shown to be necessary for the full activation of the AF-1 domain [31].

Next is the C-region which contains the highly conserved DNA binding domain (DBD). This region contains two zinc-finger motifs which are involved in the recognition of and binding to specific oestrogen-response-elements (ERE) found in the promoter sequences of oestrogen-regulated genes. The D-region which follows appears to have limited functionality, and may be responsible for the localisation of ER to the nucleus. This is followed by the E-region which, at 250 amino acids, is the largest of the 6 regions and contains the hormone binding domain (HBD), a second intrinsic transcription activator function (AF-2) and sequences important for receptor dimerisation and for the binding of chaperone proteins and co-regulators to the ER [31]. Furthermore,

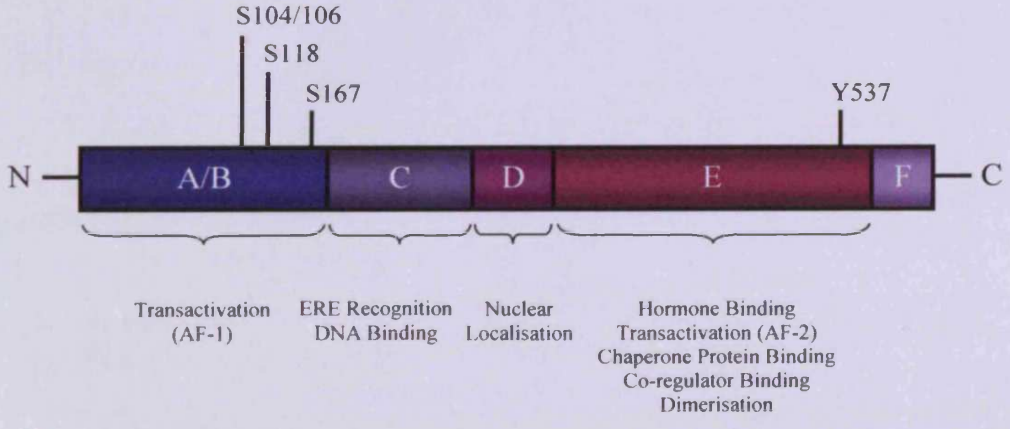

Figure 1.2 Structure of the oestrogen receptor (ER) protein.
Schematic diagram detailing the functional domains of ER (labelled A-F), in addition to phosphorylation sites involved in the promotion of ER transcriptional activity.

this region contains a tyrosine residue at position 537 which, when phosphorylated, is believed to be important for receptor dimerisation and ERE binding [34]. Additionally, this tyrosine may provide a binding site for a number of SH2-domain containing proteins (such as Src) which, when docked, promote the non-genomic signalling of ER (see section 1.3.1.2.3) [35].

Unlike AF-1, the AF-2 domain is not constitutively active and requires ligand binding to the HBD for transcriptional activation. Maximum transcriptional activity of ER usually requires the activation of both AF-1 and AF-2 domains; however, some genes only require either AF-1 or AF-2 activity, thus allowing these domains to act independently of each other [36]. This has major implications for the therapeutic use of anti-oestrogens such as tamoxifen, which will be discussed further in section 1.3.3.1.

1.3.1.2 Mechanisms of ER Activation and Signalling

The oestrogen receptor is classed as a ligand-activated nuclear transcription factor, and is a member of a super-family of nuclear hormone receptors. Three modes of oestrogen receptor signalling have so far been identified (reviewed in [29]).

1.3.1.2.1 'Classical' Genomic Oestrogen-receptor Signalling

The 'classical' genomic signalling mechanism of ER is the most well understood of the three (see figure 1.3) [29, 31, 37]. In the absence of ligand, the ER is maintained in an inactive state through the formation of a large multi-protein complex with chaperone proteins such as HSP90. Following exposure to oestrogens, the hormone molecules diffuse through the plasma-membrane of the cell and travel to the nucleus where they bind to the HBD of the ER. This causes dissociation of the chaperone proteins from the receptor which, in turn, promotes phosphorylation of the N-terminal serine residues required for maximal AF-1 activity. Together, ligand binding and receptor phosphorylation result in a conformational change in the protein which induces receptor homo-dimerisation and translocation to the ERE of oestrogen-regulated genes, where it binds to the DNA with high affinity. The binding of ER to the ERE

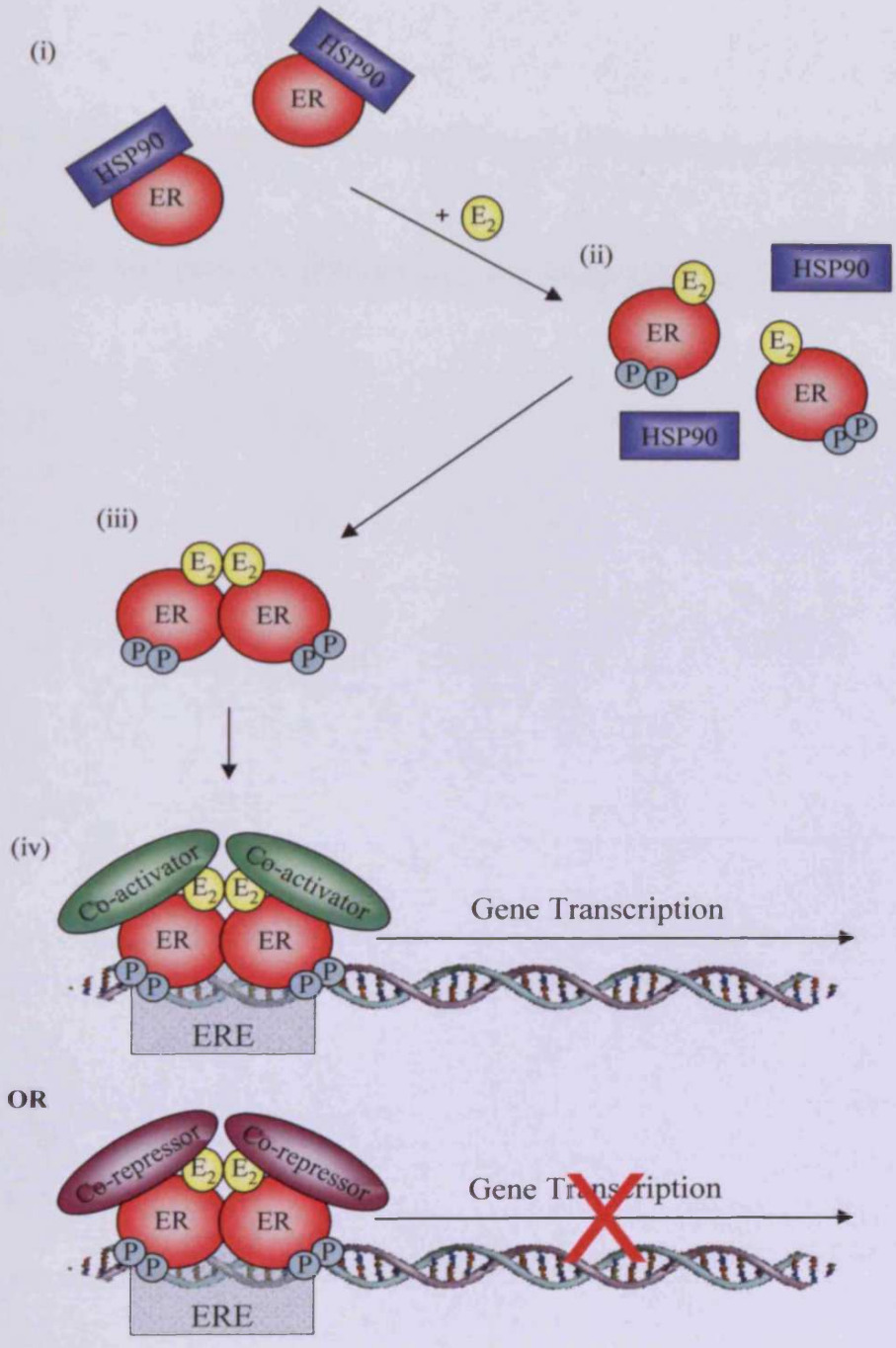

Figure 1.3 'Classical' mechanism of ER signalling in breast cancer.

When inactive, ER forms a complex with chaperone proteins such as HSP90 (i). Following the binding of E_2, the chaperone proteins dissociate from the ER and the receptor undergoes phosphorylation on Serine in the N-terminal domain (ii). The receptor then forms a homo-dimer (iii) and translocates to the ERE of an oestrogen-regulated gene (iv) where it recruits co-activators or co-repressors to promote or suppress gene transcription respectively.

then results in the recruitment of additional proteins, known as co-regulators, to the ER/DNA complex which, depending on their type, can either promote or repress gene transcription to regulate cellular processes such as cell-cycle progression, proliferation and apoptosis [29].

There are two types of co-regulator proteins: co-activators, such as SRC-1 and CBP, which promote oestrogen-receptor dependent gene transcription, and co-repressors, such as NCoR and SMRT, which repress oestrogen-receptor dependent gene transcription [37, 38]. Both co-activators and co-repressors can bind to the ER/DNA complex in the presence of oestrogen; which proteins are recruited is dependent on the promoter sequence of individual genes. Interestingly, binding of selective oestrogen receptor modulators (SERMs) such as tamoxifen typically results in the recruitment of co-repressors, leading to the inhibition of gene transcription [29]. Thus, the ratio of co-activator to co-repressor expression may have implications for the sensitivity of some breast cancers to endocrine therapy [37, 39].

1.3.1.2.2 'Non-classical' Genomic Oestrogen-receptor Signalling

The second mode of ER signalling involves the indirect regulation of gene expression in the absence of an ERE promoter sequence via the formation of protein-protein interactions with additional transcription factors (see figure 1.4) [29]. For example, by associating with the c-fos and c-jun transcription factors ER can promote the expression of genes that contain the AP-1 response element in their promoter region [36]. Thus, the ER is effectively able to act as a co-activator for other transcription factors by strengthening DNA binding and by recruiting other co-activators to the transcription-factor complex to promote gene expression [29].

Additional promoter sequences that can be targeted in this way include the SP-1, TPA and NF-κB response elements [31] which can lead to the expression of proteins important for cell proliferation and survival, such as IGF-1R, cyclin D1 and Bcl-2 [29].

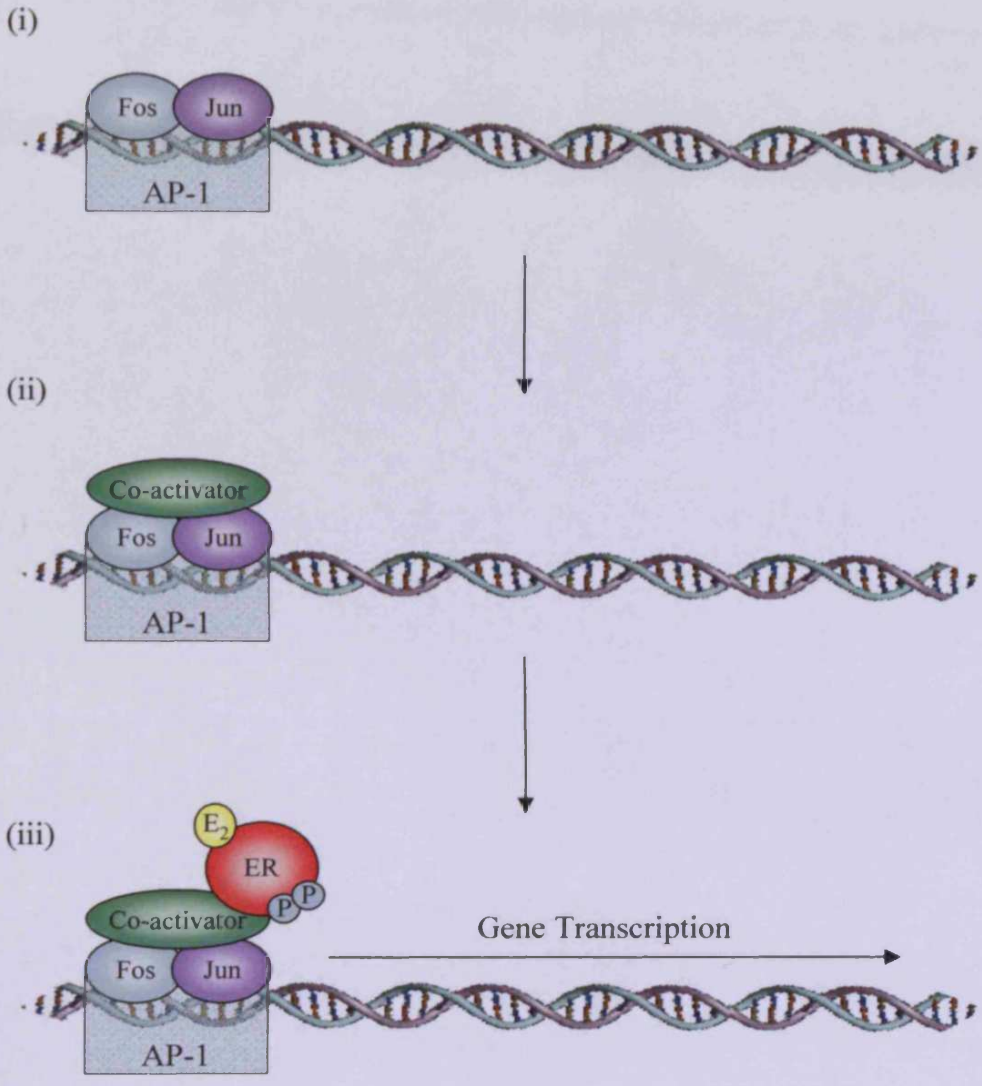

Figure 1.4 'Non-classical' mechanism of ER signalling in breast cancer.

ER is also able to promote the expression of genes that do not contain a classical ERE site. Additional transcription factors, such as Fos and Jun, can form a complex which is then directed to a specific, non-ERE gene-promoter binding site, such as AP-1 (i). This complex recruits co-activator proteins to the site (ii), followed by ligand-activated ER which can enhance the activity of the co-activator proteins to promote gene transcription (iii).

1.3.1.2.3 Non-genomic Oestrogen-receptor Signalling

The ER can also exhibit rapid signalling action in response to ligand binding which results in the activation of a number of signal-transduction molecules important for cell growth and survival, including growth-factor receptors, adapter molecules and cellular kinases such as MAPK and Akt (see figure 1.5) [29, 39]. These responses occur within minutes of exposure to oestrogens and so cannot be attributed to the genomic functions of ER described above; thus, this mechanism of ER signalling is known as 'non-genomic' [40]. Studies have revealed that non-genomic signalling takes place either at the plasma-membrane or in the cytoplasm and so requires the translocation of ER from the nucleus to these locations [40]. The mechanisms which regulate this process are poorly understood but a possible role for the non-receptor tyrosine kinase, Src, has been identified [41, 42].

Non-genomic ER signalling is believed to be facilitated by the phosphory-lation of the receptor on Y537 which acts as a docking site for SH2-domain containing proteins [43]. This allows direct, physical associations between the ER and molecules such as Shc, Src and PI3K [40]. These protein complexes can then interact with and activate other molecules such as growth-factor receptors or the ras-raf-MEK pathway, leading to the activation of ERK 1/2 and Akt which can then go on to phosphorylate nuclear ER S118 and S167 to promote genomic signalling via the AF-1 domain [32, 33]. Interestingly, the non-genomic function of ER can also be initiated by SERMs such as tamoxifen; thus, promotion of non-genomic signalling by these compounds may be a potential mechanism of tamoxifen-resistant cell growth [39].

1.3.2 Endocrine Therapies – Ovarian Ablation

The primary source of oestrogen synthesis in pre-menopausal women is the ovaries, although limited amounts are also produced in peripheral tissues such as adipose tissue [44]. These endogenous oestrogens can promote the growth of ER-positive breast cancer and so eliminating them from the body may be beneficial in the treatment of these tumours. One method of achieving this is to suppress ovarian function in order to abrogate oestrogen synthesis, and this

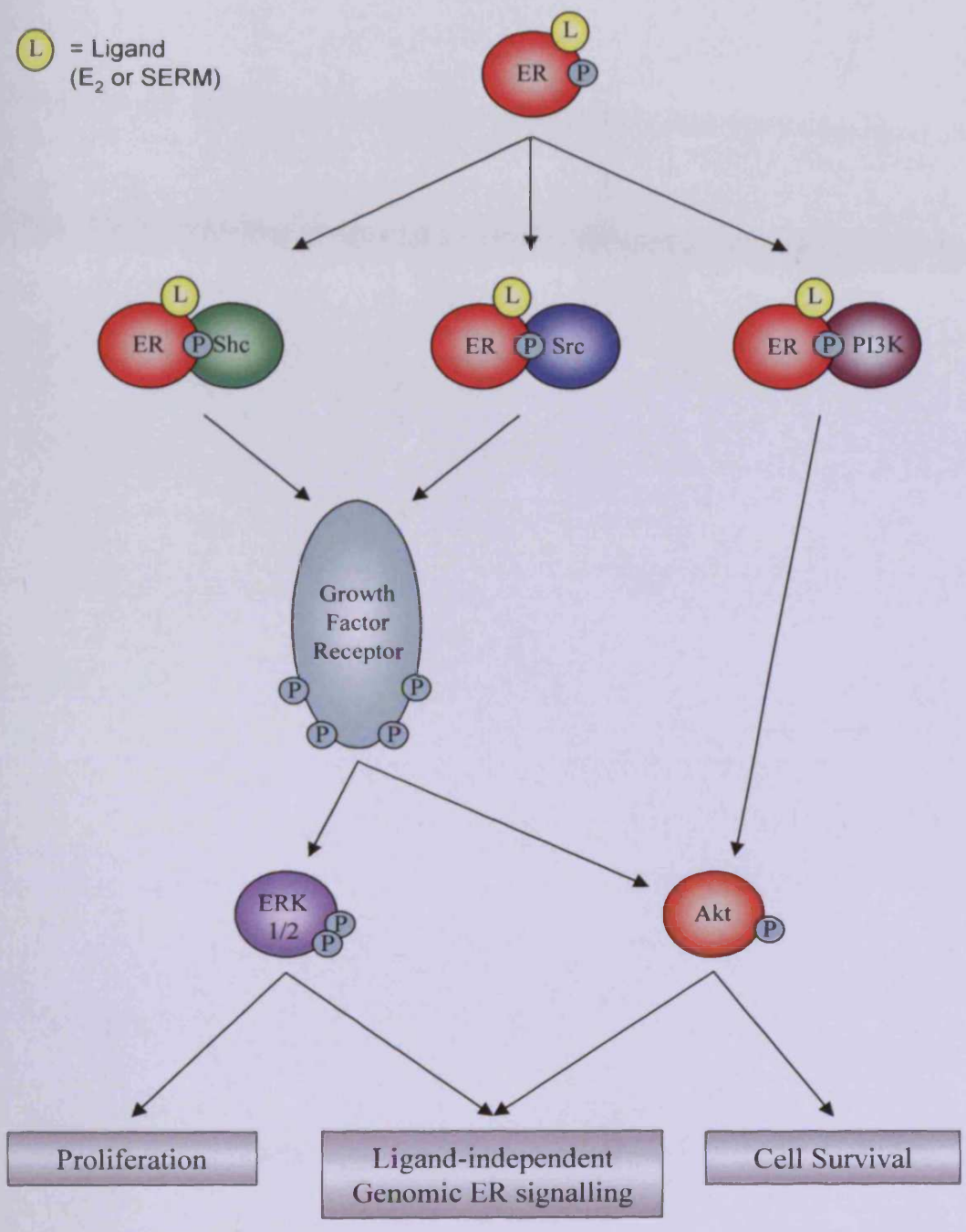

Figure 1.5 Non-genomic mechanisms of ER signalling in breast cancer.

The phosphorylation of ER at Y537 permits the binding of cytoplasmic proteins containing an SH2-domain, such as Src, Shc or PI3K. This binding can facilitate interactions between the ER and growth-factor receptor signalling pathways, resulting in the downstream activation of ERK 1/2 and Akt. In addition to their established roles in the regulation of cell proliferation and survival respectively, these proteins may also phosphorylate ER on S118 and S167 to promote ligand-independent AF-1-mediated genomic ER signalling.

can done using surgical (oophorectomy) or therapeutic (luteinising-hormone releasing hormone [LHRH] agonists) techniques [26].

Oophorectomy was first observed to reduce tumour growth following work conducted by Sir George Beatson in 1896 [45], but it wasn't until almost 60 years later that this was found to be a result of reduced oestrogen production [26]. Since then, surgical ablation of ovarian function has proven effective in the clinical management of ER-positive breast cancer; however, since the irreversible nature of this treatment strategy leads to permanent infertility [26], a number of pharmacological methods of ovarian suppression, such as LHRH agonists, have now been developed.

LHRH agonists, such as goserelin (Zoladex™), are synthetic hormones that reduce oestrogen production by the ovaries [21]. They work by down-regulating levels of the LHRH receptor in the pituitary gland to reduce secretion of luteinising hormone which is important for ovarian function [44]. Phase III clinical trials have shown that goserelin was at least as effective as chemotherapy in the adjuvant treatment of ER-positive breast cancer in pre-menopausal women [26]. However, side-effects were much less severe with goserelin (menopausal symptoms) and, importantly, menses resumed in the majority of patients within 3 years of treatment ending [26].

Effectively, ovarian ablation inhibits the synthesis of oestrogens by the ovaries to induce menopause in the patients to which they are given; however, this treatment does not reduce oestrogen production in the peripheral tissues. As such, the effects of ovarian ablation are typically augmented with additional endocrine therapies, such as tamoxifen or aromatase inhibitors, resulting in a more complete endocrine blockade [44].

1.3.3 Endocrine Therapies – Anti-oestrogens

Anti-oestrogens function by blocking the growth-stimulatory effects of oestrogen on breast cancer cells by either competitively binding to or causing the degradation of ER in the cell [21]. There are currently two main classes of

anti-oestrogen: the selective oestrogen receptor modulators (SERMs) and the selective oestrogen receptor down-regulators (SERDs).

1.3.3.1 Tamoxifen (Nolvadex™)

Tamoxifen was first developed as a contraceptive, but failed in the clinic after it was found to actually promote ovulation in humans rather than suppress it; however, through the concerted efforts of a number of scientists and investigators, tamoxifen was re-invented in the 1970s as the world's first targeted anti-breast-cancer therapy [46, 47]. It has since become the most commonly administered form of endocrine therapy, and has been the gold standard agent for the adjuvant treatment of breast cancer for over 25 years [26, 47]. Approximately 400,000 women are said to be alive today as a direct result of tamoxifen therapy [48].

Tamoxifen is a non-steroidal anti-oestrogen, the structure of which is shown in figure 1.6. It belongs to the 'selective oestrogen receptor modulator' (SERM) family of anti-oestrogens, so called because of their ability to act as both ER agonists and antagonists [49]. Tamoxifen works by competitively binding to the HBD of the ER. Much the same as with oestrogen binding, this action results in a conformational change in the receptor that causes chaperone protein dissociation, receptor dimerisation and translocation of the ER-tamoxifen complex to the promoter regions of oestrogen regulated genes [31]. However, the conformational change induced by the binding of tamoxifen to ER is incomplete, and so prevents the full activation of the ER AF-2 domain required for gene transcription [36]. This inhibition of gene transcription may be further promoted by the preferential recruitment of co-repressors to the gene promoter by the ER-tamoxifen complex [49]. Thus, tamoxifen is able to block ligand-dependent ER signalling, resulting in the disruption of regulatory mechanisms that control cell proliferation and survival in breast cancer.

However, inhibition of ER function by tamoxifen is incomplete as it is unable to affect the transcriptional activity of the AF-1 domain. Therefore, any oestrogen-regulated genes that require only the activity of the AF-1 domain may still be expressed [36]. Furthermore, the activity of AF-1 in the presence

17β-oestradiol:

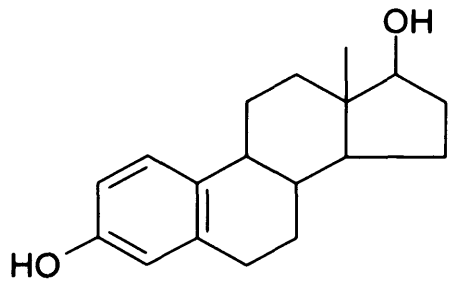

Tamoxifen (Nolvadex™):

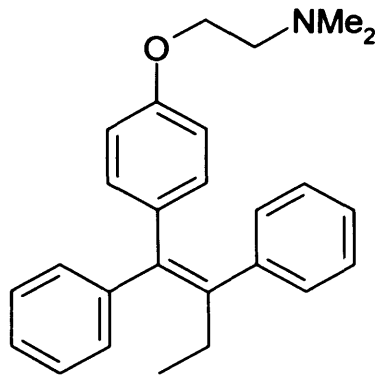

Fulvestrant (Faslodex™):

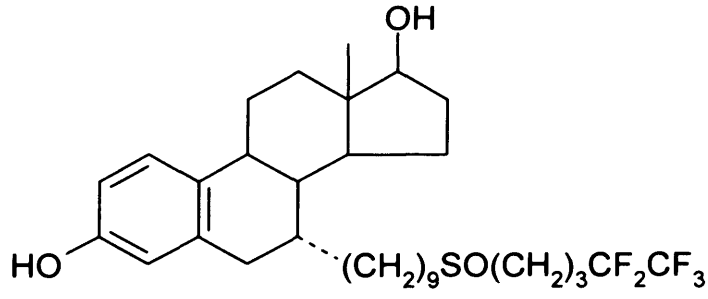

Figure 1.6 Structure of the anti-oestrogens, tamoxifen and fulvestrant, in comparison with that of 17β-oestradiol (adapted from [50]).

of tamoxifen may be enhanced by growth-factor signalling pathways which lead to the phosphorylation of ER at S118 and S167 to promote hormone-independent gene transcription and cell growth [51, 52]. Indeed, the binding of tamoxifen may act as a stimulus for non-genomic ER signalling which can promote the activation of these growth-factor signalling pathways, in addition to the activation of a number of cellular kinases which may augment this process [41]. Thus, the inability of tamoxifen to fully inhibit ER signalling may have repercussions for the development of resistance to this compound, and this will be discussed further in the next section.

In addition to drug resistance, the long-term effectiveness of tamoxifen may be complicated by some unfavourable side-effects. Although generally well tolerated in the clinic, tamoxifen has been associated with an increased risk of developing endometrial cancer due to its role as an ER agonist in this tissue, in addition to increased thromboembolic events that may lead to a stroke [24]. Because of this, tamoxifen use is often limited to a maximum of 5 years as studies have shown no additional benefit with longer treatment durations [26].

1.3.3.2 Fulvestrant (Faslodex™)

Despite being well tolerated, the side-effects associated with the agonistic effects of tamoxifen (mentioned above), in addition to the relatively frequent acquisition of resistance to this therapy, make it a less-than-ideal therapeutic agent. Thus, recent years have seen the development of a number of compounds which demonstrate equal or superior efficacy in the treatment of breast cancer compared to tamoxifen, but which lack any ER agonist activity and so may be better tolerated in the clinic [53].

One such compound is fulvestrant (Faslodex™; AstraZeneca Pharmaceuticals Ltd.) [50, 54]. Fulvestrant is an anti-oestrogen with a steroidal structure similar to that of 17β-oestradiol (E_2), but which contains an alkylsulphinyl side chain at the 7α position which is crucial for the ER antagonist activity of this compound (see figure 1.6) [30]. Fulvestrant belongs to the 'selective oestrogen receptor down-regulator' (SERD) class of anti-oestrogens [31], so called because a component of its mode of action is to down-regulate ER protein and

thus reduce their cellular levels [54]. Unlike tamoxifen, fulvestrant has been shown to possess no ER agonist activity in all tissues studied to date [36], and so is known as a 'pure' anti-oestrogen [54]. Fulvestrant is the first of this new class of 'pure' anti-oestrogens to enter clinical development [55].

Fulvestrant works by binding to the ER with high affinity (approximately 89% that of oestradiol) and inducing a conformational change in the structure of the receptor (reviewed in [30, 50, 53]). However, steric hindrance caused by the alkylsulphinyl side-chain of fulvestrant results in an abnormal conformation of the ER protein which prevents receptor dimerisation and inhibits nuclear localisation. In addition, the ER-fulvestrant complex is unstable and leads to the subsequent rapid degradation of ER to reduce the cellular levels of this protein. Furthermore, the binding of fulvestrant to ER prevents the activation of the AF-1 and AF-2 domains; thus ER mediated gene transcription is inhibited even if the down-regulation of ER protein is incomplete. The combination of cellular events that transpire as a result of treatment with fulvestrant leads to a significant reduction in ER-regulated gene transcription, with fulvestrant demonstrating 95% and 91% antagonism of E_2-upregulated and E_2-down-regulated gene expression respectively [30].

Fulvestrant has been generally well tolerated in clinical trials, with only a small number of relatively minor side-effects reported [30]. Importantly, this compound possesses no ER agonist activity in any tissue type studied thus far, and so is not associated with the increased risks of endometrial cancer or thromboembolic events that accompany long-term tamoxifen use [30].

Fulvestrant has been shown to be effective against ER-positive breast cancer in both pre-clinical *in vitro* and *in vivo* studies and in clinical trials, and results in a reduction in ER protein levels (but not mRNA) and in the expression of ER-regulated genes such as PgR and pS2 [30, 50, 54, 56]. However, data from these trials have so far failed to demonstrate superiority of fulvestrant over tamoxifen or AIs in the treatment of advanced breast cancer, and currently suggest its use as a second-line therapy following disease progression with these compounds [30, 57, 58]. As such, the importance of fulvestrant in

the treatment of breast cancer is unclear at present, but further investigations into fulvestrant as a first-line therapy in ER-positive breast cancer are ongoing.

1.3.4 Endocrine Therapies – Aromatase Inhibitors (AIs)

Due to the adverse effects associated with long-term tamoxifen use, in addition to the pervading threat of acquired resistance to this drug, aromatase inhibitors (AIs) have recently been developed as a further means of treating breast cancer.

Following menopause, the principle site of oestrogen production in the female body is in the peripheral tissues, such as adipose tissue or muscle [44]. Here, the cytochrome P450 enzyme, aromatase, converts the androgen, androstenedione, to oestrone; and this is subsequently converted into 17β-oestradiol by 17β-hydroxysteroid dehydrogenase, resulting in an increase in the circulating levels of 17β-oestradiol which can then stimulate the growth of ER-positive breast cancers. Interestingly, both enzymes can also be found in the tumour itself, thus providing a local source of oestrogen production [44].

AIs work by inhibiting the aromatase enzyme, both in peripheral tissue and in the tumour, to prevent oestrogen synthesis [55]. Therefore, in a similar fashion to ovarian ablation in pre-menopausal women, the net result of AI treatment is a significant reduction in the circulating levels of oestrogens in the body, thus removing the growth stimulus for ER-positive breast tumours [55]. Although the efficacy of first-generation AIs was blighted by low selectivity and high toxicity [59], the current third-generation AIs, of which anastrozole (Arimidex™), letrozole (Femara™) and exemestane (Aromasin™) are the most well studied, have shown promise in clinical trials for the adjuvant treatment of early breast cancer. These agents have demonstrated both high selectivity and good tolerability [26], and have been shown to reduce serum oestrogen levels by as much as 85-92% in post-menopausal women [55].

Recently, the results of the Arimidex, Tamoxifen, Alone or in Combination (ATAC) trial have challenged the 25-year reign of tamoxifen as the gold standard adjuvant therapy for early breast cancer. The data show that the AI,

anastrozole, was far superior to tamoxifen after 5 years of treatment; demonstrating prolonged disease-free survival, time-to-recurrence and time-to-distant-recurrence, in addition to a decreased risk of contralateral breast cancers [22]. The increased efficacy of anastrozole in this setting may be due to its ability to inhibit both ligand-dependent genomic and non-genomic ER signalling, unlike tamoxifen which may actually stimulate non-genomic signalling of ER [60]. Furthermore, anastrozole was better tolerated, and was associated with a reduced risk of endometrial cancer and thromboembolic events compared to tamoxifen [22]. However, bone fractures were increased in the AI group suggesting that this compound resulted in loss of bone mineral density; although this can be countered by co-treatment with bis-phosphonates to reduce bone resorption [22]. In their conclusions, the ATAC Trialists' Group recommended that anastrozole should replace tamoxifen as the preferred choice of initial adjuvant therapy in post-menopausal women with early ER-positive breast cancer [22]. However, longer follow-up studies are still required in order to ascertain the long-term effects of AIs on overall survival compared to tamoxifen [55].

Interestingly, the anastrozole-tamoxifen combined arm of the ATAC trial conclusively failed to show any benefit over tamoxifen alone, and was ended prior to completion of the study [22]. This may be because tamoxifen can act as a weak oestrogen to stimulate the non-genomic functions of ER and promote growth-factor-receptor and ligand-independent ER signalling pathways [61]. However, despite this failure, the use of AIs in combination with other endocrine therapies has also been suggested. For example, AIs in combination with fulvestrant may be superior to AIs alone as fulvestrant is able to abrogate ligand-independent ER-mediated gene transcription which is still active following AI treatment alone [60]. Indeed, ligand-independent ER activation may confer resistance to AI therapy, and this has been studied in our laboratory using an MCF7-derived cell-model of resistance to oestrogen depravation [61]. Furthermore, investigations into the efficacy of AIs in pre-menopausal women following ovarian ablation or suppression are also underway [60].

1.4 Tamoxifen Resistance in Breast Cancer

1.4.1 Acquired and de novo Resistance to Tamoxifen

Despite the success of tamoxifen in the treatment of breast cancer over the last three decades, this therapeutic agent is not without its problems or limitations. As with all endocrine therapies, tamoxifen is only beneficial in ER-positive tumours, which means that 30-40% of all breast cancers are not eligible for this treatment [19]. Sadly, of the ER-positive tumours treated with tamoxifen, a further 50% will not respond and, along with ER-negative tumours, are said to exhibit *de novo* ('from the beginning') resistance [37]. Moreover, in tumours that do initially respond to tamoxifen, the majority will acquire resistance at some point during the treatment [62]. Thus, *de novo* and acquired resistance to tamoxifen is a major obstacle in the clinical management of breast cancer and often results in disease recurrence and premature death [51].

1.4.1.1 Mechanisms of de novo tamoxifen resistance

The presence of ER in breast tumours is a significant predictive indicator of response to endocrine therapies such as tamoxifen [19, 62, 63]. Thus it should come as no surprise that the most prevalent mechanism of *de novo* tamoxifen resistance in breast cancer is the lack of ER expression [51, 55]; whereas mechanisms of *de novo* resistance in ER-positive tumours are less well defined. A strong contender for mediating *de novo* tamoxifen resistant growth in ER-positive breast cancer is the erb-B growth-factor receptor family. Studies have revealed increased expression of EGFR and/or c-erbB2 in clinical examples of *de novo* resistant breast tumours, in addition to the increased expression of TGFα and activation of ERK 1/2 [64]. This has also been reported in *in vitro* cell models, with high expression of these receptors in the ER-positive BT474 cell-line conferring *de novo* resistance to tamoxifen [64]. Furthermore, over-expression of c-erbB2 in MCF7 breast cancer cells which demonstrate high levels of the ER co-activator, AIB1, also resulted in *de novo* resistance to tamoxifen by promoting the agonist activity of this anti-hormone [65].

1.4.1.2 Mechanisms of acquired tamoxifen resistance – loss of ER

Unlike *de novo* resistance, acquired resistance develops as treatment progresses and is a result of changes that occur in the signalling profile of the cell [66]. With ER-negativity playing such a major role in *de novo* resistance mechanisms, it would be reasonable to assume that loss of ER expression may be a causative factor in acquired resistance also. Indeed, both prolonged activation of growth-factor signalling pathways [67] and epigenetic modifications such as hyper-methylation of CpG islands [51] have been shown to down-regulate ER levels under such circumstances. However, reports suggest that over 75% of tumours demonstrating acquired tamoxifen resistance retain their responsive-phase levels of ER [62], and this is also evidenced by the observed response to second-line endocrine therapies [68], such as fulvestrant [69]. Thus, loss of ER expression is unlikely to be a major factor in acquired tamoxifen resistance in the clinic [62].

1.4.1.3 Mechanisms of acquired tamoxifen resistance – aberrant growth-factor signalling and cross-talk with ER

A number of pre-clinical and clinical studies have demonstrated a positive correlation between elevated growth-factor-receptor signalling and the failure of endocrine therapies [42]. Indeed, studies in our laboratory have shown that elevated expression and activation of EGFR and c-erbB2 is responsible for the enhanced growth of our *in vitro* model of acquired tamoxifen-resistance [70]; while Nicholson *et al.* have reported an association between increased EGFR expression and the loss of hormone sensitivity in clinical breast cancers [23]. Furthermore, increased activation of ERK 1/2, which is a downstream substrate of EGFR and c-erbB2 signalling pathways, correlates with a poor response to anti-hormone therapy and decreased patient survival [71]. Interestingly, our group has also observed that tamoxifen-resistance is associated with the increased expression of growth factors both *in vitro* and *in vivo*, suggesting the presence of an autocrine mechanism for growth-factor-receptor regulated growth that circumvents the requirement for hormone stimulation in these cells [72, 73].

Moreover, increasing evidence suggests that cross-talk between growth-factor receptor and ER signalling pathways might play a significant role in enhancing tamoxifen-resistant growth in tumours that have retained ER expression and function [74, 75]. This is a bi-directional process whereby EGFR signalling is able to potentiate ER activation and *vice versa.*

In the presence of growth factors, ligand-dependent EGFR activation results in the down-stream activation of ERK 1/2, which is then able to phosphorylate the ER on S118 [32]. Under basal conditions, phosphorylation of S118 sensitises the ER to oestrogen-dependent activation and subsequent AF-1 and AF-2 mediated gene transcription; however, in the presence of tamoxifen, phosphorylation of this site enhances the transcriptional activity of the AF-1 domain only, resulting in an increase in ligand-independent gene expression [51]. Furthermore, phosphorylation of ER on S167 following EGFR dependent activation of Akt signalling may augment this process [33]. Interestingly, members of our laboratory have demonstrated increased EGFR-dependent activation of ERK 1/2 [70] and Akt [76], in addition to elevated ER phosphorylation [73], in our *in vitro* model of tamoxifen-resistance. EGFR may further promote ligand-independent gene transcription in these cells by up-regulating or down-regulating the activities of ER co-activators or co-repressors respectively [51]. Indeed, the increased expression and activity of some co-activators has been shown to promote the agonist activity of tamoxifen, resulting in the tamoxifen-stimulated growth of resistant cells [65].

Cross-talk can also occur in the opposite direction, with ligand-independent ER-mediated gene transcription in the presence of tamoxifen leading to the increased expression of growth factors, such as TGFα and amphiregulin [66, 73]. Thus, the ER-mediated expression of these growth factors can stimulate growth-factor receptor signalling in an autocrine or paracrine fashion. This process has been shown to be sensitive to treatment with fulvestrant, thus confirming a role for ER in the regulation of EGFR activity [69, 73]. Furthermore, non-genomic ER signalling has recently been shown to stimulate growth-factor receptor activation at the plasma-membrane by both direct and

indirect mechanisms. In particular, studies have revealed that ER is able to promote EGFR signalling via direct interactions with adaptor molecules such as Shc and Src [40-42]. In addition, activation of Src by membrane ER has been shown to up-regulate MMP expression and activation, leading to the cleavage and release of membrane-associated heparin-bound EGF (HB-EGF) which can then indirectly promote EGFR signalling [77].

Thus, the dependence of tamoxifen-resistant breast cancer on the co-ordinated actions of ER and EGFR signalling pathways for sustained proliferation may provide new avenues for the treatment of this disease. Indeed, the separate inhibition of ER and EGFR signalling pathways in our tamoxifen-resistant cell model with fulvestrant and gefitinib respectively was shown to have a significant inhibitory effect on their growth [69, 70, 78], while combined treatment with fulvestrant and gefitinib demonstrated synergistic growth inhibition in these cells and prevented the development of resistance to either of these compounds following long-term treatment [79].

1.4.2 Combating Tamoxifen Resistance in the Clinic

Elucidation of the mechanisms responsible for both *de novo* and acquired anti-hormone resistance is important for the development of new, improved therapeutic agents and for the strategic planning of future treatment regimens. In the last 10 years a number of novel endocrine therapies have emerged that demonstrate similar or superior efficacies to tamoxifen, but have the advantage of being better tolerated in the clinic; these include the aromatase inhibitors and the pure anti-oestrogen fulvestrant, both of which have been discussed earlier in this chapter.

Serendipitously, these new compounds possess distinct mechanisms of action both with respect to tamoxifen and each other; thus, it is highly unlikely that cross-resistance will occur between the three [58]. This means that should a patient progress on one of these treatments, they have a high chance of responding to one of the other compounds when used as a second-line therapy. For example, tamoxifen resistant breast cancer has been shown to respond to treatment with fulvestrant both *in vitro* and in the clinic [54]. Therefore, these

therapies may be sequenced following the acquisition of resistance in order to maximise the length of time where treatments with minimal toxicity can be used before more cytotoxic options are explored, and this is particularly important in advanced disease where the main aim of treatment is to maintain a high quality of life for as long as possible.

However, despite the advances in therapy sequencing already achieved, further work is required in order to ascertain the optimal sequence order and duration of treatment for these three compounds in the advent of resistance to first-line therapies, and this is particularly important at the present time since anastrozole is quickly replacing tamoxifen as the preferred first-line adjuvant therapy in early breast cancer [80]. Also, these sequencing options should include combination treatments with non-endocrine therapies such as gefitinib, as a number of pre-clinical and clinical trials assessing the efficacy of such combinations are showing positive results [78, 81, 82].

1.5 Src

1.5.1 The History of Src

The history of Src begins in the early 20th century, when Peyton Rous discovered that spindle-cell sarcomas could be transmitted between chickens by a 'filterable agent' (reviewed in [83]). However, the attitudes and beliefs of the time led to derision of the theory that tumours could be infectious; thus, the observations made by Rous were largely ignored for many years. It wasn't until the 1950s and '60s that advances in both knowledge and technology permitted intense investigation into the nature of this 'filterable agent', which was subsequently identified as the Rous sarcoma virus (RSV) [83].

By the early 1970s, the oncogene responsible for the transforming potential of the Rous sarcoma virus, namely v-src, had been identified [83]. Thus, the race was on to isolate the protein product of this gene; and this race was won by Brugge and Erikson in 1977 [84]. Using sera obtained from rabbits carrying RSV-induced tumours, Brugge and Erikson were able to immunoprecipitate a 60kDa transformation-specific polypeptide from both RSV-transformed

chicken fibroblasts and RSV-induced hamster tumour cells which was not present when a transformation-defective form of RSV was used. The identity of this polypeptide as the product of the transforming component of RSV was further confirmed in 1978 using cell-free expression systems and tryptic-digestion peptide mapping [85, 86]. Soon after, a highly-conserved cellular homologue of v-Src, designated c-Src, was identified in uninfected cells [87-89]. Further work revealed that both v-Src and c-Src demonstrated protein kinase activity [88-91], which was later found to be tyrosine specific [92-94]. Src was the first tyrosine kinase ever discovered and, as such, is the most well studied (reviewed in [95-103]); its discovery led to a surge of interest in the regulation of phospho-proteins which resulted in the subsequent identification of many other tyrosine specific kinases, such as EGFR [83, 104].

c-Src is now understood to be the prototype member of a family of cellular kinases, of which nine are known – Src, Fyn, Yes, Yrk, Lyn, Hck, Fgr, Blk and Lck [95]. All family members share significant sequence and structural homology; however, only three of the nine are ubiquitously expressed in humans (Src, Fyn and Yes), with the remaining family members restricted to haematopoietic cells and some neural tissues [95, 96]. This suggests that the family members may have distinct, tissue specific functions. Historically, the Src-family member most often associated with cancer is Src [97]. The over-expression and/or up-regulated kinase activity of Src has been reported in many different cancers [101-103], including breast [105], colorectal [106], pancreatic [107] and ovarian [108], and has been shown to correlate with disease recurrence [109] and a poor clinical prognosis [106]. As such, this thesis will focus only on the role of Src in tamoxifen-resistant breast cancer.

1.5.2 The Structure of the Src Protein

The non-receptor kinase, Src, possesses a modular structure comprised of an N-terminal Src Homology (SH) 4 domain, a unique region, SH3 and SH2 protein-binding domains, an SH1 (kinase) domain and a C-terminal negative-regulatory tail (see figure 1.7A). This structure is highly conserved among

A

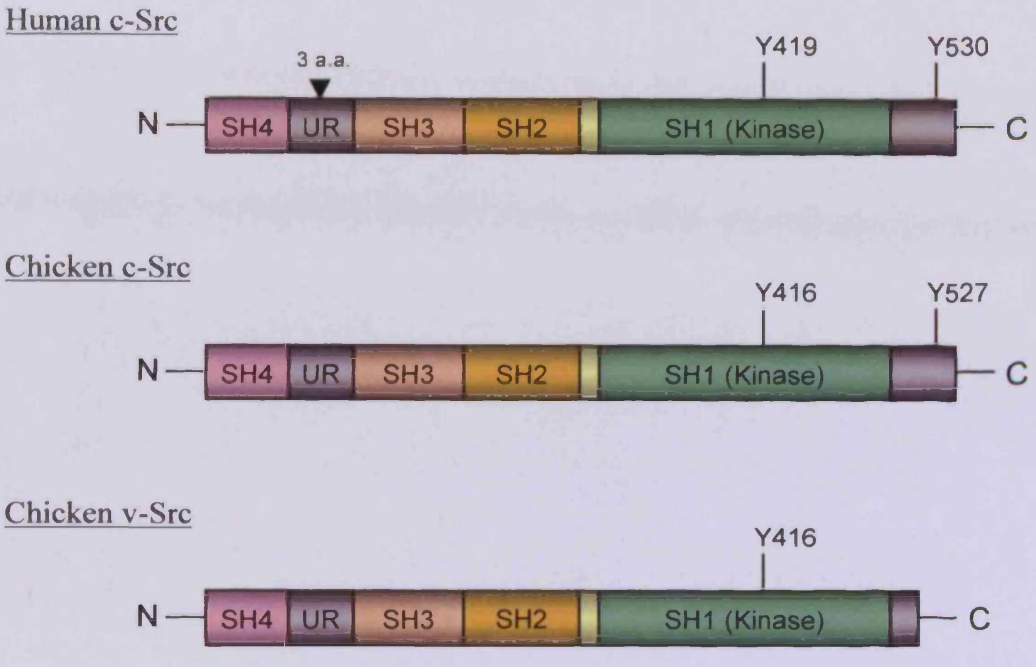

B

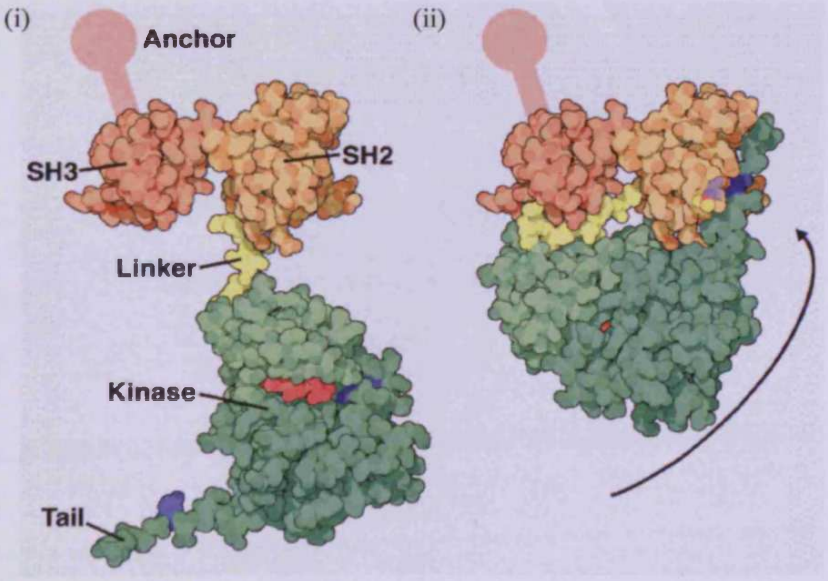

Figure 1.7 Structural organisation of the non-receptor tyrosine kinase, Src.

(A) Schematic diagram detailing the functional domains and phosphorylation sites of human Src in comparison to that of chicken c-Src and chicken v-Src (UR = unique region; adapted from [97]). (B) Schematic representation of Src in the open (i) and closed (ii) conformations. See text for details. Picture by D.S. Goodsell of The Scripps Research Institute, CA, USA. Obtained from RSCB Protein Data Bank [www.pdb.org], 'Molecule of the Month' July 2003.

Src-family members; while some components, such as the SH3 domain, have been identified in other cellular proteins including Shc and paxillin [95-97].

The first of these domains, SH4, is required for the membrane association of Src. This domain contains a conserved amino acid sequence (Met-Gly-X-X-X-Ser/Thr, where X is any amino acid) which permits the permanent binding of a 14-carbon saturated fatty-acid, known as myristate, to the N-terminal amino acid of Src following translation of the protein [110]. This process is mediated by N-myristoyltransferases [111] and promotes the attachment of Src to the cytosolic face of the plasma-membrane [112]. However, myristoylated proteins have also been found in the cytoplasm, suggesting that myristoylation alone is not sufficient for membrane association [110, 112].

A further post-translational modification which may augment myristoylation-mediated membrane association of Src-family members is palmitoylation, which has recently been shown to influence the membrane targeting of Fyn and Yes [113]. This process involves the acylation of cysteine residues at the 3 and/or 5/6 positions of the SH4 domain with a 16-carbon fatty acid, palmitate [110]. However, palmitoylation has been demonstrated in all Src-family members bar Src and Blk, as these kinases do not possess the requisite cysteine residues at these positions [110]. Instead, Src and Blk have basic amino acids at these positions which may fortify the membrane association of these two proteins through interactions with negatively charged phospho-lipids in the plasma-membrane [96, 110].

Next is the unique region, so called because of poor sequence homology between Src-family members [95]. The variability of the unique region is responsible for differences in the numbering of the amino acid sequences of Src family members from different species of origin. For example, the auto-phosphorylation site of Src originating from chickens is Y416, whereas in human Src it is Y419 due to a 3-amino-acid insertion in the unique region [100]. The function of the unique region is unclear, but the high degree of variance between family members precludes the likelihood of a generalised mechanism of action [96]. However, this region may have functions which

are distinct for each family member [95]; for example, the unique region of Lck has been shown to mediate its binding to the cytoplasmic domains of the T-cell co-receptors CD4 and CD8α [114].

The unique region is followed by the Src Homology 3 and Src Homology 2 protein-binding domains which are highly conserved throughout evolution. While these domains are found in a large number of cellular kinases and adapter molecules, they were first identified in v-Src, hence their name [115].

The SH3 domain of Src, which is approximately 60 amino acids in length, interacts with specific proline-rich sequences that fold into a left-handed helix formation (PXXP motif, where X is any amino acid) [112, 114]. The SH3 domain mediates the physical association of Src with other signalling molecules which contain these specific proline-rich sequences, such as PI3K and paxillin, and can also help stabilise protein-protein interactions formed by the SH2 domain. Furthermore, the SH3 domain may be responsible for the translocation of activated Src from the peri-nuclear region to focal adhesions at the plasma-membrane via the activation-dependent association of Src with actin stress fibres and subsequent cytoskeletal re-arrangements which are regulated by the Rho family of small GTPases [116-118].

At approximately 100 amino acids in length, the SH2 domain of Src is slightly larger than the SH3 domain [112]. The SH2 domain is responsible for the recognition of and binding to specific phosphotyrosine-containing amino acid sequences found in a number of Src substrates involved in cell-signalling, such as components of the EGFR and integrin signalling pathways. The preferred recognition sequence for the SH2 domain of Src is pTyr-Glu-Glu-Ile (pYEEI), although this domain can bind to other sequences with much lower affinity [112, 119, 120]. The secondary structure of the SH2 domain creates two 'recognition pockets' which co-ordinate the binding of the pYEEI sequence [95, 114]. The first of these pockets houses the pTyr residue itself. The recognition and binding of pTyr is facilitated by interactions with a lysine residue and two arginine residues located in the binding pocket [121]; in particular, the arginine at position 175 is highly conserved and has been

demonstrated to be necessary for SH2-mediated protein-protein interactions [115]. The second recognition pocket binds to a hydrophobic residue in the +3 position C-terminal to the pTyr [112]. However, the specificity of this pocket is not as strict as that of the pTyr-binding pocket, and so it is able to interact with a number of different hydrophobic residues, including isoleucine and proline; this may account for the variation in SH2-binding sequences seen for different proteins [114]. In Src, this pocket favours isoleucine at the +3 position of the SH2-binding sequence, promoting high affinity substrate binding to the SH2 domain [114]. Examples of Src substrates which possess high affinity SH2-recognition sequences include focal adhesion kinase (FAK; pYAEI) [96] and EGFR (pYDGI) [120], and the consequence of interactions with these proteins will be discussed in the next section.

A short linker region connects the SH2 domain to the SH1 (kinase) domain. The Src kinase domain is comprised of two lobes: a small N-terminal lobe (residues 270-340; 71 amino acids) whose main function is to anchor the ATP molecule in readiness for the phosphorylation reaction, and a larger C-terminal lobe (residues 344-523; 180 amino acids) which is primarily responsible for securing the target protein in the correct orientation [112]. The activation loop of the kinase domain is found near the N-terminal region of the large lobe (residues 407-435) and, in the inactive conformation, forms an α-helical structure which lies between the two lobes of the kinase domain. This sequesters a highly conserved tyrosine residue located in the activation loop at position 419, thus preventing its phosphorylation. Following activation of the kinase, the activation loop undergoes a conformational change which releases Y419 and promotes the auto-phosphorylation of this residue. The phosphorylation of Y419 stabilises and maintains the extended conformation of the activation loop, which now forms part of the catalytic site, to promote full activation of the kinase [112]. Indeed, the phosphorylation of Src Y419 has been shown to be a necessary requirement for the full kinase activity of Src [122, 123] and, as such, is frequently used in the laboratory as a surrogate marker for Src kinase activity in lieu of *in vitro* kinase activity assays.

The last region of the Src protein is the C-terminal negative-regulatory tail. This region contains a highly conserved tyrosine at position 530 (Y527 in chickens) which is of paramount importance for the adoption of an auto-inhibitory conformation by Src, and thus is able to regulate the activity of Src in the cell [124]. Indeed, the C-terminal negative-regulatory tail of v-Src is truncated and so lacks this conserved tyrosine, thus accounting for its constitutive activation and cell-transforming abilities [95]. Furthermore, a mutated form of the Src protein containing a tyrosine-phenylalanine substitution at this site, such as the one used in chapter five of the present study, also demonstrates constitutive activation [123]. The role of Y530 in the regulation of Src activity is discussed in further detail in the next section.

1.5.3 Regulation of Src Kinase Activity

Src can promote the activation of signalling pathways that regulate a diverse array of cellular events, including proliferation, cell survival, and cell motility and invasion [95]; thus, it is tightly regulated in normal tissue, with transient up-regulation of Src kinase activity occurring only in response to certain intra- and extra-cellular stimuli [96]. For example, in a study comparing Src activity in DCIS breast tumours versus normal breast tissue, just 12% of the normal tissue demonstrated evidence of Src activity, and this was at very low levels. This compares with the DCIS tumour samples, of which 19% demonstrated low levels of Src activity, 41% demonstrated moderate levels of Src activity and 40% demonstrated high levels of Src activity [109]. Indeed, elevated Src kinase activity has been reported in a number of cancers compared to normal tissues, including breast, colorectal and pancreatic [105-107].

Elevated Src kinase activity is sometimes, but not always, attributable to increased expression of the Src protein [105]. However, the up-regulation of the specific tyrosine-kinase activity of Src has also been reported in the absence of any corresponding increases in total Src protein [102], and this is particularly true of later stage tumours [97]. This might suggest that the regulatory mechanisms that usually keep Src activity in check are disrupted somehow following tumour development and/or progression.

The regulation of Src activity is complex, and is dependent on the conformational state of the protein. When inactive, Src is maintained in a closed conformation by intra-molecular interactions that occur between the SH2 domain and Y530 in the negative-regulatory tail and between the SH3 domain and the SH2-kinase linker, and this closed conformation imposes steric hindrance on the kinase (see figure 1.7Bii) [95-97]. Free movement of the lobes that comprise the kinase domain is required to allow access to the catalytic site of the enzyme and to promote the auto-phosphorylation of Y419 in the activation loop; thus, any restrictions placed on this movement will have an inhibitory effect on the protein [112]. For activation of the kinase domain, Src must first undergo a conformational change in order to adopt an open configuration (see figure 1.7Bi) [95-97]. This releases the steric constraints imposed on the lobes of the kinase domain, thus permitting access to the catalytic site and promoting the auto-phosphorylation of Y419 for full kinase activity. However, this conformational change can only occur following the disruption or displacement of Y530 from the SH2 domain, and so the mechanisms by which this can occur are crucial to the regulation of Src activity.

1.5.3.1 Phosphorylation and de-phosphorylation of Y530

For Y530 to interact with the SH2 domain it must first be phosphorylated; thus, one potential regulatory mechanism of Src activity involves the phosphorylation and de-phosphorylation of this residue (see figure 1.8). While a number of kinase and phosphatase enzymes that are able to regulate the phosphorylation status of Y530 have been identified [124], the proteins most often associated with the regulation of Src are C-terminal Src kinase (CSK) [125] and protein tyrosine phosphatase 1B (PTP1B) [126]. CSK has been shown to phosphorylate Src Y530 and promote its interaction with the SH2 domain, leading to the inactive conformation of the Src protein. PTP1B, on the other hand, is able to de-phosphorylate Src at this site and promote dissociation of the negative-regulatory tail from the SH2 domain, thus allowing the adoption of an active conformation. Therefore, the regulation of Src activity may depend on the balance between the intra-cellular levels of these two proteins.

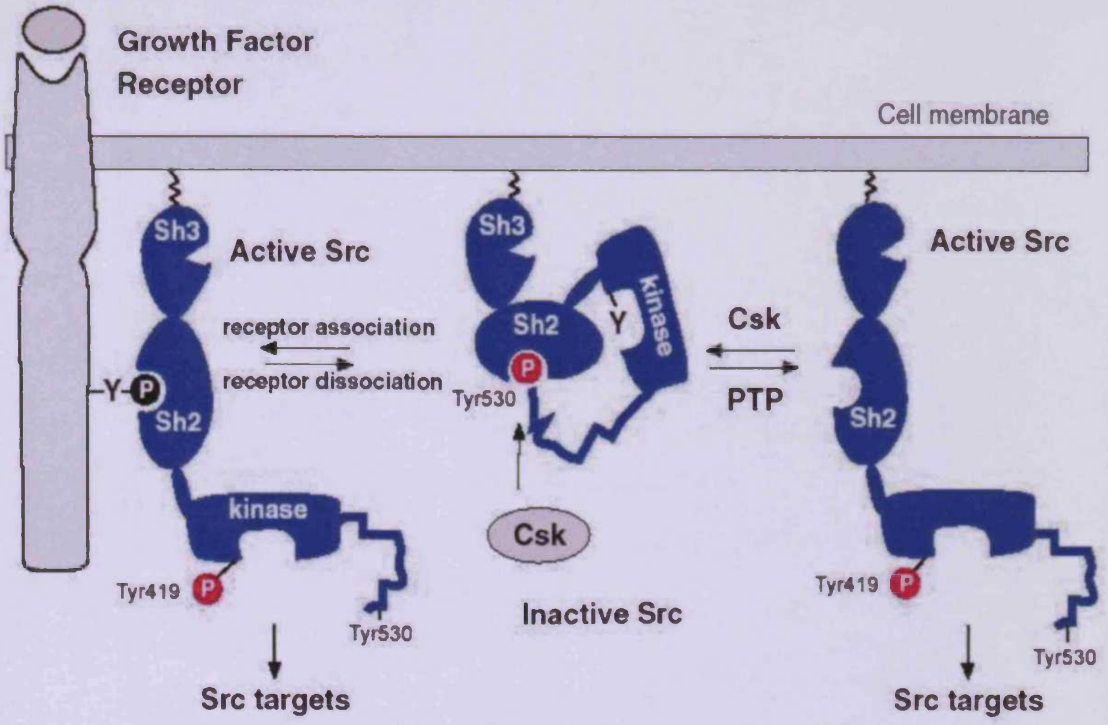

Figure 1.8 Mechanisms of Src activation.

Schematic diagram describing the two most common mechanisms of Src activation in the cell. The first mechanism involves the regulation of Src Y530 phosphorylation by kinases (e.g. CSK) or phosphatases (e.g. PTP1B), which in turn controls the association between Y530 and the SH2-domain to dictate the conformation of the Src protein. The second mechanism relies on the displacement of Y530 from the SH2-domain following direct physical interactions with a phospho-tyrosine-containing protein for which the Src SH2-domain has high affinity (e.g. growth-factor receptors).

Figure adapted from: Bjorge, J.D., Jakymiw, A. and Fujita, D.J. (2000). Oncogene 19(49), pp. 5620-5635.

Some studies, however, have shown that Src is able display full kinase activity even in the presence of phosphorylated Y530 [127-129]. This may be due to the phosphorylation of a conserved tyrosine residue in the SH2 domain (Y215) [124], which can be mediated by growth-factor receptors such as PDGF-R or c-erbB2 [120, 130]. Interestingly, while the phosphorylation of Y215 prevents the interaction between Y530 and the SH2 domain to promote the open, kinase-active conformation of Src, it does not affect the binding of Src substrates such as EGFR or FAK; thus, Src is still able to regulate the activity of these cell-signalling pathways [120].

1.5.3.2 Protein-protein interactions

A further mechanism of Src activation involves the displacement of the phosphorylated Y530 residue from the SH2 domain following interactions between Src and another phospho-tyrosine containing protein for which Src has a higher binding affinity (see figure 1.8) [96].

The intra-molecular interactions which maintain the inactive conformation of Src are weak due to the relatively low affinity of the SH2 domain for the phosphorylated Y530 in the negative-regulatory tail [119, 120]. This is because the SH2 recognition sequence adjacent to Y530 (pYQPG) lacks an isoleucine residue, or indeed any hydrophobic residue, in the +3 position which would normally locate to the hydrophobic pocket of the SH2 domain to ensure a tight association (see section 1.5.2). Moreover, the low affinity for Y530 is compounded by the proline residue in the +2 position which results in a sharp bend in the secondary structure of this sequence, thus hindering binding further [120].

A number of well-established Src substrates which contain the optimal SH2 recognition sequence for Src have been identified [131], and these include FAK (pYAEI) [96], EGFR (pYDGI) [120] and the ER (pYDLL) [40]. As such, these proteins are able to bind to the SH2 domain of Src with high affinity, thus displacing the phosphorylated Y530 residue and activating Src in the process. Once the negative-regulatory tail has been displaced, the Y530 residue may undergo enzymatic de-phosphorylation to prevent re-association

[96]. This mode of Src activation is particularly important as it enables Src to directly associate with potential substrates [100]. Interestingly, interactions between the SH3 domain of Src and the proline-rich sequences of its target proteins may also induce a conformational change to promote Src activation, but this mechanism is far less common [100].

1.5.3.3 Alternative mechanisms of Src regulation

A number of cancers are caused either by activating mutations in proto-oncogenes, such as $p21^{RAS}$, or by inactivating mutations in tumour suppressor genes, such as p53 [132]. However, evidence of activating mutations in Src is limited, with only one naturally occurring example reported [133]. This activating mutation, which was identified in a sub-set of colon cancer liver metastases and advanced colon cancer primary lesions, resulted in a premature stop codon at codon 531 which produced a truncated form of the Src protein when expressed. This mutant Src lacks a functional C-terminal negative-regulatory tail and results in the constitutive activation of the kinase domain, thus accounting for the increased activity of Src in the tissues analysed. However, attempts to confirm these findings have so far failed [134-137], suggesting that activating mutations of Src in cancer are rare.

A number of additional mechanisms of Src regulation have also been proposed. For example, on-going work at the Tenovus Centre for Cancer Research has suggested Src may be aberrantly activated following increases in intra-cellular levels of zinc, which can be caused by the over-expression of zinc-transporter proteins found in the plasma-membrane of the cell [138]. One possible explanation for this could involve the ability of zinc to act as an inhibitor of phosphatase enzymes such as PTP1B [139]; thus, elevated levels of zinc could lead to the accumulation of tyrosine-phosphorylated proteins in the cell, some of which may be able to bind to Src via interactions with the SH2 domain and promote Src activation. Data from our laboratory shows that the zinc-dependent activation of Src may result in increased activation of EGFR signalling pathways, (K.M. Taylor, unpublished), and this has also been reported by others [140, 141].

In some cancers, increased Src activity is associated with an increase in total Src protein levels [105]. Therefore, a further mechanism for the up-regulation of Src activity may involve aberrations in the degradation pathways responsible for the down-regulation of activated Src kinase. Reports demonstrate that Src may be poly-ubiquitinated following activation of the kinase domain, thus committing the protein to the proteosome-mediated degradation pathway [142]. However, disruption of either the ubiquitination or degradation mechanisms could result in an accumulation of both total and activated Src protein in the cell. Therefore, these pathways may be of importance in the development and/or progression of cancer.

1.5.4 The Role of Src in Cancer

The over-expression and/or up-regulated activity of Src has been reported in many cancers compared to normal tissue [101-103], including breast [105], colorectal [106], pancreatic [107] and ovarian [108]. The role of Src in normal tissue is unclear at present, but Src activity has been linked to both foetal development and wound healing. However, the de-regulation of Src activity in cancer would appear to have more significant consequences, and can correlate with disease progression and a poor patient prognosis [106, 109].

In cancer, Src is able to potentiate tumour cell growth by augmenting signalling pathways that emanate from membrane-localised receptors, such as the growth-factor [143-145] or steroid-hormone receptors [35, 146]. Furthermore, Src has been shown to be important for cell-cycle progression from G1 to S-phase via the simultaneous up-regulation of both cyclin D1 expression [147] and $p27^{Kip1}$ proteolysis [148]; and also, for the progression of the cell cycle through M-phase following association with and phosphorylation of a nuclear protein named SAM68 [100, 149]. Despite this evidence, however, a consistent role for Src in tumour growth remains elusive; with some investigators showing no effect on cell growth following the modulation of Src activity [150, 151], whilst others have shown modest growth inhibition following pharmacological and molecular abrogation of Src activity [152, 153]. Indeed, *in vivo* animal studies frequently demonstrate reduced tumour

volume following treatment with Src inhibitors, thus supporting a role for Src in cell proliferation [154-157]. Moreover, in addition to potentiating growth, Src can also augment signalling pathways that promote cell survival. For example, Src is able to phosphorylate the p85 subunit of PI3K to activate this protein, leading to the downstream activation of Akt which can then initiate a number of anti-apoptotic mechanisms to prevent cell death [158, 159].

However, the characteristic most often associated with elevated Src activity in cancer is the progression to metastatic disease [160-162]. Src can increase the metastatic potential of a tumour, and therefore increase the likelihood of tumour spread, by de-regulating cell-cell and cell-matrix attachment to promote cell motility and invasion [97]. The elucidation of the mechanisms which underlie this is of vast importance, as approximately 90% of all cancer related deaths can be attributed to tumour metastasis [132, 163].

Cell-cell attachment is mediated via adherens junctions, which are homotypic calcium-dependent interactions that form between the extra-cellular domains of cadherin molecules on adjoining cells [97]. In epithelia, these adhesions are mediated by E-cadherin, which is linked to the actin cytoskeleton of the cell via α- and β-catenin [97]. The loss of cell-cell adhesions is a prerequisite for the promotion of a motile and invasive phenotype, allowing the dissemination of single cells from the tumour [164]; and this process can be regulated by Src in a number of ways. For example, it has been suggested that the localisation of β-catenin at adherens junctions is dependent on its phosphorylation status [165]. As such, Src is able to phosphorylate β-catenin, causing its dissociation from the E-cadherin complex and thus reducing the integrity of cell-cell contacts in the process. Furthermore, Src can regulate cell-cell attachment by controlling the number of available E-cadherin molecules on the cell surface. Studies have shown that the phosphorylation of E-cadherin by Src leads to the poly-ubiquitination and subsequent endocytic internalisation of E-cadherin, and this can result in increased cell motility [166].

Cell-matrix attachment, on the other hand, is mediated through the formation of focal contacts, which are large, integrin-dependent protein complexes that

link the actin cytoskeleton of the cell to the extra-cellular matrix (ECM) [97]. Focal contacts can exist between the main body of the cell and the ECM (focal adhesions), or in cellular protrusions known as lamellipodia and filopodia (focal complexes); focal adhesions are usually larger, more stable structures, while focal complexes can be fairly small in size and of a more transient nature [167]. Focal adhesions are highly complex in both nature and regulation, and can comprise over 50 different proteins [97]. Some of these proteins, such as FAK, not only provide structural and mechanical support for the focal adhesion, but can also facilitate integrin signalling to incite a number of cellular responses including cell motility and invasion [168, 169].

Integrin mediated motility involves the formation of new focal contacts at the leading edge of the cell, along with the simultaneous detachment of focal contacts at the trailing edge; a process known as focal adhesion turnover [170]. The regulation of focal adhesion turnover is mediated by a Src/FAK signalling complex which forms following the auto-phosphorylation of FAK at Y397, a high affinity Src SH2-binding site [167]. This enables the now active Src to phosphorylate FAK on a number of additional sites (Y576, Y577, Y861 and Y925) to further enhance the activity of the Src/FAK complex [171, 172]. Src/FAK localises to focal contacts, where it recruits and phosphorylates numerous additional cytosolic proteins, such as paxillin and $p130^{CAS}$, to both strengthen the attachment and to initiate the various signalling cascades involved in integrin signalling [97]. One such cascade leads to the activation of the Rho-family of GTPase proteins which can regulate the production and rearrangement of actin stress fibres [173, 174]. Rho-dependent re-modelling of the actin cytoskeleton in this way not only enhances existing focal contacts at the leading edge of the cell, but also generates the contractile forces required for cell motility and spreading [168, 173].

The mechanisms of focal adhesion disassembly at the trailing edge of the motile cell are less well known, but one possibility may involve the binding of Grb2 to FAK following the Src-dependent phosphorylation of FAK at Y925 [175]. This binding initiates the sos-raf-MEK signalling pathway which cul-

minates in the ERK 2-dependent activation of Calpain-2 [168, 176]; a protease which has been shown to degrade a number of focal adhesion associated proteins, including FAK and Talin, thus resulting in the disassembly of the focal adhesion complex [170, 176]. This mechanism is particularly interesting as it may potentially be augmented by EGFR signalling [170].

In addition to increased motility, the up-regulation of Src activity in cancer also promotes an invasive phenotype [97]. As already discussed, the Src-mediated disruption of cell-cell and cell-matrix attachments leads to enhanced cell motility, which is a necessary requirement for cell invasion. In addition, Src can promote invasion by up-regulating the expression of matrix-metallo-proteases (MMP), enzymes that are able to digest components of the ECM. The localisation of Src/FAK to focal adhesions leads to the subsequent recruitment and phosphorylation of $p130^{CAS}$; this results in the increased activation of JNK via the Crk-Dock180-Rac pathway, which then translocates to the nucleus where it promotes the expression of MMP 2 and 9 [177]. The increased expression and secretion of these MMP proteins results in the degradation of the extracellular matrix, thus enabling the cell to pass through the basal membrane and invade into the surrounding area [177].

Therefore, the evidence suggests that Src may play a crucial role in the regulation of many cellular events important for the progression of cancer; however, a complete understanding of the mechanisms which underlie the involvement of Src in these events has not yet been achieved. Thus, Src remains an important subject for continued investigation in order to fully appreciate its potential as a future therapeutic target in the clinical management of cancer.

1.6 Aims

Preliminary experiments conducted on our cell model of ER-positive tamoxifen-resistant breast cancer (Tam-R) have suggested that these cells may possess an aggressive cell-phenotype *in vitro*. The increased activation of growth-factor receptors such as EGFR, which has been demonstrated in the Tam-R cells [70], is associated with an aggressive cell-phenotype and a poor prognosis in the clinic [178, 179]; however, inhibition of EGFR signalling in the Tam-R cell-line using gefitinib (Iressa™) had only a modest effect on the aggressive behaviour of these cells [180]. Thus, additional cell-signalling mechanisms must be involved in mediating this phenotype.

Given that Src activity is often increased in aggressive tumours, in addition to its established role as a promoter of cell migration and invasion, this thesis therefore investigates the hypothesis that elevated Src kinase activity is responsible for the increased aggressive cell-phenotype exhibited by the Tam-R cells *in vitro*. In order to test this hypothesis, the present study aims to:

- fully characterise the MCF7wt and Tam-R cells with respect to their *in vitro* aggressive behaviour, including an assessment of their morphology, growth rate and affinity for extracellular-matrix components, in addition to their migratory and invasive capabilities.
- characterise MCF7wt and Tam-R cells for the expression and activation of the non-receptor tyrosine kinase Src, in addition to the activation of signalling pathways which Src is known to regulate.
- inhibit Src activity in Tam-R cells using a pharmacological agent and to assess these cells for any phenotypic changes that occur as a result in order to determine a role for Src in the regulation of their aggressive phenotype.
- use molecular-based techniques to generate a stably transfected cell-line that expresses a constitutively-active Src mutant. The *in vitro* behaviour of this stably transfected cell-line will then be characterised in order to ascertain whether increased Src kinase activity is sufficient for the acquisition and maintenance of an aggressive phenotype in these cells.

Chapter Two

Materials and Methods

"We vivisect the nightingale to probe the secret of his note."

T.B. Aldrich (1836-1907). US Writer and Editor.

2 Materials and Methods

2.1 Materials

A list of the materials used throughout this study, along with the companies from which they were obtained, is given in Table 2.1.

Table 2.1 List of materials used in the study and their suppliers

Material	*Company*
3-(4,5-dimethylthiazol-2-yl)-2,5-diphenyl-tetrazolium bromide (MTT)	Sigma-Aldrich, Poole, Dorset, UK
Acrylamide/bis-acrylamide (30% solution (v/v), 29:1 ratio)	Sigma-Aldrich, Poole, Dorset, UK
Activated charcoal	Sigma-Aldrich, Poole, Dorset, UK
Agarose	Bioline Ltd, London, UK
Ammonium persulphate (APS)	Sigma-Aldrich, Poole, Dorset, UK
Amphotericin B (Fungizone)	Invitrogen, Paisley, UK
Ampicillin	Sigma-Aldrich, Poole, Dorset, UK
Antibiotics (penicillin/streptomycin)	Invitrogen, Paisley, UK
Anti-mouse horseradish-peroxidase-linked IgG (source: sheep)	Amersham, Little Chalfont, UK
Anti-rabbit horseradish-peroxidase-linked IgG (source: donkey)	Amersham, Little Chalfont, UK
Anti-rabbit/Anti-mouse EnVision™+ System, Peroxidase (DAB) kits	DAKO, Cambridgeshire, UK
Aprotinin	Sigma-Aldrich, Poole, Dorset, UK
Bio-Rad D_C Protein Assay (Reagents A, B and S)	Bio-Rad Laboratories Ltd, HERTS, UK
Bovine serum albumen (BSA)	Sigma-Aldrich, Poole, Dorset, UK
Bromophenol blue (BPB)	BDH Chemicals Ltd, Poole, UK
Cell culture medium: RPMI 1640 and Phenol-red-free RPMI 1640	Invitrogen, Paisley, UK
Cell culture medium: Phenol-red-free DCCM	Biological Industries Ltd, Israel
Cell scrapers	Greiner Bio-One Ltd, Gloucestershire, UK
Chemilluminescent Supersignal® West HRP Substrate (Pico, Dura and Femto)	Pierce and Warriner Ltd, Cheshire, UK
Corning Standard Transwell® inserts (6.5mm diameter, 8μm pore size)	Fisher Scientific, Leicestershire, UK
Coulter Counter counting cups and lids	Sarstedt AG and Co., Nümbrecht, Germany

Cryotube™ vials (1.8ml, starfoot, round)	Nunc Int., Roskilde, Denmark
Crystal violet	Sigma-Aldrich, Poole, Dorset, UK
Dextran 70	Amersham, Little Chalfont, UK
Di-butylpthalatexylene (DPX)	Raymond A Lamb Ltd, Eastbourne, UK
Dimethyl sulphoxide (DMSO)	Sigma-Aldrich, Poole, Dorset, UK
Di-potassium hydrogen orthophosphate anhydrous (K_2HPO_4)	Fisher Scientific UK Ltd, Loughborough, UK
Disposable Cuvettes	Fisher Scientific UK Ltd, Loughborough, UK
Di-thiothreitol (DTT)	Sigma-Aldrich, Poole, Dorset, UK
dNTPs (dGTP, dCTP, dATP, dTTP; 100mM)	Amersham, Little Chalfont, UK
DyNAmo qPCR kit	Finnzymes Oy, Espoo, Finland
EcoR1 restriction enzyme (and buffer)	Promega, Southampton, UK
Ethidium bromide (EtBr)	Sigma-Aldrich, Poole, Dorset, UK
Ethylene diamine tetraacetic acid (EDTA)	Sigma-Aldrich, Poole, Dorset, UK
Ethylene glycol-bis(2-amino-ethylether)-N,N,N',N'-tetraacetic acid (EGTA)	Sigma-Aldrich, Poole, Dorset, UK
Fibronectin (from Human Plasma; 1mg/ml in 0.05M TBS; pH 7.5)	Sigma-Aldrich, Poole, Dorset, UK
Filter paper (Grade 3)	Whatman, Maidstone, UK
Filter Paper (No. 4)	Whatman, Maidstone, UK
Foetal calf serum (FCS)	Invitrogen, Paisley, UK
Gelatine	Sigma-Aldrich, Poole, UK
General laboratory glass- and plasticware	Fisher Scientific UK Ltd, Loughborough, UK
Geneticin (G418)	Sigma-Aldrich, Poole, UK
Glacial Acetic Acid	Fisher Scientific UK Ltd, Loughborough, UK
Glass coverslips (thickness no. 2, 22mm^2)	BDH Chemicals Ltd, Poole, Dorset, UK
Glass slides	Fisher Scientific UK Ltd, Loughborough, UK
Glycerol	Fisher Scientific UK Ltd, Loughborough, UK
Glycine	Sigma-Aldrich, Poole, Dorset, UK
Hydrochloric acid (HCl; 5M)	Fisher Scientific UK Ltd, Loughborough, UK
Hyperladder™ I and Hyperladder™ IV	Bioline Ltd, London, UK
Isoton® II azide-free balanced electrolyte solution (see section 8.1.6 for constitution)	Beckman Coulter Ltd, High Wycombe, UK
Kodak MXB Autoradiography film (blue sensitive; 18 cm x 24 cm)	Genetic Research Instrumentation (GRI), Rayne, UK
LB-Agar EZMix™ powder	Sigma-Aldrich, Poole, Dorset, UK
LB-Broth EZMix™ powder	Sigma-Aldrich, Poole, Dorset, UK
Leupeptin	Sigma-Aldrich, Poole, Dorset, UK

L-glutamine	Invitrogen, Paisley, UK
Lipofectamine 2000™	Invitrogen, Paisley, UK
Liquid DAB$^+$ substrate chromogen system	DAKO, Cambridgeshire, UK
Lower buffer for SDS-PAGE Gels (Tris 1.5M, pH 8.8)	Bio-Rad Laboratories Ltd, HERTS, UK
Magnesium chloride ($MgCl_2$)	Sigma-Aldrich, Poole, Dorset, UK
Matrigel™ Basement Membrane Matrix	BD Biosciences, Oxford, UK
Methyl green	Sigma-Aldrich, Poole, Dorset, UK
Micro-centrifuge tubes (0.5ml and 1.5ml)	Elkay Laboratory Products, Basingstoke, UK
Molony-murine leukaemia virus (MMLV) reverse transcriptase	Invitrogen, Paisley, UK
N,N,N',N'-tetramethylene-diamine (TEMED)	Sigma-Aldrich, Poole, Dorset, UK
Nalgene® Supor® Mach V Bottle Top Filter unit (0.2μm)	Fisher Scientific UK Ltd, Loughborough, UK
Nitrocellulose transfer membrane (Protran® BA85; 0.45μm pore size)	Schleicher and Schuell, Dassell, Germany
pH calibration buffer tablets (pH 4, 7 and 10)	Fisher Scientific UK Ltd, Loughborough, UK
Phenylarsine oxide	Sigma-Aldrich, Poole, Dorset, UK
Phenylmethylsulfonyl fluoride (PMSF)	Sigma-Aldrich, Poole, Dorset, UK
Pipette tips	Greiner Bio-One Ltd, Gloucestershire, UK
Polyoxyethylene-sorbitan monolaurate (Tween 20)	Sigma-Aldrich, Poole, Dorset, UK
Ponceau S solution (0.1% [w/v] in 5% acetic acid)	Sigma-Aldrich, Poole, Dorset, UK
Potassium chloride (KCl)	Sigma-Aldrich, Poole, Dorset, UK
Potassium di-hydrogen orthophosphate (KH_2PO_4)	Fisher Scientific UK Ltd, Loughborough, UK
Precision Plus Protein™ All Blue Standards (10-250kDa)	Bio-Rad Laboratories Ltd, HERTS, UK
Random hexamers (RH)	Amersham, Little Chalfont, UK
RNase-free H_2O	Sigma-Aldrich, Poole, Dorset, UK
RNasin® ribonuclease inhibitor	Promega, Southampton, UK
SOC Medium	Sigma-Aldrich, Poole, Dorset, UK
Sodium azide	Sigma-Aldrich, Poole, Dorset, UK
Sodium chloride (NaCl)	Sigma-Aldrich, Poole, Dorset, UK
Sodium dodecyl sulphate (SDS)	Sigma-Aldrich, Poole, Dorset, UK
Sodium fluoride (NaF)	Sigma-Aldrich, Poole, Dorset, UK
Sodium hydroxide (NaOH; 5M)	Fisher Scientific UK Ltd, Loughborough, UK

Sodium molybdate (Na_2MoO_4)	Sigma-Aldrich, Poole, Dorset, UK
Sodium orthovanadate ($NaVO_4$)	Sigma-Aldrich, Poole, Dorset, UK
Solvents (acetone, chloroform, ethanol, formaldehyde, isopropanol and methanol)	Fisher Scientific UK Ltd, Loughborough, UK
Sterile bijou vials (5ml)	Bibby Sterilin Ltd, Stone, UK
Sterile cell culture plasticware (i.e. flasks, Petri-dishes, 12-, 24- and 96-well plates)	Nunc Int., Roskilde, Denmark
Sterile Falcon tubes (15ml and 50ml)	Sarstedt AG and Co., Nümbrecht, Germany
Sterile phosphate buffered saline (PBS)	Invitrogen, Paisley, UK
Sterile syringe filters (0.2µm)	Corning Inc., Corning, NY, USA
Sterile syringe needles (BD Microbalance™ 3; 25G x 5/8")	Becton Dickinson (BD) UK Ltd, Oxford, UK
Sterile syringe needles (Sherwood Medical Monoject; 21G x 1½")	Sherwood - Davis & Geck, Gosport, Hampshire, UK
Sterile syringes (BD Plastipak™; 1ml, 5ml and 10ml)	Becton Dickinson (BD) UK Ltd, Oxford, UK
Sterile universal containers (30ml)	Greiner Bio-One Ltd, Gloucestershire, UK
Sterile, disposable serological pipettes (5ml, 10ml and 25ml)	Sarstedt AG and Co., Nümbrecht, Germany
Sucrose	Fisher Scientific UK Ltd, Loughborough, UK
Taq DNA polymerase (BioTaq™; 5U/µl)	Bioline Ltd, London, UK
Tris HCl	Sigma-Aldrich, Poole, Dorset, UK
Triton X-100	Sigma-Aldrich, Poole, Dorset, UK
Trizma (Tris) base	Sigma-Aldrich, Poole, Dorset, UK
Trypsin/EDTA 10x Solution	Invitrogen, Paisley, UK
Upper buffer for SDS-PAGE Gels (Tris 0.5M, pH 6.8)	Bio-Rad Laboratories Ltd, HERTS, UK
VectorShield® hard-set mounting medium containing DAPI nuclear stain	Vector Laboratories, Inc., Peterborough, UK
Virkon	Antec International Ltd, Suffolk, UK
Vybrant® Apoptosis Assay Kit #4	Invitrogen, Paisley, UK
Western Blocking Reagent	Roche Diagnostics, Mannheim, Germany
X-ray film developer solution (X-O-dev)	X-O-graph Imaging System, Tetbury, UK
X-ray film fixative solution (X-O-fix)	X-O-graph Imaging System, Tetbury, UK

2.2 Cell Culture

2.2.1 Cell-lines

The hormone-sensitive MCF7 wild-type cell-line (MCF7wt) was a kind gift from AstraZeneca Pharmaceuticals (Macclesfield, Cheshire, UK), and was originally obtained from the American Type Culture Collection (ATCC® Number HTB-22™). These cells were routinely maintained in RPMI 1640 containing phenol-red pH indicator (rRPMI) supplemented with 5% (v/v) foetal calf serum (FCS), antibiotics (penicillin 100units/ml and streptomycin 100μg/ml), and an antifungal agent (amphotericin B; 2.5μg/ml). This medium will be referred to as R+5%.

Prior to any experimental work MCF7wt cells were washed three times with Dulbecco's phosphate-buffered saline (PBS) and cultured for 24 hours in phenol-red-free RPMI 1640 (wRPMI) supplemented with 5% (v/v) charcoal-stripped foetal calf serum (SFCS), L-glutamine (200mM) and antibiotic/anti-fungal agents (as above). This was to remove any exogenous oestrogenic effects from either the phenol-red pH indicator in the media or from steroidal hormones present in the serum. This medium will be referred to as W+5%. The charcoal-stripping procedure used to remove steroidal hormones from FCS can be found in appendix 1 (section 8.1.2).

The tamoxifen-resistant MCF7 cell-line (Tam-R) was generated in-house following the long-term culture of MCF7wt cells in W+5% supplemented with 4-hydroxytamoxifen (Tam; 100nM final concentration) [70]. After an initial period of growth inhibition (approximately 2-3 months) outgrowths of resistant cells occurred. These cells were maintained and, when necessary, passaged for a further 3 months until the resistant cell-line was established and could be characterised. Tam-R cells were routinely maintained in W+5% supplemented with 4-hydroxytamoxifen (100nM).

2.2.2 Cell Culture Techniques

All cell-culture was carried out under sterile conditions in a MDH Class II laminar-flow safety cabinet (BIOQUELL UK Ltd, Andover, UK). All

equipment and consumables were either purchased sterile for single use or were sterilized at 119°C using a Denley BA852 autoclave (Thermoquest Ltd, Basingstoke, UK).

Cells were maintained in 75cm^2 flasks (T-75) and grown in a Sanyo MCO-17AIC incubator (Sanyo E&E Europe BV, Loughborough, UK) at 37°C with a humidified atmosphere containing 5% CO_2. The culture medium was changed every 3-4 days. Cells were visually assessed using a Nikon Eclipse TE200 phase-contrast microscope (Nikon UK Ltd, Kingston-upon-Thames, UK) and passaged upon reaching 80-100% confluency (typically once a week).

For routine passaging, medium was removed and cell monolayers dispersed following the addition of 10ml of trypsin (0.05%)/EDTA (0.02%) in PBS (see appendix 1 [section 8.1.3]). The flasks were returned to the incubator for 3-5 minutes until the cells were in suspension. Trypsin/EDTA was neutralised with an equal volume of serum-containing medium (R+5% or W+5%, depending on cell-line) and the cells were pelleted by centrifugation (Jouan C312 [Thermo Fisher Scientific Inc., MA, USA]; 1000rpm, 5 min). The cell pellet was re-suspended in the appropriate medium (1ml) and mixed gently using a pipette until no cell clumps were evident. A proportion of this cell suspension was diluted in the appropriate medium and used to seed additional T-75 flasks (typically 1/10th of the cell suspension in 15ml of medium per flask), which were then cultured as normal. Cell-lines were passaged up to a maximum of 25 times or cultured for approximately 3 months, whichever was sooner. To ensure an adequate supply of cellular material, stocks of established cell-lines were generated by freezing down cells with a low passage number in liquid nitrogen (see appendix 1 [section 8.1.4.1]). When required, cells were raised from frozen using the method out-lined in section 8.1.4.2.

To seed cells for experimental analysis, cell monolayers were washed twice with PBS prior to trypsin/EDTA dispersion, centrifugation and re-suspension as above. The cells were then passed through a sterile 25G syringe needle to obtain a single-cell suspension. A 50µl aliquot of this suspension was added to Isoton® II solution (10ml) and cell number was determined using a

Coulter™ Multisizer II (Beckman Coulter UK Ltd, High Wycombe, UK). Cells were then seeded in the appropriate medium at a density dictated by the experimental design. For a comprehensive list of cell seeding densities see appendix 1 (section 8.1.5).

2.2.3 Treatments

During the course of this study cells were treated with various compounds including anti-hormones, growth-factors and inhibitors (see Table 2.2). Where stated, cells were serum starved in phenol-red-free DCCM containing L-glutamine and antibiotic/anti-fungal agents (as above) for 24 hours prior to treatment (wDCCM; see appendix 1 [section 8.1.1]). Detailed information regarding the concentration and duration of treatments used for particular experiments can be found in the relevant results chapters.

2.3 Gene Expression Analysis

Gene expression in MCF7wt and Tam-R cell-lines was investigated using both semi-quantitative reverse transcription-polymerase chain reaction (RT-PCR) [181, 182] and Real-Time (quantitative) PCR (qPCR) [183]. For both procedures, RNA and DNA were prepared as follows.

2.3.1 RNA Extraction

Cells in W+5% ± Tam (100nM) were seeded into 100mm Petri-dishes at a density of $1x10^6$ cells per dish and cultured until they had reached log-phase growth (~60% confluency). Total RNA was then extracted using a QIAGEN RNeasy mini kit (QIAGEN Ltd, Crawley, UK) following the manufacturer's instructions and using buffers and solutions supplied with the kit.

Briefly, cell culture medium was removed and the cells lysed in RLT buffer (600µl). Cellular material was then collected using a cell scraper and transferred to a 1.5ml micro-centrifuge tube for subsequent homogenisation by passing through a 21G syringe needle 5 times. Ethanol (70% v/v in H_2O; 1 volume) was added to the lysate and mixed thoroughly by pipetting. The sample was then transferred to an RNeasy spin column fitted with a collection

Table 2.2 Treatments used in cell culture experiments

Treatment	*Classification*	*Target Protein*	*Final Concentration Routinely Used*	*Vehicle*	*Company*
4-hydroxytamoxifen	Anti-hormone	ER	100nM	EtOH	Sigma-Aldrich, Poole, Dorset, UK
AG1024	Inhibitor	IGF-1R	5μM	DMSO	Calbiochem, Nottingham, UK
Amphiregulin	Growth factor	EGFR	10ng/ml	PBS	Sigma-Aldrich, Poole, Dorset, UK
AZM 555130	Inhibitor	Src	1μM	DMSO	AstraZeneca Pharmaceuticals, Cheshire, UK
EGF	Growth factor	EGFR	10ng/ml	PBS	Sigma-Aldrich, Poole, Dorset, UK
Fulvestrant (Faslodex™)	Anti-hormone	ER	100nM	EtOH	AstraZeneca Pharmaceuticals, Cheshire, UK
Gefitinib (Iressa™)	Inhibitor	EGFR	1μM	DMSO	AstraZeneca Pharmaceuticals, Cheshire, UK
Herceptin	Inhibitor	c-erbB2	100nM	H_2O	Roche, Basel, Switzerland
Heregulin-β	Growth factor	c-erbB2	10ng/ml	PBS	Sigma-Aldrich, Poole, Dorset, UK
IGF II	Growth Factor	IGF-1R	10ng/ml	PBS	Sigma-Aldrich, Poole, Dorset, UK
PD098059	Inhibitor	MEK	50μM	DMSO	Alexis Corporation Ltd, Nottingham, UK
SU6656	Inhibitor	Src	1-5μM	DMSO	Calbiochem, Nottingham, UK
TGFα	Growth factor	EGFR	10ng/ml	PBS	Sigma-Aldrich, Poole, Dorset, UK

tube and centrifuged (Labofuge 400R; Heraeus, Hanau, Germany) at 10,000rpm for 15 seconds. Since the maximum volume of an RNeasy spin column is 700µl the sample was passed through the column in two stages.

The flow-through was discarded and the column washed once with RW1 buffer (700µl) and once with RPE buffer (500µl). Following each wash the columns were centrifuged as above and the flow-through discarded. The RPE buffer wash was repeated and the column centrifuged at 10,000rpm for 2 minutes. The flow-through was discarded and the column re-centrifuged (10,000rpm; 1 minute) to remove all traces of RPE buffer. The RNA was then eluted from the column into a fresh RNase-free 1.5ml micro-centrifuge tube with RNase-free H_2O (2 x 30µl) and stored at -80°C.

2.3.2 RNA Quantitation

RNA concentration was determined by measuring the optical density (OD) of a 1:100 dilution of the column eluate obtained above in RNase-free H_2O at wavelengths of 260nm and 280nm. The ratio between the two OD values gives a measure of the purity of the RNA, with a ratio of 1.9-2.1 representing a pure RNA solution. The OD_{260} value is substituted into the following formula to give the RNA concentration in µg/ml.

$$[RNA] = OD_{260} \times 40 \times \text{Dilution Factor}$$

2.3.3 Reverse Transcription (RT)

RNA was reverse transcribed to generate complementary DNA (cDNA) using the Molony-murine leukaemia virus (MMLV) reverse transcriptase enzyme.

The RT reaction mixture comprised (per sample) 1µg of total RNA (made up to 7.5µl with RNase-free H_2O), 5µl dNTP mix (0.625mM each of dGTP, dCTP, dATP and dTTP), 2µl PCR Buffer (10x; see section 8.2.1.1), 2µl di-thiothreitol (DTT; 0.1M) and 2µl random hexamer oligonucleotides (100µM). The reaction mix was heated in a PTC-100 thermocycler (MJ Research Ltd, Massachusetts, USA) to 95°C for 5 minutes to denature the RNA, followed by rapid cooling on ice.

1µl MMLV-reverse transcriptase enzyme (200U/µl) and 0.5µl RNasin™ RNase inhibitor (40U/µl) were added to the reaction mixture to give a final volume of 20µl. The reaction was run in the PTC-100 thermocycler using the temperature cycling conditions detailed in table 2.3 and the resultant cDNA was stored at -20°C.

Table 2.3 Thermocycler program conditions for the reverse transcription of RNA

Step	*Temperature*	*Duration*
1 (Annealing)	22°C	10 minutes
2 (Extension)	42°C	42 minutes
3 (Denaturing)	95°C	5 minutes

2.3.4 Polymerase Chain Reaction (PCR)

All PCR reaction mixes were set up in a Labconco Purifier PCR Enclosure (GRI, Rayne, UK) using sterile pipette tips and reaction tubes. All equipment and work surfaces were wiped with 70% ethanol and allowed to air-dry prior to the commencement of work.

2.3.4.1 Reaction Mixtures and Thermocycling Conditions

Since the present study is concerned with Src expression PCR was optimised for the detection of Src as follows. A reaction mixture for the amplification of the Src gene consisted of 2.5µl PCR buffer (10x; see section 8.2.1.1), 2µl dNTP mix (0.625mM each of dGTP, dCTP, dATP and dTTP), 0.6µl Src forward primer (20mM), 0.6µl Src reverse primer (20mM), 0.1µl Taq polymerase (5U/µl) and 0.5µl cDNA, with the final volume made up to 25µl with sterile H_2O. The sequences for the Src primers used can be found in table 2.4 [184]. A negative control in which cDNA was substituted with an equal volume of sterile H_2O was also run for each experiment.

The reaction tubes were mixed gently, pulsed in a micro-centrifuge (IEC Micromax RF, Thermo Electron Corporation, Hampshire, UK) and placed in

Table 2.4 Primer sequences used for the PCR amplification of Src and β-actin genes

Gene		*Primer Sequence*	*Amplicon Size (bp)*
Src	Forward	5'-CAGTGTCTGACTTCGACAAC-3'	433
	Reverse	3'-CTCCTCTGAAACCACAGCAT-5'	
β-actin	Forward	5'-GGAGCAATGATCTTGATCTT-3'	204
	Reverse	3'-CCTTCCTGGGCATGGAGTCCT-5'	

a PTC-100 thermocycler with the heated lid set to 100°C. The PCR reaction was then run using the temperature cycling conditions stated in table 2.5.

PCR data was normalised using amplification of the β-actin housekeeping gene. The PCR reaction mix and thermocycling conditions for the amplification of β-actin were similar to those for Src. However, due to the increased abundance of β-actin the volume of the β-actin primers used was decreased to 0.3µl (with a corresponding increase in H_2O of 0.6µl) to avoid premature saturation of the PCR reaction system

Table 2.5 Thermocycler program conditions for PCR amplification of Src and β-actin

	Step	*Temperature*	*Duration*	*Cycle Number*
1	(Denaturing)	95°C	5 minutes	x 1
2	(Denaturing)	95°C	60 seconds	x 33 (Src) x 27 (β-actin)
	(Annealing)	55°C	30 seconds	
	(Extension)	72°C	90 seconds	
3	(Final Extension)	72°C	10 minutes	x 1
4	(Short-term storage)	4°C	∞	

2.3.4.2 Agarose Gel Electrophoresis

Samples were resolved using a 1% (w/v) agarose gel in Tris-Acetate-EDTA buffer (TAE; see section 8.2.1.2) containing ethidium bromide (1µl of a 10mg/ml solution per 50ml gel solution). Gels were cast and run using the

Sub-cell® Agarose Electrophoresis System connected to a Powerpac 1000 power pack (both Bio-Rad Laboratories Ltd, HERTS, UK) following the manufacturer's instructions.

PCR products for Src and β-actin (7.5μl of each) were added to sample loading buffer (10μl; see section 8.2.1.3) and dispensed into the wells of the gel, along with a DNA size marker (Hyperladder™ IV 100-1000bp; 5μl). TAE buffer was added to the electrophoresis tank and the gel was run at 70V constant voltage for approximately 45-60 minutes. Gels were visualised under UV light using a FOTODYNE 3-3002 UV trans-illuminator and photographed with a Polaroid GelCam camera (both GRI, Rayne, UK) for densitometry. The images were scanned using a Bio-Rad GS-690 Imaging Densitometer (Bio-Rad Laboratories Ltd, HERTS, UK) connected to a computer running Molecular Analyst Version 1.5 (also Bio-Rad). Densitometry was measured as 'adjusted volume OD x mm^2'.

2.3.4.3 Optimisation of PCR Thermocycling Conditions

The number of amplification cycles used in step 2 of the thermocycling program was determined empirically for each gene to ensure the reaction did not reach saturation before analysis. PCR amplifications of Src and β-actin using basal MCF7wt cDNA were run using the cycling conditions stated in table 2.5; with step 2 repeated 35 times for both genes. Following each cycle between cycle 25 and 35 a sample tube was removed and put on ice. On completion of the program the samples were resolved on a 1% agarose/ethidium bromide gel as described above. Cycle numbers of 33 and 27 were selected as optimal for the amplification of Src and β-actin genes respectively in this experimental system as there was sufficient amount of product for analysis, but the reaction had not yet reached saturation (see figure 2.1).

2.3.5 Real-Time PCR (qPCR)

Real-time PCR, also known as quantitative PCR (qPCR), is a relatively new technique that enables the accurate quantitation of gene expression levels [183]. qPCR uses fluorescence to measure the amount of DNA material

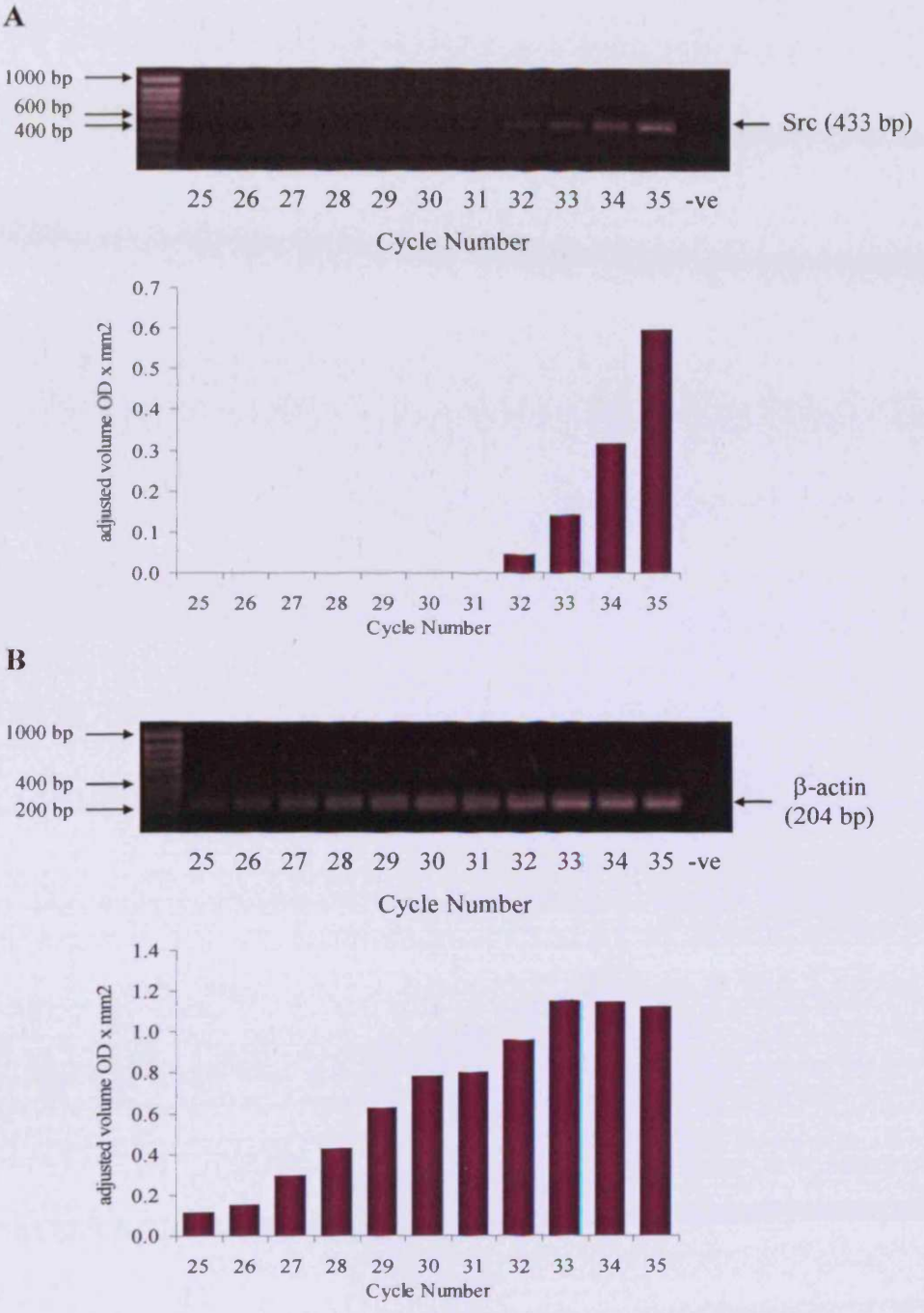

Figure 2.1 Optimisation of PCR thermocycling conditions for Src and β-actin

RNA from MCF7wt cells grown under basal conditions was extracted and reverse transcribed to generate cDNA. The cDNA was subjected to PCR for Src (A) and β-actin (B) genes as described in section 2.3.4.3. Following each amplification cycle between cycle 25 and 35 a sample was removed from the thermocycler and placed on ice. On completion of the thermocycling program the samples were resolved on a 1% agarose/ethidium bromide gel and the bands obtained were analysed using densitometry.

present in a PCR reaction after each temperature cycle and, thus, follows the amplification of a gene in 'real-time' until the system becomes saturated. Following the reaction, the amount of starting template material in an unknown sample can be quantified by comparing its fluorescence at a suitable cycle number to that of a pre-defined standard curve. The present study used the DyNAmo™ qPCR kit (Finnzymes Oy, Espoo, Finland) to confirm the Src gene expression levels obtained in MCF7wt and Tam-R cell-lines with RT-PCR. The DyNAmo™ kit uses SYBR green – an intercalating DNA dye that is only fluorescent when bound to double-stranded DNA. SYBR green is a reliable source of fluorescence for use in qPCR analysis and is much more cost effective than other techniques which utilize specific fluorescently-labelled DNA probes. However, due to its inability to discriminate between different double-stranded DNA fragments it is unsuitable for use in co-amplifications.

The qPCR reaction mixture consisted of 10µl 2x DyNAmo PCR solution (containing buffering solution, dNTP mix, Taq polymerase and SYBR green dye), 0.375µl forward primer (20mM), 0.375µl reverse primer (20mM) and 0.5µl cDNA, made up to a final volume of 20µl with sterile H_2O. Primers used were the same as those used for RT-PCR above. The qPCR reaction was run on an Opticon 2™ real-time PCR machine (MJ Research Ltd, Massachusetts, USA) using the same temperature cycling program as for RT-PCR (table 2.5), but with an increased number of amplification cycles (35-40 cycles). The Opticon 2™ was programmed to read the levels of fluorescence of the samples immediately after each cycle thus ensuring an accurate profile of gene amplification was obtained.

For quantitation, a standard curve was generated in each run using starting template material at a range of known concentrations. This template material was the amplicon produced from an RT-PCR of either Src or β-actin (as appropriate). The amplicon was purified using a QIAquick PCR purification kit following the manufacturer's instructions (QIAGEN Ltd, Crawley, UK) and quantified using a GeneQuant RNA/DNA Calculator (Biochrom Ltd

Cambridge, UK). The template material was serially diluted as required to produce a range of concentrations, which were then run as normal samples.

Using a cycle threshold of 10x the standard deviation of baseline readings between cycles 3-15, the concentrations of starting template material in the unknown samples were extrapolated from the standard curve using Opticon 2™ computer software (OpticonMONITOR™ Version 2.01).

2.4 Analysis of Protein Expression/Activation

Changes in the basal expression and/or activation of proteins between hormone-sensitive and hormone-insensitive cells and in response to various treatments were assessed using SDS-PAGE [185] and Western blotting [186, 187], followed by subsequent immuno-probing of the blots using phospho-specific antibodies where appropriate.

2.4.1 Cell Lysis

Cells were seeded into 60mm or 100mm Petri-dishes at an appropriate density and cultured until they had reached log-phase growth; at which point any treatments being used were added for the required duration. After this time the cells were washed twice with ice-cold PBS and lysed into Triton-X100 lysis buffer containing a cocktail of protease and phosphatase inhibitors (sodium orthovanadate 2mM, phenylmethylsulfonyl fluoride 1mM, sodium fluoride 25mM, sodium molybdate 10mM, phenylarsine 20μM, leupeptin 10μg/ml and aprotinin 8μg/ml). The volume of lysis buffer used was dependent on vessel size and cell confluency, and ranged from 50-250μl. See appendix 2 for more information regarding the lysis buffer (section 8.2.2.1) and inhibitors (section 8.2.2.2).

Cellular material was collected using a cell-scraper and transferred to a 1.5ml micro-centrifuge tube. This lysate was homogenised briefly using a pipette and left on ice for 20 minutes, with further occasional mixing. Cell lysates were then clarified by centrifugation (IEC Micromax RF micro-centrifuge [Thermo Electron Corporation, Hampshire, UK]; 13,000rpm, 15 minutes, 4°C) and the supernatants stored at -20°C until required.

2.4.2 Protein Concentration Assay

The concentration of total soluble protein in cell lysates was determined using the Bio-Rad D_C Protein Assay kit (Bio-Rad Laboratories Ltd, HERTS, UK), a modified version of the Lowry protein assay [188].

The lysates were diluted 1:10 with lysis buffer (as above) to give a final volume of 50µl. To this, 0.25ml of Reagent A (containing 5µl of Reagent S) and 2ml of Reagent B were added. The solutions were vortexed, left for 15 minutes for full colour development and read on a Cecil CE2041 spectrophotometer (Cecil Instruments, Cambridge, UK) at 750nm. These readings were compared with those of a BSA standard curve (0-1.45mg/ml; see appendix 2 [section 8.2.2.3]) to give the concentration of total soluble protein in the lysates.

2.4.3 SDS-PAGE Analysis

Sodium-Dodecyl-Sulphate-Polyacrylamide Gel Electrophoresis (SDS-PAGE) was performed using the Bio-Rad Mini-Protean® III apparatus powered by a Powerpac Basic™ power pack (both Bio-Rad Laboratories Ltd, HERTS, UK) following the manufacturer's instructions. The gel system used was discontinuous, comprising of a 5% (w/v) acrylamide/bis-acrylamide stacking gel at pH 6.8 and an 8-10% (w/v) acrylamide/bis-acrylamide resolving gel at pH 8.8. The recipes for the stacking and resolving gels can be found in tables 2.6 and 2.7 respectively.

Table 2.6 Recipe for the Stacking Gel used in SDS-PAGE

	5% (w/v) For 10ml:	Final Concentration in Gel
Acrylamide/bis-acrylamide solution*	1.65ml	5% (w/v)
H_2O	5.7ml	-
Tris (0.5M, pH 6.8)	2.5ml	125mM
SDS (10% solution in H_2O)	100µl	0.1% (w/v)
APS (10% solution in H_2O)	50µl	0.05% (w/v)
TEMED	20µl	0.2% (v/v)

* Acrylamide used was a 30% solution with an acrylamide:bis-acrylamide ratio of 29:1

Table 2.7 Recipe for the Resolving gel used in SDS-PAGE

	8% Gel (w/v) (70-200 kDa) For 10ml:	10% Gel (w/v) (20-100 kDa) For 10ml:	Final Concentration in Gel
Acrylamide/bis-acrylamide solution*	2.7ml	3.3ml	% as required
H_2O	4.6ml	4.0ml	-
Tris (1.5M, pH 8.8)	2.5ml	2.5ml	375mM
SDS (10% solution in H_2O)	100µl	100µl	0.1% (w/v)
APS (10% solution in H_2O)	100µl	100µl	0.1% (w/v)
TEMED	40µl	40µl	0.4% (v/v)

* Acrylamide used was a 30% solution with an acrylamide:bis-acrylamide ratio of 29:1

A set of glass plates were cleaned with ethanol and assembled in the gel casting apparatus. The constituents of the resolving gel, with the exception of TEMED, were added to a universal container and mixed thoroughly (see table 2.7). TEMED was added to the gel solution immediately before pouring as it catalyses the polymerisation and cross-linking of the acrylamide/bis-acrylamide, causing the gel to set. The gel solution was carefully dispensed between the glass plates until the level reached was approximately 1.5cm below the top of the smaller plate (to allow room for the stacking gel). The gel solution was then overlaid with 0.05% (w/v) SDS in H_2O and allowed to set for approximately 30 minutes at room temperature.

Once set, the SDS solution was discarded and the gel was rinsed with distilled water. The plates were then left to drain; with any excess water remaining between the plates carefully removed using a strip of filter paper. The stacking gel solution was prepared as described in table 2.6 and poured between the glass plates on to the resolving gel. A 10-well comb was inserted into the stacking gel solution and the gel was allowed to set for 45-60 minutes at room temperature. The gel was then placed in the electrophoresis apparatus and SDS-PAGE running buffer (see appendix 2 [section 8.2.2.4]) added to the

inner and outer reservoirs of the tank. The comb was removed from the stacking gel and the resultant wells were washed gently with running buffer.

Cell lysates containing a known amount of total soluble protein (20-150µg) were diluted as appropriate with 3x or 5x Laemmli sample loading buffer [185] (see appendix 2 [section 8.2.2.5]) and heated to 100°C for 5-10 minutes to denature and reduce the proteins in the sample. The cell lysates, along with a protein molecular weight marker (Precision Plus Protein™ All Blue Standards 10-250kDa; 5µl), were loaded into the wells of the stacking gel. Electrophoresis was then performed at 80mA constant current until the sample buffer dye had run the length of the gel (approximately 1 hour).

2.4.4 Western Blotting

Proteins were transferred from SDS-PAGE gels to a nitrocellulose membrane using the Bio-Rad Mini-Protean® III apparatus powered by a Powerpac Basic™ power pack (both Bio-Rad Laboratories Ltd, HERTS, UK).

For each gel to be transferred, two pieces of grade 3 filter paper and one piece of Protran B85 nitrocellulose membrane (0.45µm pore size) were cut to the same size as the gel and pre-soaked, along with two Teflon sponge pads, for at least 30 minutes in Western blot transfer buffer (see appendix 2 [section 8.2.2.6]). Following electrophoresis the gel plates were separated, the stacking gel gently removed and discarded, and the resolving gel carefully transferred to a tray containing distilled H_2O to wash off any excess SDS.

The Western blot transfer cassette was assembled following the manufacturer's instructions as shown in figure 2.2. A serological pipette was drawn across the surface of the assembled 'sandwich' with gentle pressure to ease out any air bubbles that formed between the layers as they can disrupt the transfer of proteins from gel to membrane. The cassette was then placed into the transfer apparatus with the gel (black side of cassette) nearest the negative (black) electrode and the membrane (clear side of cassette) positioned nearest the positive (red) electrode. This ensures the proteins, which are negatively charged after being boiled in the presence of SDS, migrate in the correct

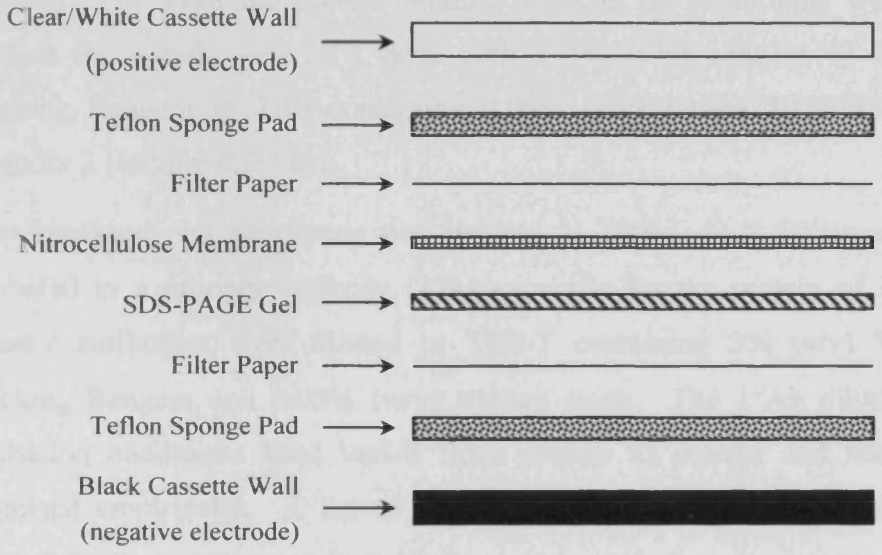

Figure 2.2 Assembly of Western blot transfer cassette

A pre-soaked Teflon sponge pad was put onto the black wall of the transfer cassette, followed by a piece of pre-soaked grade 3 filter paper. The gel was then carefully placed, in the correct orientation, onto the filter paper, avoiding the formation of air bubbles. The gel was covered with transfer buffer to prevent it drying out and the nitrocellulose membrane laid on top, again avoiding air bubbles. Finally, another piece of filter paper and a Teflon sponge pad were put in place before the cassette was closed and inserted into the transfer apparatus.

direction (i.e. from gel to membrane). The transfer apparatus was placed into a tank along with an ice-block to prevent over-heating of the gel during transfer. The tank was then filled with chilled Western blot transfer buffer and the transfer run at 100V constant voltage for 1 hour.

2.4.5 Immunoprobing of Western Blots

The membrane was removed from the transfer cassette and washed twice in Tris buffered saline (TBS; see appendix 2 [section 8.2.2.7]), each time for 5 minutes. The available protein binding sites on the membrane were then blocked for a minimum of 1 hour with a 5% (v/v) solution of Western Blocking Reagent in TBS containing 0.05% (v/v) Tween 20 (TBS-T; see appendix 2 [section 8.2.2.8]).

After blocking, the membrane was washed in TBS-T (2 x 5 minutes) and incubated in a primary antibody (1°Ab) specific for the protein of interest. Primary antibodies were diluted in TBS-T containing 5% (v/v) Western Blocking Reagent and 0.05% (w/v) sodium azide. The 1°Ab dilution and incubation conditions used varied from protein to protein and had to be optimised empirically. A list of the primary antibodies used in this study, along with their corresponding dilutions and incubation conditions, can be found in Table 2.8.

Following 1°Ab incubation the membrane was washed with TBS-T (3 x 10 minutes) and incubated with the appropriate horseradish-peroxidase-linked secondary antibody (2°Ab) diluted in TBS-T containing 5% (v/v) Western blocking reagent. The 2°Ab used was dependent on the source of the 1°Ab, with all 1°Abs used in this study being either rabbit or mouse (see table 2.8). Secondary antibodies were typically used at a dilution of 1:10,000 (or in the case of β-actin, 1:20,000), and incubation was for 1 hour at room temperature. Further washes in TBS-T (4 x 10 minutes) and TBS (2 x 10 minutes) followed, before antibodies bound to the protein of interest were visualised using chemiluminescence [189].

Table 2.8 Antibodies used in the immunoprobing of Western blots

Epitope	*Source*	*Dilution*	*Incubation Conditions*	*Company*	*Catalogue number*
Src Y418	Rabbit	1:1000	2 hrs RT	Biosource	44-660G
Src Y527	Rabbit	1:1000	O/N 4°C + 2hrs RT	Cell Signalling Technologies	#2105
T-Src	Rabbit	1:1000	O/N 4°C + 2hrs RT	Biosource	44-656G
FAK Y397	Rabbit	1:1000	2 hrs RT	Biosource	44-624G
FAK Y576	Rabbit	1:1000	O/N 4°C + 2hrs RT	Upstate	07-157
FAK Y861	Rabbit	1:1000	2 hrs RT	Biosource	44-626G
FAK Y925	Rabbit	1:1000	O/N 4°C + 2hrs RT	Cell Signalling Technologies	#3284
T-FAK	Rabbit	1:1000	2 hrs RT	Biosource	AHO0502
Pax Y31	Rabbit	1:1000	O/N 4°C + 2hrs RT	Biosource	44-720G
T-Pax	Mouse	1:500	O/N 4°C + 2hrs RT	Biosource	AHO0492
EGFR Y845	Rabbit	1:1000	O/N 4°C + 2hrs RT	Biosource	44-784G
EGFR Y1068	Rabbit	1:1000	O/N 4°C + 2hrs RT	Cell Signalling Technologies	#2234
T-EGFR	Rabbit	1:1000	O/N 4°C + 2hrs RT	Cell Signalling Technologies	#2232
c-erbB2 Y1248	Rabbit	1:2000	2 hrs RT	Biosource	44-904
T-c-erbB2	Rabbit	1:2000	2 hrs RT	Cell Signalling Technologies	#2242
ERK 1/2 T202/Y204	Rabbit	1:1000	2 hrs RT	Cell Signalling Technologies	#9101
T-ERK 1/2	Rabbit	1:1000	2 hrs RT	Cell Signalling Technologies	#9102
T-CSK	Rabbit	1:1000	O/N 4°C + 2hrs RT	Santa Cruz Biotechnology	SC-13074
T-PTP1B	Rabbit	1:1000	O/N 4°C + 2hrs RT	Upstate	07-088
AKT S473	Rabbit	1:1000	O/N 4°C + 2hrs RT	Cell Signalling Technologies	#9271
T-AKT	Rabbit	1:1000	O/N 4°C + 2hrs RT	Cell Signalling Technologies	#9272
β-actin	Mouse	1:20,000	2 hrs RT	Sigma	A2228

N.B. T = Total protein; RT = Room Temperature; O/N = Over Night

Chemiluminescence was performed using a luminol/peroxide based enhanced chemiluminescence (ECL) reagent (Supersignal™ West Pico, Supersignal™ West Dura or Supersignal™ West Femto) [190]. The ECL reagent (500µl) was made following the manufacturer's instructions and added to the blot for 5 minutes. Luminol (in the ECL reagent) is oxidised by HRP in the presence of peroxide to produce an excited state product, which then decays to a lower energy state by releasing photons of light. This light is captured on x-ray film, with exposures ranging from seconds to a few hours depending on signal strength. X-ray films were developed using an X-O-graph Compact X2 x-ray developer (X-O-graph Imaging System, Tetbury, UK) and the bands obtained were scanned and analysed using a Bio-Rad GS-690 Imaging Densitometer as mentioned in section 2.3.4.2.

2.5 Immunocytochemistry (ICC)

2.5.1 Fixation of Cells

Cells ($1x10^5$) were seeded onto TESPA-coated coverslips and grown to approximately 70% confluency, at which time they were treated as required. The cells were then fixed using either ER-ICA (for Src Y419/T-Src assays) or formal-saline (for Ki67 assay) fixes prior to immunocytochemical staining. The assays for Src and Ki67 are standard assays in our laboratory and the decision to use these fixatives was based upon the expert advice of members of our ICC department. PBS used in these experiments was made in-house using the recipe shown in appendix 2 (section 8.2.3.1).

2.5.1.1 ER-ICA

The (o)estrogen-receptor immunocytochemical assay, or ER-ICA, fix was originally developed for the detection of the oestrogen receptor, but has now been found to be effective for a number of proteins, including Src.

Coverslips were placed in a rack and sub-merged in a bath containing 3.7% (v/v) formaldehyde in PBS (see appendix 2 [section 8.2.3.2]) for 15 minutes. Following a PBS wash (≥5 minutes) the coverslips were sequentially placed into baths containing methanol (between -10°C and -30°C; 5 minutes) and

acetone (between -10°C and -30°C; 3 minutes). After a final PBS wash (≥5 minutes) the coverslips were either used immediately or stored at -20°C in sucrose storage medium (SSM; see appendix 2 [section 8.2.3.3]).

2.5.1.2 Formal-saline

Medium was removed from the coverslips and replaced with formal-saline solution (1 ml per coverslip) for 10 minutes. Formal-saline solution was made as described in appendix 2 (section 8.2.3.2). The cells were then washed with 100% ethanol (5 minutes, followed by a quick ethanol rinse) and PBS (5 minutes, followed by a quick PBS rinse). The coverslips were stored for at least 24 hrs in SSM at -20°C before use.

2.5.2 Immunocytochemical Staining of Fixed Cells

The SSM in which the fixed cells were stored was discarded and the coverslips washed gently, but thoroughly, with PBS (2 x 5 minutes). The coverslips were then rinsed with PBS containing 0.02% (v/v) Tween-20 for approximately 30 seconds to reduce surface tension and help the 1°Ab spread evenly over the cells. Primary antibody, diluted in PBS containing 0.5% (w/v) BSA, was added to each coverslip (50µl) and incubated in a humidified atmosphere overnight at 23°C. As with immunoprobing of Western blots, 1°Ab dilution varied from protein to protein and had to be determined empirically. The 1°Ab dilutions used in this study can be found in Table 2.9.

Table 2.9 Antibodies used in immunocytochemistry

Epitope	*Source*	*Dilution*	*Company*
Src Y419	Rabbit	1:50 – 1:100	Biosource
T-Src	Rabbit	1:300 – 1:600	Biosource
Ki67 (clone MIB I)	Mouse	1:100	DAKOcytomation

Following 1°Ab incubation the coverslips were washed with PBS (2 x 5 minutes) and incubated with an HRP-labelled polymer conjugated to either goat

anti-rabbit or goat anti-mouse immunoglobulins (supplied with the DAKO EnVision™+ system, peroxidase [DAB] kit) for 2 hours at 23°C. Following two further washes with PBS (5 minutes each) the cellular location of the protein of interest was visualised by the addition of 3,3'-diaminobenzidine (DAB), a chromogenic HRP substrate. Colour development typically took 6-10 minutes depending on signal strength.

Cells were counter-stained with methyl-green (0.5% [w/v] in H_2O) for up to 2 minutes. After thorough rinsing with distilled H_2O to remove excess methyl-green the coverslips were dried at 40°C for 1 hour and mounted onto glass slides using di-butylpthalatexylene (DPX), a xylene-based mounting medium. DPX was allowed to set overnight at room temperature and the slides were assessed on an Olympus BH-2 phase contrast microscope fitted with an Olympus DP-12 digital camera system (both Olympus, Oxford, UK).

2.6 Assessment of Cell Morphology

Representative images of live cells were obtained using a Leica DM-IRE2 inverted microscope (Leica Microsystems Imaging Solutions Ltd, Cambridge, UK) fitted with a Hoffman condenser and a Hamamatsu C4742-96 digital camera (Hamamatsu Photonics UK Ltd, HERTS, UK). The microscope was attached to a PowerMAC G5 computer (Apple Computer Inc., CA, USA) running Improvision® OpenLab V4.04 software (Improvision®, Coventry, UK). Unless stated otherwise, all images were captured at 20x magnification.

2.7 Growth Assays

Two methods were utilised to assess cell growth: the MTT-based cell proliferation assay and cell counting experiments using a Coulter™ Multisizer II. The MTT-based cell proliferation assay was sufficiently sensitive to detect small changes in the growth of our cell-lines and was much less labour-intensive than manual counting. However, the design of the assay limits cell growth experiments to 5 days. Therefore, for longer growth experiments (7 days or more) cell counting was used.

2.7.1 MTT Cell Proliferation Assay

The MTT cell proliferation assay involves the metabolism of a soluble yellow compound, 3-(4,5-dimethylthiazol-2-yl)-2,5-diphenyl-2H-tetrazolium bromide (MTT), by mitochondrial dehydrogenase enzymes in the cell to produce insoluble purple formazan crystals. When the cells are lysed the formazan crystals can dissolve and the absorbance of the resultant solution is proportional to cell number [191, 192].

Cells were harvested using trypsin/EDTA as described in section 2.2.2, and seeded in W+5% ± Tam (100nM) into a 96-well plate at a density of $5x10^3$ cells/well (day 1). The cells were allowed to settle for 24 hours before treatments were added as required (day 2). The plate was incubated at 37°C in a humidified atmosphere containing 5% CO_2 for 5 days. On day 7 the medium was removed and the cells washed gently with PBS. Sterile-filtered MTT in wRPMI (0.5mg/ml; 150µl) was added to the cells and left to incubate at 37°C for 4 hours. The MTT solution was then aspirated and the cells lysed in 10% (v/v) Trition-X100 in PBS (150µl/well) overnight at 4°C. The following day the plate was brought to room temperature, tapped gently to mix the samples and read on a Multiskan® MCC/340 plate-reader (Titertek, USA) at 540nm.

2.7.2 Cell Counting

Cells were harvested using trypsin/EDTA as previously described and seeded in W+5% ± Tam (100nM) into a 24-well plate at a density of $4x10^4$ cells/well. The cells were allowed to settle for 24 hours prior to the addition of treatments. The plate was then incubated at 37°C in a humidified atmosphere containing 5% CO_2 for the required length of time. Typically, growth assays were run for 7, 10, 12 or 14 days, with medium changed every 3-4 days.

Once the experiment had run its course the medium was removed and replaced with trypsin/EDTA (1ml/well). The plate was returned to the incubator for approximately 5 minutes until the cells were in suspension. Cells were drawn up into a 5ml syringe through a 25G needle three times to obtain a single-cell suspension. The wells were then washed with fresh Isoton II solution (1ml)

which was also taken up into the syringe; this was repeated twice more to give a final volume in the syringe of 4ml. The cells were added to a counting cup containing 6 ml of Isoton II solution to give a total volume of 10ml.

The dilute cell suspension was counted using a Coulter™ Multisizer II following the manufacturer's instructions. The Coulter™ Multisizer II was set to count the number of cells in a fixed volume of 500µl. Therefore, the counts obtained were multiplied by 20 to give the total number of cells per well. A minimum of two counts were taken from each well.

2.8 Fluorescence Assisted Cell Sorting (FACS)

Apoptosis, the mechanism of programmed cell death used to remove damaged or unwanted cells, was measured using the Vybrant® Apoptosis Assay Kit #4 (Invitrogen, Paisley, UK) which utilises YO-PRO®-1 (green) and propidium iodide (PI; red) fluorescent dyes to assess the viability of cells. Cells undergoing apoptosis have many defining characteristics, one of which is increased cell-membrane permeability. YO-PRO®-1 is able to permeate the membrane of apoptotic cells, but not healthy cells; whilst PI is excluded from both due to its larger size. PI can, however, be taken up by necrotic cells. This means that any cells containing only the YO-PRO®-1 dye will be apoptotic, whereas any cells containing both YO-PRO®-1 and PI will be necrotic. Thus, a distinction can be made between healthy, apoptotic and necrotic cells by measuring the fluorescence of individual cells using a FACS machine.

For FACS, MCF7wt and Tam-R cells were harvested as previously described and seeded into 100mm Petri-dishes in W+5%. The cells were then left to attach for approximately 48-72 hrs before being treated as required. On the day of the assay, 1 dish of each cell-line was treated with N,N,N',N'-tetrakis(2-pyridylmethyl)ethylenediamine (TPEN; 12.5µM) for 4 hrs to act as a positive control. TPEN is an intra-cellular chelator of heavy metals, with a particular affinity for zinc ions, and is a potent inducer of apoptosis in the MCF7 cell-line [193]. Following treatments, cells were harvested into suspension using trypsin/EDTA and washed twice with ice-cold PBS, with each wash followed

by centrifugation (1000rpm, 5min). The cells were then re-suspended in PBS (1ml) and counted. An aliquot containing $1x10^6$ cells was transferred to a sterile 1.5ml centrifuge tube and pelleted by centrifugation (1000rpm, 3min). After carefully removing the supernatant, the cells were re-suspended in PBS (100µl) containing YO-PRO®-1 (0.1µl) and propidium iodide (0.1µl) fluorescent dyes and left on ice for 20 minutes prior to analysis.

FACS analysis was carried out using a FACSCalibur FACS machine (Becton Dickinson (BD) UK Ltd, Oxford, UK) connected to a Power Macintosh G3 computer (Apple Computer Inc., CA, USA) running CellQuest™ Version 3.3 software (also Becton Dickinson). Positive and negative controls for the apoptosis assay were used to calibrate the FACS machine and associated software for optimal data collection.

2.9 Cell Attachment Assays

Cell attachment assays were used to measure the affinity of the cell-lines for either uncoated tissue culture plastic or matrix components (e.g. fibronectin) coated surfaces. All cell attachment assays were carried out in 96-well plates under sterile conditions. To assess cell attachment to plastic the plates were used as supplied. However, for attachment to fibronectin-coated surfaces the plates required pre-treatment. Fibronectin, diluted to 10µg/ml in wRPMI containing no supplements, was added to the wells of a 96-well plate (50µl/well). The plate was gently tapped to ensure even coating and placed at 37°C for 2 hours. The fibronectin solution was then aspirated and the wells washed with PBS. The plate was left to air-dry at room temperature.

Cells were harvested using trypsin/EDTA as previously described and seeded into the wells of untreated or fibronectin-coated 96-well plates at a density of $4x10^4$ cells/well (in 100µl). Cells were seeded in W+5% ± TAM (100nM) containing the required treatments, with 8 replicates per treatment. The plate was incubated at 37°C for 50 minutes, after which the medium (containing unattached cells) was removed and the wells gently washed with PBS. The PBS was removed and the number of attached cells measured using the MTT

assay as described in section 2.7.1. In the case of time course experiments the medium containing unattached cells was removed at given time points, typically 10, 20, 30, 40 and 50 minutes after seeding, and replaced with PBS. The cells were kept in PBS until the end of the experiment when the MTT assay was carried out as usual.

When cell attachment is presented as a percentage of the total number of cells seeded, the cells in one well per treatment were not removed after the required time; instead 10µl of MTT solution (5.5mg/ml in wRPMI) was added directly to the cells (in 100µl medium) to give a final MTT concentration of 0.5mg/ml (as standard). After 4 hours at 37°C the cells were lysed by the addition of 40µl of a 37.5% (v/v) Triton-X100 solution in PBS, to give a final volume of 150µl and a final Triton-X100 concentration of 10%. The absorbance of these wells was read at 540nm as normal.

2.10 Cell Migration Assays

Cell migration assays were carried out using Corning Standard Transwell® inserts with a 6.5mm diameter and an 8µm membrane pore size (figure 2.3). The undersides of the Transwell® insert membranes were first coated with fibronectin as follows. Fibronectin (10µg/ml in wRPMI containing no supplements; 200µl) was added to the wells of a 24-well plate (supplied with the inserts) and the Transwell® insert placed such that the membrane was just submerged in the fibronectin solution. The plate was incubated at 37°C for 2 hours after which the inserts were washed with PBS and allowed to air-dry.

Cells were harvested using trypsin/EDTA as previously described and seeded into the upper compartment of the Transwell® inserts at a density of $5x10^4$ cells/insert in W+5% ± TAM (100nM) ± treatments (200µl). Each treatment condition was run in duplicate. W+5% ± TAM (100nM) ± treatments (650µl) was added to the lower compartment of the insert and the experiment allowed to proceed for 24 hours at 37°C.

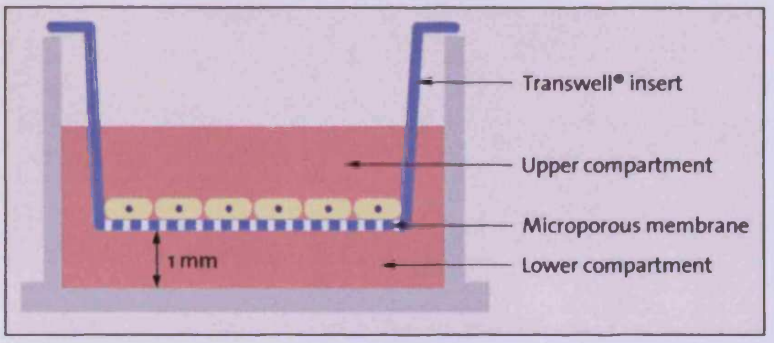

Figure 2.3 Schematic diagram of a Corning Standard Transwell® insert

A schematic diagram of a Corning Standard Transwell® insert in a well of a 24-well plate as used in cell migration (section 2.10) and cell invasion (section 2.11) assays. Figure acquired from

http://www.corning.com/lifesciences/ technical_information/techdocs/transwell_guide.pdf

After this time the medium in the upper compartment of the Transwell® inserts was aspirated and the non-migratory cells (i.e. those still on top of the membrane) removed using a cotton swab. The remaining migratory cells were fixed in 3.7% (v/v) formaldehyde in PBS for 10 minutes. The fixed cells were then washed with PBS and stained with crystal violet (0.5% [w/v] in H_2O) for 15-30 minutes. Following thorough washing in PBS to remove excess crystal violet stain the inserts were air-dried at room temperature.

Cells were counted in 5 random fields of view at 10x magnification using an Olympus BH-2 phase contrast microscope (see section 2.5.2), and the data presented as mean cell count/field.

2.11 Cell Invasion Assay

As with cell migration assays, invasion assays were carried out using Corning Standard Transwell® inserts with a 6.5mm diameter and an 8μm membrane pore size (figure 2.3). However, for invasion assays the top of the porous membrane of the Transwell® insert was coated with Matrigel™ - a biologically active synthetic basement membrane comprised of a number of extra-cellular matrix (ECM) proteins, primarily laminin and collagen IV. A stock solution of Matrigel™ (~12mg/ml but can vary) was diluted 1 in 3 with ice-cold wRPMI (no supplements) and dispensed (50μl) into the upper compartment of the Transwell® inserts. The inserts, in a 24-well plate, were then placed at 37°C for 2 hours to allow the Matrigel™ to set.

Cells were harvested using trypsin/EDTA as previously described and seeded into the upper compartment of the Transwell® inserts at a density of $5x10^4$ cells/insert in W+5% ± TAM (100nM) ± treatments (200μl). Each treatment condition was run in duplicate. W+5% ± TAM (100nM) ± treatments (650μl) was added to the lower compartment of the inserts and the plate was incubated at 37°C for 72 hours. After this time the medium in the upper compartment of the Transwell® inserts was aspirated and the non-invasive cells (i.e. those still on top of the membrane) removed using a cotton swab.

Cells which had invaded through the matrigel and passed through the membrane were fixed in 3.7% (v/v) formaldehyde in PBS for 10 minutes, washed with PBS and allowed to air-dry for 3-4 minutes at room temperature. The membranes containing the fixed cells were excised from the inserts with a scalpel blade and mounted, cell-side up, onto glass slides using VectorShield® hard-set mounting medium containing DAPI nuclear stain. Slides were stored at 4°C in the dark.

The number of invading cells was assessed by counting the DAPI stained nuclei on each membrane using a Leica DM-IRE2 fluorescent microscope and the data presented as the mean cell count/membrane.

2.12 Expression of a constitutively-active Src Mutant in MCF7wt Cells

2.12.1 Plasmids

The mutant Src Y529F gene construct in a pUSEamp eukaryotic expression vector (figure 2.4A) was purchased from Upstate Biotechnology (Lake Placid, NY, USA). The pUSEamp expression vector is controlled by a CMV promoter and also contains genes that confer resistance to ampicillin and neomycin, antibiotics used for the selection of positively transformed bacteria and positively transfected eukaryotic cells respectively. The pUSEamp empty vector was also purchased for use as a control in the transfection experiments (figure 2.4B).

Expression of the Src Y529F gene results in a constitutively active form of the Src protein. This is due to a mutation in the gene sequence which leads to a tyrosine-phenylalanine substitution at position 529 of the protein (see appendix 2 [sections 8.3.4.1 and 8.3.4.2]). This substitution prevents the negative-regulatory tail of Src from interacting with the SH2 domain, enabling Src to maintain an open conformation and promoting full activation of the kinase domain via the phosphorylation of Y419. It is important to note that the position of the negative-regulatory tyrosine mutated in the Src Y529F construct differs to the position given in chapter 1. This is due to slight

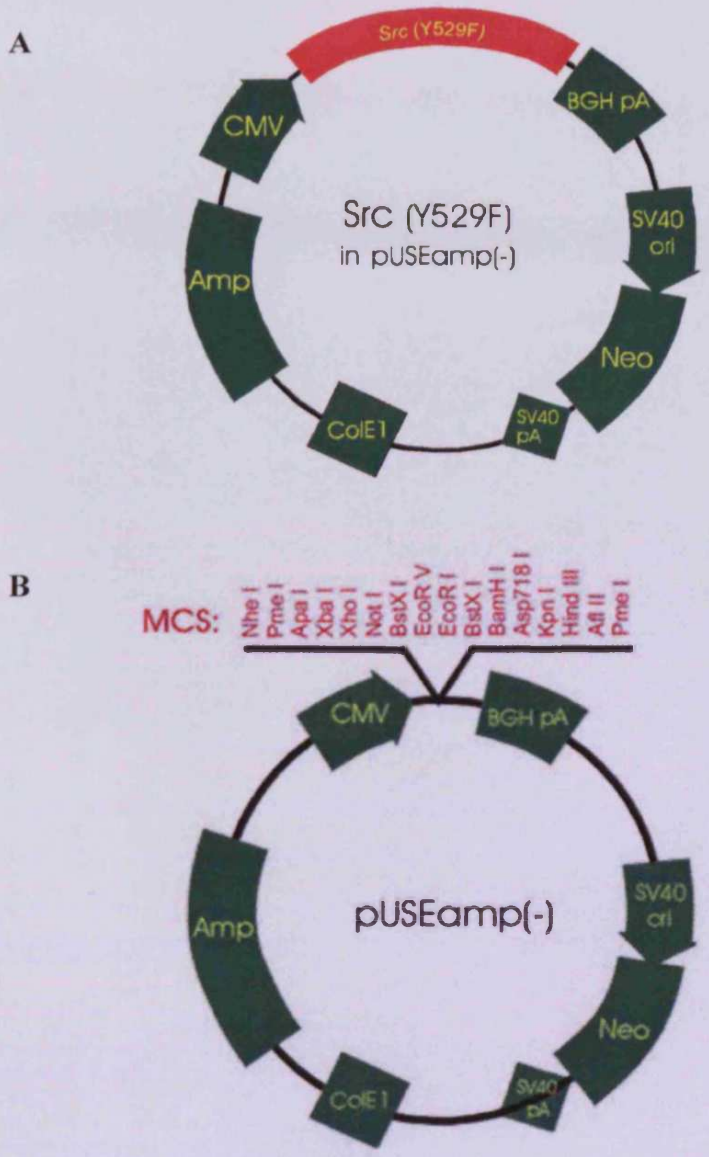

Figure 2.4 Plasmid maps for SrcY529F gene construct in a pUSEamp expression vector and the pUSEamp empty vector

(A) Plasmid map for the mutant Src Y529F gene construct in a pUSEamp eukaryotic expression vector under the control of a CMV promoter. Also shown are the genes for ampicillin and neomycin resistance used in the selection of positively transformed bacteria and positively transfected eukaryotic cells respectively. (B) Plasmid map, showing the multiple cloning site (MCS), for the pUSEamp empty vector control.

Images obtained from http://www.upstate.com/browse/productdetail.q.ProductID.e.21-115/%3CI%3ESrc%3C%2FI%3E+cDNA++activated++in+pUSEamp# (figure 2.4A) and http://www.upstate.com/browse/productdetail.q.ProductID.e.21-148/pUSEamp++++# (figure 2.4B).

variations in the amino acid sequence of the 'unique' region of Src between species of origin, which leads to differences in the numbering of residues in the protein. As such the Y529 in the constitutively-active Src construct, which is a mouse/chicken chimera, corresponds to Y530 in human Src.

As Src is an oncogene the transfection of mammalian cells with a constitutively-active Src mutant constitutes a class II genetic manipulation project and so all work with this plasmid involving mammalian cell culture was conducted in a specialised containment II genetic manipulation suite fitted with a Faster BHA48 Laminar-Flow Safety Cabinet (Faster SRL, Ferrara, Italy).

2.12.2 Transformation of Competent Bacteria

Transformation of competent *E.coli* bacteria was performed to obtain stocks of Src Y529F and pUSEamp empty vector plasmids used in the transfection experiments. The transformation protocol was identical for both plasmids. All bacterial transformation work was conducted under sterile conditions in an MDH Class II laminar-flow safety cabinet (BIOQUELL UK Ltd, Andover, UK) housed in a specialised Containment I genetic manipulation suite.

The plasmid stock was diluted in sterile H_2O to give a concentration of 5ng/µl. The diluted plasmid (2µl) was added to a tube containing 20µl of One Shot® TOP10 Chemically Competent *E.coli* (Invitrogen Ltd, Paisley, UK) and the solution mixed by gentle inversion. The tube was placed on ice for 20 minutes after which the *E.coli* were heat-shocked at 42°C for 30 seconds and placed immediately back on ice. SOC medium (250µl; see section 8.3.1) was added to the tube prior to incubation at 37°C for 1 hour with vigorous shaking. The tube was then pulse centrifuged and 25µl of the transformed bacteria spread on a selective Luria-Bertani (LB) agar plate (see section 8.3.2) containing ampicillin (100µg/ml). Cultures were grown overnight at 37°C. A single *E.coli* colony was picked from the plate and used to inoculate a starter culture in LB-broth (3ml; see section 8.3.3) containing ampicillin (100µg/ml), which was grown at 37°C for approximately 8 hours with vigorous shaking. The

starter culture was then diluted 1:750 with LB-ampicillin broth (100ml) and grown for a further 14-16 hours at 37°C with vigorous shaking.

2.12.3 Plasmid Purification and Isolation

Plasmid DNA was extracted from the transformed bacteria using a QIAGEN Endofree Plasmid Purification Maxi Kit (QUIAGEN Ltd, Crawley, UK) following the manufacturer's instructions. Plasmid isolation and purification was carried out under sterile conditions, and all buffers and solutions used were supplied with the kit.

Briefly, the transformed *E.coli* (100ml) were harvested by centrifugation at 6500rpm for 15 minutes (Sorvall® RC5B Plus fitted with a SLA-1500 rotor; Thermo Fisher Scientific Inc., MA, USA). The bacteria were then lysed using buffers supplied with the kit, and the lysate passed through a QIAfilter MAXI cartridge to remove contaminants such as proteins and genomic DNA. Following the addition of the endotoxin removal buffer the lysate was passed through a QIAGEN-tip 500 column which binds the plasmid DNA. The column was then washed twice with QC buffer and the plasmid DNA eluted with QN buffer. Plasmid DNA was then precipitated using isopropanol, pelleted by centrifugation (Sorvall® RC5B Plus fitted with a SLA-600TC rotor, 10,000rpm, 30 minutes), washed with 70% ethanol and allowed to air-dry. The plasmid DNA pellet was dissolved in sterile H_2O (500µl; pH 8.0), aliquotted and stored at -20°C.

To ensure the quality and purity of the plasmid obtained, samples were taken at various points throughout the isolation/purification procedure for analysis (as described in the manufacturer's instructions). These points were: following filtration of the lysate (FL), from the flow-through following addition of the lysate to a QIAGEN-tip 500 column (FT), from 2 washes (W1 and W2) and from the eluted plasmid DNA (E). The aliquots taken were precipitated with isopropanol and washed with 100% ethanol as described above, and the resultant DNA pellet dissolved in Tris-EDTA buffer (10µl; supplied with kit). The samples (10µl sample in 6µl of sample loading buffer)

were then analysed on a 0.6% (w/v) agarose/ethidium bromide gel running at 70V for approximately 60-75 minutes and viewed under UV light.

The gels show that Src Y529F (figure 2.5A) and empty vector (figure 2.5B) plasmid DNA, which can be seen in the filtered lysate (FL), has been retained by the QIAGEN-tip 500 column - as demonstrated by the near complete absence of bands in the flow-through (FT) or wash (W1 and W2) lanes. Following elution (E) and isopropanol precipitation/ethanol washing, the position of the bands for the purified plasmid (PP) compare with those of the plasmid stock (PS) supplied by Upstate Biotechnology.

The two bands seen in each lane of the gels represent the coiled (upper band) and super-coiled (lower band) forms of the plasmid DNA. However, in figure 2.5B additional bands can be seen in lanes FL, E and PP which are outside the range of the DNA size marker (i.e. greater than 10,000 bp in size). These bands are not contamination with bacterial genomic DNA, which can sometimes occur due to errors in the plasmid purification process; rather they are multimeric forms of the pUSEamp empty vector plasmid being purified. The two can be distinguished following a restriction digest assay using the *EcoR1* restriction enzyme: digestion of multimeric plasmids will result in distinct bands on an agarose gel, whereas digestion of genomic DNA will produce smearing (see figure 2.7A).

2.12.4 Plasmid Quantitation

The concentrations of the purified plasmids were determined by measuring the optical density (OD) of a 1:200 dilution in sterile H_2O at wavelengths of 260nm and 280nm. The ratio of these two values gives a measure of the purity of the DNA, with a ratio of 1.8 representing a pure DNA solution. The value for OD_{260} was substituted into the following formula to give the DNA concentration in μg/ml:

$$[\text{Plasmid}] = OD_{260} \times 50 \times \text{Dilution Factor}$$

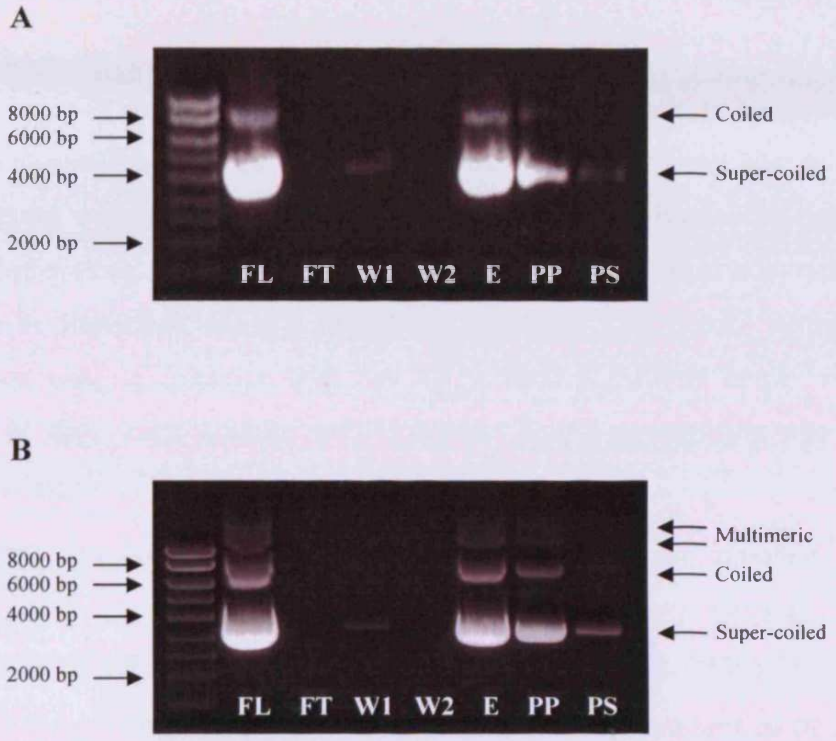

Figure 2.5 Monitoring of the plasmid purification process for Src Y529F and pUSEamp empty vector plasmids

Src Y529F (A) and pUSEamp empty vector (B) plasmids were isolated and purified from transformed *E.coli* using the QIAGEN Endofree Plasmid Purification MAXI kit. To ensure the quality and purity of the plasmid obtained a number of aliquots were taken at various points throughout the purification procedure and analysed on a 0.6% agarose/ethidium bromide gel. The points sampled were following filtration of the lysate (FL), the flow-through from the QIAGEN-tip 500 column following addition of the filtered lysate (FT), the 2 washes (W1 and W2) and from the eluted plasmid DNA (E). For comparison, the final purified plasmid (PP) and the plasmid stocks obtained from Upstate Biotechnology (PS) were also run. The gels show that, for both plasmids, the isolation/purification process proceeded without any problems.

2.12.5 Verification of Purified Plasmids

Following quantitation, the identities of the purified Src Y529F and pUSEamp empty vector plasmids were verified using restriction digestion assays and PCR (with primers specific for the Src gene as detailed in section 2.3.4).

2.12.5.1 Confirmation of the Size of the Src Y529F and pUSEamp Empty Vector Plasmids Using an EcoR1 Restriction Digest Assay

Due to their non-linear nature, plasmids do not run at the correct size relative to a molecular weight marker (Hyperladder™ I) when resolved using agarose gel electrophoresis. Therefore, to verify the size of a plasmid accurately it must first be linearized using a restriction enzyme. The *EcoR1* restriction enzyme was used to linearize both Src Y529F and pUSEamp empty vector plasmids as they each contain only a single *EcoR1* recognition site (see appendix 3 [section 8.3.4.3 and section 8.3.5.2]).

The *EcoR1* digestion mix consisted of 10x buffer (5µl; supplied with restriction enzyme), Src Y529F *or* pUSEamp empty vector plasmid DNA (1µg) and the *EcoR1* restriction enzyme (1.2U), made up to 50µl with sterile H_2O. The reactions were overlaid with mineral oil and incubated at 37°C overnight. The digested DNA products were then resolved using 0.6% agarose/ethidium bromide gel electrophoresis and visualised under UV light as described in section 2.12.3. Digestion of the Src Y529F plasmid by *EcoR1* resulted in a single band which ran at between 6000 and 8000bp (figure 2.6A); whereas digestion of the pUSEamp empty vector produced a single band which ran between 5000 and 6000bp (figure 2.7A). These sizes are consistent with those of 7200bp for Src Y529F and 5400bp for the pUSEamp empty vector which were obtained from the manufacturer.

2.12.5.2 PCR of Src Y529F Plasmid for Src Gene

To ensure the mutated Src gene had been retained in the Src Y529F plasmid following transformation of bacteria and plasmid isolation/purification the purified plasmid was subjected to PCR analysis for Src as previously described in section 2.3.4. As a positive control, the Src Y529F plasmid stock

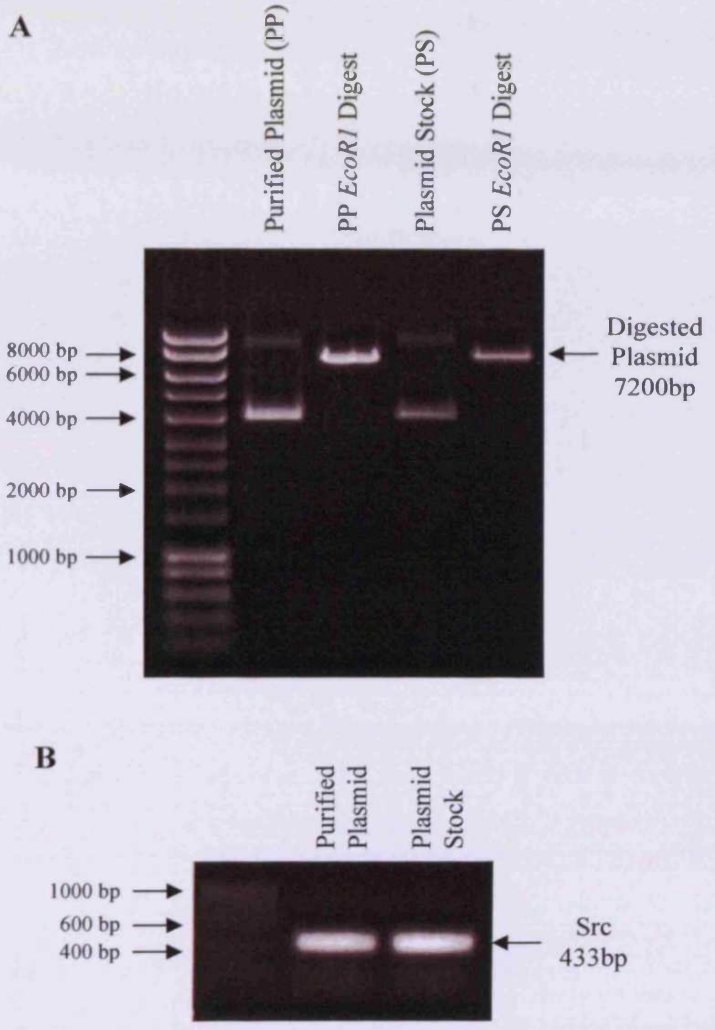

Figure 2.6 Verification of the Src Y529F plasmid by restriction digestion and PCR

The size of the Src Y529F plasmid obtained following transformation of bacteria and subsequent isolation/purification was verified as 7200bp using an *EcoR1* restriction digest assay (A). Furthermore, the presence of the Src gene in the plasmid both before and after bacterial transformation and plasmid isolation/purification was confirmed with PCR analysis using primers specific for the Src gene (B).

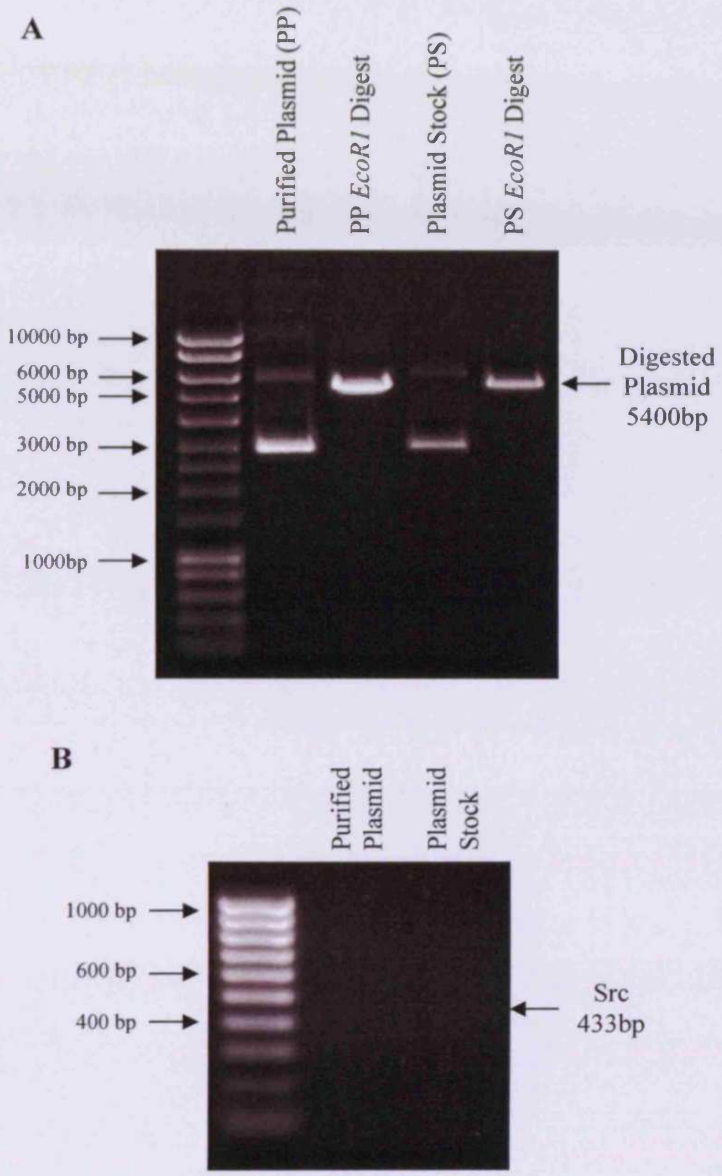

Figure 2.7 Verification of the pUSEamp Empty Vector plasmid by restriction digestion and PCR

The size of the pUSEamp empty vector plasmid obtained following transformation of bacteria and subsequent isolation/purification was verified as 5400bp using an *EcoR1* restriction digest assay (A). Furthermore, the presence of a distinct band at 5400bp following digestion confirms that the additional bands seen during the isolation/purification procedure (figure 2.5B) were multimeric forms of the plasmid, as opposed to bacterial genomic DNA contamination. The absence of the Src gene in the empty vector plasmid stock and isolated/ purified plasmid was confirmed with PCR analysis using primers specific for the Src gene (B).

purchased from Upstate Biotechnology (diluted 1:20 with sterile H_2O) was also run. The PCR showed that the Src gene was present in both the stock plasmid and the purified plasmid (figure 2.6B).

2.12.5.3 PCR of pUSEamp Empty Vector Plasmid for Src Gene

To confirm the absence of the Src gene in the pUSEamp empty vector the purified plasmid was subjected to PCR analysis for Src as above. As a positive control, the pUSEamp empty vector plasmid stock purchased from Upstate Biotechnology (diluted 1:20 with sterile H_2O) was also run. The PCR showed that the Src gene was not present in either the stock plasmid or the purified plasmid (figure 2.7B).

2.12.6 Transfection of MCF7wt cells with Mutated Src Gene Construct (Src Y529F)

Lipofectamine™ 2000 (Invitrogen Ltd, Paisley, UK) was used to transfect MCF7wt cells with Src Y529F and pUSEamp empty-vector plasmid constructs. Initially, the cells were transiently transfected in order to optimise conditions for maximum transfection efficiency (i.e. amount of plasmid DNA used and the ratio of DNA to lipid). Once determined, these conditions were then used in the generation of a stably transfected cell-line. Further details of the optimisation procedure can be found in chapter 5.

2.12.6.1 Transfection Protocol

The protocol described below pertains to cells grown in 35mm Petri-dishes; if cells are grown in smaller or larger vessels then the volumes used must be altered proportionally, based on the relative surface area of the vessel used compared to that of a 35mm Petri-dish.

MCF7wt cells were grown in R+5% to approximately 60-70% confluency and changed into W+5% 24 hours prior to transfection. On the day of transfection the medium was removed and replaced with antibiotic-free wRPMI (2ml) containing 5% SFCS and L-glutamine (200mM). The optimal amount of plasmid DNA for transfection, as determined in chapter 5, was added to a 250µl aliquot of antibiotic- and serum-free wRPMI containing L-glutamine;

while a corresponding volume of Lipofectamine™ 2000, dependent on the DNA:lipid ratio selected, was added to another. The DNA and Lipofectamine™ 2000 solutions were then combined and left for 20 minutes at room temperature to allow the formation of DNA-lipid complexes.

The DNA-lipid mixture was added drop-wise, with gentle agitation, to the dishes and the cells were placed at 37°C in a humidified atmosphere containing 5% CO_2 for 6 hours. The DNA/lipid-containing medium was then replaced with fresh antibiotic-free medium, and the cells were left for a further 48-72 hours before being either characterised using Western blotting and ICC or used in the generation of stably transfected cell-lines.

2.12.7 Generation of Stably Transfected Src Y529F (MCF7-S) and pUSEamp Empty Vector (MCF7-EV) Cell-lines

Geneticin, or G418, is an analogue of the antibiotic neomycin and is used for the selection of mammalian cells positively transfected with plasmids containing the neomycin resistance gene, such as pUSEamp, in order to generate stably transfected cell-lines. However, the toxicity of G418 varies from cell-line to cell-line, and so 'kill-curves' were used to elucidate the concentration of G418 that was optimal for the selection of stably transfected cells derived from the MCF7wt cell-line (see chapter 5).

To generate cell-lines stably transfected with either Src Y529F (MCF7-S) or pUSEamp empty vector (MCF7-EV) MCF7wt cells were transfected with the appropriate plasmid using the protocol described above. Approximately 60 hours post-transfection the transfected cells were changed into medium containing G418 at the concentration deemed optimal for the selection of MCF7-derived cell-lines (800μg/ml; see chapter 5). Cells were then assessed on a daily basis using phase-contrast microscopy, with the selection medium changed every 2-3 days.

When the confluency of the cells had been reduced to 5-10% (approximately 7 days), G418 in the culture medium was decreased to a concentration more suitable for routine maintenance - i.e. a concentration sufficiently high to kill

any remaining non-transfected cells, but not high enough to be toxic to the transfected cells (400μg/ml; see chapter 5). From this point onwards the stably transfected cells were cultured as normal in medium containing G418 (400μg/ml) and passaged when necessary. Following 3-4 passages, the cell-lines were characterised, and stocks frozen down using the method described in appendix 2 (section 8.1.4.1). For more information regarding the generation of the stably transfected cell-lines see chapter 5.

2.13 Statistical Analysis

Where data allowed, the statistical significance of the results obtained when comparing between cell-lines or when comparing treated cells versus controls was analysed using independent, two-tailed Student's t-test. The software used for these analyses was Microsoft® Excel 2002 containing the 'Data Analysis' add-in (Microsoft Corporation, USA).

Where multiple data points were present (e.g. dose response experiments), data were analysed using ANOVA with post-hoc tests (Dunnett's t-test and Tamhane's T2 test). These analyses were conducted using the statistical analysis program, SPSS v12.0.2 (SPSS Inc., Illinois, USA).

Chapter Three: Results

Acquired Tamoxifen Resistance in MCF7 Cells is Accompanied by Increased Aggressive Behaviour and Elevated Src Kinase Activity

"A disease known is half cured."

Proverb

3 Acquired Tamoxifen Resistance in MCF7 Cells is Accompanied by Increased Aggressive Behaviour and Elevated Src Kinase Activity

3.1 Introduction and Aims

Tamoxifen is currently the gold standard therapy for the treatment of ER-positive breast cancer in post-menopausal women, with approximately 50% of these patients benefiting from this treatment. However, despite its effectiveness as an anti-hormone therapy, resistance to tamoxifen can develop in a high proportion of initially responsive patients, leading to disease recurrence and increased mortality. This represents a major obstacle in the treatment of breast cancer in the clinic. To help overcome this problem, the Tenovus Centre for Cancer Research has developed an *in vitro* model of tamoxifen resistance using the ER-positive MCF7 breast cancer cell-line in order to elucidate the changes that occur within the cell to bring about a drug-resistant state.

MCF7 cells are epithelial in nature and were derived from the pleural effusion of a 69 year old Caucasian female with mammary adenocarcinoma [194]. They display many characteristics of differentiated mammary epithelium including the expression of oestrogen and progesterone receptors and the ability to synthesize and process oestradiol for growth [195], making them a good cell-model for the study of ER-positive breast cancer *in vitro*. The tamoxifen resistant MCF7 cell-line (Tam-R) was developed following the long-term culture of MCF7 cells in the presence of 4-hydroxytamoxifen as described in materials and methods (chapter 2). Characterisation of this cell-line has shown that, unlike the parental MCF7 cells, Tam-R cells are unresponsive to either the growth-stimulatory effects of E_2 or to the growth-inhibitory effects of tamoxifen. However, despite being insensitive to hormone manipulation Tam-R cells were found to be ER-positive, with ER expression levels similar to those seen in MCF7 cells [69]. Moreover, the ER in Tam-R cells appears to have retained a partial role in the regulation of cell

growth, as evidenced by the observation that Tam-R cells are sensitive to further challenge with the pure anti-oestrogen, fulvestrant (Faslodex™) [69].

Studies have also revealed a fundamental role for growth-factor receptor signalling in tamoxifen-resistant breast cancer, with both EGFR and erbB2 being over-expressed and demonstrating increased activity in Tam-R cells compared to MCF7wt [70]. The data suggest that Tam-R cells are dependent on these growth-factor signalling pathways to drive proliferation, and that this process may be augmented by cross-talk mechanisms that exist between growth-factor and steroid-hormone signalling pathways [69, 73] and also, between different growth-factor signalling pathways, such as the EGFR and IGF-1R pathways [196]. Furthermore, Tam-R cells demonstrate increased phosphorylation of PKB/Akt which appears to be regulated by EGFR/c-erbB2 signalling and may be important for survival and proliferation in this cell-line [76].

The majority of research into the mechanisms of tamoxifen resistance has, thus far, been focussed on the modifications to cell signalling pathways that enable Tam-R cells to circumvent the growth-inhibitory effects of tamoxifen treatment. However, the aim of this chapter was to shift that focus onto how the acquisition of tamoxifen resistance can affect the behaviour of cancer cells. Failure of tamoxifen in the clinic is evidenced by disease relapse, with recurring tumours being more aggressive in nature and correlating with a poor prognosis [197]. Preliminary studies on Tam-R cells *in vitro* have suggested that they too may exhibit enhanced aggressive behaviour in comparison to their wild-type counterparts. With this in mind, the Tam-R cells are further characterised in this chapter with respect to their *in vitro* aggressive behaviour by assessing their morphology, growth, cell-matrix attachment, and migrational and invasive capabilities under basal conditions. Possible cause(s) of these phenotypic changes are also considered. Given the established association between increased Src activity and an aggressive cell-phenotype, the hypothesis that increased Src expression/activation in the Tam-R cells might be responsible for their aggressive *in vitro* behaviour is investigated.

3.2 Results

3.2.1 *Tam-R cells display an aggressive* in vitro *phenotype compared to MCF7wt cells*

The morphology of MCF7wt and Tam-R cells was assessed by phase contrast microscopy using a Leica DM-IRE2 inverted microscope fitted with a Hoffman condenser. Representative images of live cells are shown in figure 3.1. Tam-R cells were seen to have a spiky, more angular appearance than that of the MCF7wt cells and demonstrated membrane ruffling with increased lamellipodia and filopodia formation. Furthermore, MCF7wt cells grew in distinct, tightly packed colonies, whereas Tam-R cells had a predilection for growth in a much looser fashion lacking cell-cell contacts, with identifiable colonies only seen as the cells approached confluency.

The growth rates of MCF7wt and Tam-R cell-lines were measured using cell counting experiments as described in section 2.7.2. Figure 3.2 shows that the Tam-R cell-line possessed a markedly higher rate of growth compared to basal MCF7wt cells when measured over a period of 12-14 days, with Tam-R cell number increasing 34-fold within this time-frame compared to a 12.6-fold increase observed for MCF7wt cells. Furthermore, this figure demonstrates that, while the Tam-R cells were able to grow in the presence of tamoxifen, the growth of MCF7wt cells was significantly inhibited by this anti-hormone.

Acquired tamoxifen resistance is associated with disease relapse, frequently at distant sites, leading to a poor prognosis. As such, the intrinsic metastatic potential (i.e. the migrational and invasive capacity) of Tam-R cells in comparison to the parental MCF7wt cell-line was investigated using *in vitro* migration and invasion assays (sections 2.10 and 2.11 respectively).

Representative images of the Transwell® insert membranes following a migration assay are shown in figure 3.3A, with both the pores in the membrane for the cells to pass through (white) and the crystal-violet stained cells (purple) clearly visible. From these images it is evident that an increased number of Tam-R cells had migrated through the fibronectin-coated membrane compared to MCF7wt. These observations were confirmed following quantitation of the

A MCF7wt

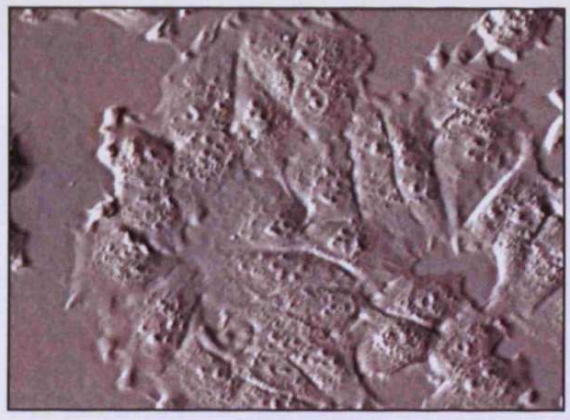

B Tam-R

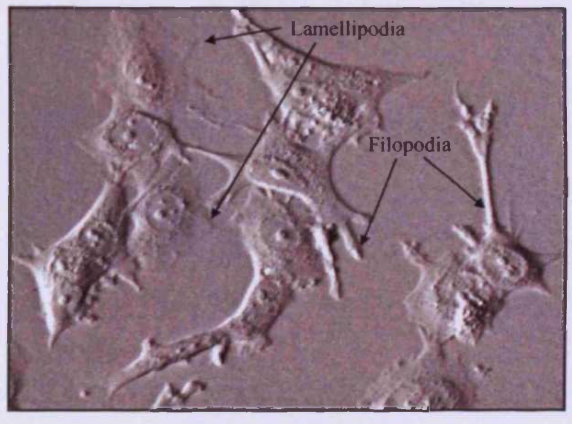

Figure 3.1 Basal morphology of MCF7wt and Tam-R cell-lines.

MCF7wt (A) and Tam-R (B) cells were grown in 100mm Petri-dishes under basal conditions (W+5% ± Tam [100nM]). When the cells had reached log-phase growth, representative images of the live cells were captured at 20x magnification using a Leica DM-IRE2 inverted microscope fitted with a Hoffman condenser and a Hamamatsu C4742-96 digital camera.

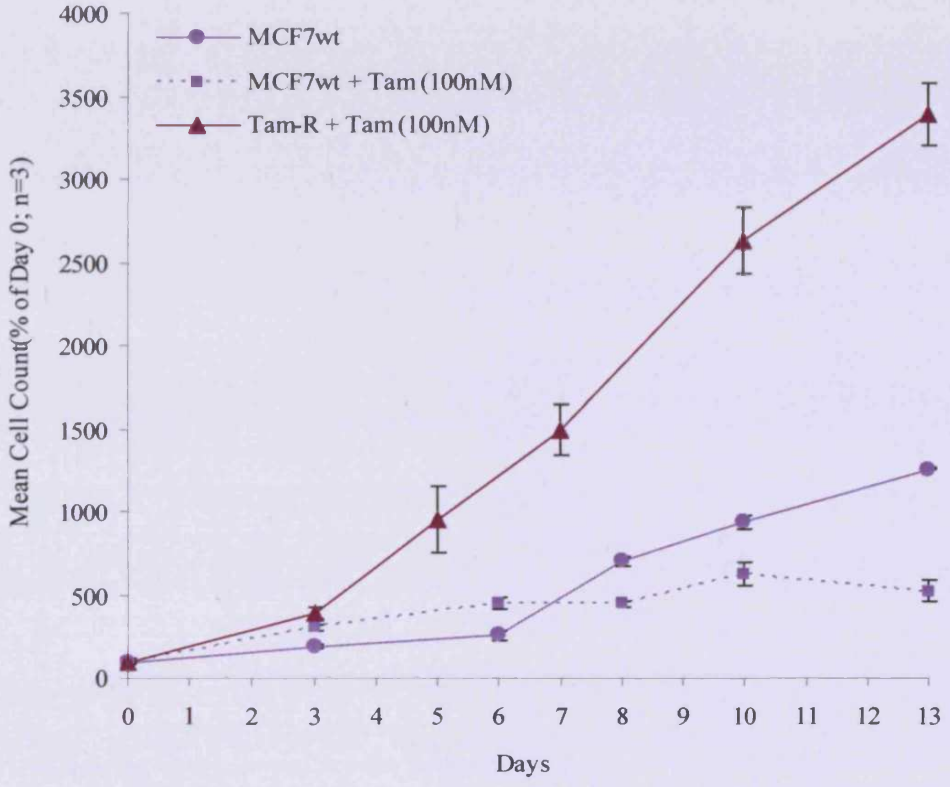

Figure 3.2 Growth rates of MCF7wt and Tam-R cell-lines.

MCF7wt and Tam-R cells were seeded in W+5% ± Tam (100nM) into a 24-well plate at a density of 30,000 cells/well. The cells were cultured as normal and cell number was determined on days 3, 5/6, 7/8, 10 and 13 using a Beckman Coulter™ Multisizer II. Each time point was counted in triplicate and the experiment was repeated at least 3 times. Shown is a representative experiment displaying mean cell count as % of Day 0 ± S.D.

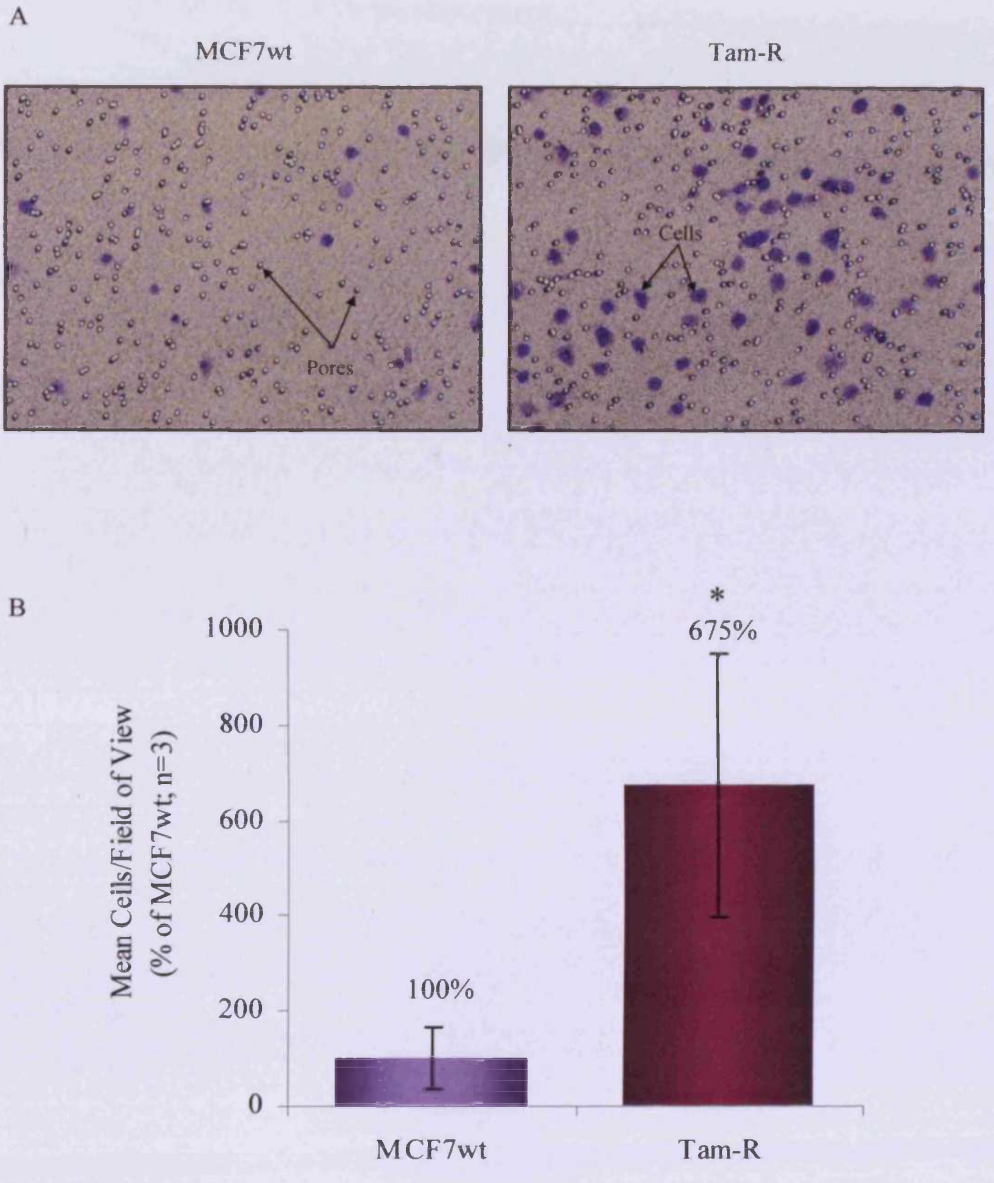

Figure 3.3 Basal migration of MCF7wt and Tam-R cell-lines.

The migrational capabilities of the MCF7wt and Tam-R cell-lines were assessed using *in vitro* migration assays as described in materials and methods (section 2.10). Representative images of crystal-violet-stained cells captured using light microscopy at 20x magnification show that an increased number of Tam-R cells had migrated through the fibronectin-coated membrane of the Transwell™ insert compared to MCF7wt (A). To quantify the migration assays, the number of migratory cells in 5 random fields of view were counted using light microscopy and the data (mean cells/field of view) presented as % of MCF7wt ± S.D. (* $p<0.01$ vs. MCF7wt; n=3) (B).

migration assays, which was done by counting the number of migratory cells present in five random fields of view at 20x magnification for each insert. Data obtained from three independent experiments confirmed that basal migration of the Tam-R cells was approximately 6.75-fold higher than that of MCF7wt cells, as shown in figure 3.3B. Similar results were also seen for the invasive capabilities of these cell-lines. Representative images, this time captured using fluorescent microscopy to visualise the DAPI-stained cell nuclei, show that an increased number of Tam-R cells had invaded through the Matrigel™-coated membrane of the Transwell® insert compared to MCF7wt cells (figure 3.4A). Quantitation of the invasion assays was carried out by counting the number of invasive cells present on each membrane. Results from three independent experiments showed that basal Tam-R cell invasion was 4.5-fold greater than that of MCF7wt cells (figure 3.4B).

Increased migratory and invasive activity is associated with altered cell-matrix attachment. To examine whether this was also true in the Tam-R cell-line, the affinities of MCF7wt and Tam-R cells for uncoated and fibronectin-coated surfaces were assessed using cell attachment assays (section 2.9). These assays were quantified using the MTT assay which produces a coloured solution, the OD_{540} of which is proportional to cell number. Figure 3.5 shows that the attachment of Tam-R cells to an uncoated plastic surface was significantly higher than for MCF7wt cells (OD_{540} of 333 compared to 51 respectively). Likewise, the number of adherent Tam-R cells on a fibronectin-coated surface after 50 minutes was greater than the number of adherent MCF7wt cells (OD_{540} of 595 compared to 399). Interestingly, attachment of both cell-lines was augmented in the presence of a fibronectin matrix.

These data demonstrate that Tam-R cells possess an enhanced aggressive cell-phenotype *in vitro*, displaying an altered morphology, increased growth rate, increased migration and invasion, and a greater degree of adherence to plastic and matrix-coated surfaces compared to endocrine-sensitive MCF7wt cells.

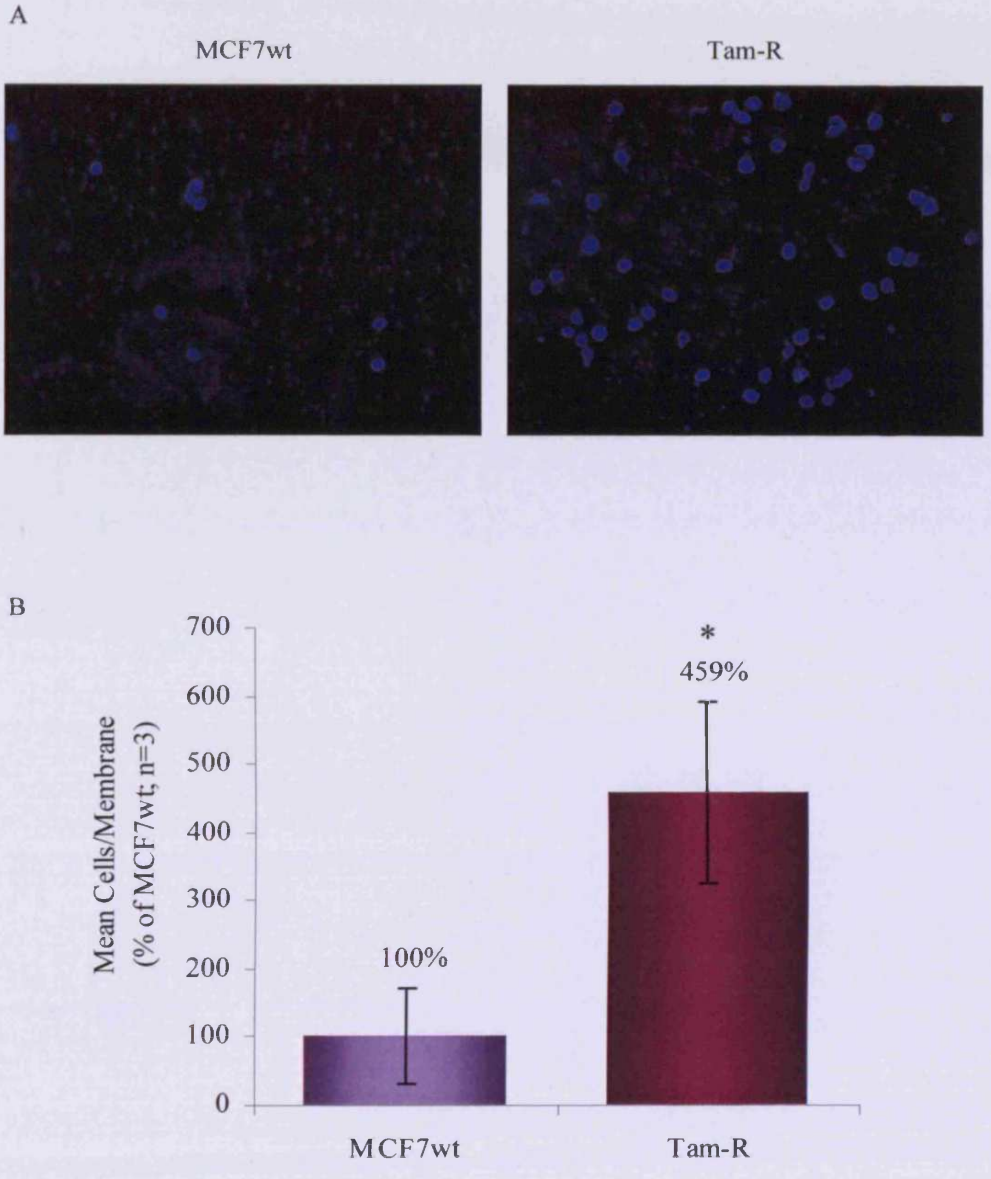

Figure 3.4 Basal invasion of MCF7wt and Tam-R cell-lines.

The invasive capabilities of the MCF7wt and Tam-R cell-lines were assessed using *in vitro* invasion assays as described in materials and methods (section 2.11). Representative images captured using fluorescent microscopy (20x magnification) to visualise DAPI-stained cell nuclei show that an increased number of Tam-R cells had invaded through the Matrigel™-coated membrane of the Transwell™ insert compared to MCF7wt (A). To quantify the invasion assays, the number of invasive cells on each membrane were counted using fluorescent microscopy and the data (mean cells/membrane) presented as % of MCF7wt ± S.D. (* $p<0.01$ vs. MCF7wt; n=3) (B).

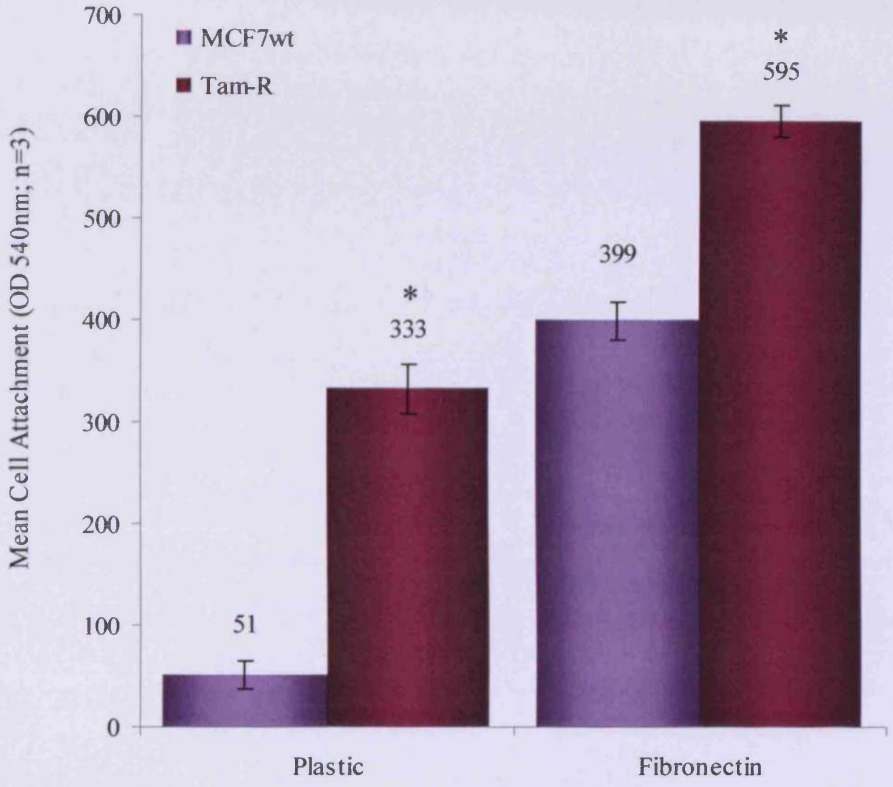

Figure 3.5 Affinity of MCF7wt and Tam-R cells for uncoated and matrix-coated surfaces.

The affinity of MCF7wt and Tam-R cells for uncoated or fibronectin-coated surfaces was measured using cell attachment assays. Cells ($4x10^4$) were seeded in W+5% ± Tam (100nM) into the wells of a 96-well plate which were either uncoated or had been pre-coated with fibronectin. Cells were left to attach for 50 minutes at 37°C after which the wells were washed with PBS and the number of attached cells assessed using the MTT assay. Each condition was run 6 times per experiment, with each experiment repeated at least 3 times. Data is presented as Mean Cell Attachment (OD_{540}) ± S.D. (* $p<0.001$ vs. MCF7wt; $n \geq 3$).

3.2.2 Analysis of Src expression and activation in Tam-R cells

3.2.2.1 Src mRNA

Increased Src expression and activation is often associated with the acquisition of an aggressive cell-phenotype. In the previous section, Tam-R cells were shown to exhibit an aggressive cell-phenotype *in vitro*, and so it was important to investigate whether aberrant Src expression and/or activity in these cells might be involved. Src mRNA levels in both cell-lines were determined by semi-quantitative RT-PCR using total RNA extracted from cells grown under basal conditions. PCR products were resolved using agarose/ethidium bromide gel electrophoresis, and the bands obtained were analysed by densitometry (figure 3.6). No significant difference in Src expression at the mRNA level was observed between the two cell-lines. Subsequent quantitative analysis of Src gene expression was performed using 'real-time' qPCR. These studies confirmed the RT-PCR data, again showing no significant change in Src expression between the MCF7wt and Tam-R cells (figure 3.7).

Affymetrix cDNA array technology is currently being used within our group to profile gene expression patterns in cell-models of resistance to a number of breast cancer therapies, including anti-hormones (tamoxifen and fulvestrant), anti-growth-factor therapies (gefitinib) and oestrogen deprivation. To take advantage of this on-going process, the expression of Src in the MCF7wt and Tam-R cell-lines was also assessed using the Affymetrix array database. Gene expression profiles for Src in MCF7wt and Tam-R cells were obtained from median-normalised, log-transformed data using an on-line software package (www.genesifter.net) and are shown in figure 3.8. The profiles were consistent with the data obtained using RT-PCR and qPCR, and showed no significant difference in Src mRNA levels between the two cell-lines. This data was provided courtesy of Dr Julia Gee and Mr Richard McClelland.

3.2.2.2 Src Protein (Phosphorylated and Total)

Levels of total and activated Src kinase were assessed in MCF7wt and Tam-R cells by Western blotting. The extent of Src activation was determined using a

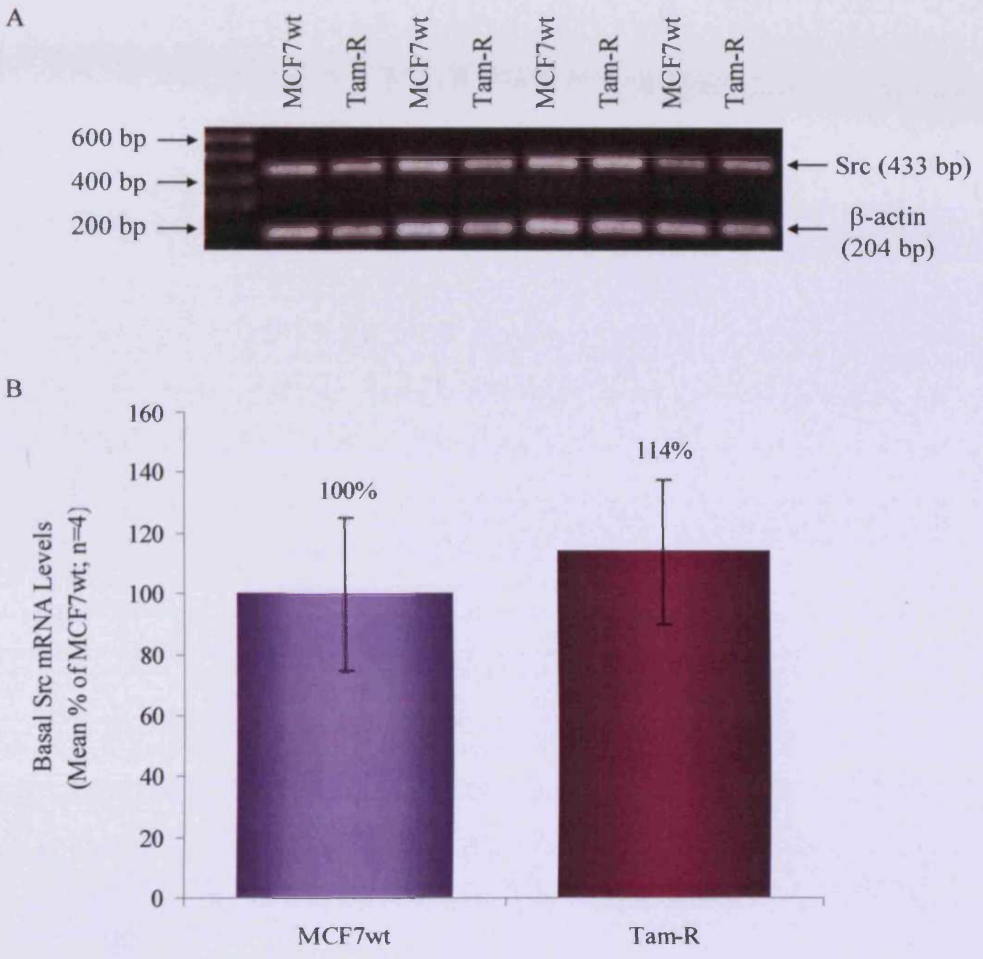

Figure 3.6 Basal Src mRNA levels in MCF7wt and Tam-R cells as measured by semi-quantitative RT-PCR.

MCF7wt and Tam-R cells were cultured under basal conditions until log-phase growth was reached. Total RNA was then extracted from these cells using the QIAGEN RNeasy mini-kit following the manufacturer's instructions. Src expression levels were determined by RT-PCR using primers specific for Src, and the PCR products were resolved using agarose/ethidium bromide gel electrophoresis. Bands were analysed using densitometry and the data, corrected for loading with β-actin, presented as Mean % of MCF7wt ± S.D. (n=4).

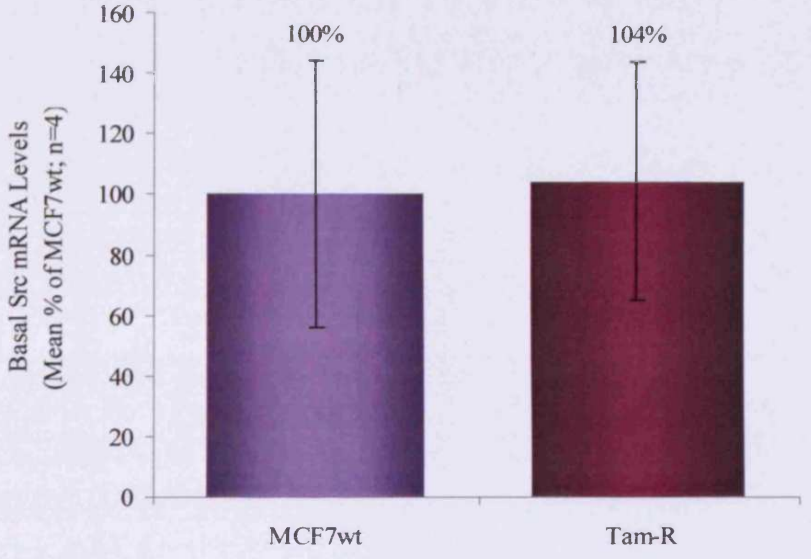

Figure 3.7 Basal Src mRNA levels in MCF7wt and Tam-R cells as measured by quantitative 'real-time' qPCR.

Total RNA was extracted from MCF7wt and Tam-R cells cultured under basal conditions as described in figure 3.6. Confirmation of Src expression levels in these cell-lines was obtained by qPCR using the DyNAmo™ SYBR-green qPCR kit and primers specific for Src. The fluorescence of the unknown samples was measured after each temperature cycle and compared, at an appropriate cycle threshold number, with the fluorescence of a defined standard curve in order to extrapolate amounts of starting template material present. The data, corrected for loading with β-actin, is presented as Mean % of MCF7wt ± S.D. (n=4).

Probe Set ID: 221281_at

Accession No: NM_005417

t-test: non-significant

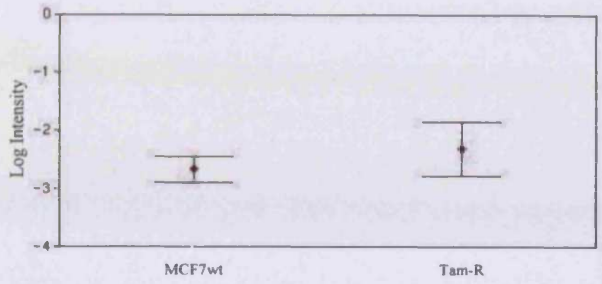

Probe Set ID: 213324_at

Accession No: AK024281

t-test: non-significant

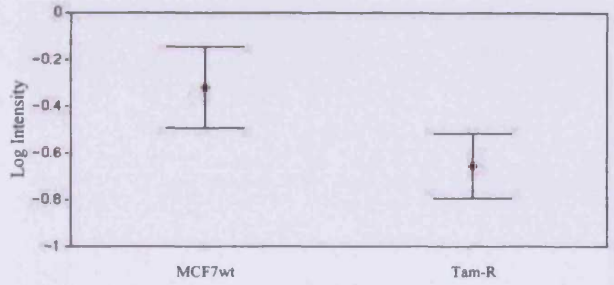

Probe ID: 221284_s_at

Accession No: NM_005417

t-test: non-significant

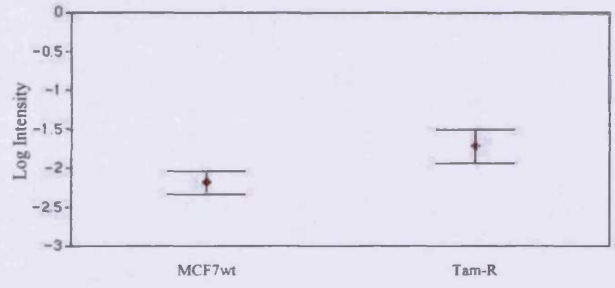

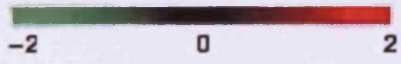

Figure 3.8 Expression profile of Src in MCF7wt and Tam-R cell-lines using the Affymetrix HG-U133A cDNA array.

MCF7wt and Tam-R cells were cultured under basal conditions to log-phase growth, at which point they were harvested for total RNA using TriReagent (Sigma) following the protocol supplied. RNA samples were DNase1 treated to remove any genomic DNA contamination and purified using the QIAGEN RNeasy mini kit. RNA samples were then quantified and tested for RNA integrity before being used for Affymetrix HG-U133A Genechip analysis (Central Biotechnology Services, Cardiff University, Cardiff, UK). The Genechip arrays were scanned and analysed using Microarray Suite 5.0 software (Affymetrix) and the quality of the data was verified through analyses of internal control gene expression. The gene expression profiles for Src shown above (presented as mean signal intensity for each transcript) were generated from median-normalised, log-transformed data for three independent probe sets using an on-line software package (www.genesifter.net). Data was provided courtesy of Dr. Julia Gee and Mr Richard McClelland.

phospho-specific antibody which recognises the phosphorylation of Src at Y419, an auto-phosphorylation site found in the activation loop of the kinase domain of Src and the phosphorylation of which is required for full kinase activity [123]. Densitometric analysis of the bands obtained revealed that phosphorylation of Src at Y419, and hence Src activation, was markedly higher in Tam-R cells, showing a highly significant 14.2-fold increase over MCF7wt cells (figure 3.9). A small, but non-significant, increase (1.4-fold) was seen for total Src protein in Tam-R cells versus MCF7wt (figure 3.9).

The increase in Src pY419 in Tam-R cells compared to MCF7wt was also evident with immunocytochemistry (figure 3.10). Using this technique it was also possible to observe the localisation of activated Src kinase within the cells. The small amount of Src detected in MCF7wt cells appeared to be predominantly cytoplasmic (figure 3.10A). In the Tam-R cells, however, Src pY419 was found both in the cytoplasm and at the plasma-membrane, and was particularly noticeable in membrane protrusions such as filopodia (figure 3.10B). The plasma-membrane localisation of Src pY419 in Tam-R cells was more evident when the cells were approaching confluency and thus forced to grow in closer proximity to neighbouring cells (figure 3.10C).

3.2.2.3 Src Substrates (Surrogate Markers of Src Activation)

If the activity of Src is increased in Tam-R cells then a corresponding increase in the activation of downstream components of Src signalling pathways might also be expected. To ascertain whether this was the case, the phosphorylation status of FAK and paxillin was examined in MCF7wt and Tam-R cells. These proteins were selected for two reasons: firstly, the Src-dependent phosphorylation of FAK and paxillin on specific tyrosine residues has been well established, and secondly, both of these proteins are known to be involved in the mechanisms that control cell attachment, motility and invasion, all of which are altered in the Tam-R cell-line.

SDS-PAGE/Western blotting was performed using phospho-specific anti-bodies to determine total and phosphorylated levels of FAK (Y397 and Y861) and paxillin (Y31) in MCF7wt and Tam-R cells. Figure 3.11 shows a modest,

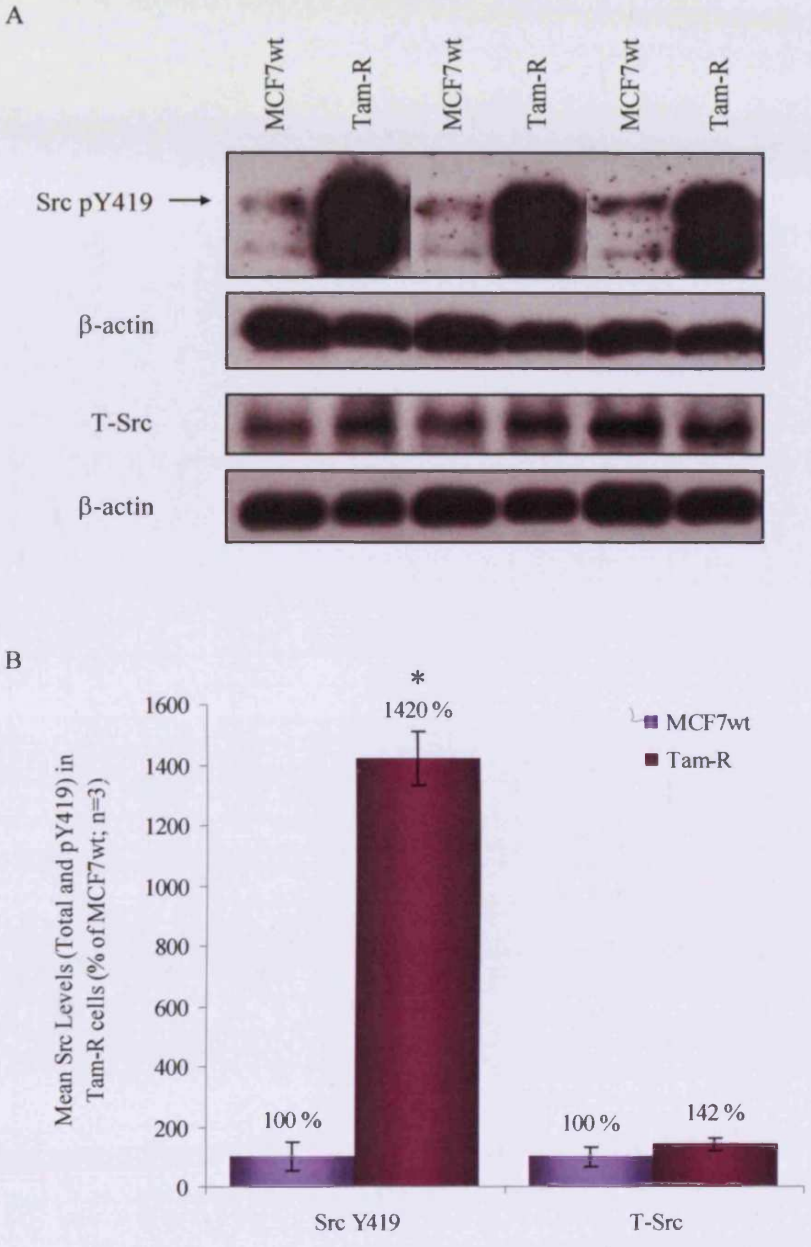

Figure 3.9 Basal levels of total and activated Src tyrosine kinase in MCF7wt and Tam-R cells as determined by Western blotting.

MCF7wt and Tam-R cells were cultured until they reached log-phase growth and then lysed for proteins as described in materials and methods (section 2.4.1). Total soluble protein (40μg) was subjected to SDS-PAGE/Western blot analysis and the membranes probed with antibodies specific for Src pY419 and total Src (A). Densitometry was conducted on the bands obtained and the data, corrected for loading with β-actin, presented as Mean % of MCF7wt ± S.D. (* $p<0.001$ vs. MCF7wt; n=3) (B).

A MCF7wt (x20)

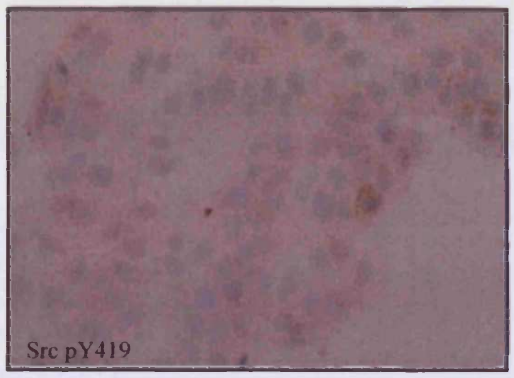

B Tam-R (x20)

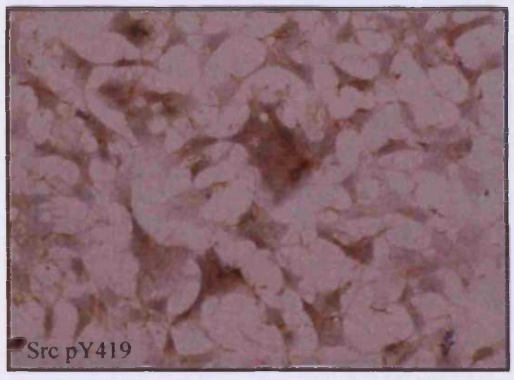

C Tam-R (x40)

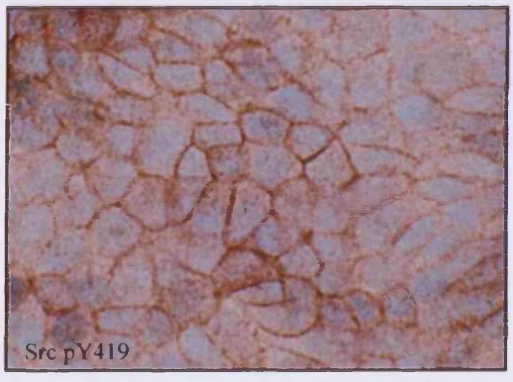

Figure 3.10 Levels and localisation of activated Src tyrosine kinase in basal MCF7wt and Tam-R cells as determined by immunocytochemistry.

MCF7wt and Tam-R cells were cultured on coverslips until they reached log-phase growth and then fixed using the ERICA technique as described in materials and methods (section 2.5.1.1). The fixed cells were assayed for Src pY419 using a phospho-specific antibody and the protein localisation was visualised using the DAKO EnVision™+ system peroxidase [DAB] kit as described in section 2.5.2. Representative images of MCF7wt (A) and Tam-R (B & C) cells were captured at x20 or x40 magnification using an Olympus BH-2 phase contrast microscope fitted with an Olympus DP-12 digital camera system.

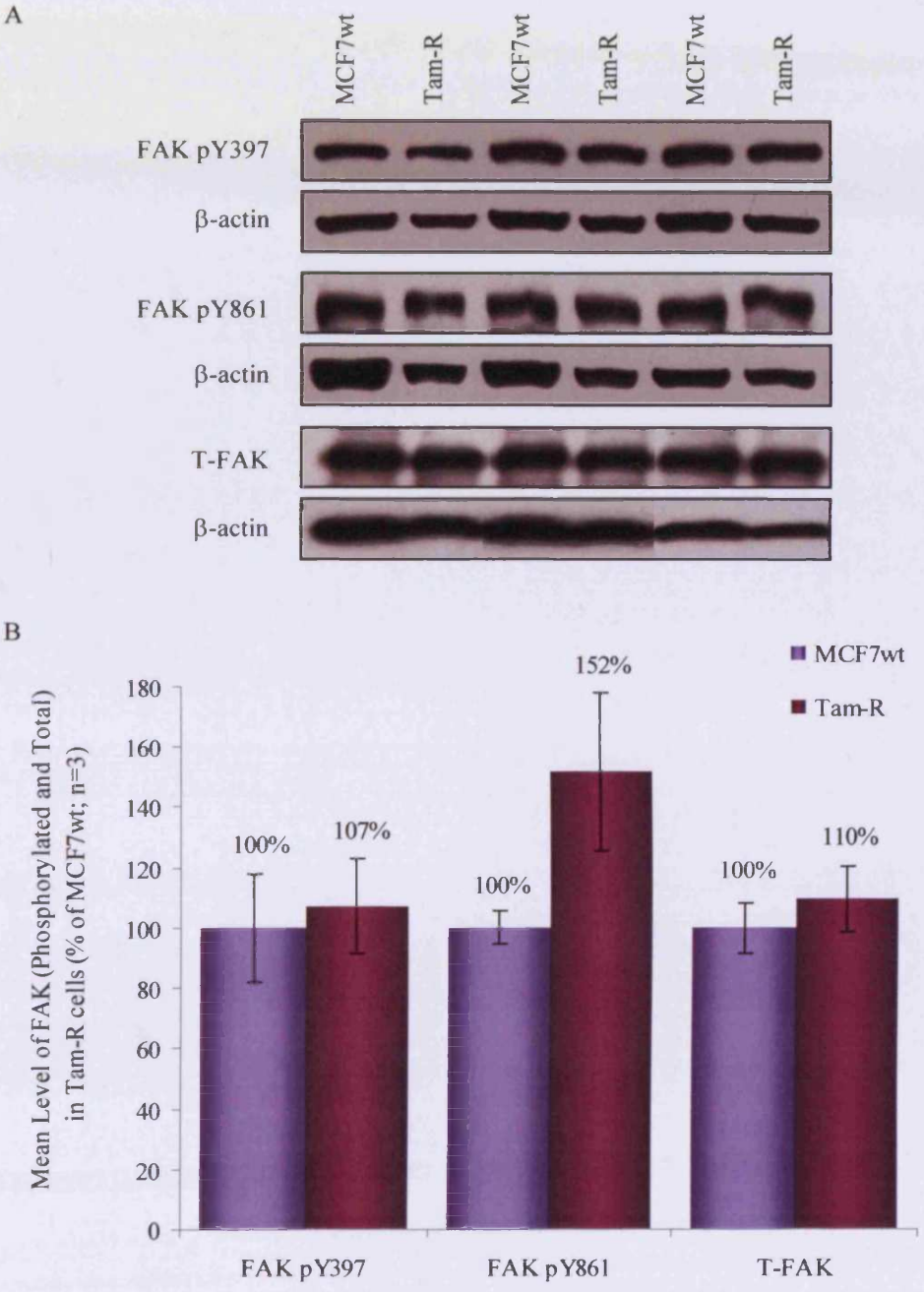

Figure 3.11 Basal levels of total and phosphorylated (Y397 & Y861) FAK in MCF7wt and Tam-R cell-lines as determined by Western blotting.

MCF7wt and Tam-R cells were cultured until they reached log-phase growth and then lysed for proteins as described in materials and methods (section 2.4.1). Total soluble protein (40μg) was subjected to SDS-PAGE/Western blot analysis and the membranes probed with antibodies specific for FAK pY397, pY861 and total FAK (A). Densitometry was conducted on the bands obtained and the data, corrected for loading with β-actin, presented as Mean % of MCF7wt ± S.D. (n=3) (B).

but non-significant, 1.5-fold increase in the phosphorylation of FAK at the Src-specific Y861 site in Tam-R cells compared to MCF7wt. Furthermore, measurement of paxillin phosphorylation at Y31 revealed a corresponding 1.6-fold increase in the Tam-R cells (figure 3.12). However, no differences were seen in either the phosphorylation of FAK at its auto-phosphorylation site (Y397), or in the total levels of either FAK or paxillin.

Focal adhesions are integrin-mediated sites of cell attachment whereby large protein complexes at the plasma-membrane link the cytoskeleton of the cell to the extra-cellular matrix. FAK phosphorylation and activation is important in cell-matrix attachment, motility and invasion due to its involvement in the regulation of focal adhesion formation and turnover. FAK is auto-phosphorylated on Y397 following integrin engagement and subsequent clustering on the plasma-membrane, which creates a docking site for the SH2 domain of Src. Src is then able to bind to FAK, being activated in the process, and goes on to phosphorylate additional residues on FAK. As this process is initiated by integrins, the auto-phosphorylation and Src-dependent phos-phorylation of FAK in MCF7wt and Tam-R cells grown on a fibronectin matrix was examined. Two time-points were used in order to look at both the immediate and longer-term effects of integrin stimulation with fibronectin.

MCF7wt and Tam-R cells were seeded onto fibronectin-coated dishes and left to attach for 30 minutes or cultured to log-phase growth (5 days) at 37°C before being lysed for total soluble proteins as described previously. SDS-PAGE/Western blot analysis revealed that phosphorylation of FAK Y397 and Y861 were both significantly increased (by 1.6-fold and 2.2-fold respectively) in Tam-R cells compared to MCF7wt following seeding on fibronectin for 30 minutes (figure 3.13). However, the differences in FAK phosphorylation at both sites between the two cell-lines were diminished after 5 days growth on fibronectin, with no significant difference in the levels of FAK Y397 or Y861 observed at this time point. No change in total FAK protein was seen between the two cell-lines at either time point.

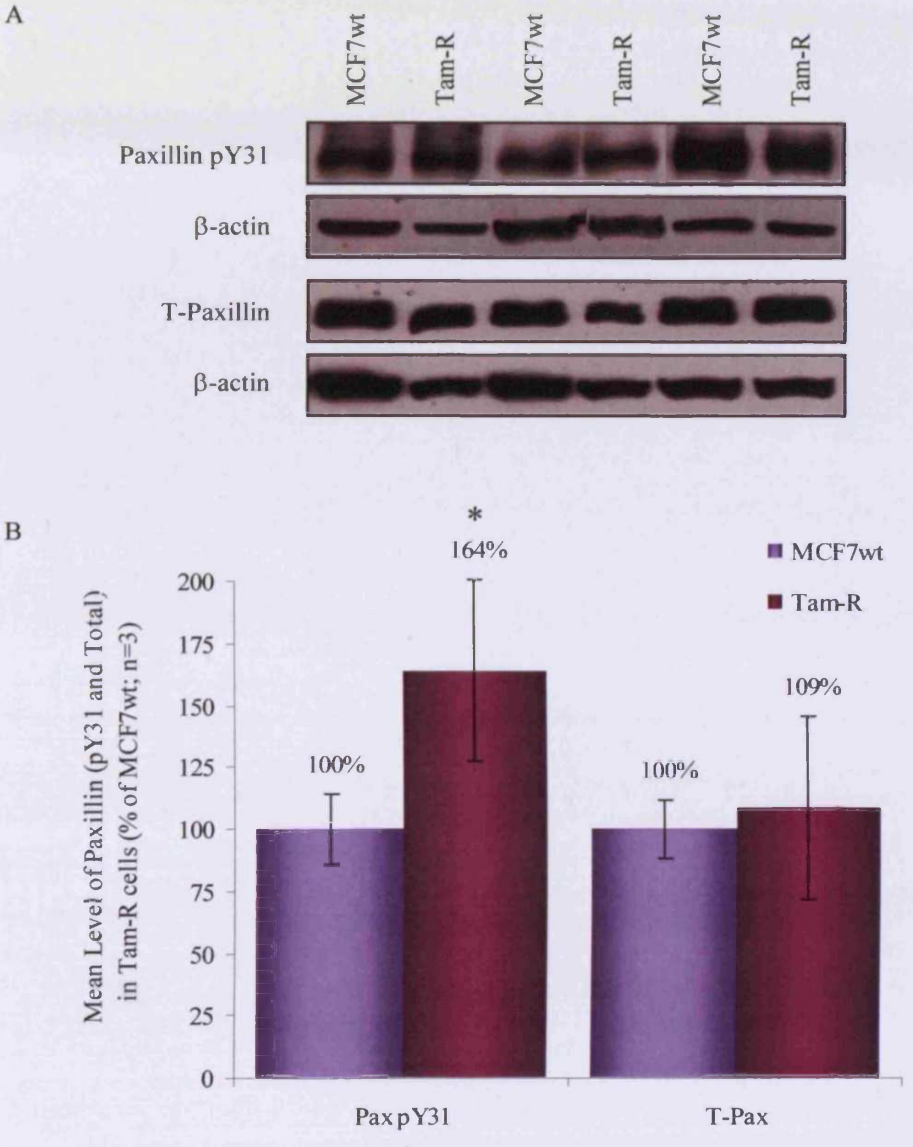

Figure 3.12 Basal levels of total and phosphorylated (Y31) paxillin in MCF7wt and Tam-R cell-lines as determined by Western blotting.

MCF7wt and Tam-R cells were cultured until they reached log-phase growth and then lysed for proteins as described in materials and methods (section 2.4.1). Total soluble protein (40μg) was subjected to SDS-PAGE/Western blot analysis and the membranes probed with antibodies specific for Paxillin pY31 and total Paxillin (A). Densitometry was conducted on the bands obtained and the data, corrected for loading with β-actin, presented as Mean % of MCF7wt ± S.D. (* $p<0.05$ vs. MCF7wt; n=3) (B).

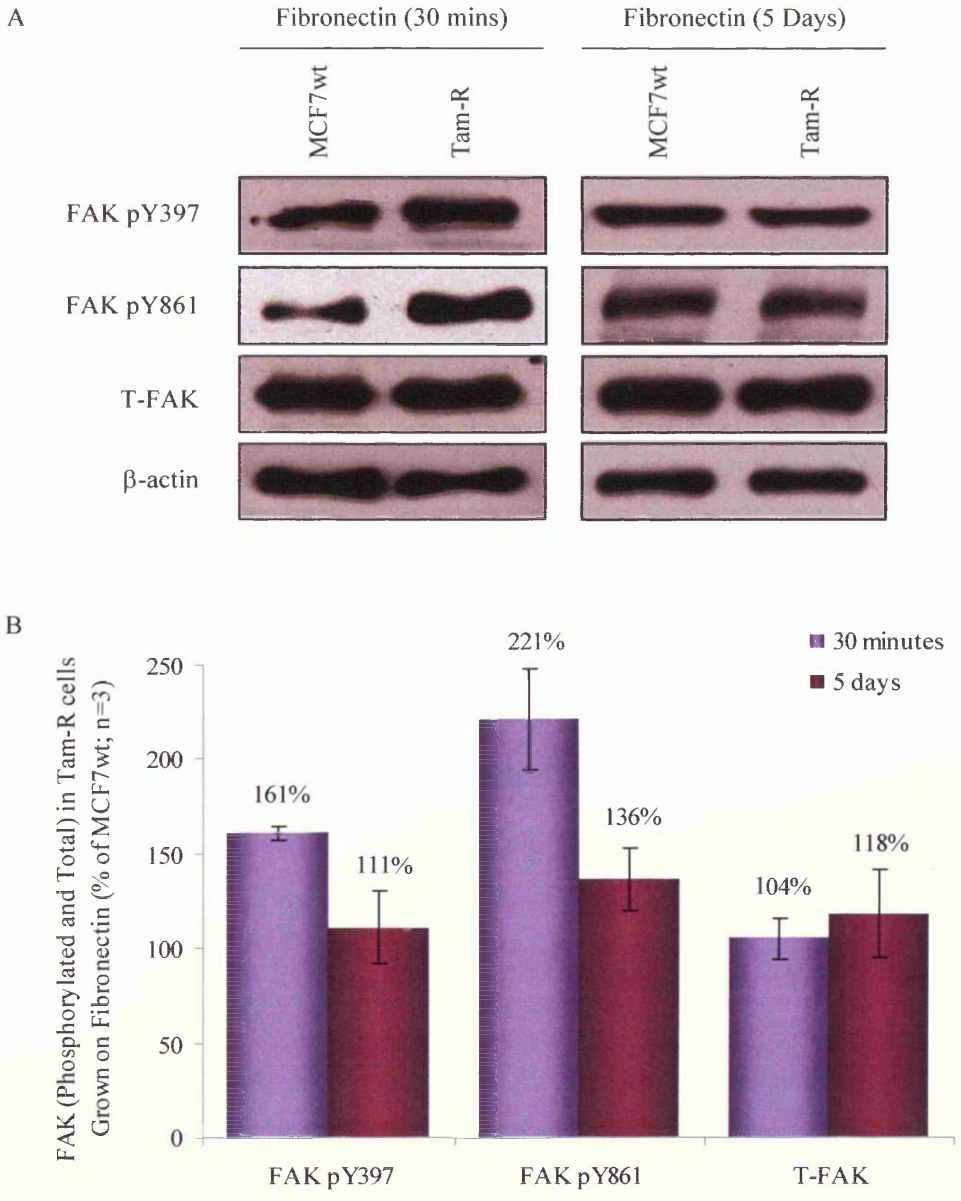

Figure 3.13 Levels of total and phosphorylated (Y397 and Y861) FAK in MCF7wt and Tam-R cell-lines exposed to a fibronectin matrix for either 30 minutes or 5 days.

MCF7wt and Tam-R cells were seeded onto 60mm fibronectin-coated Petri-dishes and left to either attach to the matrix for 30 minutes or to grow on the matrix for 5 days before being lysed for proteins as normal. Total soluble protein (40μg) was subjected to SDS-PAGE/ Western blot analysis and the membranes probed with antibodies specific for FAK pY397, FAK pY861 and total FAK (A). Densitometry was conducted on the bands obtained and the data, corrected for loading with β-actin, presented as Mean % of MCF7wt ± S.D. (n=3). N.B. MCF7wt values (100%) are not represented on the graph (B).

Phosphorylation of FAK by Src leads to the recruitment of additional proteins, such as paxillin and talin, to promote the formation of focal adhesion complexes. Moreover, FAK phosphorylation can also lead to the subsequent ERK 1/2-dependent activation of Calpain 2 which can result in proteolytic cleavage of FAK and focal adhesion disassembly. Thus, Src is able to regulate the rate at which focal adhesions are both formed and disassembled, a process known as focal adhesion turnover [170].

To examine the extent to which FAK is phosphorylated in response to fibronectin, the levels of pY397 and pY861 in MCF7wt and Tam-R cells that were either kept in suspension or seeded onto a fibronectin matrix for 30 minutes were compared. Figure 3.14 shows that the phosphorylation of FAK Y397 was increased in both MCF7wt and, to a greater extent, Tam-R cells following seeding onto a fibronectin matrix in comparison with the cells maintained in suspension. Additionally, a marked increase in the phosphorylation of FAK at the Src-specific Y861 site was also seen in Tam-R cells (375% of cells in suspension); however, the corresponding increase observed in MCF7wt cells was more modest (159% of cells in suspension). Furthermore, a small increase in Src activation was evident in both cell-lines following seeding onto a fibronectin matrix, possibly due to the increased FAK Y397 phosphorylation reported above. Once again, the levels of total FAK and Src in either cell-line were unchanged.

These results suggest that the extent of FAK phosphorylation, and hence the rate of focal adhesion formation/turnover, might be increased in Tam-R cells. An increase in the rate of focal adhesion formation might affect the rate of cell attachment, and so this was investigated in the Tam-R cell-line using a cell attachment time-course assay. These assays are similar to the normal cell attachment assay in that cells were seeded into a 96-well plate and left to attach for 50 minutes at 37°C. However, during the time-course assay, medium containing unattached cells was removed at given time-points, namely 10, 20, 30 40 and 50 minutes, and replaced with PBS. The cells were kept in PBS until the end of the experiment when the number of attached cells

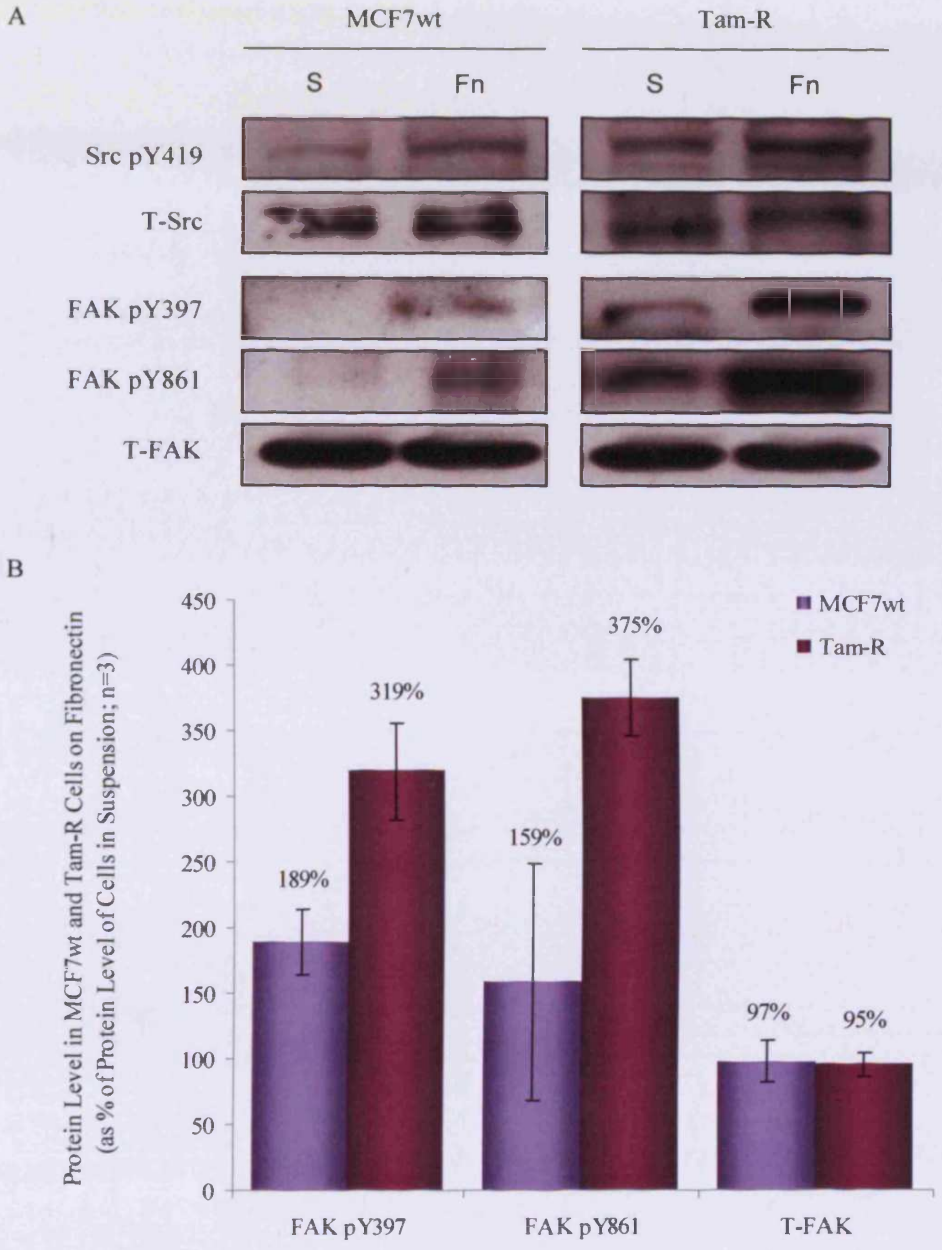

Figure 3.14 Induction of FAK phosphorylation (Y397 and Y861) in MCF7wt and Tam-R cells either in suspension or seeded onto a fibronectin matrix (30 minutes).

Following Trypsin/EDTA dispersion, MCF7wt and Tam-R cells were either kept in suspension (S) or seeded onto 60mm fibronectin-coated Petri-dishes (Fn) for 30 minutes before being lysed for proteins as normal. Total soluble protein (40µg) was subjected to SDS-PAGE/ Western blot analysis and the membranes probed with antibodies specific for Src pY419, total Src, FAK pY397, FAK pY861 and total FAK (A). Densitometry was conducted on the bands obtained for pY397, pY861 and total FAK and the data, corrected for loading with total FAK, presented as Mean % of Protein Levels in Cells in Suspension ± S.D. (n=3) (B). N.B. Values for protein levels in cells in suspension (100%) are not represented on the graph.

was quantified using the MTT assay as normal. Figure 3.15 shows the rate of cell-attachment for MCF7wt and Tam-R cells on uncoated (A) or fibronectin-coated (B) surfaces. In both cases, the rate of cell-attachment in the Tam-R cells was greater than that of MCF7wt cells, with the largest difference seen within the initial 20 minute period.

To expand upon these findings, the rate of cell-spreading in MCF7wt and Tam-R cells following attachment was also examined. Cells were seeded onto either uncoated or fibronectin-coated 60mm dishes and placed at 37°C. Then, to monitor the progress of the cells as they attached and spread, representative images of the live cells were captured 1-, 3-, 6- and 24-hours after seeding using a Leica DM-IRE2 inverted microscope fitted with a Hoffman condenser.

Figure 3.16 shows that the MCF7wt cells had attached to the uncoated surface after 1-3 hours, but were yet to show any signs of spreading and still displayed a rounded appearance. After 6 hours, however, it was evident that the cells were in the early stages of spreading as they appeared larger and changes in their morphology were more noticeable. After 24 hours, attachment and spreading of the MCF7wt cells was complete. In contrast, cell-spreading in Tam-R cells was observed just 1 hour after seeding, with a high number of cells appearing to be fully attached and displaying characteristic morphological traits such as filopodia after just 3 hours. Similar patterns were seen for both cell-lines when seeded onto a fibronectin-coated surface (figure 3.17); however, attachment and spreading of the Tam-R cells on fibronectin seemed to occur at a faster rate, with the proportion of spread cells after just 1 hour being much higher than that seen on the uncoated surface.

3.2.3 Regulation of Src Kinase Activity in Tam-R Cells

Src activity can be regulated in a number of different ways as discussed in chapter one. The most well studied mechanisms of Src regulation, however, involve either the modulation of the phosphorylation status of conserved tyrosine residues found in the protein, such as Y530, or direct protein-protein interactions via the SH2 and SH3 protein binding domains. As such, these are the two mechanisms that are examined in this thesis.

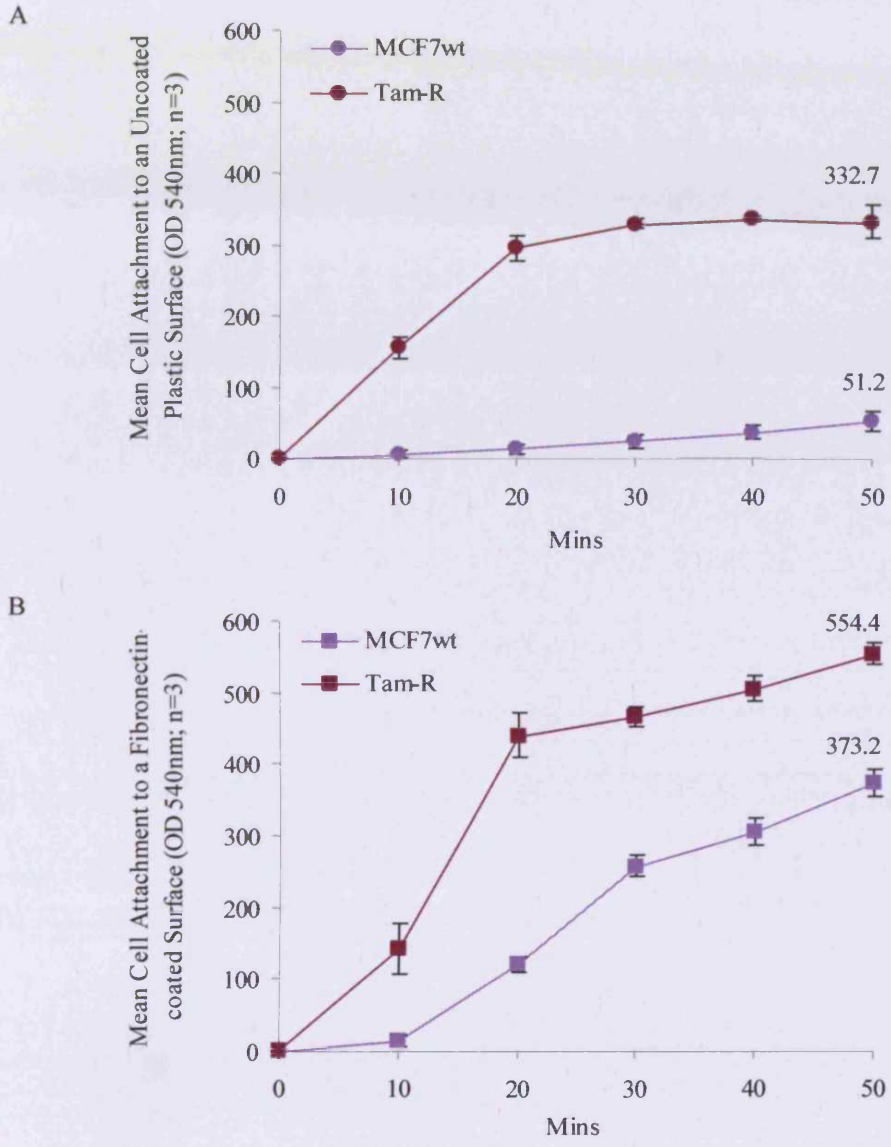

Figure 3.15 Rate of MCF7wt and Tam-R cell-attachment on uncoated and matrix-coated surfaces as measured using a cell attachment time-course assay.

The rate of MCF7wt and Tam-R cell attachment to uncoated (A) or fibronectin-coated (B) surfaces was measured using a cell attachment time-course assay. Cells ($4x10^4$) were seeded in W+5% ± Tam (100nM) into the wells of a 96-well plate which were either uncoated or had been pre-treated with fibronectin. Cells were left to attach for up to 50 minutes at 37°C. During the course of the assay, medium containing unattached cells was removed at the given time points and replaced with PBS. The attached cells were kept in PBS until the end of the experiment when the MTT assay was carried out as normal. Data is presented as Mean Cell Attachment (OD_{540}) ± S.D. ($n \geq 3$).

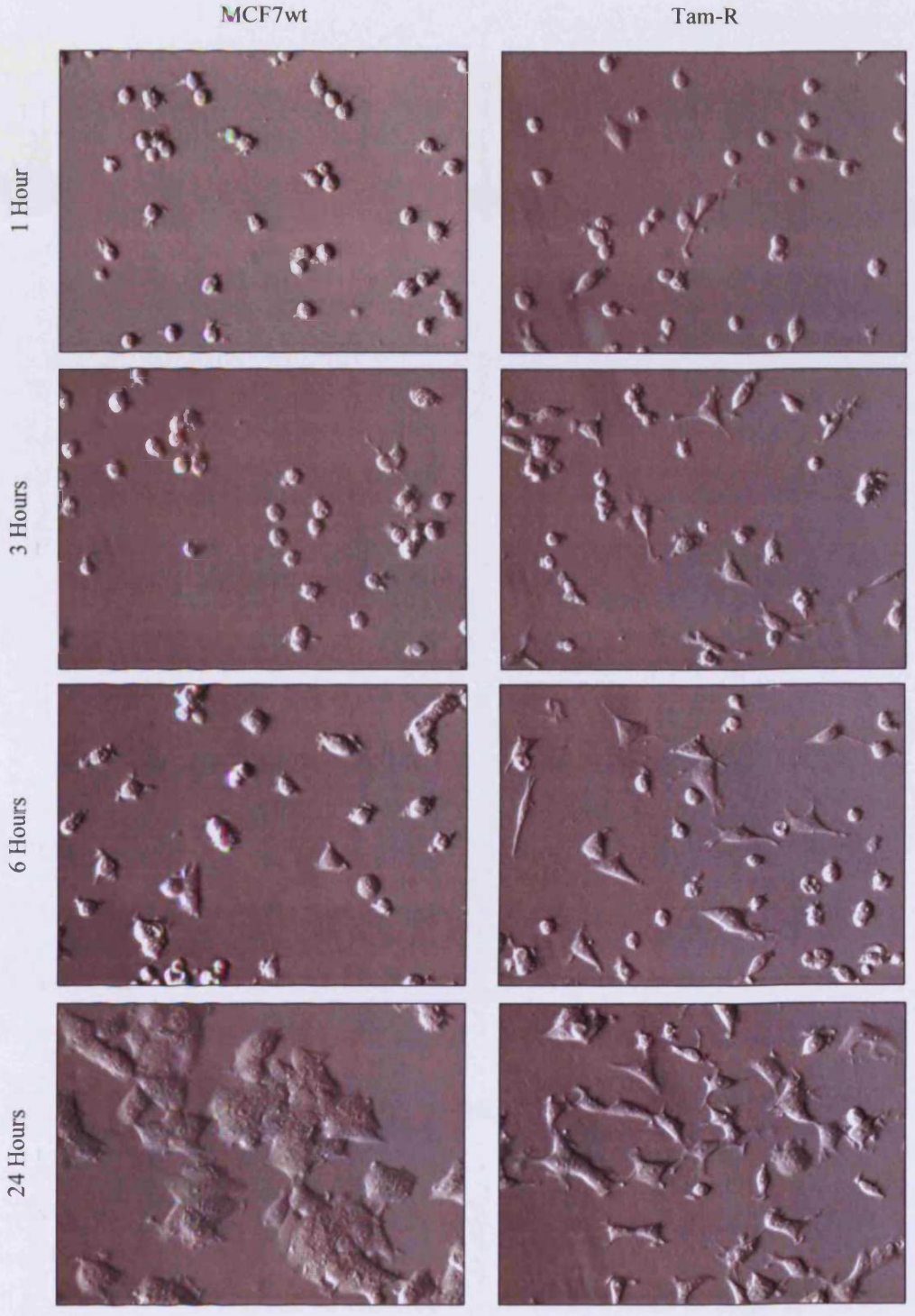

Figure 3.16 MCF7wt and Tam-R cell-spreading on an uncoated plastic surface.

MCF7wt and Tam-R cells were seeded onto an uncoated 60mm dish and placed at 37°C. Representative images of the live cells at 20x magnification were captured 1-, 3-, 6- and 24-hours after seeding using a Leica DM-IRE2 inverted microscope fitted with a Hoffman condenser and a Hamamatsu C4742-96 digital camera.

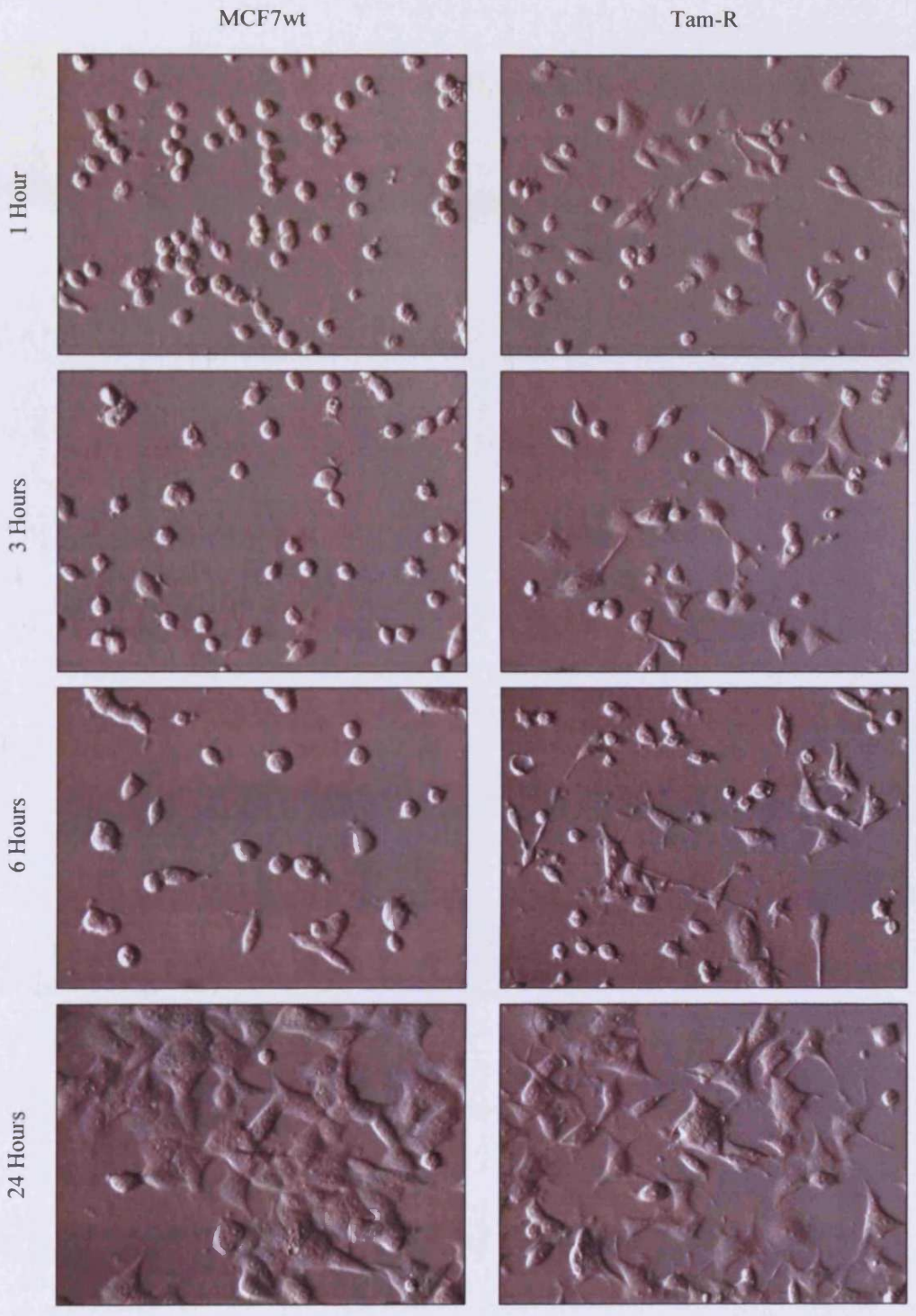

Figure 3.17 MCF7wt and Tam-R cell-spreading on a fibronectin-coated surface.

MCF7wt and Tam-R cells were seeded onto a fibronectin-coated 60mm dish and placed at 37°C. Representative images of the live cells at 20x magnification were captured 1-, 3-, 6- and 24-hours after seeding using a Leica DM-IRE2 inverted microscope fitted with a Hoffman condenser and a Hamamatsu C4742-96 digital camera.

3.2.3.1 Modulation of Src Y530 phosphorylation is unlikely to play a role in the regulation of Src activity in Tam-R cells.

Y530 is a conserved amino acid found in the negative-regulatory tail of Src which, when phosphorylated, is able to interact with the SH2 domain of Src and induce a conformational change in the protein structure that blocks the active site of the kinase domain, thus inactivating the kinase. There are a number of kinase and phosphatase enzymes known to regulate Y530 phosphorylation; two major contributors are CSK, which phosphorylates Y530 to inactivate Src, and PTP1B, which can de-phosphorylate Y530 leading to Src kinase activation.

To determine whether this mechanism might play a role in the regulation of Src activity in MCF7wt and Tam-R cells, levels of CSK and PTP1B were measured using SDS-PAGE/Western blotting. The results revealed no significant differences in the levels of CSK or PTP1B between the two cell-lines, suggesting that the differences in Src activity observed are not a result of the aberrant activity of these two proteins (figure 3.18). In support of this, measurement of basal Src Y530 phosphorylation in MCF7wt and Tam-R cells also showed no significant difference between the two cell-lines (figure 3.19). This result, therefore, serves to preclude the involvement of other kinase and phosphatase enzymes that may also regulate Src kinase activity in this manner.

3.2.3.2 Growth-factor-receptor signalling may contribute to the up-regulation of Src activity in Tam-R cells.

Another mechanism of Src activation is via the direct interaction of Src with other proteins, including receptor tyrosine kinases such as EGFR and c-erbB2. Over-expression and/or up-regulation of EGFR is associated with increased Src activity both *in vitro* and in the clinic [131, 198, 199], and can lead to a synergistic relationship between the two proteins in the cell [131, 145, 200, 201]. Increased EGFR activity has also been linked to tumour progression and metastasis [178, 202], possibly via increased MAP kinase activation [203, 204] or through interactions with FAK [205], and can lead to a poor prognosis [179]. Furthermore, increased expression and activation of EGFR is

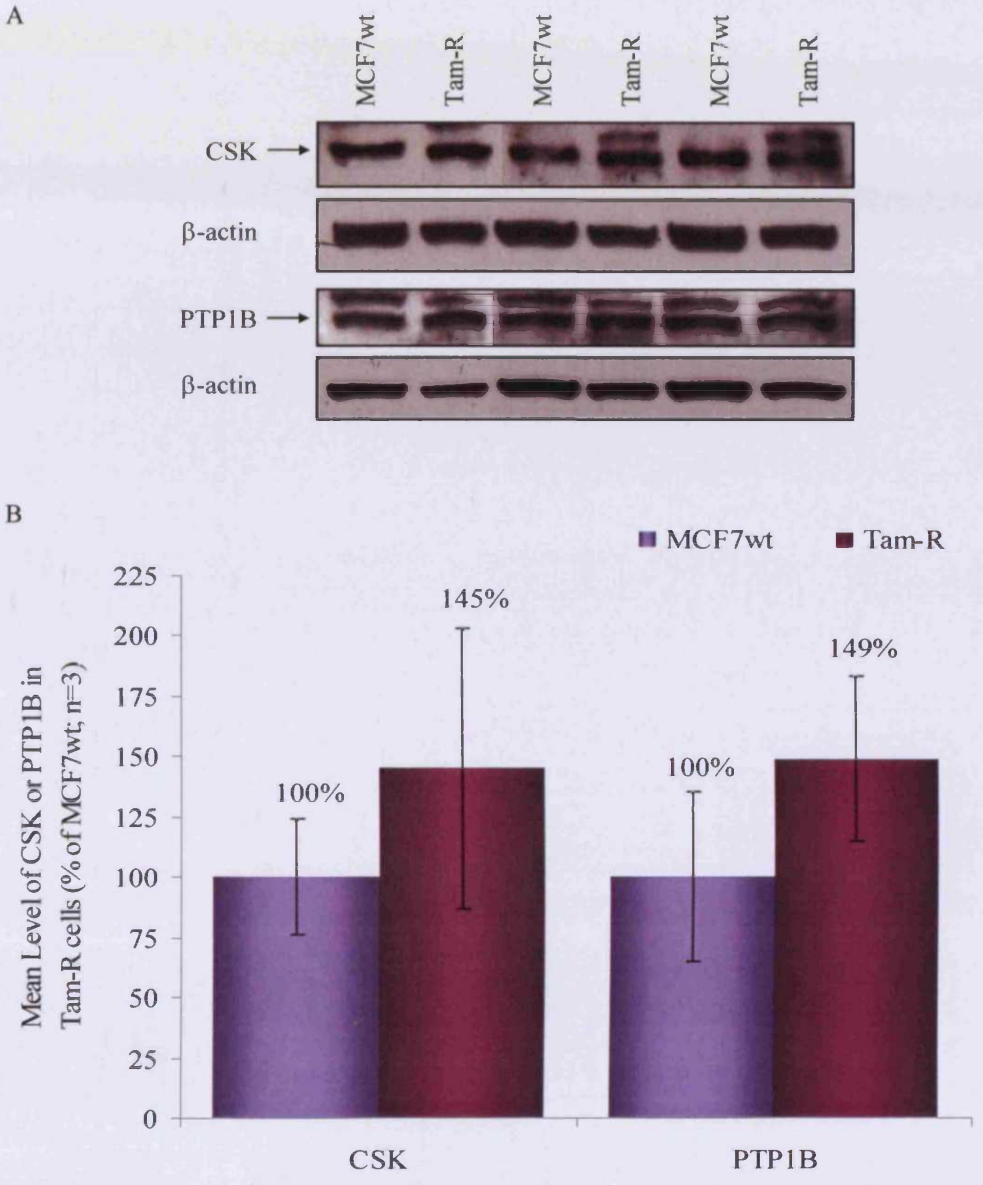

Figure 3.18 Basal levels of CSK and PTP1B in MCF7wt and Tam-R cells as determined by Western blotting.

MCF7wt and Tam-R cells were cultured until they reached log-phase growth and then lysed for proteins as described in materials and methods (section 2.4.1). Total soluble protein (40μg) was subjected to SDS-PAGE/Western blot analysis and the membranes probed with antibodies specific for CSK and PTP1B (A). Densitometry was conducted on the bands obtained and the data, corrected for loading with β-actin, presented as Mean % of MCF7wt ± S.D. (n=3) (B).

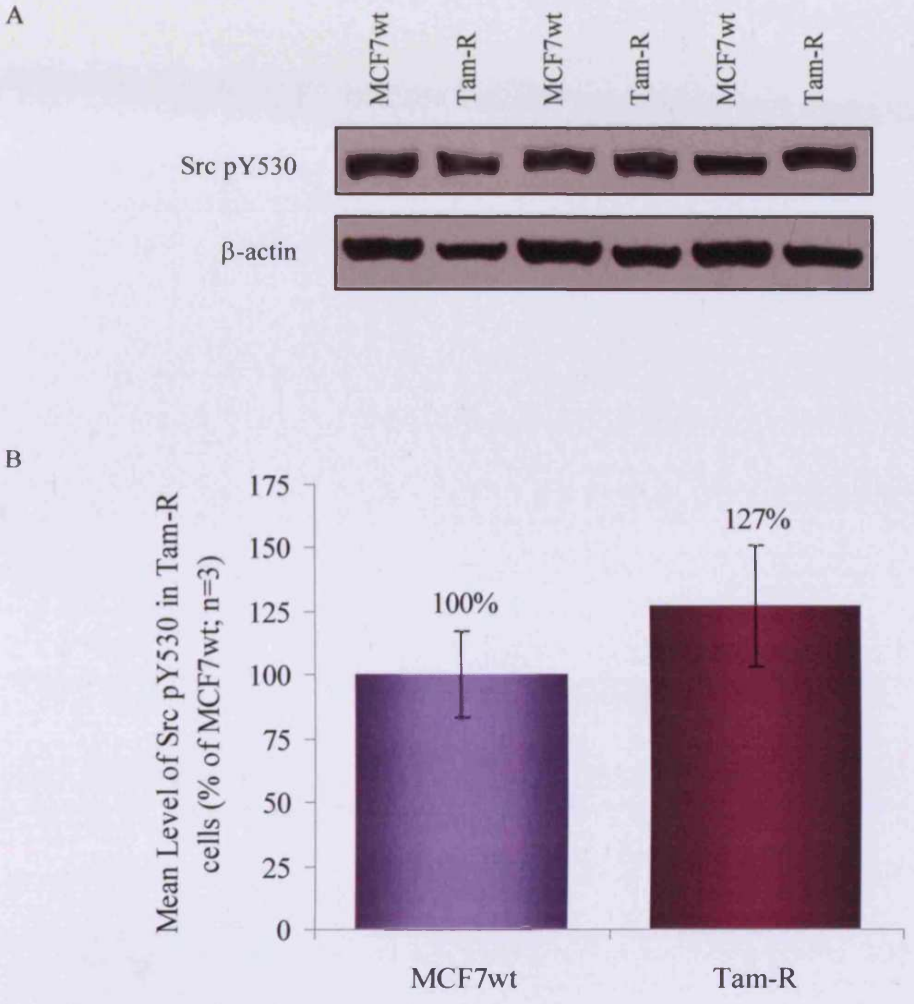

Figure 3.19 Basal levels of Src tyrosine kinase phosphorylated at Y530 in MCF7wt and Tam-R cells as determined by Western blotting.

MCF7wt and Tam-R cells were cultured until they reached log-phase growth and then lysed for proteins as described in materials and methods (section 2.4.1). Total soluble protein (40μg) was subjected to SDS-PAGE/Western blot analysis and the membranes probed with an antibody specific for Src pY530 (A). Densitometry was conducted on the bands obtained and the data, corrected for loading with β-actin, presented as mean % of MCF7wt ± S.D. (n=3) (B).

associated with resistance to both tamoxifen and the pure anti-oestrogen, fulvestrant [23, 206, 207]. Since our laboratory has previously shown EGFR activation and signalling to be important for the proliferation of Tam-R cells *in vitro* [66, 70, 75], its potential role in the aberrant activation of Src kinase in these cells was also investigated.

To study the relationship which may exist between Src and EGFR in Tam-R cells, verification of the published reports that demonstrate increased EGFR activity in these cells was first required. For this, SDS-PAGE/Western blotting was used to measure the levels of phosphorylated and total EGFR protein in both cell-lines (figure 3.20). The phosphorylation sites selected as markers for EGFR activity were Y845, as this is a known Src-specific phosphorylation site, and Y1068, which is important for the EGFR-MAP kinase mitogenic signalling pathway shown to be up-regulated in Tam-R cells. Densitometric analysis of the bands obtained showed a 3.1- and 8.8-fold increase in EGFR phosphorylation at Y845 and Y1068 respectively in the Tam-R cells. Furthermore, these experiments confirmed increased EGFR expression in the Tam-R cells, which demonstrated total EGFR protein levels 8.3-fold higher than those in the MCF7wt cell-line.

EGFR activity was modulated in Tam-R cells in order to ascertain any consequential effects on the activation of Src. TGFα was used to stimulate EGFR signalling in the Tam-R cells as Knowlden *et al.* have previously shown it to be expressed by these cells as part of an autocrine regulatory mechanism [70]. To down-regulate EGFR activity, the small molecule tyrosine-kinase-inhibitor gefitinib (Iressa™; TKI), which is an effective inhibitor of the intrinsic kinase activity of EGFR [70], was used. Tam-R cells were serum starved in wDCCM for 24 hours before being treated with TGFα (10ng/ml; 30 minutes) or gefitinib (1μM; 24 hours), with the appropriate vehicle added to the control cells for the same duration. SDS-PAGE/Western blotting analysis confirmed that TGFα increased phosphorylation of EGFR on Y1068 (figure 3.21A). Conversely, phosphorylation of EGFR at this site was virtually undetectable following treatment with gefitinib. Further analysis of these samples for Src

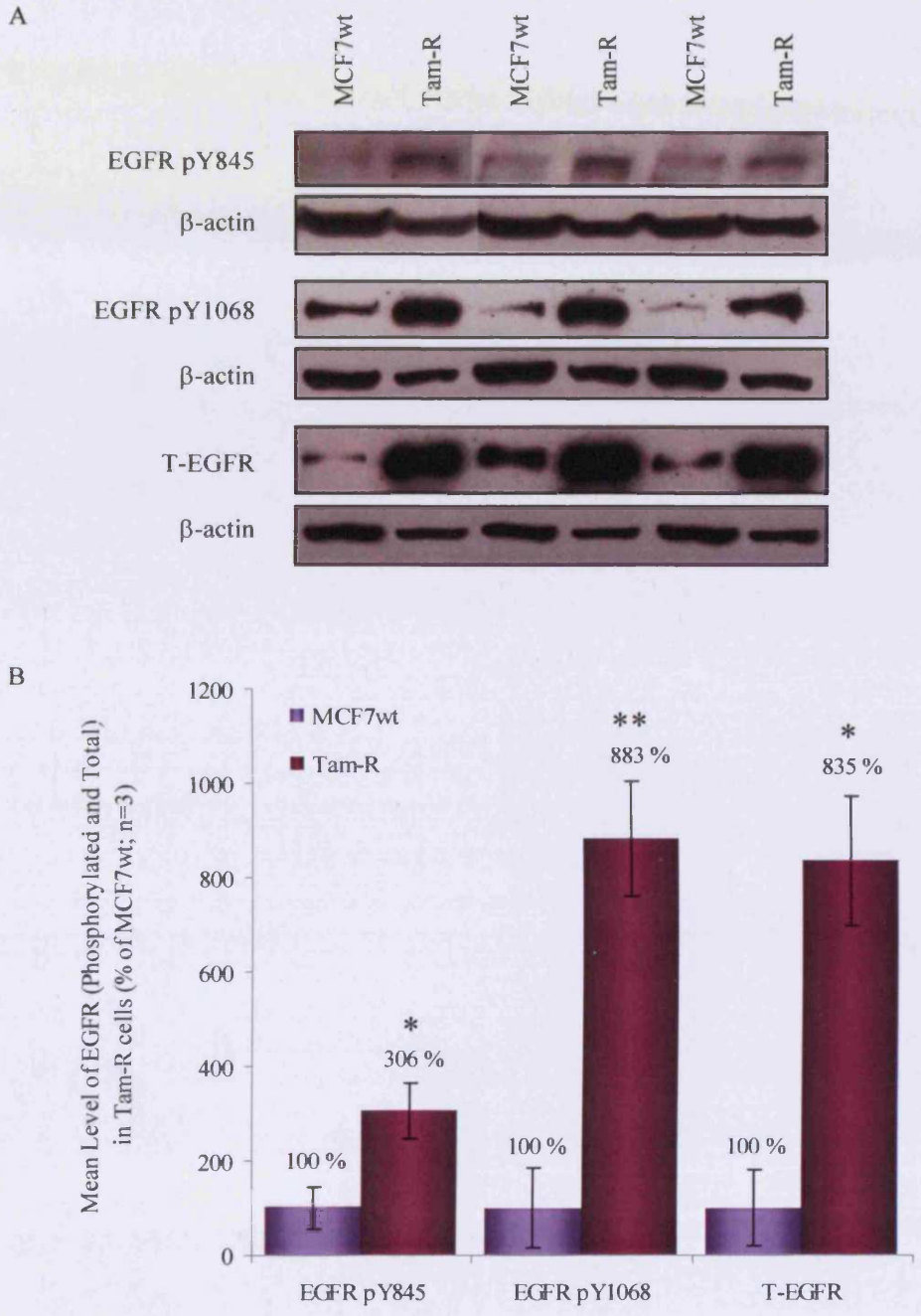

Figure 3.20 Basal levels of total and phosphorylated (Y845 & Y1068) EGFR in MCF7wt and Tam-R cell-lines as determined by Western blotting.

MCF7wt and Tam-R cells were cultured until they reached log-phase growth and then lysed for proteins as described in materials and methods (section 2.4.1). Total soluble protein (40μg) was subjected to SDS-PAGE/Western blot analysis and the membranes probed with antibodies specific for EGFR pY845, pY1068 and total EGFR (A). Densitometry was conducted on the bands obtained and the data, corrected for loading with β-actin, presented as Mean % of MCF7wt ± S.D. (* $p<0.01$ vs. MCF7wt ** $p<0.001$ vs. MCF7wt; n=3) (B).

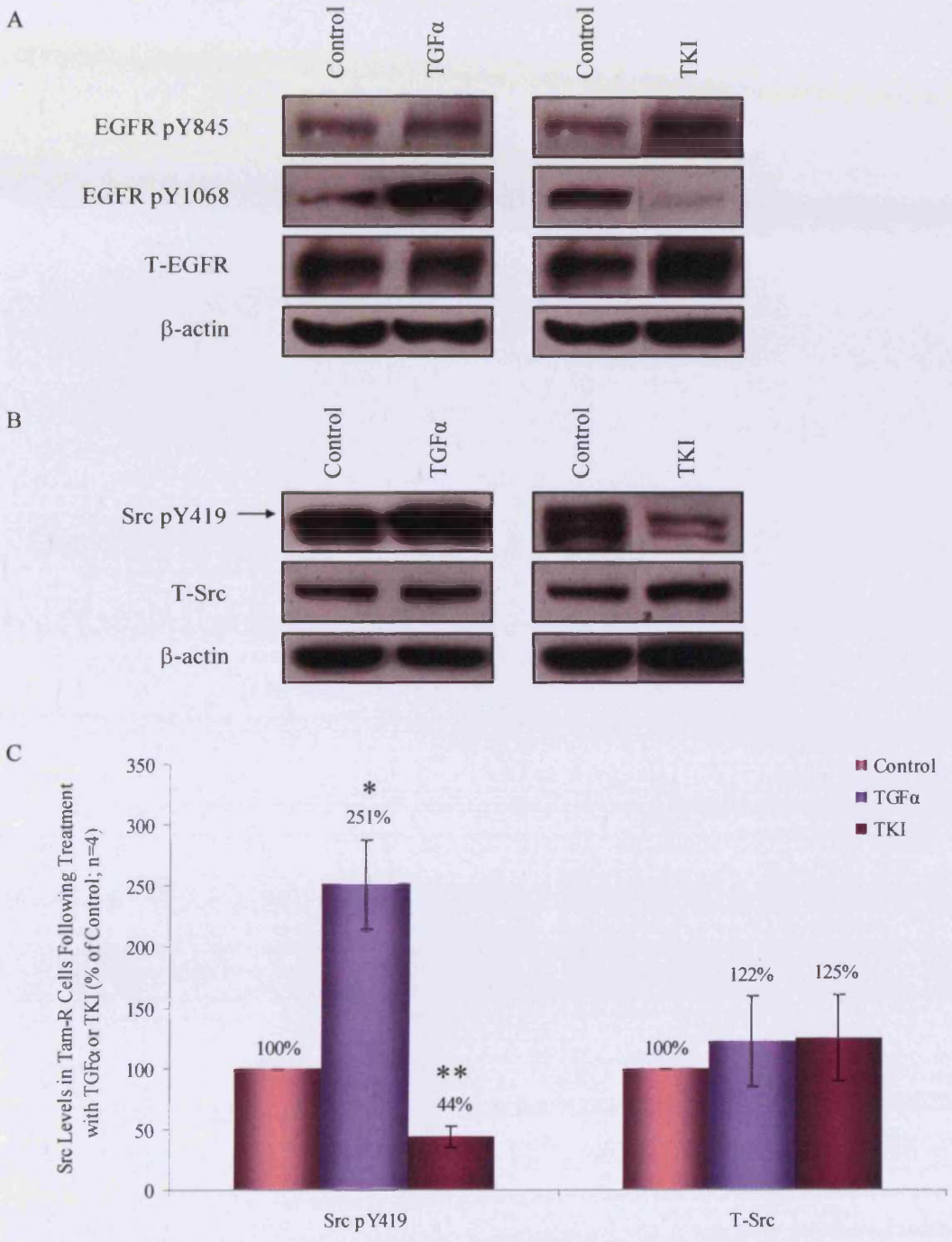

Figure 3.21 Src kinase activity in Tam-R cells following modulation of EGFR signalling as determined by Western blotting.

Tam-R cells were cultured to log-phase growth. Following a period of serum starvation (wDCCM; 24hrs) cells were treated with TGFα (10ng/ml; 30 mins), gefitinib (Iressa™ [TKI]; 1μM; 24 hrs) or vehicle only. Cells were lysed and total soluble protein (40μg) subjected to SDS-PAGE/Western blot analysis. Membranes were then probed with antibodies specific for EGFR pY845, pY1068 and total EGFR (A), and for Src pY419 and total Src (B). Densitometry was conducted on the bands obtained for Src and the data, corrected for loading with β-actin, presented as Mean % of Control ± S.D. (* $p<0.01$ vs. Control ** $p<0.001$ vs. Control; n=4) (C).

revealed a corresponding 2.5-fold increase in Src activation following stimulation of these cells with TGFα, whereas treatment with gefitinib reduced Src activity by over 50%. In both cases, no significant change in total Src protein levels was seen (figure 3.21B and figure 3.21C).

Tam-R cells express additional receptor tyrosine kinases, such as c-erbB2 and IGF-1R, which, as well as promoting cell growth, may also affect Src kinase activity. Therefore, the contribution of these receptor tyrosine kinases to Src activation in Tam-R cells was investigated by using the appropriate ligands to stimulate receptor activation. On reaching log-phase growth, Tam-R cells were serum starved in wDCCM for 24 hours and treated with EGF, TGFα, amphiregulin, heregulin-β1 or IGF II. All growth-factors were used at 10ng/ml and treatment duration was 30 minutes. SDS-PAGE/Western blotting of the cell lysates showed increases in Src activity of between 2.7- and 4.5-fold compared to control following treatment with erb B receptor ligands, with amphiregulin and heregulin-β1 eliciting the greatest effects (figure 3.22). A modest 2-fold increase was also seen with stimulation of IGF-1R with IGF II.

To further elucidate a role for these receptor tyrosine kinases in the activation of Src in Tam-R cells, a panel of specific pharmacological inhibitors was used to reduce their activity. Tam-R cells were serum starved in wDCCM for 24 hours and then treated with gefitinib (Iressa™ [TKI]; 1μM), trastuzumab (Herceptin® [HRC]; 100nM), AG1024 (5μM), PD098059 (25μM) or vehicle only. AZM555130 (1μM), a potent inhibitor of Src activity (see chapter 4), was also used in these experiments as a positive control for Src inhibition. All treatments were for 24 hours, after which the cells were lysed and subjected to SDS-PAGE/Western blot analysis for Src pY419 and total Src protein levels (figure 3.23). As already seen in figure 3.21, treatment of Tam-R cells with gefitinib reduced Src activation by approximately 50%; however, inhibition of c-erbB2 with trastuzumab did not appear to have any effect on Src activation. Inhibition of MAP kinase with the MEK inhibitor PD098059 did not alter Src activation levels, which suggests that regulation of Src by EGFR is not a down-stream effect of this signalling pathway. Furthermore, inhibition of

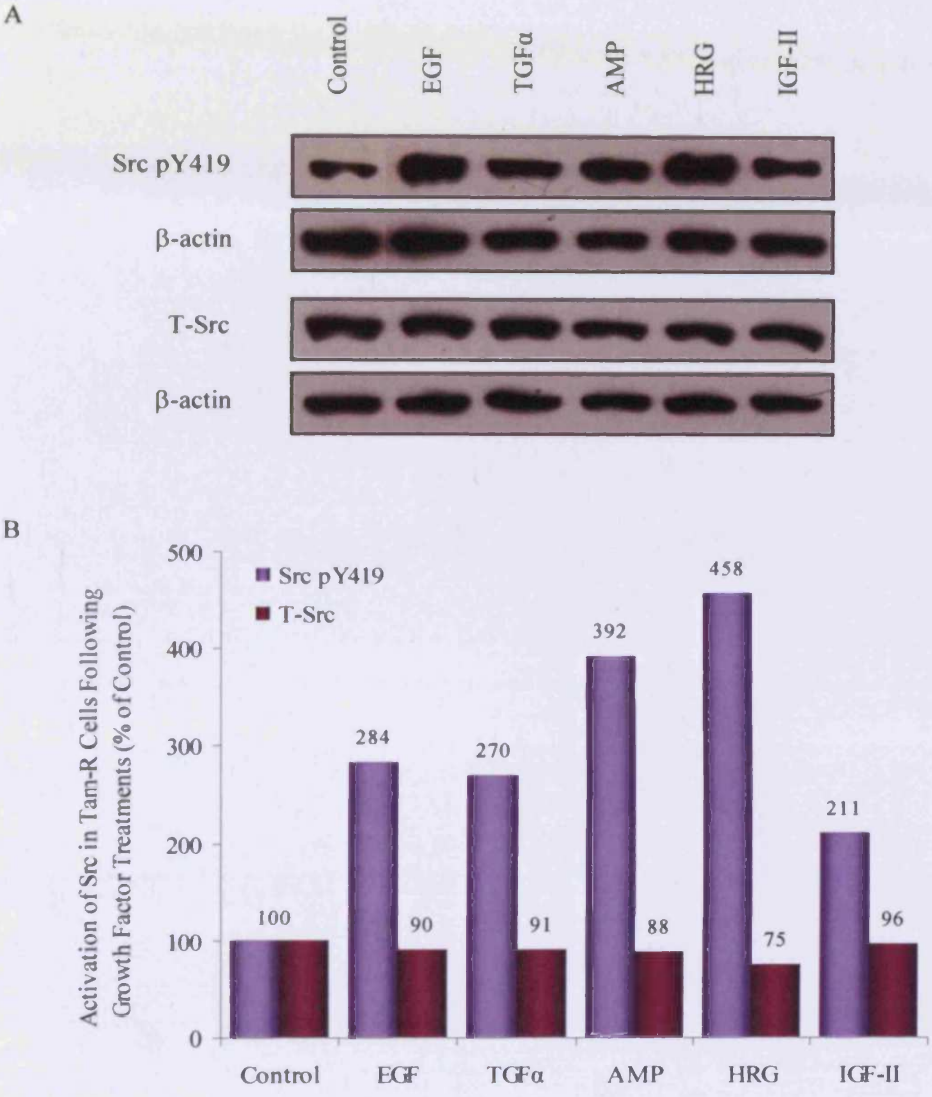

Figure 3.22 Effect of growth factor treatment on Src activation in Tam-R cells as determined by Western blotting.

Tam-R cells were cultured until they reached log-phase growth. Following a period of serum starvation (wDCCM; 24hrs) cells were treated with EGF (10ng/ml), TGFα (10ng/ml), amphiregulin (10ng/ml), heregulin-β1 (10ng/ml), IGF-II (10ng/ml) or vehicle only. All treatments were for 30 minutes, after which the cells were lysed for proteins. Total soluble protein (40μg) was subjected to SDS-PAGE/Western blot analysis and the membranes probed with antibodies specific for Src pY419 and total Src (A). Densitometry was conducted on the bands obtained and the data, corrected for loading with β-actin, presented as % of Control (B).

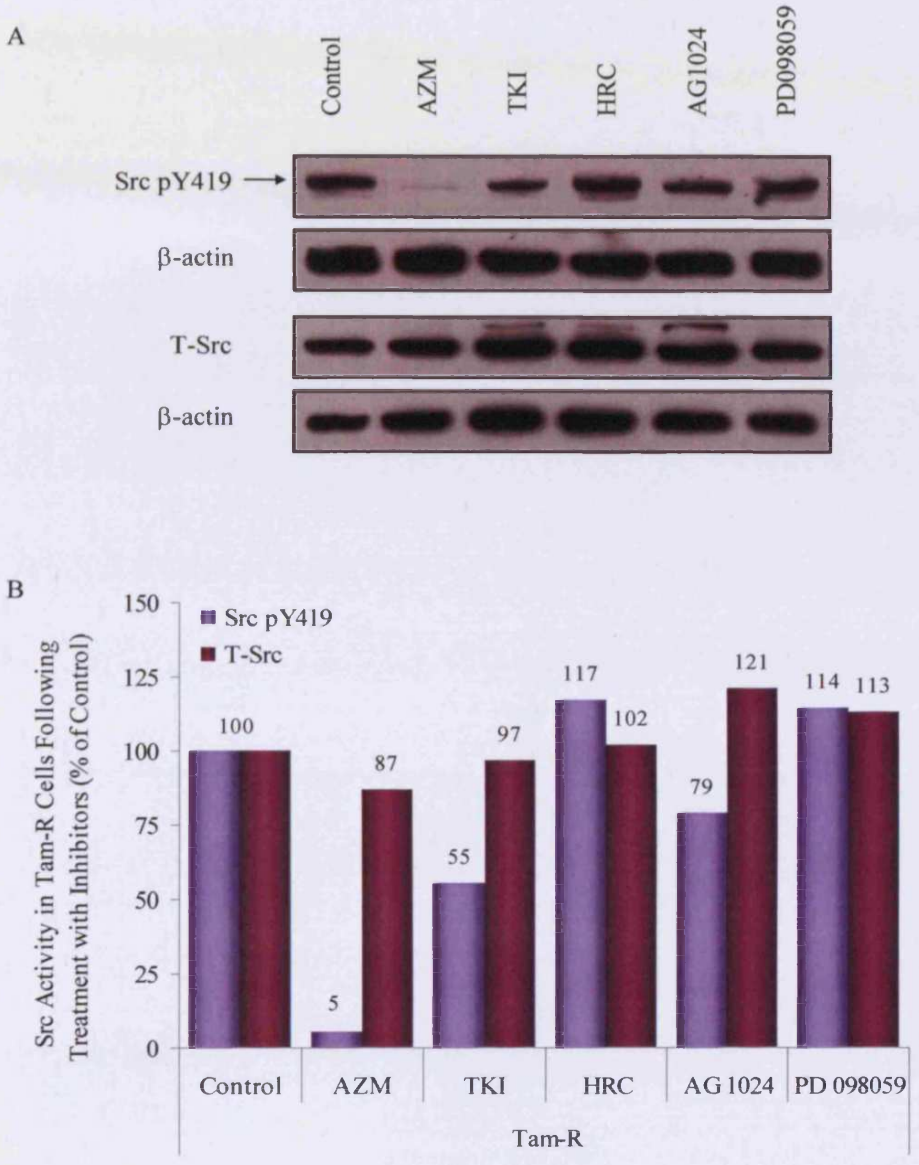

Figure 3.23 Effect of inhibition of various cell-signalling pathways on Src activation in Tam-R cells as determined by Western blotting.

Tam-R cells were cultured until they reached log-phase growth. Following a period of serum starvation (wDCCM; 24hrs) cells were treated with AZM555130 (1μM), gefitinib (Iressa™ [TKI]; 1μM), trastuzumab (Herceptin® [HRC]; 100nM), AG1024 (5μM), PD 098059 (25μM) or vehicle only. All treatments were for 24 hours, after which the cells were lysed for proteins as described in materials and methods (section 2.4.1). Total soluble protein (40μg) was subjected to SDS-PAGE/Western blot analysis and the membranes probed with antibodies specific for Src pY419 and total Src (A). Densitometry was conducted on the bands obtained and the data, corrected for loading with β-actin, presented as % of Control (B).

IGF-1R with AG1024 had only a modest effect on Src activation. Thus, while IGF-1R signalling in the Tam-R cell-line is obviously able to modulate Src activation, it is unlikely to be the predominant mechanism responsible for the increased Src activity seen in these cells.

3.3 Discussion

3.3.1 Characterisation of the tamoxifen-resistant cell-phenotype

Resistance to anti-hormone therapies is a major obstacle in the successful treatment of hormone-dependent breast cancer and so interest in the delineation of the mechanisms responsible is high. Using an *in vitro* model for tamoxifen resistance (Tam-R), our laboratory has previously demonstrated one such mechanism to involve elevated EGFR expression and activity [70]. Aberrant growth-factor signalling is associated with resistance to both tamoxifen and fulvestrant [23, 206, 207], and can lead to the development of an aggressive cell phenotype [178, 208-210]. Thus, this chapter investigates whether Tam-R cells display characteristics of an aggressive cell-phenotype which can lead to the enhanced metastatic potential of tumours *in vivo*.

Measurement of cell proliferation showed that Tam-R cells have a significantly enhanced rate of growth compared to MCF7wt cells under basal conditions. This is consistent with previously published data reporting similar increases following the acquisition of tamoxifen resistance, and which propose that the increased growth rate is due to enhanced activation of erb B-receptor signalling pathways in these cells [70]. Indeed, increased EGFR activity has been positively correlated to staining of Ki67, a marker for cell proliferation, in immuno-histochemical analysis of hormone-insensitive breast cancers [23]. More recently, however, it is becoming clear that these signalling pathways do not act independently and may cross-talk with additional pathways, such as the ER and IGF-1R pathways, to augment the effects on cell growth [69, 73, 196].

Tam-R cells also display an altered morphology compared to MCF7wt cells, with increased membrane ruffling and filopodia formation evident, giving the cells a more angular appearance. Differences were also seen in the way in

which the two cell-lines grow under basal conditions; with MCF7wt cells consistently growing in neat, tightly-packed colonies while Tam-R cells were seen to grow in a looser, more disorganised fashion. These observations suggest that the regulatory mechanisms for focal adhesions and adherens junctions, which control cell-matrix and cell-cell attachment respectively, are altered in the Tam-R cell-line. Indeed, figure 3.5 demonstrated that cell-matrix attachment in Tam-R cells was significantly enhanced over that of the MCF7wt cells on both plastic and fibronectin-coated surfaces, and similar results have been seen with laminin, collagen and vitronectin matrices [211]. Additionally, Hiscox *et al.* have previously shown that EGFR driven tyrosine phosphorylation of β-catenin and its subsequent dissociation from E-cadherin is increased in Tam-R cells, resulting in the loss of cell-cell contacts [165]. Furthermore, antibody-mediated neutralisation of E-cadherin in MCF7wt cells discouraged the formation of tightly-packed colonies and promoted invasion in this cell-line [165].

De-regulation of cell-cell and cell-matrix adhesion is important in the promotion of cell migration, which can then lead to an invasive phenotype [117]. Investigation of the migratory nature of the MCF7wt and Tam-R cell-lines across a fibronectin coated surface revealed that the Tam-R cells were significantly more motile than the parental MCF7wt cells. Parallel studies within our laboratory have also revealed that not only are the Tam-R cells able to migrate a greater distance than their MCF7wt counterparts, but that the migration was directional in nature [180], a process that may be influenced by growth-factor receptor signalling [212]. Furthermore, increased migration in the Tam-R cells was accompanied by a concomitant increase in their ability to invade through an artificial basement membrane (Matrigel™).

The increases observed in the migration and invasion of Tam-R cells in comparison to MCF7wt were not due to differences in the growth rates of the two cell-lines as figure 3.2 shows no difference in cell number after 1-3 days, the time over which the migration and invasion assays were performed. Furthermore, blockade of the cell cycle using aphidicholin has been shown to

have no significant effect on Tam-R cell invasion [180]. These results are consistent with observations in the clinic in which recurring tumours following tamoxifen resistance are often more aggressive, leading to increased tumour metastasis and a poor prognosis [197].

3.3.2 Investigations into the mechanisms involved in regulating the aggressive cell-phenotype of Tam-R cells

The mechanisms involved in the acquisition of an aggressive cell-phenotype are complex in nature due to the potentially high number of signalling pathways that may play a role. Whilst the identity and precise regulation of such pathways are still not fully understood, great progress has been made in identifying possible candidates.

Increased expression and activation of members of the erb B receptor family is often associated with tumour progression and increased metastatic potential [178, 202, 213]. EGFR up-regulation in particular frequently correlates with increased migration and invasion [178, 202, 209], and is thought to act by altering cell-matrix attachment either directly (via interactions with FAK/integrins to increase focal adhesion formation and turnover [205, 214]) or indirectly (via the down-stream activation of ERK 1/2 MAP kinases [203, 204]). EGFR has also been implicated in the regulation of intestinal epithelial cell migration via the Src-dependent activation of p38 [215], a mechanism which is distinct from that which controls EGFR-driven proliferation in these cells [216]. It is clear from the literature that an association between EGFR and an aggressive phenotype does exist; however, inhibition of EGFR in Tam-R cells using the small molecule tyrosine-kinase inhibitor, gefitinib, had only a modest effect on their aggressive cell phenotype, with only an approximate 50% reduction seen in levels of migration and invasion [180]. This implies that additional mechanisms must be involved which augment this behaviour in the Tam-R cells.

Altered integrin expression and signalling is another potential explanation for the changes seen in cell behaviour following the acquisition of tamoxifen resistance, as they are fundamental in the formation and degradation of cell-

matrix attachments which facilitate cell motility and invasion [217]. The large number of integrin receptor sub-units identified, in combination with their ability to form multiple heterodimers with other sub-units, prevented characterisation of the MCF7wt and Tam-R cell-lines for integrin expression within the time frame of this project. However, early work has suggested that integrin expression is increased in Tam-R cells, particularly $\alpha_V\beta_3$ (S Hiscox, unpublished observations) which is able to bind to a number of different matrices such as fibronectin, vitronectin, collagen and laminin [217] and which has been shown to promote spontaneous metastasis of breast tumours to bone [218]. Increased expression of integrins in Tam-R cells may partially explain the increased attachment seen in these cells. Therefore, further profiling of integrin expression in MCF7wt and Tam-R cells is an obvious area for future work in order to fully assess the role that they may play in the progression of tamoxifen resistant breast cancer.

Attention then turned to the non-receptor tyrosine kinase, Src, since it is widely associated with the acquisition of an aggressive cell-phenotype. The over-expression and up-regulation of Src has been reported in a number of human cancers [101, 103], including colorectal [106], breast [105], pancreatic [107], ovarian [108], and liver [219]. Furthermore, Src has been implicated in the regulation of a number of diverse cellular functions [95, 97, 220], and is known to play an important role in the mediation of both EGFR [145, 200, 201, 221] and integrin [95, 222] signalling to enhance aggressive cell behaviour. For example, González *et al.* have shown that the expression of a dominant-negative form of Src in MCF7 cells resulted in decreased cell attachment, spreading and migration, and was able to reduce both serum- and EGF-induced cell proliferation [152].

Profiling of Src gene expression using multiple approaches (RT-PCR, qPCR and Affymetrix cDNA arrays) revealed no significant difference in Src mRNA levels between the MCF7wt and Tam-R cell-lines. This was also apparent at the protein level, with SDS-PAGE/Western blotting showing no significant difference in total Src protein levels. However, when the activation of Src was

investigated there was a striking difference between the two cell-lines, with Src Y419 phosphorylation increased by approximately 14-fold in Tam-R cells. Whilst elevated Src activity has previously been linked to an aggressive cell-phenotype and increased metastatic potential [199], an association between up-regulated Src activity and tamoxifen resistance had not been reported prior to this work. However, in agreement with this data, Planas-Silva *et al.* have recently demonstrated similar increases in their model of tamoxifen resistance which was also derived from the MCF7 breast cancer cell-line [160].

Early studies have suggested that increased Src activity in breast cancer is a result of increased Src protein levels [105]. Biscardi *et al.* reviewed a number of studies that showed increased Src activity in over 70% of the tumour samples and cell-lines analysed, but found that this increase was due solely to increased levels of Src protein [145]. The data presented in this chapter, however, reflect the work of others who have reported increased Src activity independent of total protein levels [102]. It has recently been suggested that both situations might be true depending on how advanced the cancer is; in colorectal cancer, for example, increases in both protein level and activation are seen in the early stages of tumour development, with up-regulation of Src activity alone seen as the cancer continues to progress [97].

Src is known to mediate integrin signalling via interactions with FAK to regulate cell-matrix attachment, motility and invasion (reviewed in [167, 169, 176]). Since the Tam-R cells have been shown to display augmented cell-matrix attachment, motility and invasion, the possibility that Src may regulate these phenotypic changes through increased FAK phosphorylation was investigated. While no change was observed in basal levels of pY397, there was a modest increase in the Src-specific phosphorylation of Y861 in Tam-R cells compared to MCF7wt. This was accompanied by a corresponding increase in paxillin phosphorylation at Y31. The recruitment of FAK to focal adhesions and the subsequent phosphorylation of paxillin have been shown to be important for cell migration [223, 224]. Also, Src specific phosphorylation of FAK Y861 is crucial for ras transformation of fibroblasts, with Y861F-

mutant expressing cells demonstrating reduced association of FAK with $p130^{CAS}$ and decreased migration and invasion [225]. This suggests, therefore, that the elevated Src activity in Tam-R cells may contribute to their migratory and invasive nature by enhancing FAK-dependent integrin signalling.

As FAK auto-phosphorylation and the subsequent binding of Src is thought to be initiated primarily by integrin engagement, the effect of attachment to a fibronectin matrix on FAK phosphorylation was assessed. To determine both immediate and longer term effects two time points were used (30 minutes and 5 days). Interestingly, FAK Y397 auto-phosphorylation and the subsequent Src-specific phosphorylation of Y861 were both increased in Tam-R cells compared to MCF7wt following seeding onto a fibronectin matrix for 30 minutes. However, these increases diminished over time, with only small increases observed after 5 days. This may suggest that increased Src activity in the Tam-R cells promotes initial cell attachment through the phosphorylation of FAK and the formation of focal adhesions. However, as Src is also required for the subsequent disassembly of focal adhesions necessary for cell motility [117], the promotion of focal adhesion formation and attachment is likely to be transient. Eventually, an equilibrium between focal adhesion formation and disassembly is reached, leading to the steady state of FAK phosphorylation seen after 5 days.

To support this hypothesis, the extent to which FAK was phosphorylated in MCF7wt and Tam-R cells seeded onto a fibronectin matrix was assessed in comparison to cells in suspension. FAK phosphorylation on Y397 and Y861 was increased in both cell-lines following seeding onto fibronectin compared to the cells maintained in suspension. However, the level of FAK phosphorylation at both sites was markedly higher in Tam-R cells than in MCF7wt cells at the same time-point, suggesting an increased rate of FAK phosphorylation in these cells. Interestingly, attachment time-course assays revealed a corresponding increase in the initial rate of Tam-R cell attachment to a fibronectin matrix compared to MCF7wt cells. Moreover, the difference between the number of MCF7wt and Tam-R cells attached to fibronectin after 30 minutes

(figure 3.15) correlates with the difference in FAK phosphorylation seen following the seeding of these cells onto a fibronectin matrix for the same duration (figure 3.13).

Early work suggests that integrin expression in Tam-R cells might be increased compared to their wild-type counterparts (S. Hiscox, unpublished observations), which may account for the increase in Y397 phosphorylation seen. However, as Y861 is Src-specific, the increase in phosphorylation at this site might indicate an increase in the formation of Src/FAK signalling complexes which could then go on to promote initial focal adhesion formation and cell attachment. It is also interesting to note that the levels of FAK Y397 and Y861 phosphorylation were higher in Tam-R cells compared to MCF7wt cells when both cell-lines were kept in suspension. This may be a result of the increased Src activity in Tam-R cells, and might act to prime the cells ready for attachment to matrix components. Together, these data further suggest a role for Src in the regulation of cell-matrix attachment in Tam-R cells.

Surprisingly, differential rates of attachment were also observed on uncoated plastic. The apparent absence of matrix components might suggest that these observations are integrin (and hence FAK) independent and, therefore, do not involve Src. However, attachment assays were conducted in the presence of serum which, although charcoal-stripped, may still contain fibronectin at levels sufficient to enhance cell attachment. Alternatively, gene expression profiling using Affymetrix cDNA arrays has shown that fibronectin expression is increased in Tam-R cells (S Hiscox, unpublished observations). Thus, it is possible that the Tam-R cells themselves are able to express and lay-down a fibronectin matrix to provide an attachment advantage over MCF7wt.

In conclusion, the data presented suggest that increased Src kinase activity in Tam-R cells promotes increased FAK phosphorylation, which may in turn alter cell-matrix attachment and lead to the increased motility and invasion seen in these cells.

3.3.3 Regulation of Src kinase activity in Tam-R cells

As discussed earlier, the increase in Src activation observed in Tam-R cells cannot be accredited to an increase in Src gene expression; therefore, other changes that have occurred within the cell following the acquisition of tamoxifen resistance must be responsible. Src can be activated in a number of ways, the most widely reported of which involve either the de-phosphorylation of the negative-regulatory tail at Y530 or the formation of protein-protein interactions with SH2- and SH3-binding proteins. Additional mechanisms identified may also include activating mutations of the Src gene sequence. However, these are rare and the only reported incidence of a naturally occurring mutation was found in a sub-set of colon cancer liver metastases and advanced colon cancer primary lesions [133]. The mutation, identified in codon 531 of the Src sequence, led to the expression of a truncated form of Src, resulting in activation of its kinase domain. However, attempts to repeat these findings since have not been forthcoming [134-137].

Another potential mechanism of Src activation involves the regulation of Src protein levels. Increases in Src protein levels are seen early in the development of some colon cancers, and may be responsible for the concomitant increase in Src activity also seen [97]. In addition to altered gene expression, protein levels may also be modified by protein degradation mechanisms. Ubiquitination of certain proteins by ubiquitin-protein ligases results in their degradation via a proteosome-dependent pathway. It has been proposed that, following activation, Src can be ubiquitinated and subsequently degraded in this manner [226], and that this may require the function of CSK [142]. Therefore, aberrations in the ubiquitination or proteosome degradation pathways may allow activated Src to accumulate in the cell. However, as this would also result in increased levels of total Src protein [142], which were not observed in the Tam-R cells, it is doubtful that this mechanism is responsible for the increased Src activation seen.

A novel mechanism of Src activation may involve the activity of proteins called N-myristoyltransferases (NMT), which can myristoylate certain pro-

teins, including Src, and thus modify their cellular location by facilitating membrane association. Ducker *et al.* showed that siRNA knock-down of NMT proteins, which are over-expressed in colon cancer cells, resulted in decreased Src activity and down-regulation of FAK phosphorylation [111]. However, alterations in the activity of these proteins would also appear to result in changes in Src mRNA and protein levels. Again, as no such changes were observed, it is unlikely that this is occurring in our cell-lines.

Whilst these possible mechanisms are interesting, the infrequency in which they are reported suggests that their incidence is low and their relevance is limited. As such, they will not be discussed further in this thesis.

One of the primary mechanisms of Src regulation involves the phosphorylation status of the conserved Y530 amino acid residue found in the negative-regulatory tail of Src. Phosphorylation of Y530 allows the formation of intramolecular interactions between the negative-regulatory tail and the SH2 domain of Src, resulting in a closed conformation of the protein and inactivation of the kinase domain. It is said that approximately 90-95% of Src is phosphorylated at Y530 *in vivo* [124].

The level of Src phosphorylation at Y530 is governed by the balance of kinase and phosphatase activity within the cell [100, 124]. While a number of proteins that can facilitate this have been identified, two in particular stand out as key components. The first is CSK, a protein tyrosine kinase able to phosphorylate Src on Y530 resulting in the down-regulation of its activity [125]. Phosphorylation of Y530 by CSK in a cell-free system has previously been shown to reduce Src activity to 0.2% of initial levels [129]. The second key component in Src Y530 regulation is the phosphatase PTP1B, which can dephosphorylate Src at Y530 and thus promote kinase activation. PTP1B has been shown to be the primary tyrosine phosphatase responsible for the increased activation of Src in a number of human breast cancer cell-lines [126]. Furthermore, inhibition of PTP1B using selective small molecule inhibitors resulted in an increase in Src Y530 phosphorylation, accompanied

by equivalent decreases in cell-spreading, migration and the phosphorylation of FAK, $p130^{CAS}$ and ERK 1/2 [127].

With this in mind, the aberrant modulation of Src Y530 phosphorylation was investigated as a potential explanation for the increased Src activity seen in Tam-R cells. However, no significant differences were observed in the levels of CSK and PTP1B between the MCF7wt and Tam-R cell-lines. To confirm this, and to preclude the possibility of other kinase/phosphatase proteins being involved, Src Y530 phosphorylation was also measured. Again, no significant differences were observed between the MCF7wt and Tam-R cells. Taken together, these data suggest that the increased Src activity in Tam-R cells is not a result of altered Src Y530 phosphorylation in these cells.

The conventional paradigm of Src regulation is that when Src is active Y419 and Y530 are phosphorylated and de-phosphorylated respectively; with the reverse being true with the inactivation of Src. Therefore, in view of the considerable increase in Src Y419 phosphorylation seen in the Tam-R cells, one might expect to see a corresponding decrease in the levels of Src phosphorylation at Y530. However, the data do not show such a decrease.

Interestingly, while some studies have demonstrated a direct correlation between CSK expression and Src activation [219], others have suggested that this is not always the case [107]. Furthermore, it has also been reported that Src can possess kinase activity even if Y530 is phosphorylated [120, 127-129]. A possible explanation for this may involve the platelet-derived growth-factor receptor (PDGF-R) [120] and/or c-erbB2 [130], which are able to selectively phosphorylate Src on a conserved tyrosine residue found at position 215 in the SH2 binding domain. Phosphorylation of Y215 has been shown to alter the binding specificity of the SH2 domain such that interactions with Y530 are prevented regardless of phosphorylation status, whereas binding to other SH2 docking sites is unaffected [120]. Therefore, it is possible that the increased Src phosphorylation at Y419 seen in the Tam-R cells in the absence of a corresponding decrease in phosphorylation at Y530 is a result of the phosphorylation of Src at Y215 by c-erbB2, which is up-regulated in these

cells [70]. This would prevent interactions between the negative-regulatory tail and the SH2 domain and promote full kinase activation of Src, even in the presence of phosphorylated Y530. Further work to characterise these cell-lines for Src Y215 phosphorylation is, therefore, required to test this theory.

The other key mechanism of Src activation is through protein-protein interactions. Src has been called a "promiscuous" tyrosine kinase due to its ability to directly interact with many different proteins. Src contains one SH2 and one SH3 protein binding domain which work to facilitate interactions between Src and other proteins in a highly specific manner; the SH2 domain recognises phosphorylated tyrosine residues flanked by specific sequences of amino acids, whereas the SH3 domain binds to proteins containing proline-rich sequences that fold in a left-handed helix [114]. The interaction between Src and other proteins via these domains results in Src adopting an open conformation, thus promoting the auto-phosphorylation and activation of its kinase domain [100]. SH2- and SH3-protein binding domains, along with the target sites they recognise, are found in a wide variety of proteins, and so elucidating the aetiology of Src activation by this mechanism is complicated by the vast number of proteins that may contribute to it [131].

FAK is a favoured binding partner of Src and their association has been well documented [131, 167, 169, 175, 176]. Phosphorylation of FAK at Y397, which is usually initiated by integrin engagement and clustering, creates an SH2-binding site to which Src can bind, becoming activated in the process. However, Western blot analysis of basal MCF7wt and Tam-R cells showed no significant differences in FAK phosphorylation at Y397 between the two cell-lines. Furthermore, immunoprecipitation experiments indicate that there is no difference in the levels of Src/FAK association between basal MCF7wt and Tam-R cells (S Hiscox, personal communication). Taken together, these observations would suggest that increased association of Src with FAK is not responsible for the increased Src activation seen in the Tam-R cells.

Src can also be activated through interactions with receptor tyrosine kinases [143], such as the erb B family of growth-factor receptors [227]. The most

well-studied of these interactions occurs between Src and EGFR [145, 228]. It has been suggested that Src and EGFR share a synergistic relationship, with the activities of both proteins being greater when they are co-over-expressed than when either protein is over-expressed on its own [200, 201]. Our laboratory has previously reported that EGFR signalling is important for driving hormone-independent growth in Tam-R cells [70] and may also contribute to the regulation of their enhanced aggressive cell-phenotype [180]. Therefore, whether the increased expression of EGFR in Tam-R cells might also be responsible for the increased Src activation seen was investigated.

Figure 3.20 confirmed that basal levels of total and phosphorylated EGFR were increased in the Tam-R cell-line, with both phosphorylation at Y1068 (an important site for the EGFR-Grb2-MAPK mitogenic signalling pathway) and total protein levels increased 8-fold over MCF7wt. Interestingly, a 3-fold increase in the phosphorylation of EGFR at Y845, a Src specific phosphorylation site [229], was also observed.

Next, EGFR activation and signalling were modulated using growth-factor (TGFα) stimulation and pharmacological inhibition (gefitinib) in order to observe any subsequent effects on Src activation. As expected, TGFα stimulation resulted in increased phosphorylation of EGFR at both Y845 and Y1068. However, a 2.5-fold increase in Src activation was also observed. Correspondingly, gefitinib inhibited EGFR phosphorylation at Y1068 and reduced Src activation by over 50%. The effect of gefitinib on Src activation positively correlates with the effect seen on Tam-R cell migration and invasion [180]. The modulation of Src activity following ligand-stimulation or pharmacological inhibition of EGFR has been reported previously [198, 199, 230]. Furthermore, Osherov and Levitzki have proposed that the activation of Src by EGFR is dependent on the level of EGFR expression [198]. As EGFR expression is increased 8-fold in Tam-R cells compared to MCF7wt, these data suggest that up-regulated EGFR expression may be at least partially responsible for the concomitant increase in Src activation seen in these cells.

Interestingly, increases were observed in both EGFR pY845 and total protein levels following gefitinib treatment. This may be because Src is thought to be involved in the internalisation of EGFR following ligand binding, which commits the receptor to the degradation or recycling pathways [231, 232]. Thus, if Src activity is reduced by gefitinib then these mechanisms might be disrupted, resulting in the accumulation of EGFR on the plasma-membrane. Residual active Src may be sufficient to phosphorylate this EGFR on Y845, which is not dependent on the intrinsic kinase activity of EGFR, thus accounting for the increase in phosphorylated Y845 also seen.

The effect of alternative EGFR ligands, in addition to the stimulation of other receptor tyrosine kinases, on the activation of Src in Tam-R cells was investigated next. The receptors chosen were c-erbB2 and IGF-1R, as both have previously been shown to be active in Tam-R cells [70, 196]. Treatment of Tam-R cells with EGF, TGFα and amphiregulin all resulted in increased activation of Src, with amphiregulin eliciting a greater response than either EGF or TGFα. Interestingly, recent work in our laboratory has demonstrated that cross-talk between ER and EGFR signalling pathways in Tam-R cells promotes the expression of amphiregulin as part of an autocrine growth mechanism [73], and thus these cross-talk mechanisms may also indirectly stimulate Src activation.

Furthermore, the MEK inhibitor PD098059, which inhibits the EGFR-stimulated activation of ERK 1/2, had no effect on Src activity in Tam-R cells. This suggests that the activation of Src by EGFR is direct, rather than a downstream effect of the EGFR signalling pathway. Indeed, Luttrell *et al.* have shown that Src is able to directly associate with phosphorylated EGFR in breast cancer cells via its SH2-binding domain [144], which could then lead to the subsequent activation of its kinase domain. However, immuno-precipitation experiments are required in order to confirm whether this is occurring in the Tam-R cells.

Heregulin is a ligand for the c-erbB3 and c-erbB4 members of the erb B family of receptor tyrosine kinases which, upon ligand binding, are able to

form hetero-dimers with other family members. Treatment of Tam-R cells with heregulin produced the greatest increase in Src activity, with Src pY419 levels increased 4.6-fold over control. Knowlden *et al.* have previously reported that, while c-erbB4 is not present in the Tam-R cells, c-erbB3 is expressed and is able to form homo-dimers or undergo hetero-dimerisation with EGFR under basal conditions [70]. Furthermore, it is possible that c-erbB2/c-erbB3 hetero-dimers, which were not detectable under basal conditions in Tam-R cells, may also form following ligand binding to c-erbB3.

Whilst data on direct interactions between Src and c-erbB3 homo-dimers is limited, heregulin may still activate Src in two additional ways. The first is following hetero-dimer formation between c-erbB3 and either EGFR or c-erbB2, which would result in the trans-activation of EGFR or c-erbB2, facilitating interactions with, and thus activation of, Src in the classical manner. Secondly, increased c-erbB2 activation following c-erbB3 hetero-dimer formation may, as already discussed, result in the phosphorylation of Src Y215 in the SH2 domain, thus preventing intra-molecular interactions between the SH2 domain and negative-regulatory tail and promoting Src activation via auto-phosphorylation of Y419 [120, 130]. However, treatment of Tam-R cells with the c-erbB2 inhibitor trastuzumab (Herceptin™) appeared to have no effect on Src activation. Therefore, if c-erbB2 is able to potentiate Src activation in the Tam-R cells via the phosphorylation of Y215 then this mechanism would seem to be cooperative rather than essential. Thus, the data suggests that stimulation of Tam-R cells with heregulin could potentially initiate two mechanisms of Src activation, which may account for the high levels of activation seen.

Tam-R cells were also either stimulated with IGF-II or inhibited with AG1024, a specific IGF-1R inhibitor, in order to modulate IGF-1R activity. IGF-II was used to stimulate IGF-1R in the Tam-R cells as it has previously been demonstrated that these cells do not express IGF-I [196]. The effects seen on Src activation were modest, with Src activation at 211% and 79% of control following IGF-1R stimulation and inhibition respectively. Therefore,

while IGF-1R activity is able to modulate the activation of Src in Tam-R cells, it is unlikely to contribute greatly to the increase in Src activation seen following the acquisition of tamoxifen resistance. However, work is currently on-going in our laboratory to look at the role of Src in cross-talk mechanisms between EGFR and IGF-1R signalling pathways that may ultimately aid the development of resistance to anti-growth-factor therapies [196].

Taken together, this evidence may suggest a role for protein-protein interactions, particularly those between Src and EGFR, as a contributory factor for the increased activation of Src tyrosine kinase in tamoxifen resistant MCF7 breast cancer cells. Furthermore, formation of a Src/EGFR complex may be facilitated by the phosphorylation of Src Y215 by c-erbB2 to prevent competitive binding of the phosphorylated negative-regulatory tail.

3.4 Chapter Summary

- Tam-R cells possess an enhanced aggressive cell phenotype compared to MCF7wt cells, displaying altered morphology, increased growth rates, increased motile and invasive capabilities, and altered cell-matrix attachment.
- Src activity is significantly increased in Tam-R cells, an effect independent of changes in Src gene expression or total protein levels.
- Increased Src activation in Tam-R cells leads to an increase in the Src-dependent phosphorylation of FAK and paxillin, proteins which are important in the regulation of cell attachment, migration and invasion.
- While the mechanisms that underlie the increase in Src activation following the acquisition of tamoxifen resistance are still unclear, aberrant modulation of Src phosphorylation at Y530 is unlikely to be a causative factor. However, protein-protein interactions, particularly those between Src and EGFR, may have an important role to play.
- Therefore, this chapter provides circumstantial evidence for a role for Src in mediating the aggressive phenotype of tamoxifen-resistant MCF7 breast cancer cells *in vitro*.

Chapter Four: Results

Src Kinase is Central to the Regulation of the Aggressive *in vitro* Phenotype of Tam-R Cells

"There are no such things as incurable, there are only things for which man has not yet found a cure."

Bernard Baruch (1870-1965). US Financier and Statesman.
Speech, 30th April 1954; quoting his father, the surgeon Simon Baruch.

4 Src Kinase is Central to the Regulation of the Aggressive *in vitro* Phenotype of Tam-R Cells

4.1 Introduction and Aims

Src is a 60kDa non-receptor tyrosine kinase which was first discovered as the product of a viral oncogene (v-src) following studies on the transforming Rous sarcoma virus in the 1970s [83], with a cellular homologue of v-Src, named c-Src, identified in uninfected cells soon after [87]. Further work revealed that both v-Src and c-Src demonstrated protein kinase activity [90] which was later found to be tyrosine specific [94]. Src was the first tyrosine specific kinase to be discovered and, as such, is the most well studied [95-100].

Src activity is tightly regulated in a normal cellular environment; however, both Src expression and activation have been shown to be increased in many types of cancer, such as colon, breast and pancreatic [105-107]. Furthermore, Src has been implicated in the regulation of a diverse number of cellular processes which can promote tumour progression, including cell growth, survival, attachment, motility and invasion [95-97]. Thus, Src presents a promising therapeutic target in cancer, and this is reflected by the emergence of several Src inhibitors which are now entering clinical trials [233].

The previous chapter showed that Tam-R cells possess an increased aggressive cell-phenotype compared to their wild-type counterparts, demonstrating enhanced growth, attachment, motility and invasion. Furthermore, these cells also had significantly elevated levels of Src kinase activation. Thus, the aim of this chapter was to establish whether Src plays a role in the regulation of the aggressive cell-phenotype exhibited by Tam-R cells, and to do this, a pharmacological inhibitor (AZM555130) was employed to reduce Src kinase activity in the MCF7wt and Tam-R cell-lines.

AZM555130 is one of a new series of 4-anilinoquinazoline based Src-family-kinase inhibitors that have been recently developed by AstraZeneca [234-236]. AZM555130 is a probe compound arising from studies which have since led

to the development of AZD0530, a highly selective and potent inhibitor of Src-family-kinases currently being assessed in phase I clinical trials [236]. The anilinoquinazoline-based structure common to both AZM555130 and AZD0530 is shown in figure 4.1.

Although AZD0530 was the lead compound in the development of this series of Src-family-kinase inhibitors it was unavailable for use on commencement of this study. Thus, the work presented in this thesis was conducted using AZM555130 to reduce Src activation in MCF7wt and Tam-R cells. For experimental use, AZM555130 was dissolved in DMSO at a stock concentration of 10mM and then diluted as appropriate in cell culture medium immediately before use. Vehicle alone (DMSO) was used to treat control cells in each experiment and had no effect on the parameters analysed in comparison with culture medium alone.

4.2 Results

4.2.1 AZM555130 decreases activation of Src kinase

AZM555130 is a novel compound which had not been used in the MCF7wt and Tam-R cell-lines prior to this work. Thus, the first priority was to determine its efficacy as an inhibitor of Src kinase activity in these cells using dose response and time course experiments. The effect of the compound on Src activation was assessed by measuring the level of Src phosphorylation at Y419 in the cells following treatment [123].

For dose response experiments, MCF7wt and Tam-R cells were cultured in W+5% ± Tam (100nM) until they had reached log-phase growth. The cells were then treated with AZM555130 at a range of concentrations (0-1μM) for 24 hours prior to lysis and immunoprobing for levels of phosphorylated (Y419) and total Src protein. Representative blots and subsequent densitometric analysis for Src in the MCF7wt and Tam-R cell-lines are shown in figures 4.2 and 4.3 respectively.

The data show AZM555130 to be an effective inhibitor of Src activation in both cell-lines at concentrations of 0.1μM and 1μM; with the phosphorylation

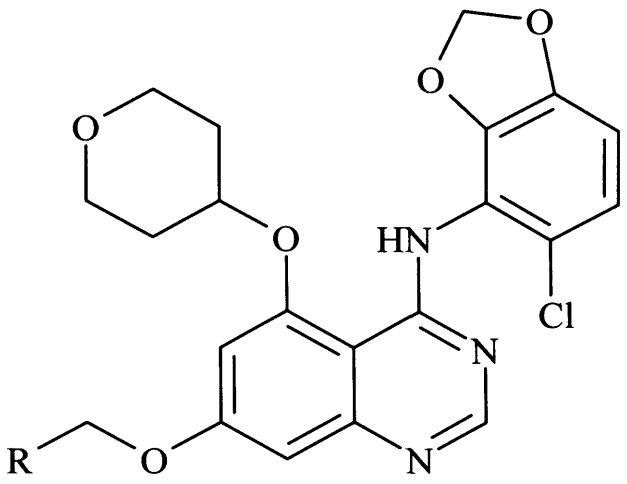

Figure 4.1 Structure of AZM555130, one of a new series of 4-anilinoquinazoline based Src-family-kinase inhibitors developed by AstraZeneca.

The novel Src-family-kinase inhibitor AZM555130 was developed and supplied by AstraZeneca (Macclesfield, UK). It is one of a new series of 4-anilinoquinazoline based Src-family-kinase inhibitors and works by competitively binding to the ATP-binding site of the kinase domain. A very similar compound also developed by AstraZeneca, AZD0530, is currently undergoing phase I/II clinical trials.

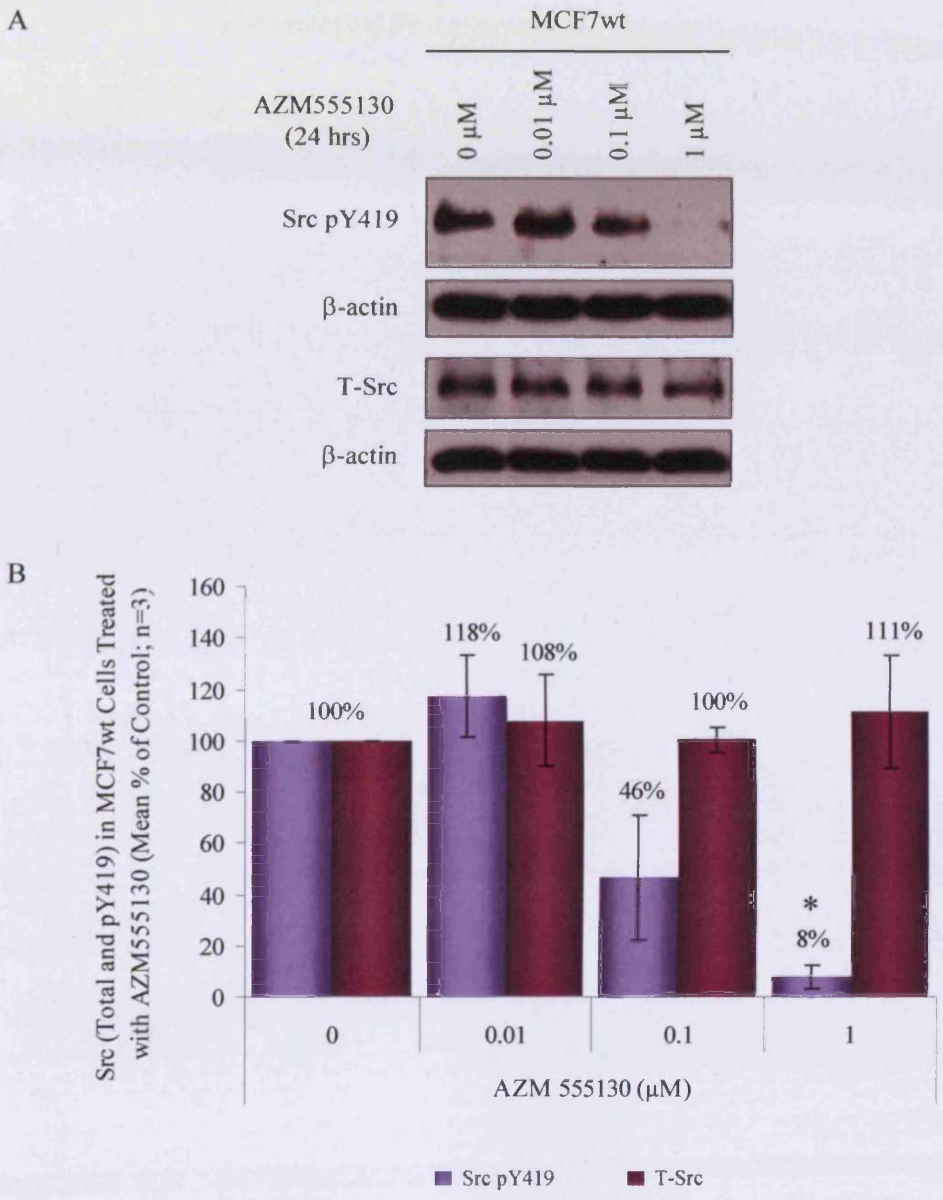

Figure 4.2 Dose-dependent effect of AZM555130 Src-family-kinase inhibitor on Src activation in MCF7wt cells as determined by Western blotting.

MCF7wt cells were cultured to log-phase growth and then treated with AZM555130 at the stated concentrations for 24 hours. Control cells were treated with vehicle (DMSO) only for the same duration. The cells were then lysed for proteins as described in materials and methods (section 2.4.1). Total soluble protein (40µg) was subjected to SDS-PAGE/Western blot analysis and the membranes probed with antibodies specific for Src pY419 and total Src (A). Densitometry was conducted on the bands obtained and the data, corrected for loading with β-actin, presented as Mean % of Control ± S.D. (* $p<0.001$ vs. Control; n=3) (B).

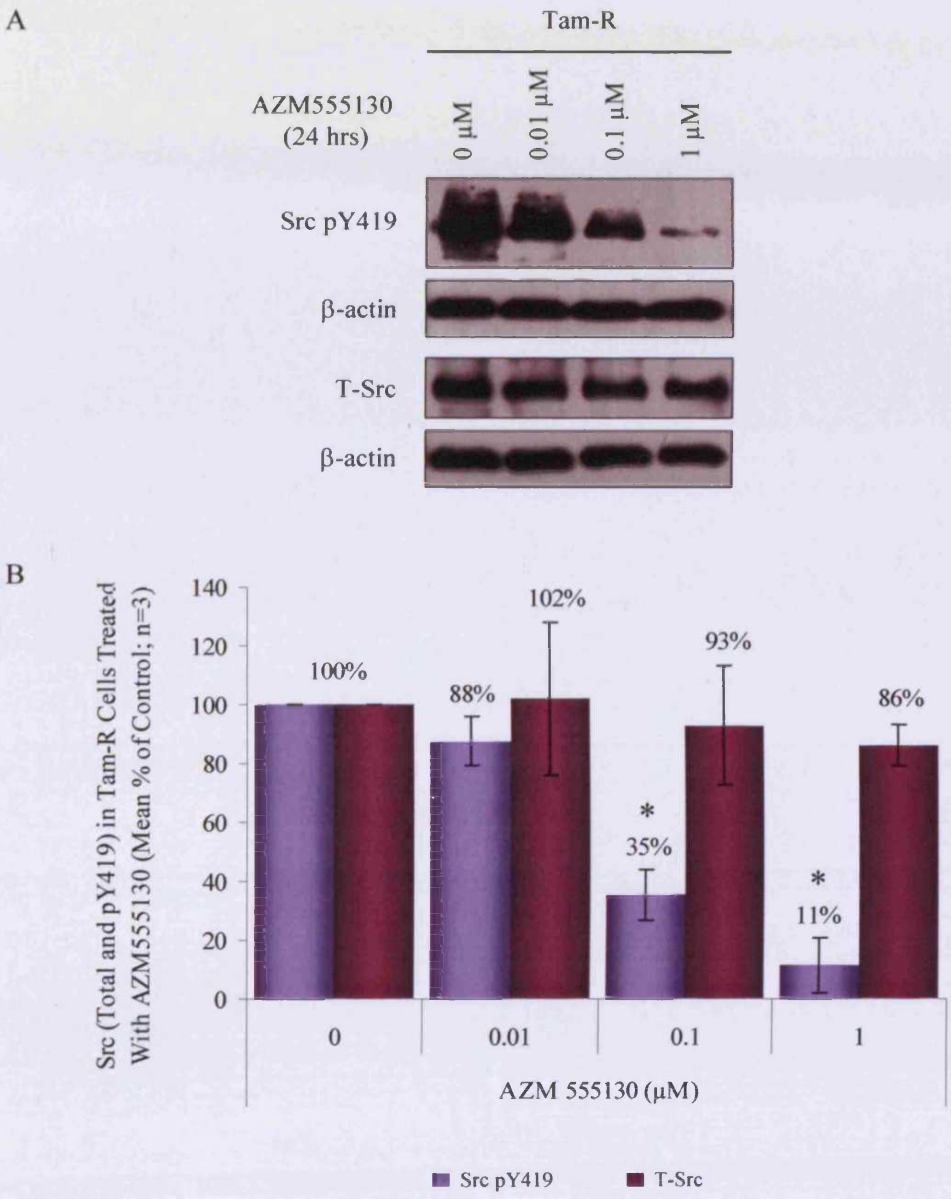

Figure 4.3 Dose-dependent effect of AZM555130 Src-family-kinase inhibitor on Src activation in Tam-R cells as determined by Western blotting.

Tam-R cells were cultured to log-phase growth and then treated with AZM555130 at the stated concentrations for 24 hours. Control cells were treated with vehicle (DMSO) only for the same duration. The cells were then lysed for proteins as described in materials and methods (section 2.4.1). Total soluble protein (40μg) was subjected to SDS-PAGE/Western blot analysis and the membranes probed with antibodies specific for Src pY419 and total Src (A). Densitometry was conducted on the bands obtained and the data, corrected for loading with β-actin, presented as Mean % of Control ± S.D. (* $p<0.01$ vs. Control; n=3) (B).

of Src Y419 reduced by 54% and 92% (MCF7wt) and by 65% and 89% (Tam-R) at these concentrations respectively. The reductions in Y419 phosphorylation observed were not a result of decreased Src protein as levels of total Src were unaffected by AZM555130 treatment. The IC_{50} values for the inhibition of Src in MCF7wt and Tam-R cells by AZM555130 were calculated as 0.07μM and 0.02μM respectively.

The effect of AZM555130 on Src activation in these cell-lines was also examined by immunocytochemistry. MCF7wt and Tam-R cells were cultured on coverslips to log-phase growth and treated with either AZM555130 (1μM) or vehicle (DMSO) for 24 hours. The cells were then fixed using the ERICA technique and immuno-probed for Src pY419 using phospho-specific antibodies as previously described (section 2.5). Representative images captured using light microscopy are shown in figure 4.4 and demonstrate a reduction in Src pY419 staining in both cell-lines following treatment with AZM555130, thus confirming the results obtained with SDS-PAGE/Western blotting.

In addition to establishing the optimum concentration of AZM555130 for the treatment of MCF7wt and Tam-R cells, various treatment durations were also profiled to ensure that the inhibitor was effective within the time frame of the experiments in which it was used. For this, MCF7wt and Tam-R cells were cultured to log-phase growth and then treated with AZM555130 at 1μM for increasing durations (1 min, 10 min, 30 min, 60 min, 4 hrs, 24 hrs and 4 days) prior to lysis and immunoprobing for phosphorylated and total Src as above. Controls were treated with vehicle only (DMSO) for 24 hrs or 4 days as appropriate. Figures 4.5 (MCF7wt) and 4.6 (Tam-R) show that AZM555130 at 1μM drastically reduced the level of Src Y419 phosphorylation after just 1 minute, and almost completely eradicated Y419 phosphorylation after 30 minutes, in both cell-lines. Total Src protein levels were unaffected by short-term treatment with AZM555130; however, a reduction in total Src was seen in MCF7wt cells after 4 day treatment with AZM555130.

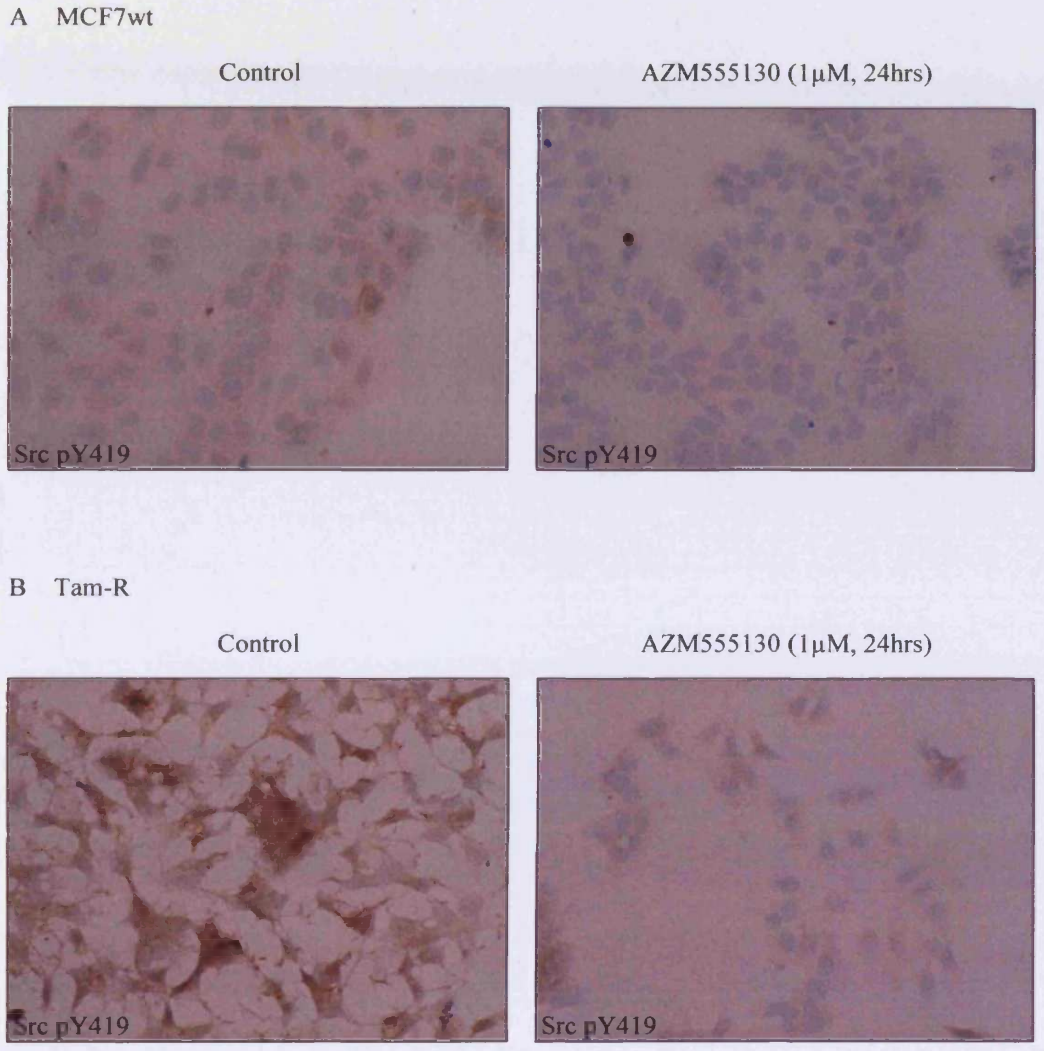

Figure 4.4 Effect of AZM555130 Src-family-kinase inhibitor (1μM, 24 hrs) on Src activation in MCF7wt and Tam-R cells as determined by immunocytochemistry.

MCF7wt and Tam-R cells were cultured on glass coverslips to log-phase growth and then treated with AZM555130 (1μM) for 24 hours. Control cells were treated with vehicle (DMSO) only for the same duration. The cells were then fixed using the ERICA technique as described in materials and methods (section 2.5.1.1). Fixed cells were assayed for Src pY419 using a phospho-specific antibody and the protein localisation was visualised using the DAKO EnVision™+ system peroxidase [DAB] kit as described in section 2.5.2. Representative images of MCF7wt (A) and Tam-R (B) cells ± AZM555130 were captured using an Olympus BH-2 phase contrast microscope at 20x magnification.

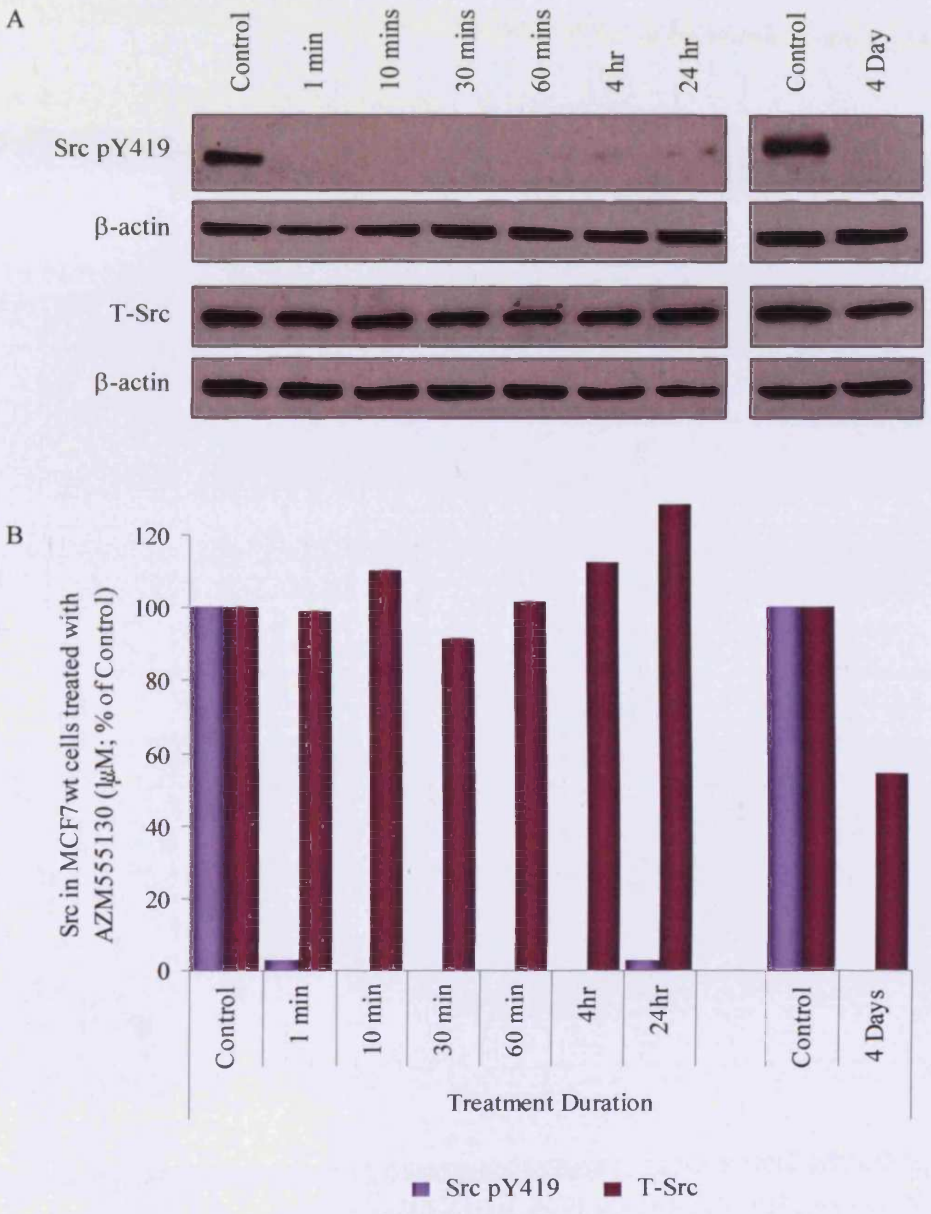

Figure 4.5 Time-course experiment to demonstrate efficacy of AZM555130 (1μM) as an inhibitor of Src activation in MCF7wt cells.

MCF7wt cells were cultured to log-phase growth and treated with AZM555130 (1μM) for 1 minute, 10 minutes, 30 minutes, 60 minutes, 4hrs, 24hrs and 4 days. Control cells were treated with vehicle (DMSO) only for 24 hrs or 4 days as appropriate. Following treatment, cells were lysed for proteins as described in materials and methods (section 2.4.1). Total soluble protein (40μg) was subjected to SDS-PAGE/Western blot analysis and the membranes probed with antibodies specific for Src pY419 and total Src (A). Densitometry was conducted on the bands obtained and the data, corrected for loading with β-actin, presented as % of Control (B).

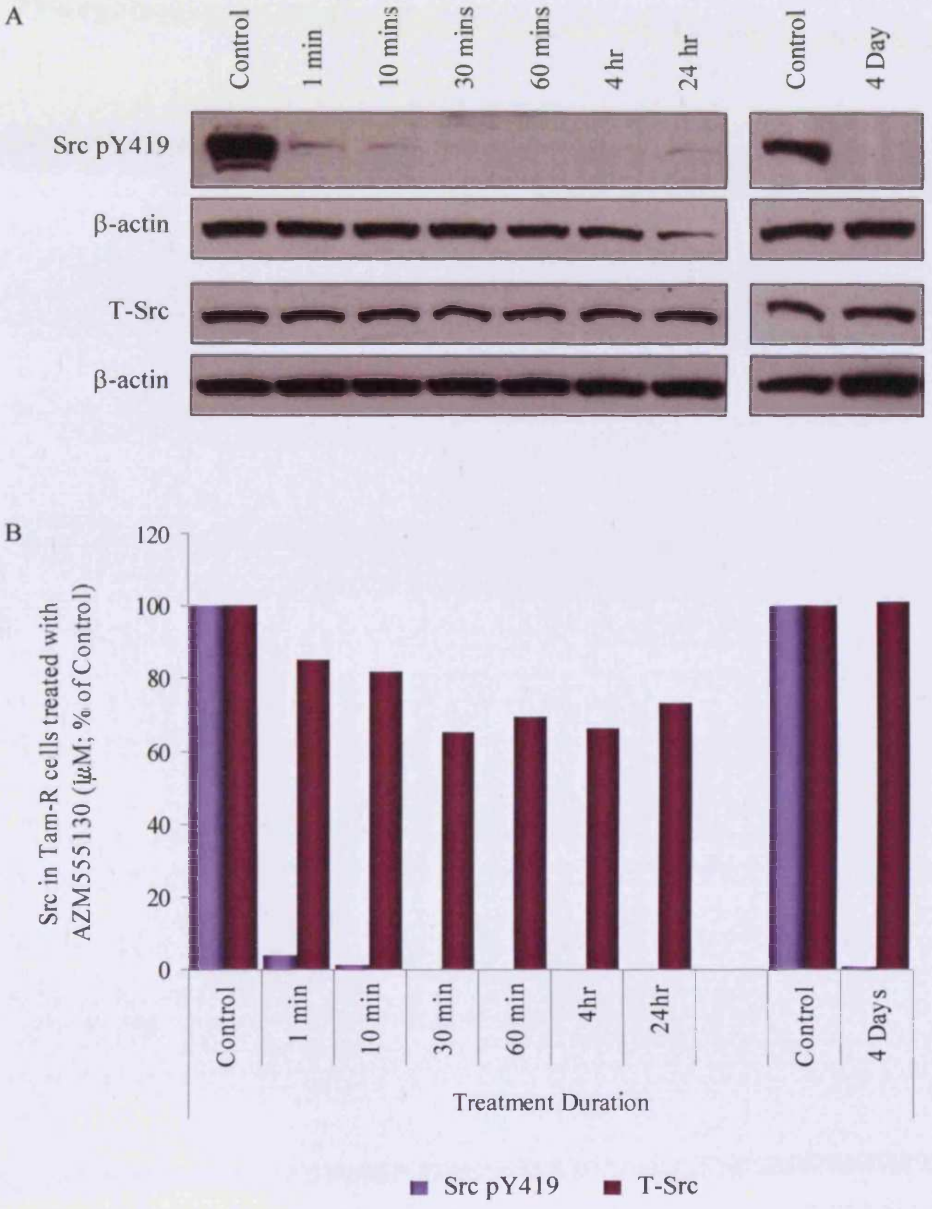

Figure 4.6 Time-course experiment to demonstrate efficacy of AZM555130 (1μM) as an inhibitor of Src activation in Tam-R cells.

Tam-R cells were cultured to log-phase growth and treated with AZM555130 (1μM) for 1 minute, 10 minutes, 30 minutes, 60 minutes, 4hrs, 24hrs and 4 days. Control cells were treated with vehicle (DMSO) only for 24 hrs or 4 days as appropriate. Following treatment, cells were lysed for proteins as described in materials and methods (section 2.4.1). Total soluble protein (40μg) was subjected to SDS-PAGE/Western blot analysis and the membranes probed with antibodies specific for Src pY419 and total Src (A). Densitometry was conducted on the bands obtained and the data, corrected for loading with β-actin, presented as % of Control (B).

One of the most prevalent inhibitors currently used for *in vitro* and *in vivo* analysis of Src activity is the proprietary compound, SU6656 (Calbiochem). As such, the efficacy of AZM555130 as an inhibitor of Src kinase activity was compared to that of SU6656. Tam-R cells were cultured to log-phase growth and then treated with SU6656 at a range of concentrations (0-10μM) for 24 hours, while control cells were treated with vehicle (DMSO) only for the same duration. SDS-PAGE/Western blot analysis revealed that, while SU6656 reduced Src Y419 phosphorylation in a dose-dependent manner, it was not as potent an inhibitor of Src activation as AZM555130 in the Tam-R cell-line (Figure 4.7). The IC_{50} for SU6656 in Tam-R cells calculated from these experiments was 1.7μM, compared to 0.02μM for AZM555130. Furthermore, phosphorylation of Src at Y419 was still evident with SU6656 at 10μM.

4.2.2 Src inhibition in Tam-R cells alters cell morphology and decreases matrix-attachment, migration and invasion

The data obtained above confirms that the novel Src-family-kinase inhibitor, AZM555130, is an effective inhibitor of Src kinase activation in the MCF7wt and Tam-R cell-lines. As such, pharmacological inhibition of Src was used as a tool with which to elucidate a role for Src in the regulation and maintenance of the aggressive Tam-R cell phenotype.

The effect of Src inhibition on cell morphology was investigated. MCF7wt and Tam-R cells were cultured to log-phase growth and then treated with either AZM555130 (1μM) or vehicle (DMSO) for 24 hours. The effect of AZM555130 on the morphology of these cells was then assessed using a Leica DM-IRE2 inverted microscope fitted with a Hoffman condenser as described in section 2.6. Representative images of the control and treated cells captured at 20x magnification are shown in figure 4.8. Under basal conditions Tam-R cells are seen to grow in diffuse colonies and possess an angular appearance due to increased membrane activity. However, inhibition of Src activity caused significant loss of membrane structures such as filopodia and lamelli-podia in the Tam-R cells, and resulted in a morphology more akin to that of

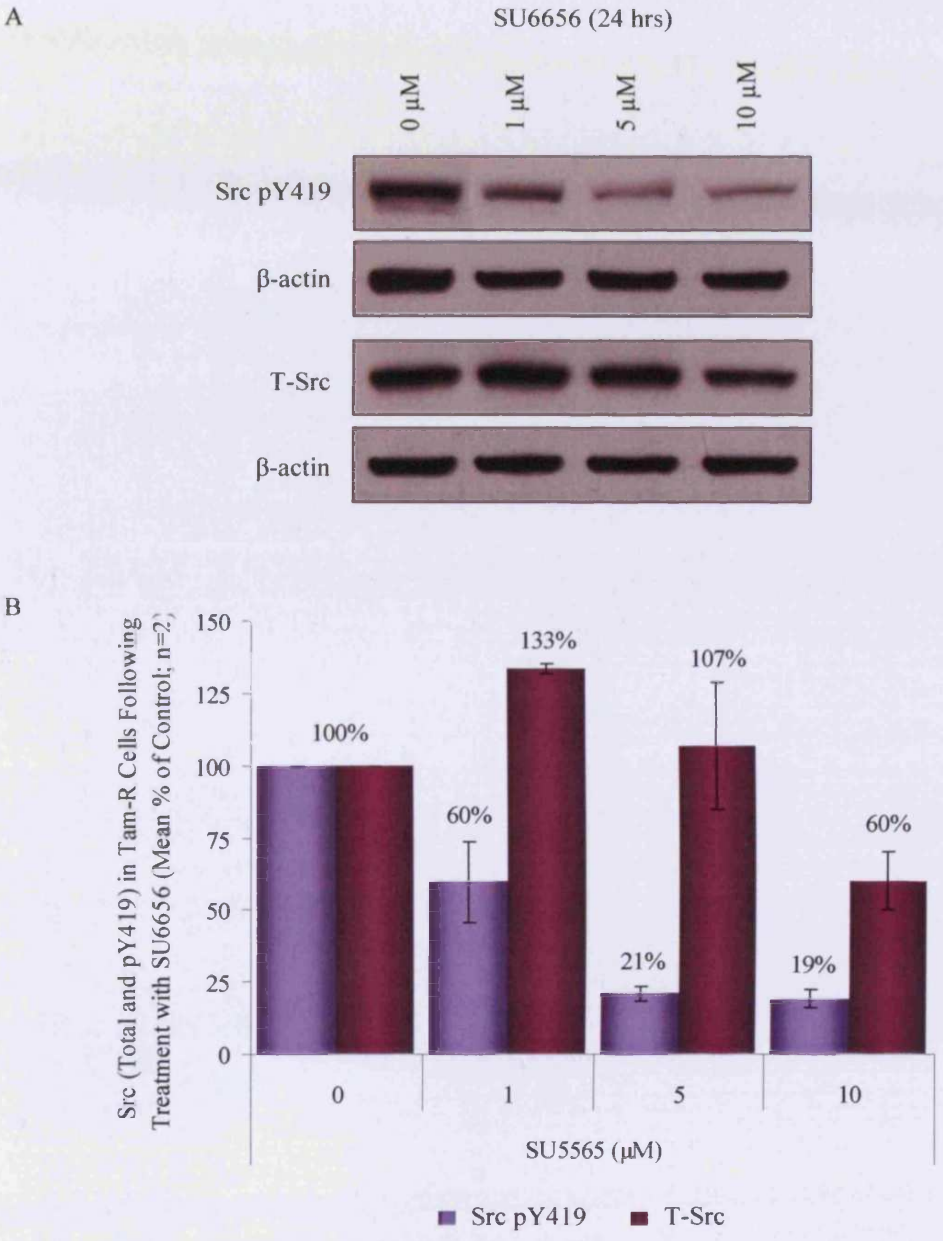

Figure 4.7 Dose-dependent effect of the proprietary Src-family-kinase inhibitor SU6656 on Src activation in Tam-R cells as determined by Western blotting.

Tam-R cells were cultured to log-phase growth and then treated with SU6656 at the stated concentrations for 24 hours. Control cells were treated with vehicle (DMSO) only for the same duration. The cells were then lysed for proteins as described in materials and methods (section 2.4.1). Total soluble protein (40μg) was subjected to SDS-PAGE/Western blot analysis and the membranes probed with antibodies specific for Src pY419 and total Src (A). Densitometry was conducted on the bands obtained and the data, corrected for loading with β-actin, presented as Mean % of Control ± S.D. (n=2) (B).

A MCF7wt

Control AZM555130 (1μM, 24hrs)

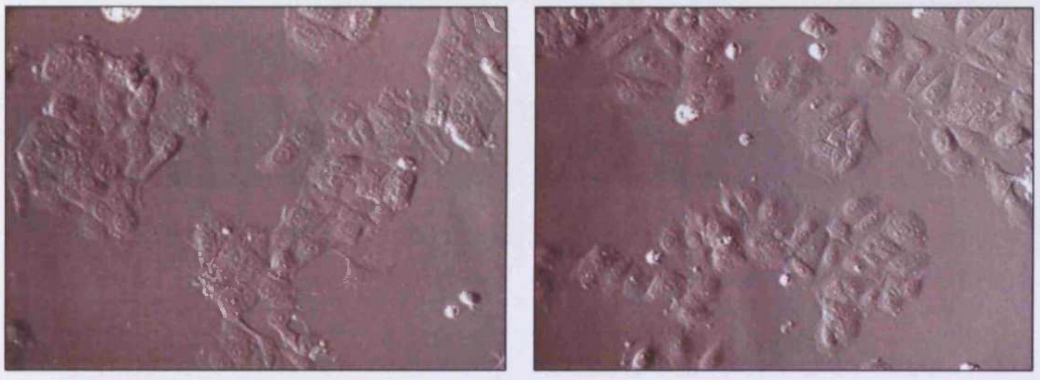

B Tam-R

Control AZM555130 (1μM, 24hrs)

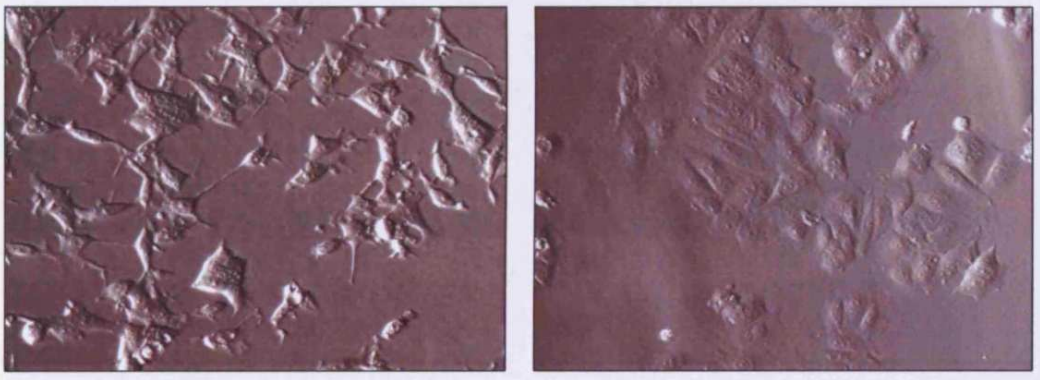

Figure 4.8 Effect of Src inhibition using AZM555130 on the morphology of MCF7wt and Tam-R cells.

MCF7wt and Tam-R cells were cultured to log-phase growth and then treated with AZM555130 (1μM) for 24 hours. Control cells were treated with vehicle (DMSO) only for the same duration. Representative images of MCF7wt (A) and Tam-R (B) cells ± AZM555130 treatment were captured at 20x magnification using a Leica DM-IRE2 inverted microscope fitted with a Hoffman condenser and a Hamamatsu C4742-96 digital camera.

the wild-type cell-line. Furthermore, treatment with AZM555130 resulted in the Tam-R cells growing in tightly-packed colonies in a manner similar to that seen with MCF7wt cells. In contrast, the morphology of the MCF7wt cells did not appear to be affected by treatment with AZM555130.

Previously, Tam-R cells have been shown to demonstrate both increased migratory and invasive capabilities and elevated Src activation compared to MCF7wt cells. Increased Src activity is often associated with increased cell migration and invasion, and so the AZM555130 Src-family-kinase inhibitor was used in order to elucidate a role for Src in the increased migratory and invasive phenotype of the Tam-R cells.

The effect of AZM555130-induced Src inhibition on the migratory and invasive capabilities of Tam-R cells was assessed using *in vitro* migration and invasion assays (see sections 2.10 and 2.11). The weakly migratory and invasive MCF7wt cells were also included for comparative purposes. Cells were seeded into the pre-coated Transwell® inserts in medium containing AZM555130 (0-1μM), while control cells were seeded in medium containing vehicle (DMSO) only. Inhibition of Src by AZM555130 resulted in significant reductions in the migration and invasion of Tam-R cells in a dose dependent manner. AZM555130 at 0.1μM and 1μM decreased Tam-R cell migration to 56% and 23% of control respectively (figure 4.9). Similarly, invasion in this cell-line was reduced to 17% and 6% of control at these concentrations (figure 4.10). Interestingly, the effect of AZM555130 at 0.1μM on Tam-R cell invasion was more pronounced than the effect seen on cell migration, which may suggest that the events involved in cell invasion are particularly reliant on higher levels of Src activity.

In the previous chapter it was proposed that the increased migration and invasion of Tam-R cells is a consequence of de-regulated cell-matrix attachment caused by increased Src-dependent FAK phosphorylation. To further test this hypothesis, the effect of Src inhibition on cell-matrix attachment was examined next.

(A) Mean % of Control (n=4).

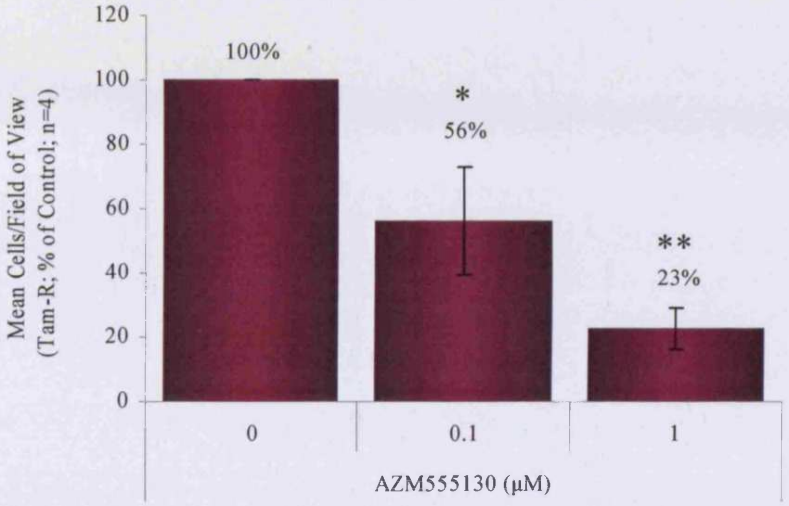

(B) Representative experiment with MCF7wt cells included for comparison.

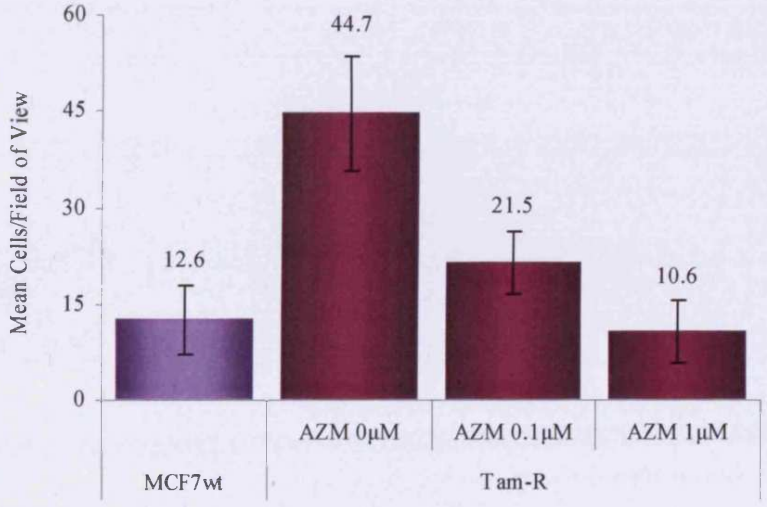

Figure 4.9 The effect of AZM555130 on migration of Tam-R cells *in vitro*.

The effect of AZM555130 on Tam-R cell migration was assessed using migration assays as described in section 2.10. MCF7wt and Tam-R cells ($5x10^4$) in W+5% ± Tam containing AZM555130 at the concentrations stated above were seeded into Transwell™ inserts which had been pre-coated with fibronectin. Control cells were seeded in W+5% ± Tam containing vehicle (DMSO) only. Cells were left for 24 hours before migratory cells were fixed and quantified as previously described. Data (mean cells/field of view) is presented as % of Control ± S.D. (* $p<0.05$ vs. Control ** $p<0.001$ vs. Control; n=4) (A). A representative experiment including MCF7wt cells for comparison is also shown (B).

(A) Mean % of Control (n=3).

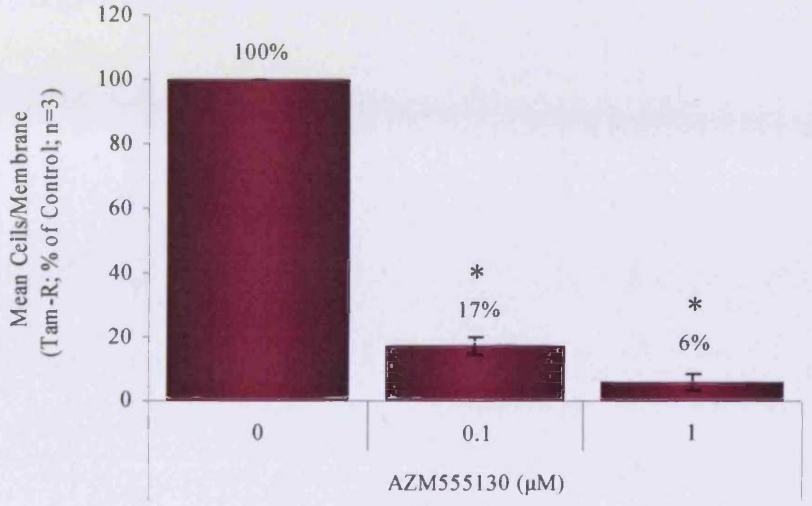

(B) Representative experiment with MCF7wt cells included for comparison.

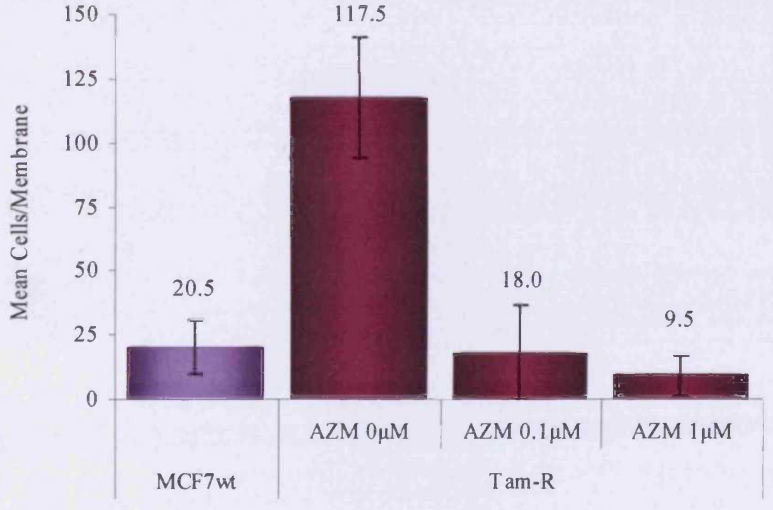

Figure 4.10 The effect of AZM555130 on invasion of Tam-R cells *in vitro*.

The effect of AZM555130 on Tam-R cell invasion was assessed using invasion assays as described in section 2.11. MCF7wt and Tam-R cells ($5x10^4$) in W+5% ± Tam containing AZM555130 at the concentrations stated above were seeded into Transwell™ inserts which had been pre-coated with Matrigel™. Control cells were seeded in W+5% ± Tam containing vehicle (DMSO) only. Cells were left for 72 hours before invasive cells were fixed and quantified as previously described. Data (mean cells/membrane) is presented as % of Control ± S.D. (* $p<0.001$ vs. Control; n=3) (A). A representative experiment including MCF7wt cells for comparison is also shown (B).

The affinities of MCF7wt and Tam-R cells for uncoated or fibronectin-coated surfaces following treatment with AZM555130 were measured using cell attachments assays (see section 2.9). The data obtained revealed that treatment with AZM555130 significantly inhibited the attachment of both cell-lines to either an uncoated or fibronectin-coated surface in a dose dependent manner (figure 4.11). Attachment of MCF7wt cells in the presence of AZM555130 (1μM) was reduced to approximately 25% and 22% of control on uncoated and fibronectin-coated surfaces respectively. The effect of AZM555130 at 1μM on Tam-R cell attachment was more modest, with the number of attached cells on an uncoated and fibronectin-coated surface reduced to approximately 69% and 59% of control respectively.

To expand upon these results, the rate of MCF7wt and Tam-R cell attachment in the absence and presence of AZM555130 was assessed using the attachment time-course assays described in section 2.9. Figure 4.12 shows that the rate of cell attachment to uncoated and fibronectin-coated surfaces was markedly reduced by AZM555130 at 1μM in both cell-lines. Interestingly, the effect of Src inhibition on the rate of cell attachment was greatest when the cells were seeded onto a fibronectin-coated surface, suggesting that treatment of cells with AZM555130 may disrupt integrin-dependent attachment which is regulated via FAK phosphorylation.

Indeed, SDS-PAGE/Western blot analysis of MCF7wt and Tam-R cells treated with AZM555130 at various concentrations (0-1μM) revealed that inhibition of Src kinase resulted in the decreased phosphorylation of FAK in a dose dependent manner. Figure 4.13 shows that phosphorylation of FAK at the Src specific Y861 site was significantly reduced by AZM555130 at both 0.1μM and 1μM. Furthermore, treatment with AZM555130 at these concentrations also resulted in a smaller reduction in the phosphorylation of FAK Y397. This is of particular interest as FAK Y397 is widely believed to be an auto-phosphorylation site. Levels of total FAK protein in these cells were unaffected by treatment with AZM555130.

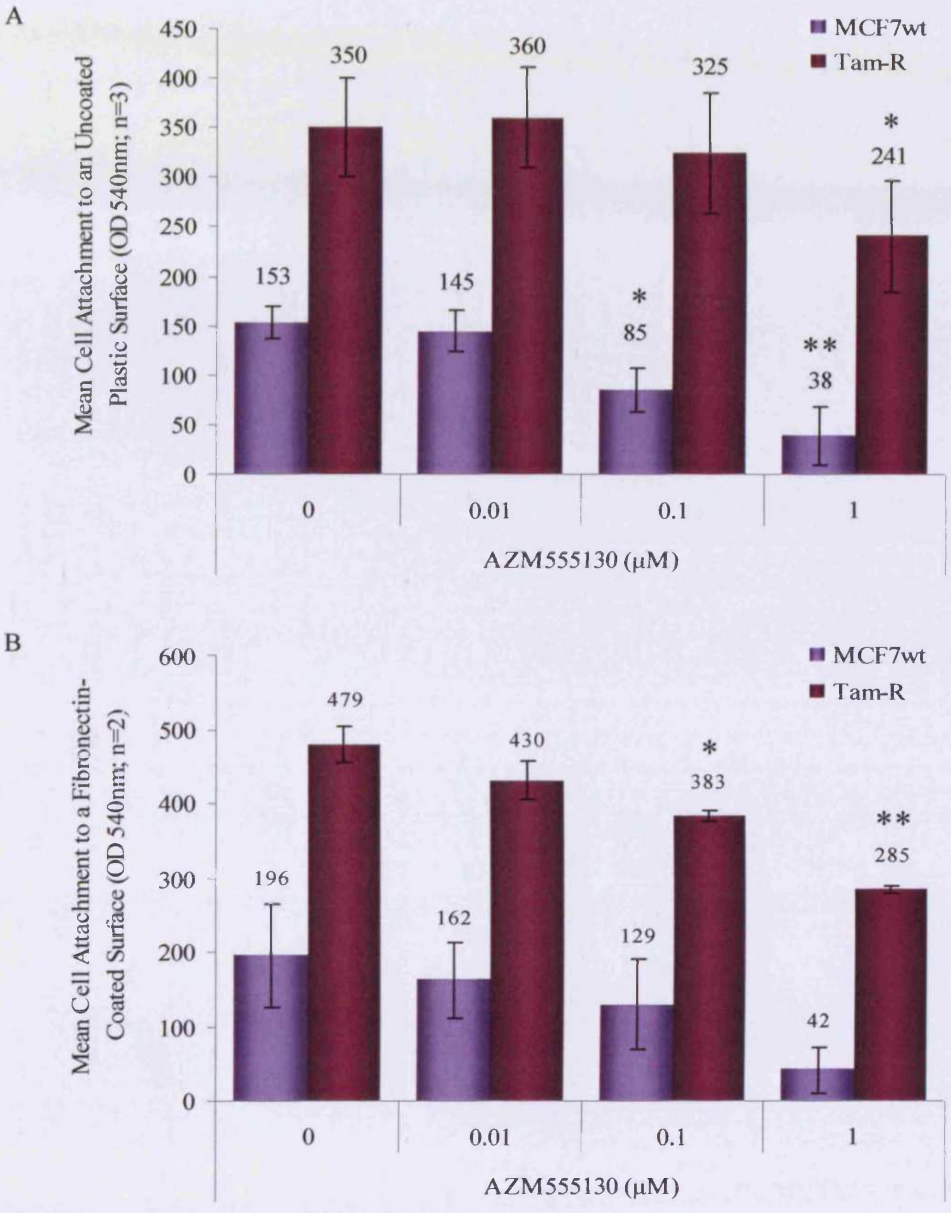

Figure 4.11 Effect of Src inhibition using AZM555130 on the affinity of MCF7wt and Tam-R cells for uncoated and fibronectin-coated surfaces.

The effect of Src inhibition on the affinity of MCF7wt and Tam-R cells for uncoated (A) or fibronectin-coated (B) surfaces was measured using a cell attachment assay. Cells ($4x10^4$) were seeded into the wells of either uncoated or fibronectin-coated 96-well plates in W+5% ± Tam (100nM) containing AZM555130 at the concentrations stated above. Control cells were seeded in W+5% ± Tam (100nM) containing vehicle (DMSO) only. Cells were left to attach for 50 minutes at 37°C after which the wells were washed with PBS and the number of attached cells assessed using the MTT assay as described in materials and methods (section 2.7.1). Each condition was run 6 times per experiment. Data is presented as Mean Cell Attachment (OD_{540}) ± S.D. (* $p<0.05$ vs. Control ** $p<0.01$ vs. Control; $n \geq 2$).

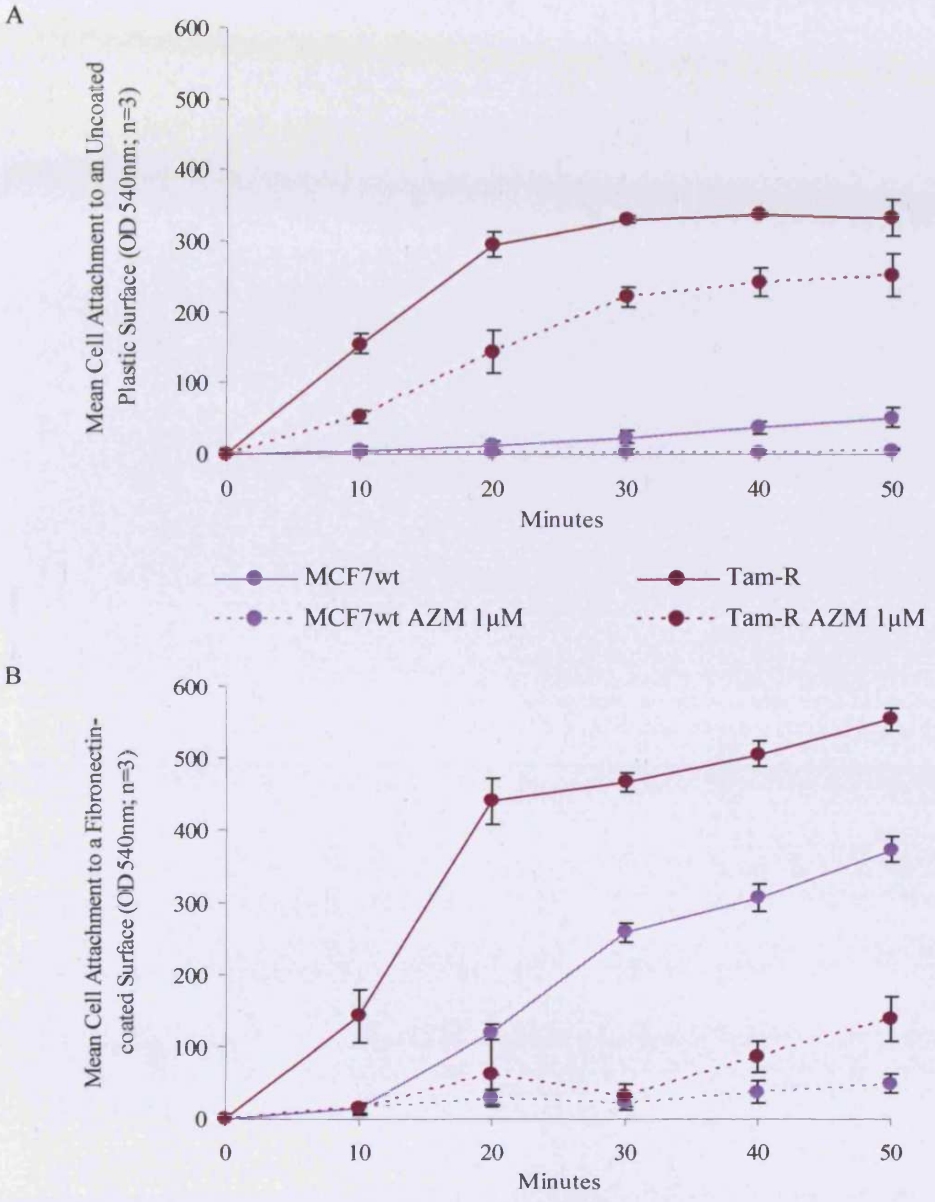

Figure 4.12 Effect of Src inhibition using AZM555130 on the rate of MCF7wt and Tam-R cell-attachment to uncoated and fibronectin-coated surfaces.

The effect of Src inhibition on the rate of MCF7wt and Tam-R cell attachment to uncoated (A) or fibronectin-coated (B) surfaces was measured using a cell attachment time-course assay. Cells ($4x10^4$) were seeded into the wells of either uncoated or fibronectin-coated 96-well plates in W+5% ± Tam (100nM) containing AZM555130 (1μM). Control cells were seeded in W+5% ± Tam (100nM) containing vehicle (DMSO) only. Cells were left to attach for up to 50 minutes at 37°C. During the course of the assay, medium containing unattached cells was removed at the given time points and replaced with PBS. The attached cells were kept in PBS until the end of the experiment when the MTT assay was carried out as normal. Data is presented as Mean Cell Attachment (OD_{540}) ± S.D. (n=3).

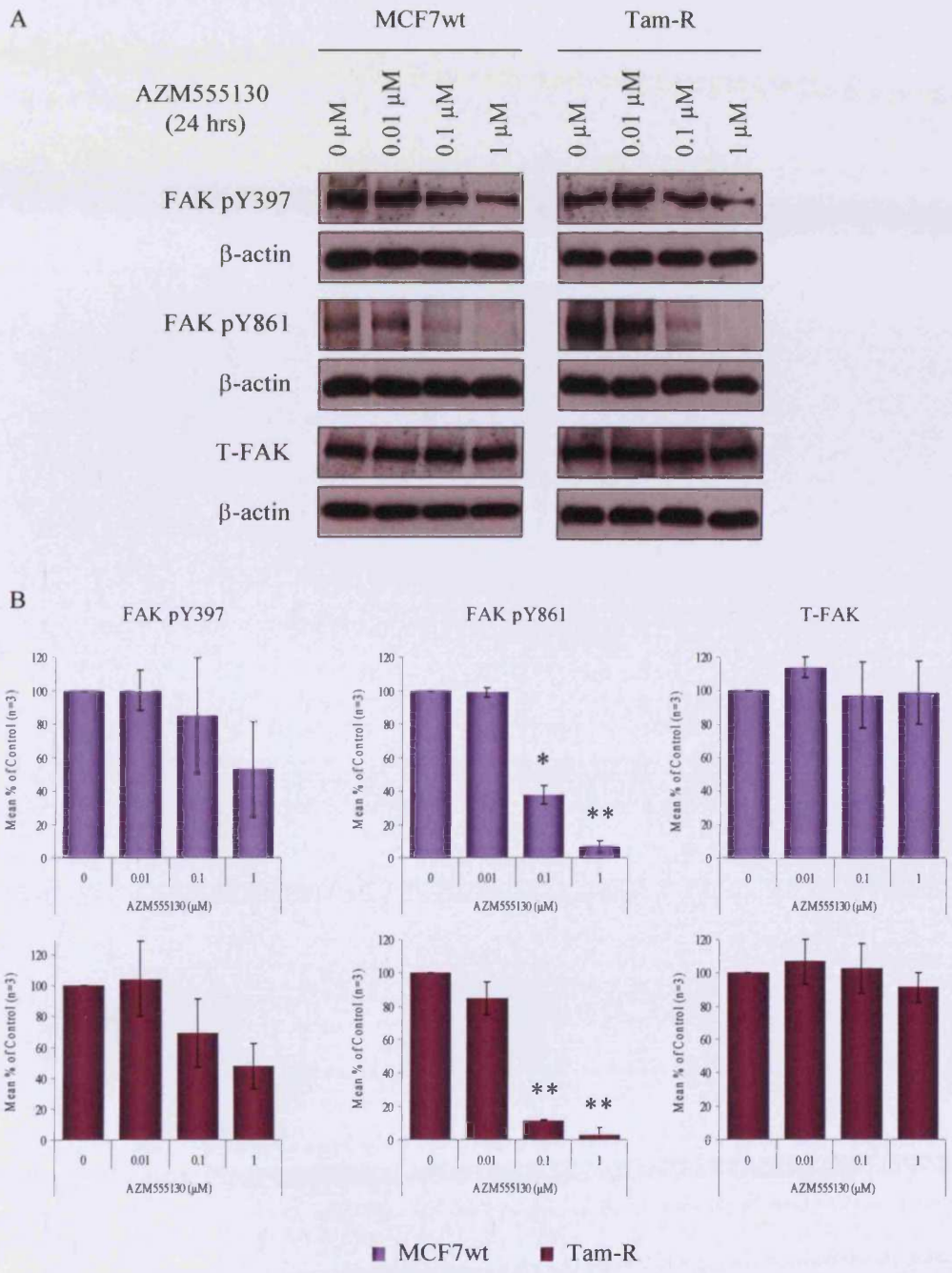

Figure 4.13 Effect of Src inhibition using AZM555130 on FAK phosphorylation (pY397 and pY861) in MCF7wt and Tam-R cells.

MCF7wt and Tam-R cells were cultured to log-phase growth and then treated with AZM555130 at the stated concentrations for 24 hours. Control cells were treated with vehicle (DMSO) only for the same duration. The cells were then lysed for proteins as described in materials and methods (section 2.4.1). Total soluble protein (40µg) was subjected to SDS-PAGE/Western blot analysis and the membranes probed with antibodies specific for phosphorylated FAK (pY397 and pY861) and total FAK (A). Densitometry was conducted on the bands obtained and the data, corrected for loading with β-actin, presented as Mean % of Control ± S.D. (* $p<0.01$ vs. Control ** $p<0.001$ vs. Control; $n \geq 3$) (B).

4.2.3 Src inhibition with AZM555130 in MCF7wt and Tam-R cells decreases cell proliferation

Tam-R cells have previously been shown to possess an increased growth rate in comparison to their wild-type counterparts, and this increased growth is reportedly driven by enhanced EGFR and c-erbB2 signalling in these cells [70]. The synergistic association between increased Src activation and enhanced EGFR signalling is well established [131, 145, 200, 201, 237]. However, a role for Src in cell proliferation is more controversial, with published reports providing evidence for both sides of the argument [150, 152, 153, 237, 238]. As such, AZM555130 was utilised to investigate the role of Src in the increased growth rate of Tam-R cells.

The effect of Src inhibition on the growth of MCF7wt and Tam-R cells was assessed using cell counting experiments (see section 2.7.2). The data obtained from three independent experiments is presented in figure 4.14 and shows that the growth of both MCF7wt and Tam-R cell-lines was significantly inhibited by AZM555130 at a concentration of 1μM only. Src has been linked to the augmentation of multiple signalling pathways that are able to promote both cell proliferation and cell survival. The cell counting experiments presented here show that the inhibition of Src with AZM555130 reduced cell number; however, it is not clear whether this reduction is a result of decreased proliferation or decreased cell survival. Therefore, whether the reduction in cell number following AZM555130 treatment was a result of the disruption of either, or both, of these cellular processes was investigated next.

The induction of apoptosis in the MCF7wt and Tam-R cell-lines following treatment with AZM555130 was measured using FACS analysis as described in section 2.8. Cells were seeded in W+5% ± Tam (100nM) and allowed to attach for 48-72 hours before being treated with either AZM555130 (0.01-1μM) or vehicle (DMSO) for a further 72 hours. Apoptosis in these cells was then assessed using the Vybrant® Apoptosis Assay Kit #4 (Invitrogen). The Vybrant® Apoptosis Assay uses Yo-Pro®-1 (green) and propidium iodide (PI; red) fluorescent dyes to assess the viability of cells. Yo-Pro®-1 is able to

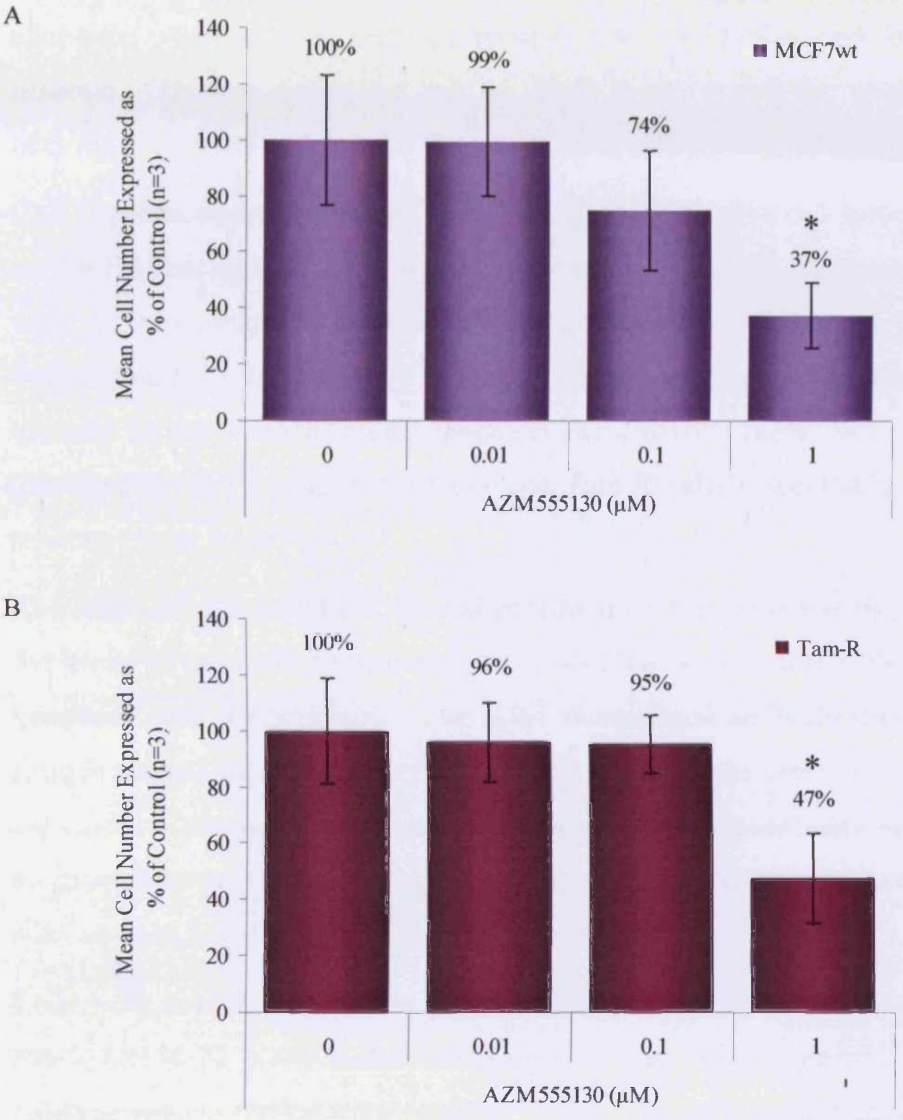

Figure 4.14 Dose-dependent effect of AZM555130 Src-family-kinase inhibitor on cell growth in MCF7wt and Tam-R cells as determined by cell counting.

MCF7wt (A) and Tam-R (B) cells were seeded in W+5% ± Tam (100nM) into a 24-well plate at a density of 40,000 cells/well. After 24hrs, the medium was replaced with W+5% ± Tam (100nM) containing AZM555130 at the stated concentrations. Control cells were cultured in the presence of vehicle (DMSO) only. The cells were cultured as normal and cell number determined on days 8 (Tam-R) and 11 (MCF7wt) using a Beckman Coulter™ Multisizer II. Each concentration was counted in triplicate per experiment and the experiment was repeated 3 times. Data is presented as Mean % of Control ± S.D (* $p<0.05$ vs. Control; n=3).

permeate the membrane of apoptotic cells, but not healthy cells; whilst PI is excluded from both due to its larger size. PI can, however, be taken up by necrotic cells. Therefore, any cells containing only Yo-Pro®-1 will be apoptotic, whereas any cells containing both Yo-Pro®-1 and PI will be necrotic. Thus, a distinction can be made between healthy, apoptotic and necrotic cells by measuring the fluorescence of individual cells using FACS.

Cell populations were analysed using CellQuest™ Version 3.3 software based on the fluorescence profile obtained. For quantitation, the number of cells in each gated population was expressed as a percentage of the total number of events counted. Figures 4.15 and 4.16 show that there was no significant increase in the levels of either apoptosis (Yo-Pro1® +ve/PI –ve) or necrosis (Yo-Pro1® +ve/PI +ve) in MCF7wt and Tam-R cells respectively following treatment with AZM555130.

The effect of Src inhibition on cell proliferation was assessed by measuring the levels of the Ki67 nuclear antigen in MCF7wt and Tam-R cells following treatment with AZM555130. The Ki67 monoclonal antibody recognises an antigen present in the nucleus of cells at all stages of the cell cycle apart from G0 [239]. Cells in G0 are said to be dormant, or quiescent, and demonstrate no growth or replication of cellular components. Thus, the presence of the Ki67 antigen is a reliable marker of cell proliferation.

Cells were seeded onto coverslips in W+5% ± Tam (100nM) and allowed to attach for 48-72 hours before being treated with either AZM555130 (0.01-1μM) or vehicle (DMSO) for a further 72hrs. The cells were then fixed using formal-saline as described in section 2.5.1.2, and assayed for the Ki67 nuclear antigen using the MIB I monoclonal antibody following the protocol outlined in section 2.5.2. The Ki67 antigen was visualised in the cells using the DAKO EnVision™+ system peroxidase [DAB] kit. Representative images of Ki67 antigen staining in MCF7wt and Tam-R cells at each concentration of AZM555130 were captured at 10x and 20x magnification, and are presented in figures 4.17 and 4.18 respectively. The images show that the proportion of Ki67 antigen expressing cells was significantly reduced by AZM555130 at

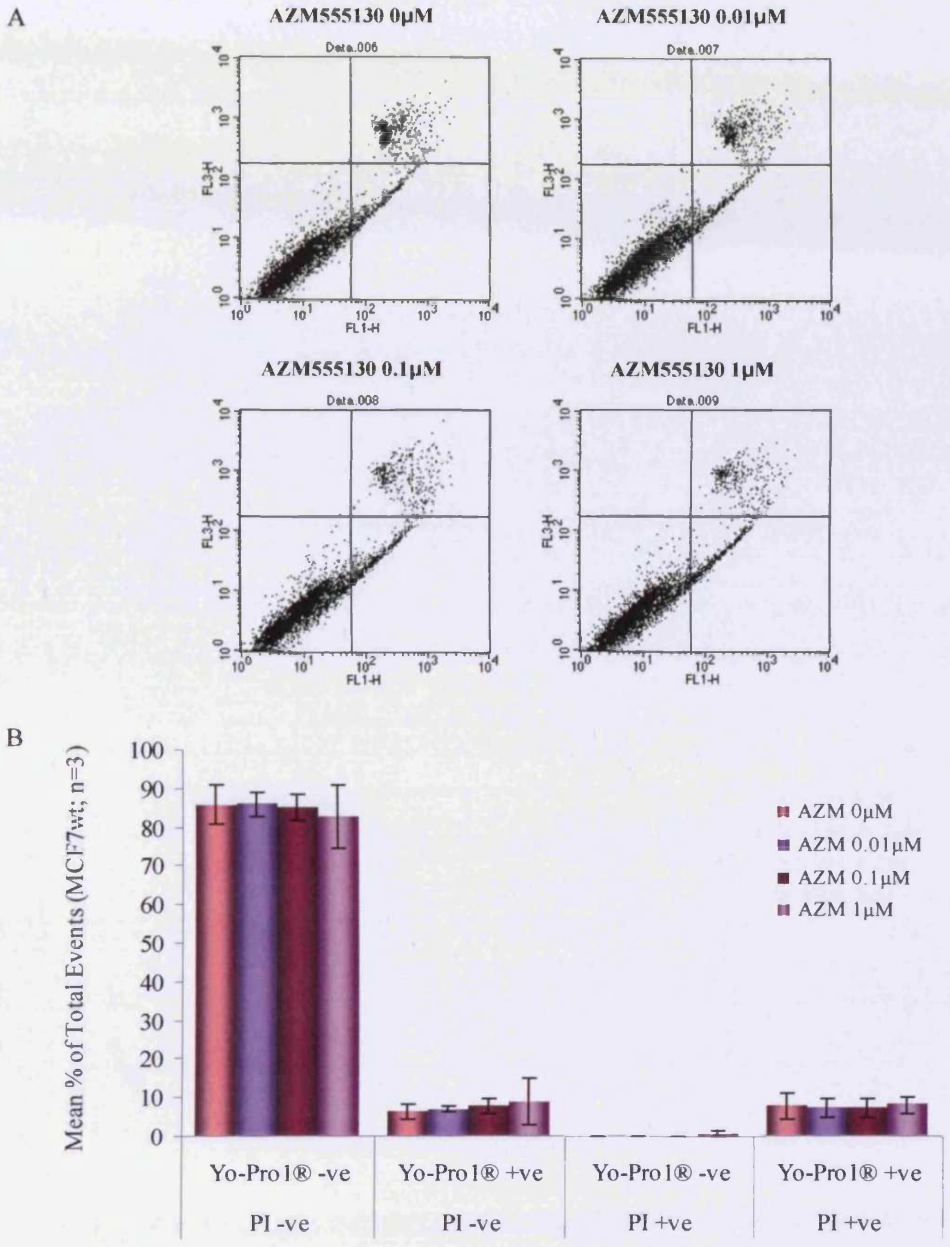

Figure 4.15 Effect of Src inhibition using AZM555130 on apoptosis in MCF7wt cells.
MCF7wt cells were treated with AZM555130 at the stated concentrations or with vehicle only (DMSO) for 72hrs. Apoptosis was then assessed using the Vybrant® Apoptosis Assay Kit #4 (Invitrogen) as described in materials and methods (section 2.8). Cell counts were measured using a FACSCalibur FACS machine. Positive (TPEN-treated) and negative (untreated) controls for the assay were used to calibrate the FACS machine for optimal data collection. A total of 5000 events were counted in each run and each sample was counted in duplicate. Cell populations were analysed using CellQuest™ Version 3.3 software based on their fluorescence profile (A). Yo-Pro®1 –ve/PI –ve cells represent the live-cell population, Yo-Pro®1 +ve/PI –ve cells are undergoing early-mid apoptosis, and Yo-Pro®1 +ve/PI +ve cells are necrotic. Data is presented as the mean number of cells in each population as a percentage of the total number of events ± S.D. (n=3) (B).

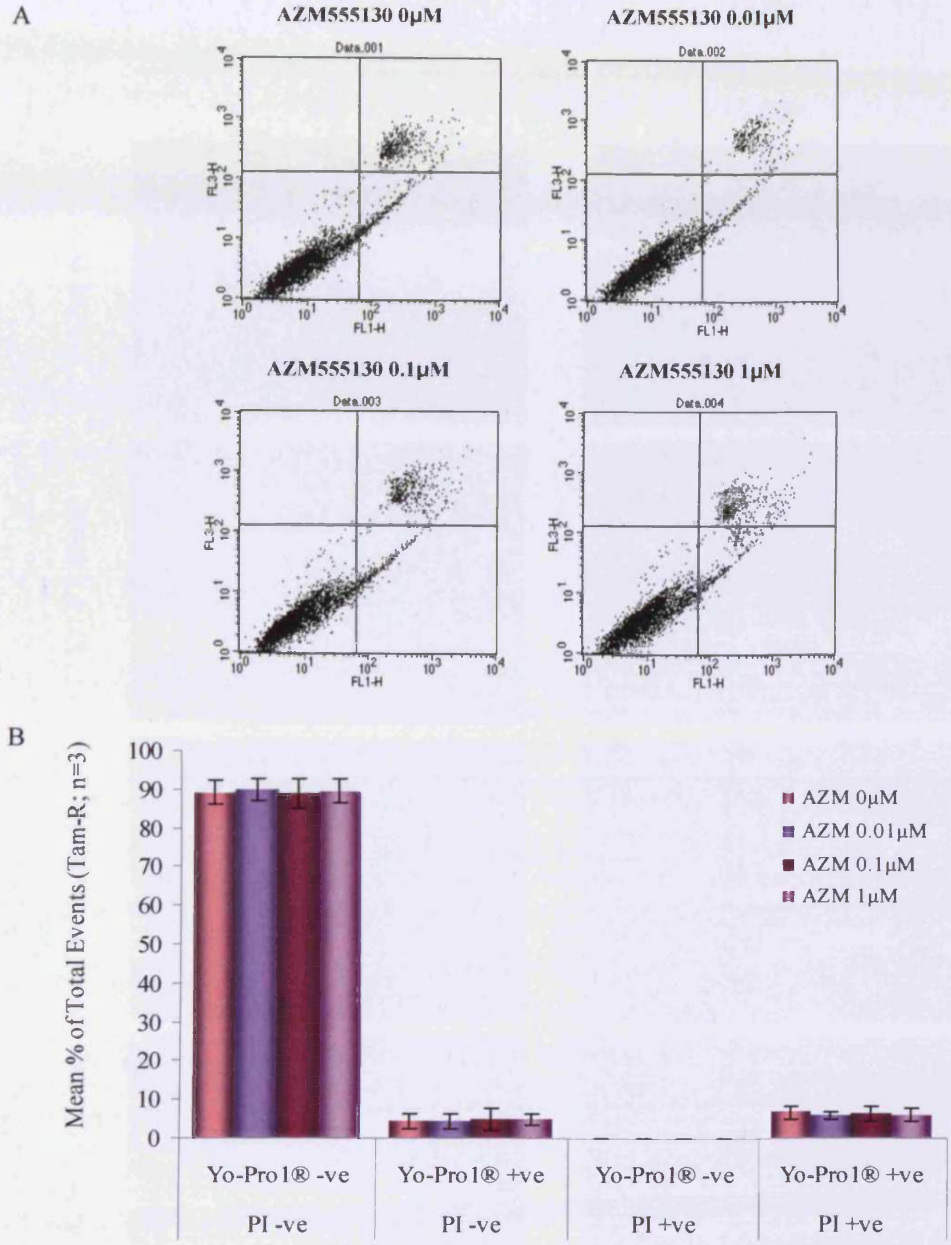

Figure 4.16 Effect of Src inhibition using AZM555130 on apoptosis in Tam-R cells.

Tam-R cells were treated with AZM555130 at the stated concentrations or with vehicle only (DMSO) for 72hrs. Apoptosis was then assessed using the Vybrant® Apoptosis Assay Kit #4 (Invitrogen) as described in materials and methods (section 2.8). Cell counts were measured using a FACSCalibur FACS machine. Positive (TPEN-treated) and negative (untreated) controls for the assay were used to calibrate the FACS machine for optimal data collection. A total of 5000 events were counted in each run and each sample was counted in duplicate. Cell populations were analysed using CellQuest™ Version 3.3 software based on their fluorescence profile (A). Yo-Pro®1 –ve/PI –ve cells represent the live-cell population, Yo-Pro®1 +ve/PI –ve cells are undergoing early-mid apoptosis, and Yo-Pro®1 +ve/PI +ve cells are necrotic. Data is presented as the mean number of cells in each population as a percentage of the total number of events ± S.D. (n=3) (B).

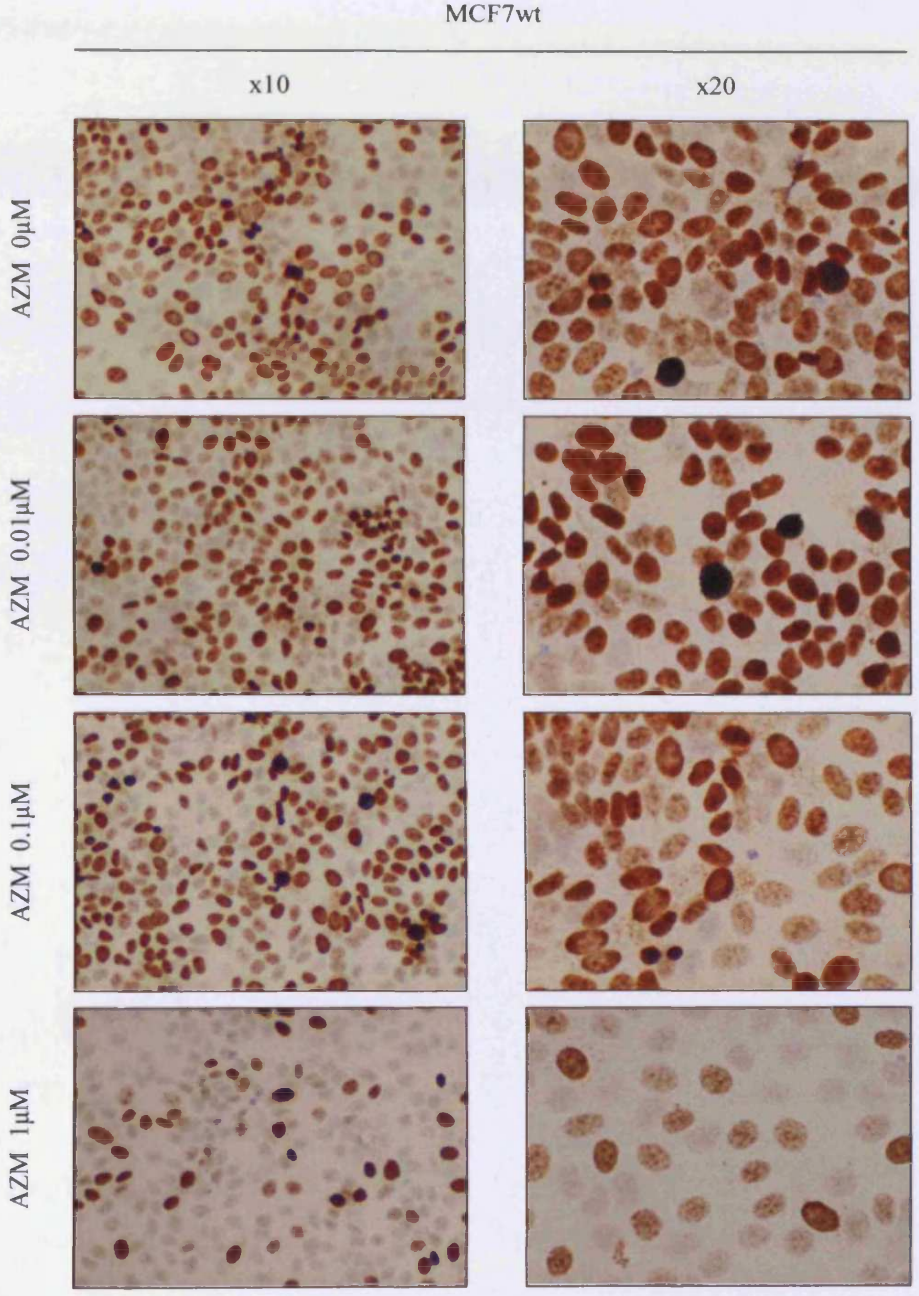

Figure 4.17 Assessment of the inhibitory effects of AZM555130 on cell proliferation in MCF7wt cells using immunocytochemical staining for the Ki67 antigen.

MCF7wt cells were cultured on glass coverslips and then treated with AZM555130 at the stated concentrations or with vehicle only (DMSO) for 72hrs. The cells were then fixed with formal-saline as described in materials and methods (section 2.5.1.2) and assayed for the Ki67 antigen using the MIB I monoclonal antibody. Ki67 antigen present in the cells was visualised using the DAKO EnVision™+ system peroxidase [DAB] kit as described in section 2.5.2. Representative images of Ki67 staining in MCF7wt cells at each concentration of AZM555130 were captured at 10x and 20x magnification using an Olympus BH-2 phase contrast microscope fitted with an Olympus DP-12 digital camera system.

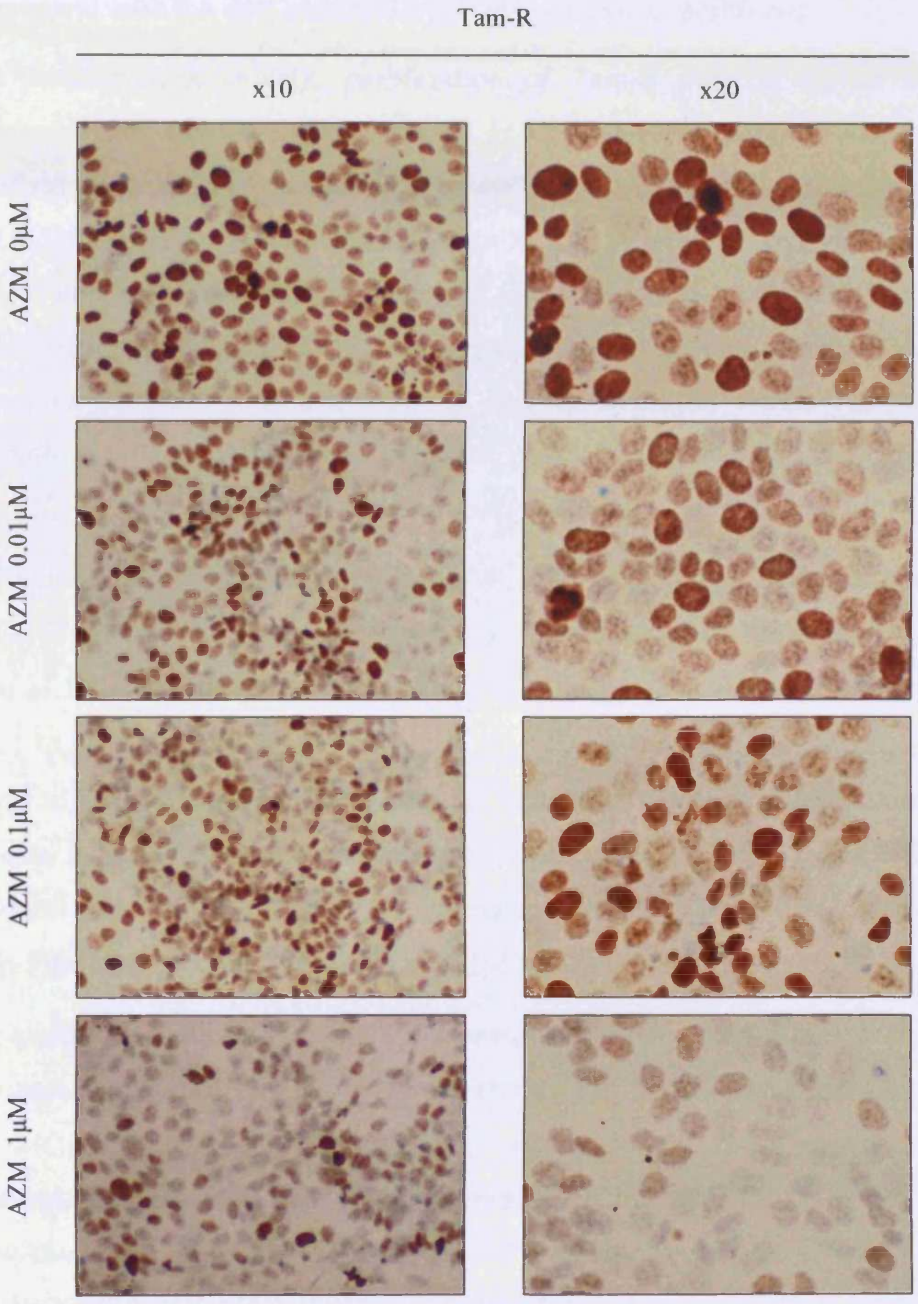

Figure 4.18 Assessment of the inhibitory effects of AZM555130 on cell proliferation in Tam-R cells using immunocytochemical staining for the Ki67 antigen.

Tam-R cells were cultured on glass coverslips and then treated with AZM555130 at the stated concentrations or with vehicle only (DMSO) for 72hrs. The cells were then fixed with formal-saline as described in materials and methods (section 2.5.1.2) and assayed for the Ki67 antigen using the MIB I monoclonal antibody. Ki67 antigen present in the cells was visualised using the DAKO EnVision™+ system peroxidase [DAB] kit as described in section 2.5.2. Representative images of Ki67 staining in Tam-R cells at each concentration of AZM555130 were captured at 10x and 20x magnification using an Olympus BH-2 phase contrast microscope fitted with an Olympus DP-12 digital camera system.

1μM only in both the MCF7wt and Tam-R cell-lines. These results are in agreement with the data obtained with cell counting experiments.

As mentioned previously, proliferation of Tam-R cells is driven by the enhanced activation of the EGFR-ERK 1/2 mitogenic signalling pathway [70]. Furthermore, Ki67 staining, which was reduced following treatment with AZM555130, is known to correlate with EGFR activity in tamoxifen-resistant breast cancer *in vivo* [23]. Therefore, given the effect of AZM555130 on proliferation and Ki67 staining in these cell-lines, in addition to Src's ability to phosphorylate EGFR at a number of sites to potentiate EGFR activity and signalling [201, 229, 240], the effect of AZM555130 on EGFR signalling in the MCF7wt and Tam-R cells was investigated.

SDS-PAGE/Western blot analysis of MCF7wt and Tam-R cells treated with AZM555130 at increasing concentrations (0-1μM) revealed that phosphorylation of EGFR Y1068 was significantly reduced at 1μM only, while levels of total EGFR were unaffected (figure 4.19). Phosphorylation of EGFR Y1068 leads to the activation of the RAS-RAF signalling pathway, which ultimately results in the downstream activation of the MAPKs, ERK 1 and ERK 2. Accordingly, figure 4.20 shows a corresponding reduction in ERK 1/2 activation following Src inhibition with AZM555130 at 1μM only.

As treatment with AZM555130 was seen to down-regulate EGFR activity at the protein level, the effect of Src inhibition on TGFα-stimulated growth in the MCF7wt and Tam-R cell-lines was next explored. These growth experiments were conducted over a short duration and so the MTT assay described in section 2.7.1 was used to quantitate cell number. MCF7wt and Tam-R cells ($5x10^3$) were cultured in a 96-well plate for 5 days in medium containing either AZM555130 (0-1μM) + TGFα (10ng/ml) or AZM555130 (0-1μM) alone before being subjected to the MTT assay for quantitation. Figure 4.21 shows that the basal growth of MCF7wt and Tam-R cells was decreased by AZM555130 at a concentration of 1μM, which confirms the data obtained using cell counting experiments in figure 4.14. Treatment of the cells with

A MCF7wt

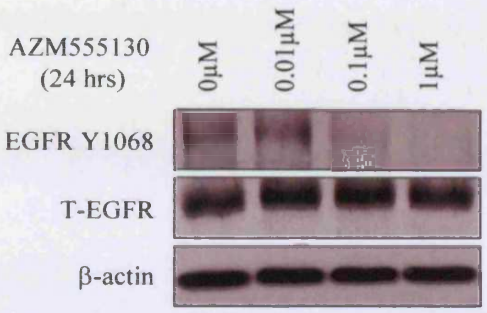

B Tam-R

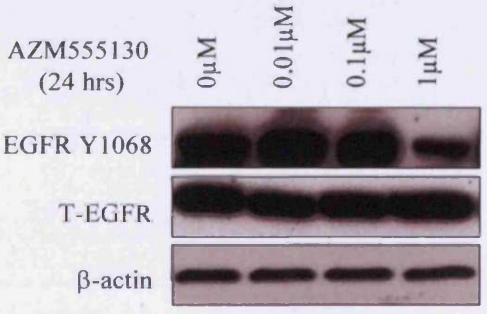

C

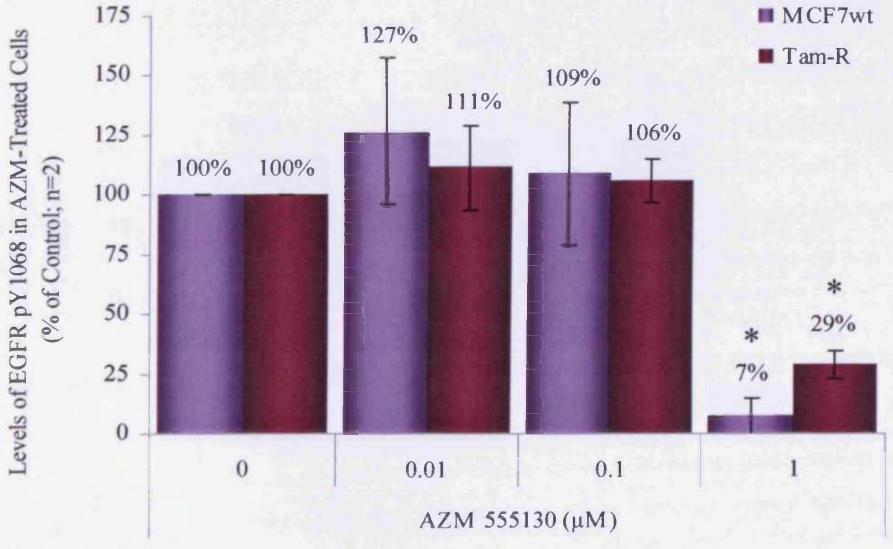

Figure 4.19 Effect of Src inhibition on EGFR activation in MCF7wt and Tam-R cells.

MCF7wt and Tam-R cells were cultured to log-phase growth and then treated with AZM555130 at the stated concentrations for 24 hours. Control cells were treated with vehicle (DMSO) only for the same duration. The cells were then lysed for proteins as described in materials and methods (section 2.4.1). Total soluble protein (40μg) was subjected to SDS-PAGE/Western blot analysis and the membranes probed with antibodies specific for EGFR pY1068 and total EGFR (A and B). Densitometry was conducted on the bands obtained and the data for pY1068, corrected for loading with β-actin, presented as % of Control (* $p<0.001$ vs. Control; n=2) (C).

A MCF7wt

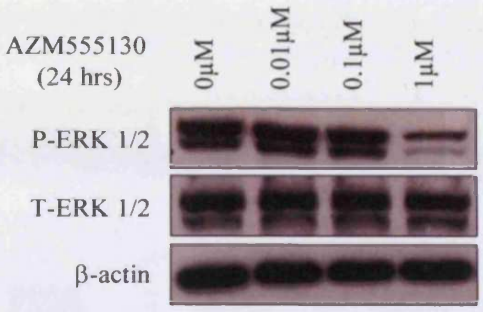

B Tam-R

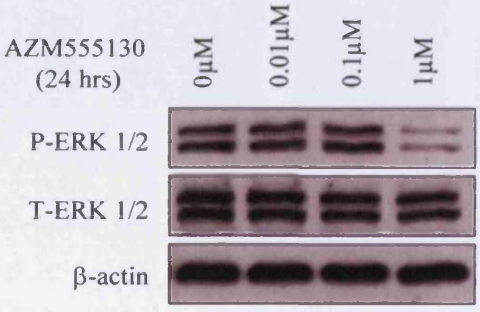

C

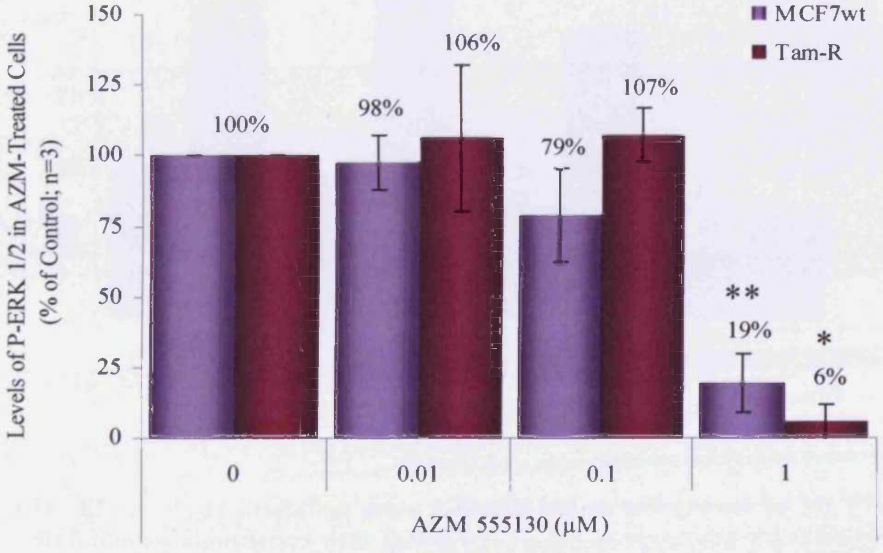

Figure 4.20 Effect of Src inhibition on ERK 1/2 activation in MCF7wt and Tam-R cells.
MCF7wt and Tam-R cells were cultured to log-phase growth and then treated with AZM555130 at the stated concentrations for 24 hours. Control cells were treated with vehicle (DMSO) only for the same duration. The cells were then lysed for proteins as described in materials and methods (section 2.4.1). Total soluble protein (40μg) was subjected to SDS-PAGE/Western blot analysis and the membranes probed with antibodies specific for active (P) and total (T) ERK 1/2 (A and B). Densitometry was conducted on the bands obtained and the data for P-ERK 1/2, corrected for loading with β-actin, presented as % of Control (* $p<0.05$ vs. Control ** $p<0.01$ vs. Control; $n \geq 3$) (C).

A MCF7wt

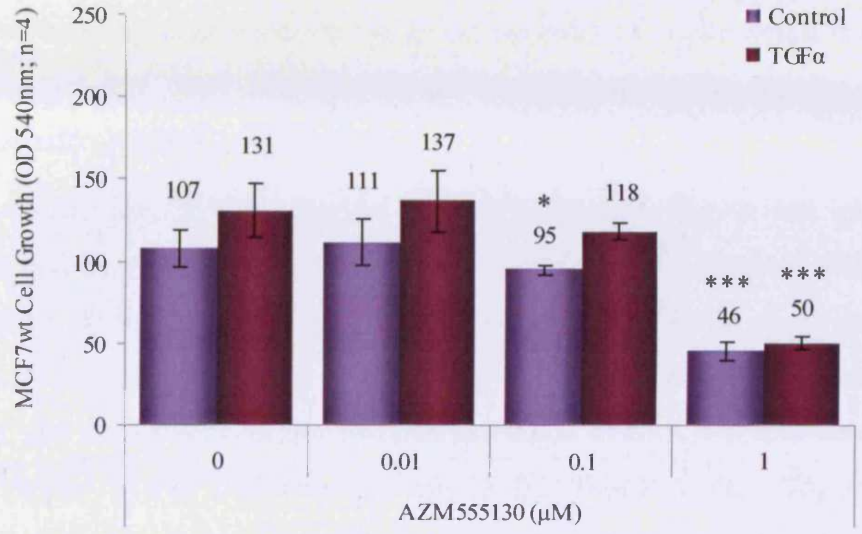

B Tam-R

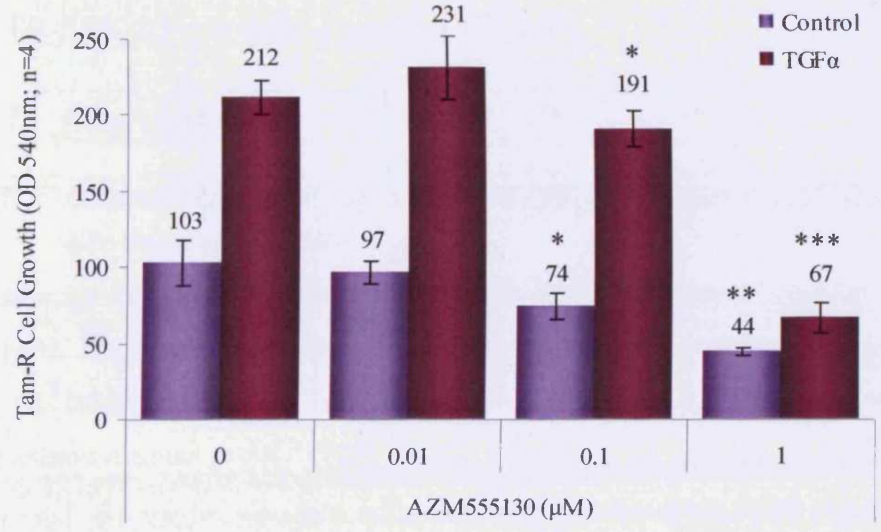

Figure 4.21 Effect of Src inhibition using AZM555130 on cell growth in MCF7wt and Tam-R cells following stimulation with TGFα.

MCF7wt (A) and Tam-R (B) cells were seeded in W+5% ± Tam (100nM) into a 96-well plate at a density of $5x10^3$ cells/well. After 24 hrs, the medium was replaced with W+5% ± Tam containing either AZM555130 + TGFα (10ng/ml) or AZM555130 alone. AZM555130 was used at the concentrations stated above, with control cells cultured in the presence of vehicle (DMSO) only. The cells were cultured at 37°C for 5 days before cell number was determined using the MTT assay as described in section 2.7.1. Data is presented as mean absorbance at 540nm, which is proportional to cell number, ± S.D. (* $p<0.05$ vs. Control ** $p<0.01$ vs. Control *** $p<0.001$ vs. Control; n=4).

TGFα resulted in a 2-fold increase in their growth. However, when treated with TGFα in the presence of AZM555130 at 1μM, the stimulatory effects of TGFα on Tam-R cell proliferation were negated. TGFα treatment was seen to have no significant effect on the growth of MCF7wt cells which is consistent with fact that these cells display lower levels of EGFR activity than their tamoxifen-resistant counterparts.

In conclusion, it was observed that MCF7wt and Tam-R cell growth was reduced by AZM555130 at 1μM only. Ki67 staining revealed that this was due to the inhibition of cell-proliferation; whereas levels of apoptosis were unaffected. Furthermore, AZM555130 at 1μM reduced EGFR phosphorylation and the subsequent downstream activation of ERK 1/2, and was also able to negate TGFα stimulated growth in the Tam-R cells. Together, these observations support a role for Src in the promotion of cell-proliferation via the potentiation of EGFR phosphorylation and the subsequent activation of the EGFR-ERK 1/2 mitogenic signalling pathway.

4.3 Discussion

4.3.1 Characterisation of AZM555130 as a potent inhibitor of Src kinase activity

Over-expression and/or increased activity of Src has been reported in many cancers, including colon, breast and pancreatic [101], and has been identified as an important factor in tumour progression and the development of metastatic disease [103]. Additionally, increased Src activity in breast cancer has been shown to correlate with increased proliferation, high tumour grade and lower 5-year recurrence-free survival rates [109].

In the previous chapter, the Tam-R model of tamoxifen-resistant breast cancer was shown to possess elevated levels of Src activity. Furthermore, these cells were seen to exhibit an aggressive cell-phenotype *in vitro*, displaying an altered morphology and enhanced cell growth, attachment, motility and invasion compared to their hormone-sensitive parental cell-line. Therefore, the aim of this chapter was to establish a causative role for Src in the

regulation of the aggressive cell-phenotype exhibited by the Tam-R cell-line. To accomplish this, a novel Src-family-kinase inhibitor was employed to reduce Src activation in MCF7wt and Tam-R cells, which were then studied for any subsequent changes in their *in vitro* behaviour.

AZM555130 is a novel Src-family-kinase inhibitor recently developed by AstraZeneca. It is one of a number of leading probe compounds, of which AZD0530 has been selected for assessment in clinical trials as an anti-invasive therapy [236]. AZM555130 and AZD0530 are very similar in structure and both belong to the anilinoquinazoline class of small molecule inhibitors [234, 235]. These have previously proven to be very successful as inhibitors of tyrosine kinase activity, with recent examples including the EGFR tyrosine kinase inhibitor gefitinib (Iressa™, ZD1839) [241, 242].

AZM555130 and AZD0530 are ATP analogues which reduce Src kinase activity by competitively binding to the active site of its kinase domain. Although AZD0530 has been carried forward into clinical trials, AZM555130 was used throughout this study as the AZD0530 compound was not available for use when work began. However, much of the data presented here has subsequently been repeated using AZD0530 with comparable results. AZM-555130 is a novel compound that had not been used in these cell models prior to this work. Therefore, the first priority was to optimise the conditions of its use and to assess it as an inhibitor of Src kinase activation in these cells.

AZM555130 inhibited the phosphorylation of Src Y419 in a dose dependent manner, with IC_{50} values in MCF7wt and Tam-R cells of 0.07μM and 0.02μM respectively. A concentration of 1μM was selected as optimal for experimental use because, not only did it have the greatest effect on Src inhibition, but it was also a concentration well tolerated by the cells. Furthermore, time course experiments revealed that the reduction of Src Y419 phosphorylation was rapid, and occurred within minutes of the initial treatment. Additionally, the effects of AZM555130 on Src activation were sustained and still evident up to 4 days post-treatment. This verifies that AZM555130 was suitable for use in both experiments with a short duration, such as attachment time course assays,

and longer-term experiments, such as growth studies. A treatment duration of 24 hours was selected for protein analysis as this ensured any downstream effects of Src inhibition were observed experimentally.

SU6656 is a proprietary Src inhibitor and is one of the most commonly used compounds in the *in vitro* study of Src at present. SU6656 is an ATP-analogue and has a similar mechanism of action to AZM555130 [243]; however, comparison of SU6656 with AZM555130 showed that AZM555130 was more efficacious, with the IC_{50} for SU6656 in Tam-R cells calculated at 1.7μM. Furthermore, phosphorylation of Src at Y419 was still evident with SU6656 at 10μM, a concentration that was proving to be cytotoxic upon visual inspection of the cells during treatment. Therefore, the lower concentrations of AZM555130 required for effective Src inhibition in MCF7wt and Tam-R cells would increase the tolerability of the compound.

4.3.2 Src and the aggressive phenotype of tamoxifen resistant breast cancer cells in vitro

To assess the effects of increased Src activity on the aggressive phenotype displayed by the Tam-R cells *in vitro*, the appearance and behaviour of MCF7wt and Tam-R cells were examined in the presence of AZM555130. As with the optimisation experiments, increasing concentrations of AZM555130 were used in order to identify any potential dose-dependent effects.

Visual assessment of MCF7wt and Tam-R cells treated with AZM555130 (1μM, 24 hrs) revealed that the Tam-R cells had undergone morphological reversion, while the MCF7wt cells were seemingly unchanged. Inhibition of Src kinase activity in Tam-R cells resulted in decreased membrane activity, with a marked absence of lamellipodia and filopodia formation evident. Src has previously been implicated in the formation of lamellipodia and filopodia through promotion of actin polymerisation and cyto-skeletal rearrangement [170, 238, 244]. The formation of lamellipodia and filopodia is important in actively motile cells as these membrane projections allow the cell to form new cell-matrix attachments distal to the main body of the cell and provide traction to enable forward movement [170].

Additionally, under basal conditions Tam-R cells grow in loose, disorganised colonies and demonstrate de-regulated E-cadherin-mediated cell-cell contact formation [165]. However, in the presence of AZM555130 Tam-R cells were seen to grow in tightly packed colonies similar to those seen with MCF7wt cells, suggesting the re-establishment of cell-cell adhesion mechanisms. Intact cell-cell contacts are important for the suppression of cell motility and invasion [164]. Increased Src kinase activity has previously been shown to disrupt cadherin-dependent cell-cell contacts [245]; while inhibition of Src with PP2 was seen to restore cell-cell attachment via increased E-cadherin expression, leading to inhibition of cancer metastasis [237].

It has been proposed that Src may act as a molecular switch that alters the predominant adhesion type in the cell from cell-cell adhesions to dynamic cell-matrix attachments, and that this may increase cell motility [166]. The data reported in this chapter suggest that increased Src activation increases membrane activity and de-regulates cell-cell attachment in Tam-R cells, which together may contribute to their motile and invasive phenotype. Inhibition of Src with AZM555130 was able to reduce membrane activity and restore cell-cell contacts in Tam-R cells, resulting in an altered morphology that may have a significant impact on these cell's ability to migrate and invade.

Indeed, investigations into the effect of Src inhibition on the migratory and invasive capabilities of Tam-R cells showed significant inhibition of both cellular processes by AZM555130 in a dose-dependent fashion. Interestingly, invasion in the Tam-R cells appeared to be more sensitive than migration to the effects of Src inhibition, with reductions of 83% and 44% seen with AZM555130 at 0.1μM respectively. This may be because Src activity is required for a number of the cellular events that, when coordinated, result in cell invasion, including decreased cell-cell adhesion, increased cell motility and the expression of matrix-metalloproteases to digest the basal membrane. This increased dependence on Src may explain the increased sensitivity of cell invasion to the effects of Src inhibition.

Cell migration and invasion are fundamentally reliant on the disruption of cell-cell contacts and the de-regulation of cell-matrix attachment. In the previous chapter it was hypothesised that Src is able to regulate cell-matrix attachment by increasing FAK phosphorylation and, thus, the rate of focal adhesion formation and turnover. Therefore, the effect of Src inhibition on cell-matrix attachment in MCF7wt and Tam-R cells was investigated next.

Attachment to uncoated and fibronectin-coated plastic surfaces was reduced in MCF7wt and Tam-R cells following seeding in medium containing AZM555130. Once again, the effects of AZM555130 were dose-dependent; although, even at 1μM, a concentration previously shown to significantly decrease Src Y419 phosphorylation, the inhibitory effects of AZM555130 on cell-matrix attachment were modest, especially in the Tam-R cell-line (approximate 40% reduction on both matrices compared to control). More pronounced, however, were the effects on the rate of cell-matrix attachment in these cells, particularly on a fibronectin-coated surface. Together, this would suggest that although Src kinase activity is not crucial for cell-matrix attachment, it is able to influence the rate at which it occurs. Indeed, attachment and spreading of Src-deficient fibroblasts has been shown to be significantly delayed on both fibronectin and vitronectin [246].

Cell-matrix attachment and motility are regulated by integrin signalling via the phosphorylation of FAK and other focal adhesion proteins. As Src is known to regulate the phosphorylation of FAK, the effects of Src inhibition on FAK activation and signalling were examined. SDS-PAGE/Western blotting experiments revealed that the phosphorylation of FAK Y861, a Src specific site, was significantly reduced by AZM555130 at both 0.1μM and 1μM. In addition, a similar decrease in the phosphorylation of paxillin Y31 was also observed, suggesting the disruption of Src/FAK signalling pathways [247]. Expression of an FAK Y861F mutant in NIH3T3 fibroblasts suppressed the association of FAK with $p130^{CAS}$ and resulted in decreased motility and invasion in these cells [225]; while the expression of a paxillin Y31F mutant in

NBT-II cells has been shown to impair cell motility and prevent the formation of paxillin-Crk complexes at focal adhesions [224].

Somewhat surprisingly, a modest decrease in the phosphorylation of FAK Y397 was also observed following treatment of MCF7wt and Tam-R cells with AZM555130. FAK Y397 is an auto-phosphorylation site that is phosphorylated following integrin engagement and clustering, although the precise mechanisms by which this occurs are largely unknown. However, the data presented here suggest a potential role for Src.

Some studies suggest that the phosphorylation of FAK can result from trans-activation by other proteins. For example, EGFR has been shown to enhance FAK Y397 phosphorylation following ligand binding to promote growth-factor induced motility [205]. Therefore, given the synergistic relationship between Src and EGFR it is possible that AZM555130 is able to reduce Y397 phosphorylation indirectly via the inhibition of EGFR. Further work using a specific inhibitor of EGFR, such as gefitinib, is required to address this.

Meanwhile, others have proposed that FAK itself may be able to promote the auto-phosphorylation of Y397. Phosphorylation of FAK Y397 leads to the binding of Src and the subsequent Src-dependent phosphorylation of FAK on Y576, Y577 and Y861. Ruest *et al.* (2000) and Leu and Maa (2002) suggest that FAK molecules phosphorylated at these sites are then able to trans-phosphorylate other FAK molecules on Y397 as part of a signal amplification mechanism [248, 249]. Disruption of Src/FAK signalling required for FAK Y861 phosphorylation following treatment with AZM555130 has been demonstrated above. Therefore, treatment with AZM555130 may result in the partial loss of this signal amplification mechanism, thus accounting for the modest reduction in Y397 phosphorylation seen.

Further studies have suggested a more direct role for Src kinase activity in the phosphorylation of FAK Y397. Src possesses a dual role as a signalling molecule in that it is able to act as both a tyrosine kinase and as an adapter molecule. The adapter molecule function of Src is mediated via direct protein-protein interactions with the SH2 and SH3 protein-binding domains, and

enables Src to activate other proteins by direct association and also, to act as a scaffold protein during the formation of protein complexes, such as focal adhesions. Src's adapter molecule function is thought to be independent of its kinase activity; however, it has been proposed that the consensus sequence recognised by the Src kinase domain is similar to that recognised by the SH2 domain of Src, meaning that sites phosphorylated by Src may also be able to act as Src ligands [98]. An example of this has been reported for EGFR where Src has been shown to both phosphorylate and bind to tyrosine residues at positions 992, 1086, 1101 and 1148 [240]. One drawback of inhibiting Src kinase activity only is that Src is still able to promote cell signalling through protein-protein interactions. However, if accurate, these observations might suggest that the inhibition of Src by AZM555130 may reduce its ability to function as an adapter molecule also.

Src/FAK signalling at focal adhesions ultimately engages pathways that lead to FAK degradation and focal adhesion disassembly, thus promoting cell motility. In accordance with this, Hiscox *et al.* have observed the formation of enlarged focal adhesions in Tam-R cells following the inhibition of Src with AZD0530, thus suggesting impaired focal adhesion turnover [247]. Also, CEF cells expressing a kinase-defective v-Src mutant have been shown to demonstrate impaired FAK degradation and enlarged focal adhesions, resulting in increased focal adhesion strength and decreased cell motility [117]. Furthermore, Hiscox *et al.* have recently reported that the knockdown of FAK using siRNA in Tam-R cells abrogated Src-dependent matrix attachment and cell motility, proving that Src/FAK signalling is indeed central to the regulation of these processes in this cell-line [211].

Therefore, the data presented in this chapter suggest that the pharmacological inhibition of Src inhibits Src/FAK signalling at focal adhesions, thus disrupting focal adhesion turnover and reducing cell motility and invasion in Tam-R cells. Together, these data provide further evidence of a causative role for Src in the regulation of the aggressive phenotype exhibited by Tam-R cells.

4.3.3 Increased Src activity in Tam-R cells enhances their growth through potentiation of EGFR signalling

Currently, there are conflicting reports concerning the role of Src in cell proliferation, with some groups showing that the modulation of Src activity in cancer cells has no effect on their growth [150, 238], while others demonstrate that the inhibition of Src using both pharmacological and molecular means reduces cell proliferation to varying degrees [152, 153, 237].

Knowlden *et al.* have previously reported that the Tam-R cells possess a significantly higher rate of growth than their hormone-sensitive MCF7wt counterparts [70]. Furthermore, they have demonstrated that EGFR mitogenic signalling via ERK 1/2 is increased in this cell-line [70]. Given the established association between Src and EGFR, in which Src is able to potentiate EGFR signalling by increasing the phosphorylation of EGFR at a number of sites, the effect of AZM555130-mediated Src inhibition on the growth of Tam-R cells was investigated. Cell counting experiments revealed that treatment of MCF7wt and Tam-R cells with AZM555130 significantly inhibited cell growth at a concentration of 1μM only. The mechanism by which Src is able to promote the growth of these cell-lines is unclear; however, Src is known to play a role in the transduction of many cell signalling pathways, including those that regulate cell proliferation and cell survival.

Inhibition of Src using PP2 has been shown to induce apoptosis in Murine B-cell leukaemia via the activation of the caspase cascade [250]. However, the *in vitro* expression of a dominant-negative form of Src in MCF7 cells reduced cell proliferation but had no effect on the levels of apoptosis [152]. Interestingly, increased Src activity has been shown to protect cells against detachment-induced apoptosis, or anoikis, by inducing MAPK-mediated expression of the anti-apoptotic Bcl-2 family of proteins, thus suggesting that Src may not be involved in the regulation of apoptosis in cells that are firmly attached to a matrix substratum [99]. The data obtained using the Vybrant® apoptosis assay revealed that treatment of MCF7wt and Tam-R cells with AZM555130 (1μM) for 72 hours did not affect the proportion of cells

undergoing apoptosis in either cell-line (figures 4.15 and 4.16). In addition, cleavage of the protein PARP, which is another characteristic of apoptosis, was not evident by SDS-PAGE/Western blotting in either MCF7wt or Tam-R cells following treatment with the AZD0530 Src inhibitor (1μM, 72hrs) (S. Hiscox, personal communication). This implies, therefore, that Src is not involved in the mechanisms that induce apoptosis in these cells.

However, when the expression of the Ki67 cell-proliferation marker was assessed in AZM555130-treated MCF7wt and Tam-R cells using ICC, the results showed reduced staining for Ki67 at 1μM only. This suggested that the proportion of cells passing through the cell-cycle was reduced by AZM555130 at this concentration, with a high proportion of cells arrested at the G0/G1 stage. Inhibition of Src has been previously shown to cause arrest of the cell cycle at G0/G1, thus preventing entry into S-phase and halting cell proliferation [159]. This effect also correlated with a significant reduction in ERK 1/2 activation [159]. Furthermore, Src has been shown to promote G1-S phase transition in quiescent cells under serum-free conditions via a mechanism involving the PI3K-MEK dependent activation of ERK 1/2 [147], and also in oestradiol-treated MCF7 cells via a mechanism requiring PI3K only [251].

A further mechanism of cell cycle progression involving Src has been proposed. Oktay *et al.* report that the formation of a Src/FAK signalling complex following integrin engagement promoted the recruitment of $p130^{CAS}$, paxillin, and Crk to focal adhesions. They discovered that the recruitment of $p130^{CAS}$ and Crk resulted in the downstream activation of JNK, which then led to the phosphorylation of JUN and the subsequent expression of genes required for cell cycle progression [252]. Interestingly, the phosphorylation of FAK Y861 and paxillin Y31, which have been shown to be necessary for the recruitment of $p130^{CAS}$ [225] and Crk [224] to focal adhesions respectively, was inhibited following treatment of MCF7wt and Tam-R cells with AZM-555130. Thus, the inhibition of Src may interrupt cell cycle progression and reduce cell proliferation by preventing $p130^{CAS}$ and Crk recruitment to focal adhesions, thus disrupting the downstream activation of JNK.

As Ki67 staining positively correlates with the expression and activity of EGFR *in vivo* [23], the effect of AZM555130 on EGFR signalling in MCF7wt and Tam-R cells was investigated. Interestingly, SDS-PAGE/Western blot analysis revealed that AZM555130 reduced both the phosphorylation of EGFR Y1068 and the subsequent downstream activation of ERK 1/2 at 1μM only. Furthermore, inhibition of Src with AZM555130 at 1μM was also able to negate TGFα-stimulated Tam-R cell growth.

It is interesting to note that, while FAK phosphorylation and cell motility/ invasion were reduced by AZM555130 at both 0.1μM and 1μM, cell proliferation and EGFR-ERK 1/2 signalling were inhibited at 1μM only. The observation that cell growth is only reduced at concentrations that also inhibit EGFR and ERK 1/2 activation suggests that Src inhibition prevents cell-cycle progression and down-regulates proliferation by directly reducing the activity of this signalling pathway. If, on the other hand, Src/FAK-JNK signalling via $p130^{CAS}$ and Crk were involved then reductions in Ki67 and cell number would have been expected with AZM555130 at 0.1μM also. Therefore, these data further support the notion of a synergistic relationship between Src and EGFR in these cell-lines. Increased expression and activation of EGFR is associated with a poor patient prognosis [179], while increased activation of ERK 1/2 correlates with a poor response to anti-hormonal therapy and decreased patient survival in the clinic [71]. Therefore, the inhibition of Src may be especially beneficial in tumours that display increased EGFR signalling in addition to increased Src activation.

EGFR is important in the growth of Tam-R cells, but less so for the growth of MCF7wt cells. This is evidenced by the lower levels of EGFR activation present in MCF7wt cells (figure 3.20) and by the lack of a proliferative response to TGFα stimulation (figure 4.21). Thus, the question remains that the inhibition of Src acts upon EGFR signalling to decrease the growth of Tam-R cells, how then does it influence the growth of the MCF7wt cell-line?

One possible mechanism may involve Src-dependent cross-talk between growth-factor signalling pathways. It has recently been suggested that Src enables uni-directional cross-talk between the IGF-receptor and EGFR [196]. IGF-1R signalling is active in MCF7wt cells and thus Src may be able to augment MCF7wt cell growth by promoting EGFR activation in response to IGF-1R stimulation. Disruption of this cross-talk mechanism following inhibition of Src may therefore negatively affect the growth of these cells.

Alternatively, Src may exert its effects on MCF7wt cell growth via interactions with the ER signalling pathway. The ER signalling pathway is the predominant mitogenic pathway in the MCF7wt cells and there is an increasing amount of data that implicate Src in the potentiation of ER signalling and *vice versa* [35, 40, 251, 253, 254]. Therefore, even though its activity is much lower in these cells, further work is required to elucidate how Src may affect ER signalling in the MCF7wt cells as there may be important implications for therapeutic response and the development of drug resistance [41, 52, 160].

The data presented here suggest that Src may have a supporting role in the proliferation of both MCF7wt and Tam-R cells via potentiation of the predominant mitogenic signalling pathways present. Furthermore, the mechanisms by which Src regulates proliferation in these cell-lines are likely to be distinct from those that regulate cell motility and invasion due to their differential sensitivities to pharmacological inhibition of Src (i.e. cell motility and invasion were reduced with AZM555130 at 0.1μM, whereas inhibition of cell growth was evident with 1μM AZM555130 only). Thus, inhibition studies using AZM555130 at 0.1μM may prove a useful tool in the identification of Src-dependent gene-expression or protein-activation profiles specific to the regulation of cell motility and invasion only, thus enabling the discovery of potential future therapeutic targets.

4.4 Chapter Summary

- AZM555130 was shown to be an effective inhibitor of Src kinase activity, with a significant reduction in Src Y419 phosphorylation observed with AZM555130 at 1μM after just one minute. Total Src protein levels were unaffected by treatment with AZM555130.
- Treatment of Tam-R cells with AZM555130 negated their aggressive cell-phenotype, resulting in morphological reversion and decreased cell migration, invasion and matrix-attachment in a dose dependent manner. This was attributable to decreased Src-dependent phosphorylation of FAK and paxillin.
- AZM555130 significantly inhibited the growth of Tam-R cells at a concentration of 1μM only. Ki67 staining of AZM555130-treated cells confirmed that this was a result of reduced cell proliferation, rather than an increase in levels of apoptosis.
- Inhibition of Tam-R cell growth by AZM555130 at 1μM was accompanied by corresponding reductions in the phosphorylation of EGFR Y1068 and in the downstream activation of ERK 1/2, suggesting that EGFR-driven proliferation in Tam-R cells was disrupted following treatment with AZM555130.
- Together, these data provide compelling evidence for a causative role for Src in the aggressive cell-phenotype displayed by ER-positive tamoxifen-resistant breast cancer cells *in vitro*.

Chapter Five: Results

Expression of Constitutively-Active Src in MCF7wt Cells Promotes an Aggressive Phenotype and Tamoxifen Insensitivity

"Disease is very old, and nothing about it has changed. It is we who change, as we learn to recognize what was formerly imperceptible."

Jean Martin Charcot (1825-1893). French Neurologist.
De l'expectation en médecine.

5 Expression of Constitutively-Active Src in MCF7wt Cells Promotes an Aggressive Phenotype and Tamoxifen Insensitivity

5.1 Introduction and Aims

Data presented thus far have demonstrated that acquired tamoxifen-resistance in MCF7wt cells is accompanied by an invasive cell-phenotype in which Src kinase activity appears to play a major role. To further confirm the role of Src in these phenomena, MCF7wt cells were transfected with a constitutively-active form of the Src protein.

MCF7wt cells were transfected with a plasmid construct containing a gene for constitutively-active Src (Src Y529F; Upstate Biotechnology, NY, USA; Cat. # 21-115). The Src Y529F gene contains an adenine to thymine substitution mutation at nucleotide 2611, which results in a tyrosine (Y) to phenylalanine (F) substitution at position 529 of the Src protein when transcribed. When phosphorylated, Y529 (located in the negative-regulatory tail) can interact with the SH2 domain of Src, locking Src in a closed conformation and inactivating the kinase domain in the process. However, the tyrosine to phenylalanine substitution in the Src Y529F mutant prevents this interaction, enabling the Src protein to adopt an open conformation and promoting full, constitutive activation of the kinase domain via the auto-phosphorylation of Y419. It is important to note that the position of the tyrosine mutated in the Src Y529F protein differs to the position of this tyrosine given in chapter 1 for human Src. This is due to slight variations in the amino acid sequence of the 'unique' region of Src between species of origin, which leads to differences in the numbering of residues in the protein. As such, Y529 in the constitutively-active Src construct, which is a mouse/chicken chimera, corresponds to Y530 in human Src.

The Src Y529F gene was supplied in a pUSEamp eukaryotic expression vector under the control of a CMV promoter. This vector also contains genes that confer resistance to the antibiotics, ampicillin and neomycin, which allow for

the selection of transformed bacteria and transfected eukaryotic cells respectively. As a control for these experiments an empty pUSEamp expression vector was used (Upstate Biotechnology; Cat. # 21-148). Schematic diagrams of the structures of the Src Y529F and pUSEamp plasmids can be found in materials and methods (figure 2.4), while additional information, such as nucleotide sequence and restriction digest maps, can be found in appendix 3 (sections 8.3.4 and 8.3.5).

Thus, the overall aim of this chapter was to create a stable, Src Y529F-expressing cell-line which could then be used to further study the role of Src in the regulation of the tamoxifen-resistant breast-cancer-cell phenotype *in vitro*. This stably transfected cell-line was characterised to ascertain any changes in its aggressive behaviour which may arise as a result of increased Src activity, including growth, matrix-attachment and motile and invasive capabilities. Furthermore, cell-signalling pathways involved in the control of these behavioural characteristics were also investigated in order to gain a fuller understanding of the importance of Src in the acquisition and regulation of an aggressive cell-phenotype.

5.2 Results

5.2.1 Stable transfection of MCF7wt cells with Src Y529F.

Cellular transfection efficiency is recognised as frequently being variable and can be influenced by both the cell-line and the DNA vector used. Therefore, prior to the generation of a stably transfected Src Y529F-expressing cell-line, the conditions used for the transfection of MCF7wt cells with the Src Y529F plasmid were optimised. To obtain maximum transfection efficiency, both the concentration of the plasmid DNA and the ratio between the concentrations of plasmid DNA and lipid-based transfection agent (Lipofectamine™ 2000) were considered.

MCF7wt cells, cultured to approximately 70-80% confluency in 35mm Petri-dishes, were transiently transfected with the Src Y529F plasmid using the protocol described in materials and methods (section 2.12.6). Plasmid

concentrations investigated were 0.1μg/ml, 0.2μg/ml, 0.4μg/ml and 0.8μg/ml, each with a DNA:lipid ratio of 1:2, 1:3 or 1:4. A control was also run by adding an equal volume of the Lipofectamine™ 2000 transfection agent only to the cells. Approximately 72 hours post-transfection, the cells were lysed and immunoprobed for activated (pY419) and total Src. Figure 5.1 shows that the transfection efficiency, measured by the amount of activated and total Src protein present, increased as the concentration of plasmid DNA used increased. Furthermore, for each concentration a DNA:lipid ratio of 1:4 resulted in the highest levels of Src Y529F expression in these cells. No cytotoxic effects were observed with the lipid transfection agent at any of the concentrations investigated. Thus, from this data a plasmid concentration of 0.8μg/ml and a DNA:lipid ratio of 1:4 were selected for the transfection of MCF7wt cells with the Src Y529F plasmid.

Transfections for the development of the stably transfected cell-lines were to be conducted in T-75 cell-culture flasks. To verify whether the selected transfection conditions were also suitable for use in T-75 flasks, the transient transfection of MCF7wt cells with Src Y529F was repeated. For comparison, a plasmid concentration of 0.1μg/ml was also used as this was shown in figure 5.1 to produce a low level of Src Y529F expression. A DNA:lipid ratio of 1:4 was used in both instances. Cells were lysed 72 hours post-transfection and immunoprobed for levels of Src pY419, Src pY530 and total Src. Figures 5.2A and 5.2B show elevated levels of both activated (pY419) and total Src protein in cells transfected with Src Y529F plasmid at a concentration of 0.8μg/ml. It is interesting to note that levels of Src Y530 phosphorylation were unaffected by transfection. The tyrosine at 530 is substituted for phenyl-alanine in the mutated Src protein and so cannot be phosphorylated. Therefore, the Src pY530 antibody should only be able to detect endogenous Src. As no change was seen in Src Y530 phosphorylation, this strongly suggests that the observed increases in both activated and total Src protein are due to the expression of the Src Y529F gene, and not a result of altered expression/activation of endogenous Src in these cells.

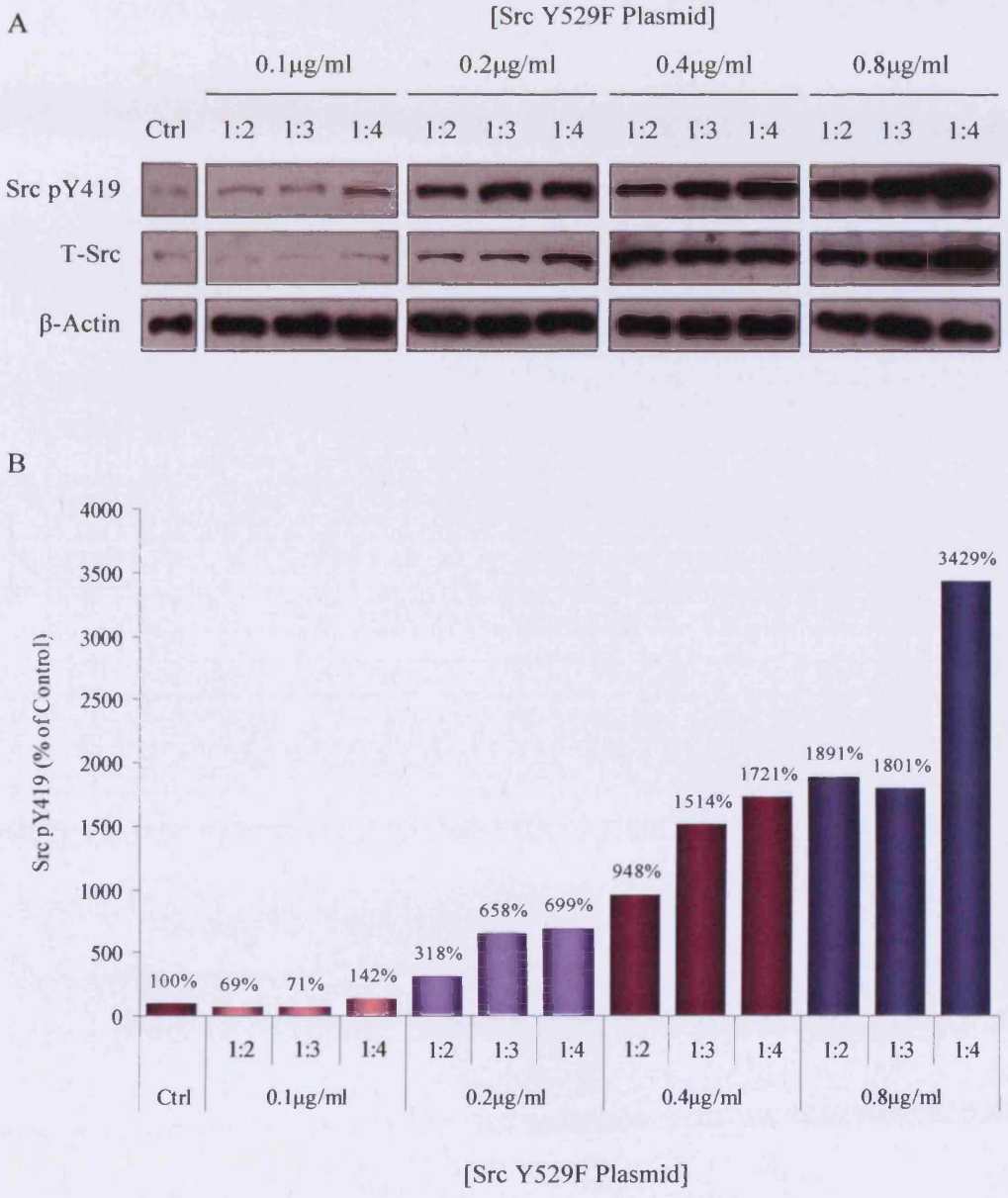

Figure 5.1 Optimisation of the experimental conditions for the transfection of MCF7wt cells with a Src Y529F plasmid construct.

To optimise transfection conditions, MCF7wt cells were transiently transfected with varying concentrations of the Src Y529F plasmid (0µg/ml, 0.1µg/ml, 0.2µg/ml, 0.4µg/ml and 0.8µg/ml) using the protocol described in materials and methods (section 2.12.6). Transfection at each concentration of plasmid was performed using DNA:Lipid ratios of 1:2, 1:3 and 1:4. Transiently transfected cells were cultured for 72hrs before being lysed for proteins. Total soluble protein (40µg) was subjected to SDS-PAGE/Western blot analysis and the membranes probed with antibodies specific for Src pY419 and total Src (A). Densitometry was conducted on the bands obtained, and the data for Src pY419, corrected for loading with β-actin, is presented as % of control (B).

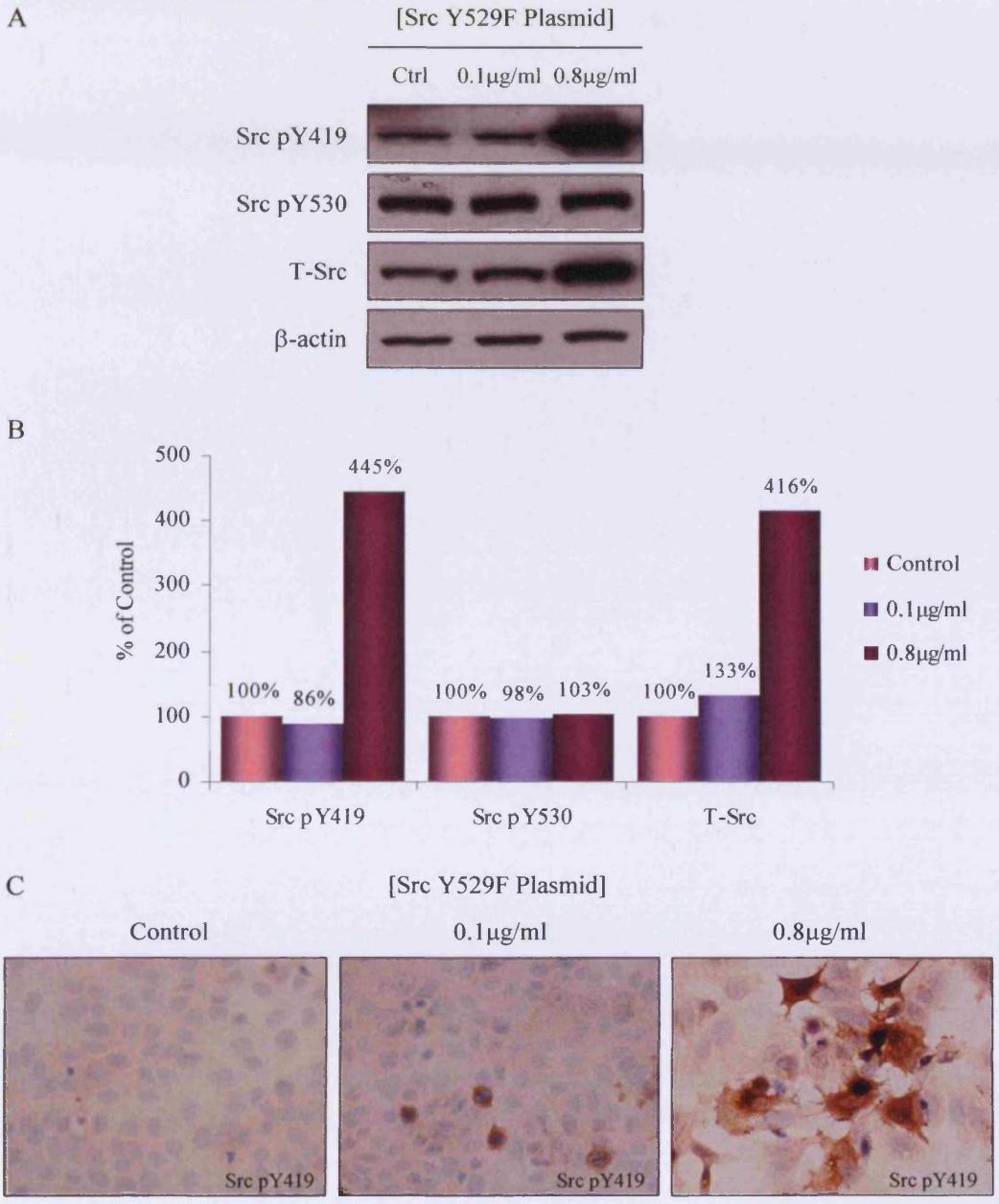

Figure 5.2 Verification of the experimental conditions selected for transfection of MCF7wt cells with a Src Y529F plasmid construct.

A plasmid concentration of 0.8µg/ml and a DNA:Lipid ratio of 1:4 were selected as optimal for the transfection of MCF7wt cells with the Src Y529F plasmid. To verify whether these conditions were also suitable for use with larger vessels, the transfection was repeated in a T-75 cell-culture flask. For comparison, a lower concentration of plasmid (0.1µg/ml) was also used. Cells were lysed 72hrs post-transfection. Total soluble protein (40µg) was subjected to SDS-PAGE/Western blot analysis and the membranes probed with antibodies specific for Src pY419, Src pY530 and total Src (A). Densitometry was conducted on the bands obtained, and the data, corrected for loading with β-actin, presented as % of control (B). ICC of the transiently transfected cells for Src pY419 revealed a pattern of Src activation similar to that seen with Western blotting. The images shown were captured using an Olympus BH-2 phase contrast micro-scope at 20x magnification (C).

To assess transfection efficiency using these conditions the transfection of MCF7wt cells with the Src Y529F plasmid was repeated with cells cultured on coverslips. The cells were fixed using the ERICA method 72 hours post-transfection (see materials and methods, section 2.5.1.1) and assayed for Src pY419 by ICC. The levels of Src Y419 phosphorylation seen with ICC for the two plasmid concentrations were in agreement with the data obtained by SDS-PAGE/Western blotting above. Transfection efficiency was visually estimated at approximately 25-30% when 0.8μg/ml plasmid DNA was used.

To generate a stably transfected cell-line, MCF7wt cells positively transfected with the Src Y529F plasmid were selected using G418 (Geneticin). G418 is an analogue of the antibiotic, neomycin, and works by blocking polypeptide synthesis, resulting in cell death. However, the Src Y529F plasmid contains a gene that confers resistance to the effects of G418. Thus, any cell transformed with the Src Y529F plasmid would be able to grow in medium containing G418, whereas non-transformed cells would not. The cytotoxicity of G418 is dependent on whether the cells are actively dividing and on the length of their cell-cycle, and so can vary between cell-lines. As such, the concentration of G418 used in the selection and maintenance of positively transfected MCF7wt cells was initially titrated to ensure an optimal rate of cell kill.

MCF7wt cells were seeded into the wells of a 24-well plate. After 24 hours, the culture medium was replaced with W+5% containing G418 at a range of concentrations (0-2000μg/ml) and the cells were counted (figure 5.3) and photographed (figure 5.4) on days 0, 2, 5, 8 and 11. The data show that MCF7wt cells were sensitive to the growth inhibitory effects of G418 at all concentrations investigated, and that the efficacy of the compound increased proportionally with concentration. A concentration of 800μg/ml was chosen for the selection of transfected MCF7wt cells as it demonstrated approximately 50% cell kill after just 2-3 days, with complete cell death after 8 days. Furthermore, this concentration is similar to that used by previous researchers in our laboratory with this cell-line, and also by others in the literature. For the routine maintenance of stably transfected cells, a concentration of

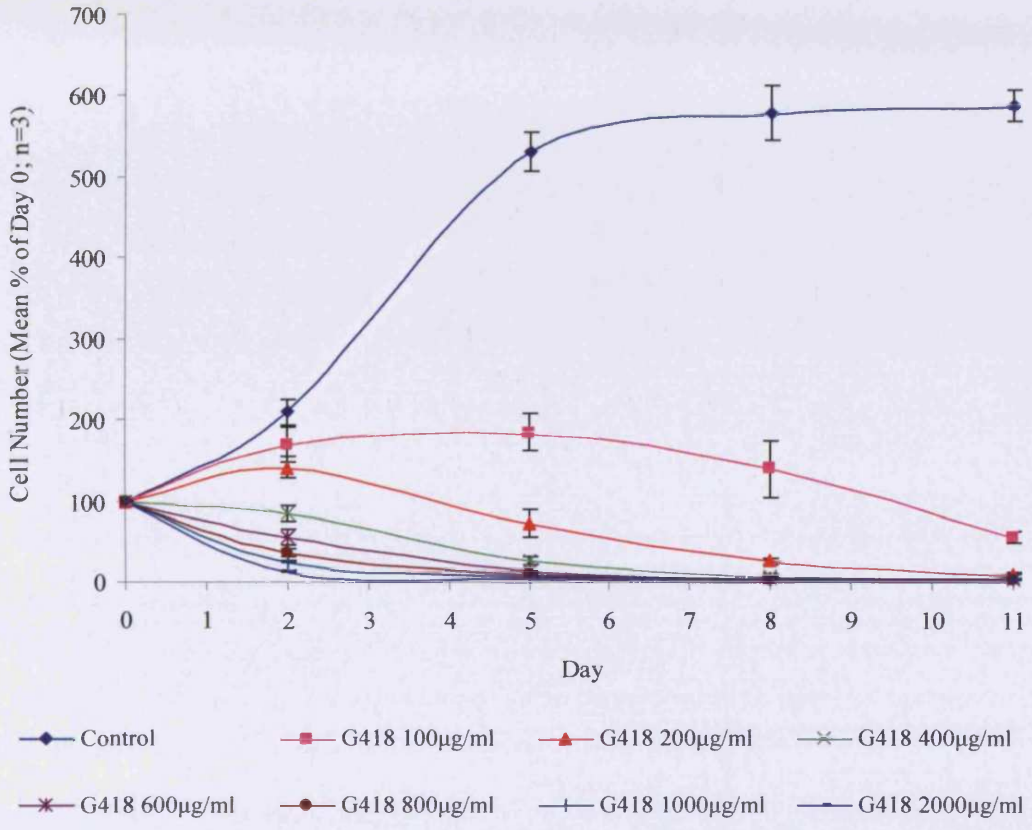

Figure 5.3 Effects of G418 (Geneticin) on MCF7wt cell growth.

MCF7wt cells were seeded in W+5% into a 24-well plate at a density of 30,000 cells/well. After 24hrs, the medium was replaced with W+5% containing the selective antibiotic, G418 (Geneticin), at the stated concentrations (0-2000µg/ml). Cell number was then determined for each concentration on days 2, 5, 8 and 11 using a Beckman Coulter™ Multisizer II. Data is presented as Mean % of Day 0 ± S.D. (n=3).

Figure 5.4 (Overleaf) Effects of G418 (Geneticin) on MCF7wt cell growth.

MCF7wt cells were seeded in W+5% into a 24-well plate at a density of 30,000 cells/well. After 24hrs, the medium was replaced with W+5% containing the selective antibiotic, G418 (Geneticin), at the stated concentrations (0-2000µg/ml). Representative images of the cells were captured for each concentration on days 0, 2, 5, 8 and 11 using a Leica DM-IRE2 inverted microscope fitted with a Hoffman condenser (20x magnification).

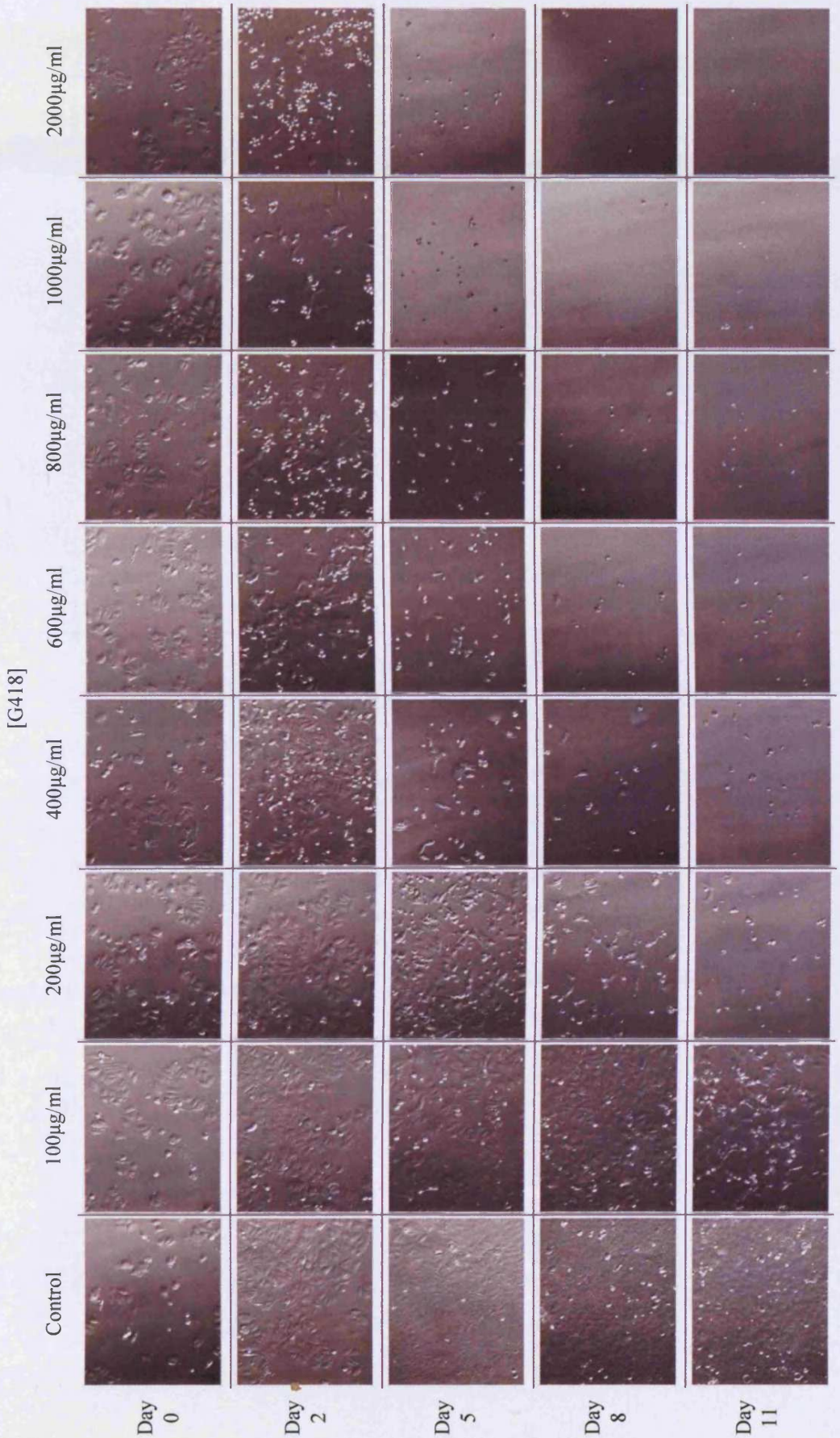
[G418]
Control
100µg/ml
200µg/ml
400µg/ml
600µg/ml
800µg/ml
1000µg/ml
2000µg/ml
Day 0
Day 2
Day 5
Day 8
Day 11

400μg/ml was selected as it was the lowest concentration of the compound that demonstrated almost 100% cell kill after 8 days.

A stably transfected, Src Y529F-expressing cell-line (MCF7-S) was created by transfecting MCF7wt cells with the Src Y529F plasmid following the protocol described in materials and methods (section 2.12.6.1), using the plasmid concentration (0.8μg/ml) and DNA:lipid ratio (1:4) optimised above. For use as an experimental control, MCF7wt cells were also stably transfected with the pUSEamp empty vector plasmid following the same protocol described above (MCF7-EV cells). Approximately 60 hours post-transfection the cells were cultured in medium containing G418 (800μg/ml) and assessed on a daily basis using phase-contrast microscopy, with the selection medium changed every 2-3 days. When the confluency of the cells had been reduced to 5-10% (~7 days) G418 in the culture medium was decreased to 400μg/ml for routine maintenance. From this point onwards the stably transfected cells were cultured as normal in medium containing G418 (400μg/ml) and passaged when necessary. Following 3-4 passages, the cell-lines were characterised.

5.2.2 Characterisation of the phenotype exhibited by the stable MCF7-S and MCF7-EV cell-lines.

5.2.2.1 Expression of neomycin resistance gene as a marker for successful transfection of MCF7wt cells with Src Y529F or pUSEamp.

To confirm that the MCF7-S and MCF7-EV cell-lines had been successfully transformed with the Src Y529F and pUSEamp empty vector plasmids respectively, and were thus expressing the neomycin resistance gene contained within the vector, the ability of these cells to grow in the presence of G418 was assessed. As with MCF7wt cells above, MCF7-S and MCF7-EV cells were seeded into a 24-well plate and, after 24 hours, cultured in medium containing G418 (0-2000μg/ml). The cells were counted and photographed on days 0, 3, 5, 7 and 10 (MCF7-S cells; figures 5.5 and 5.6) or days 0, 1, 5, 8, and 12 (MCF7-EV; figures 5.7 and 5.8). The figures demonstrate that both MCF7-S and MCF7-EV cell-lines were able to grow in the presence of G418 at all concentrations tested.

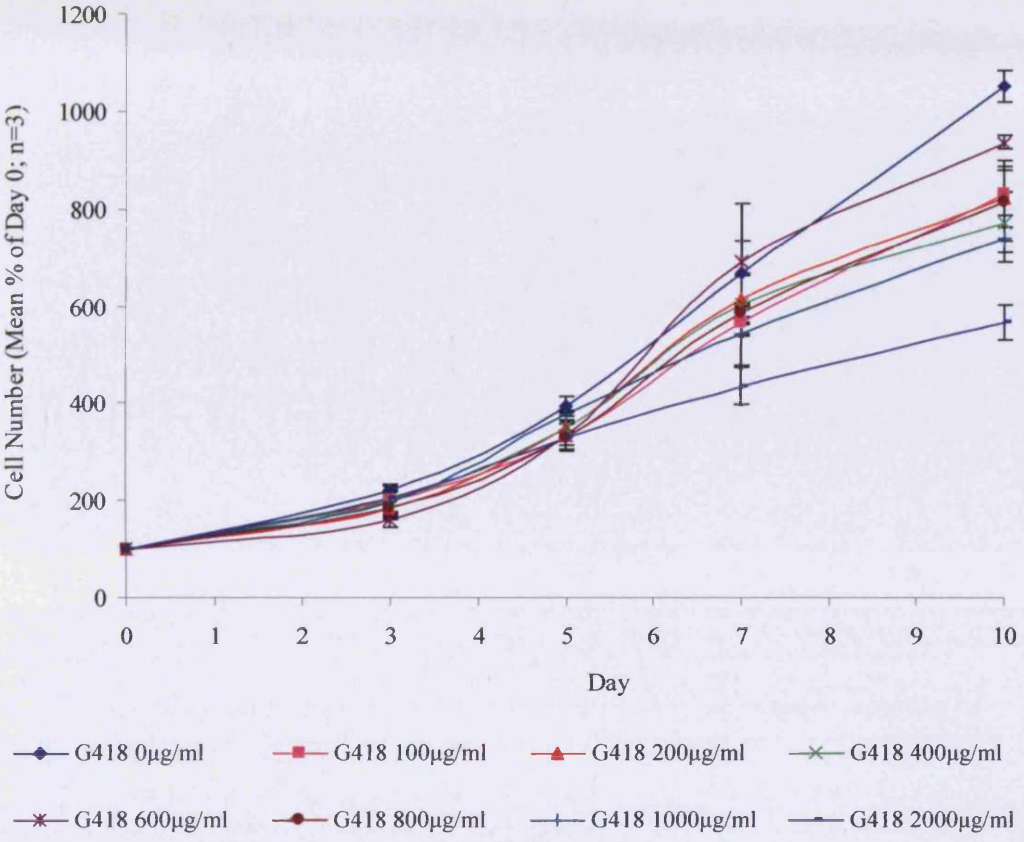

Figure 5.5 Effects of G418 (Geneticin) on MCF7-S cell growth.

MCF7wt cells stably transfected with the Src Y529F plasmid (MCF7-S) were seeded in W+5% into a 24-well plate at a density of 30,000 cells/well. After 24hrs, the medium was replaced with W+5% containing the selective antibiotic, G418 (Geneticin), at the stated concentrations (0-2000µg/ml). Cell number was then determined for each concentration on days 3, 5, 7 and 10 using a Beckman Coulter™ Multisizer II. Data is presented as Mean % of Day 0 ± S.D. (n=3).

Figure 5.6 (Overleaf) Effects of G418 (Geneticin) on MCF7-S cell growth.

MCF7-S cells were seeded in W+5% into a 24-well plate at a density of 30,000 cells/well. After 24hrs, the medium was replaced with W+5% containing the selective antibiotic, G418 (Geneticin), at the stated concentrations (0-2000µg/ml). Representative images of the cells were captured for each concentration on days 0, 3, 5, 7 and 10 using a Leica DM-IRE2 inverted microscope fitted with a Hoffman condenser (20x magnification).

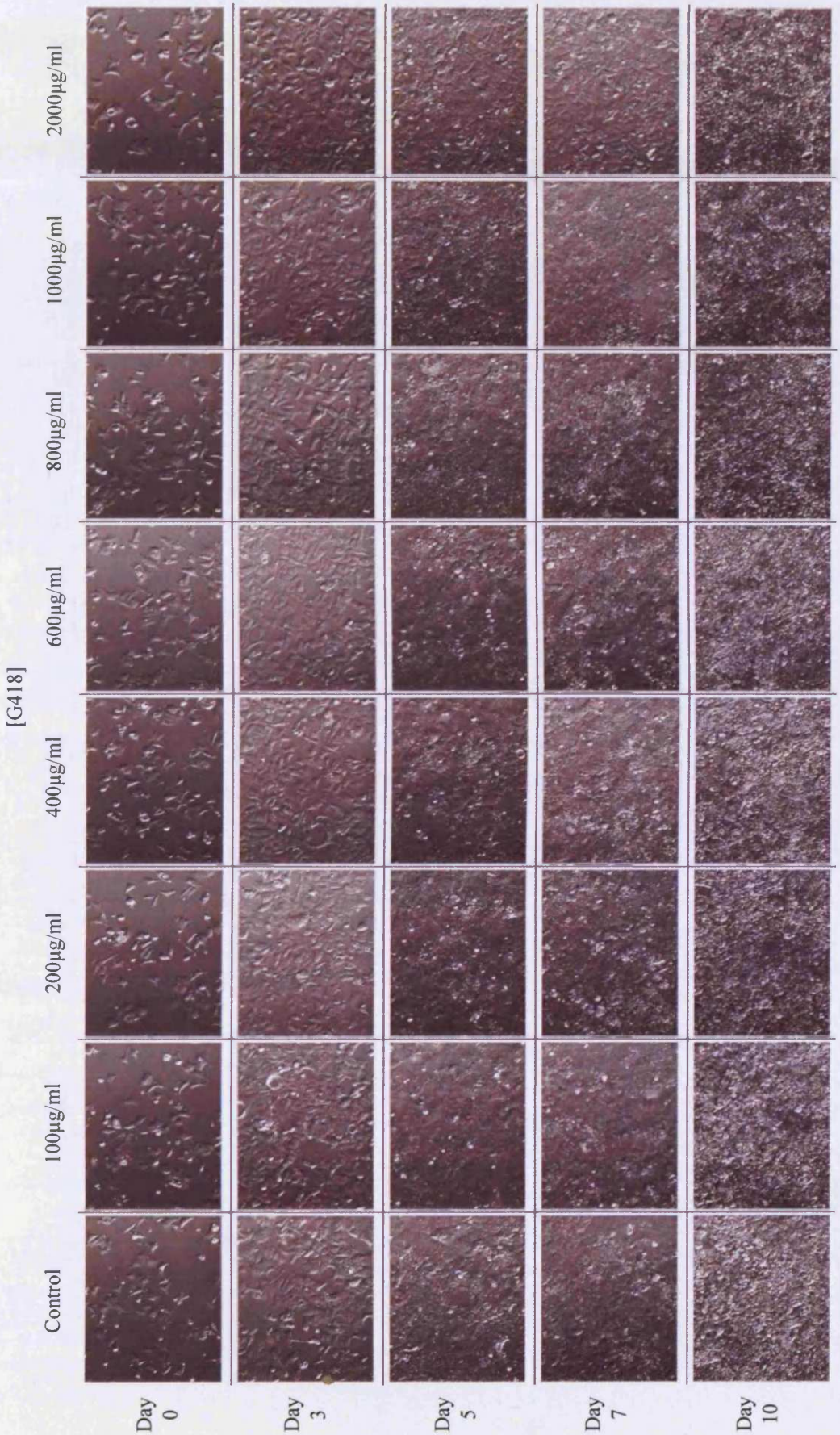
[G418]
Control
100µg/ml
200µg/ml
400µg/ml
600µg/ml
800µg/ml
1000µg/ml
2000µg/ml
Day 0
Day 3
Day 5
Day 7
Day 10

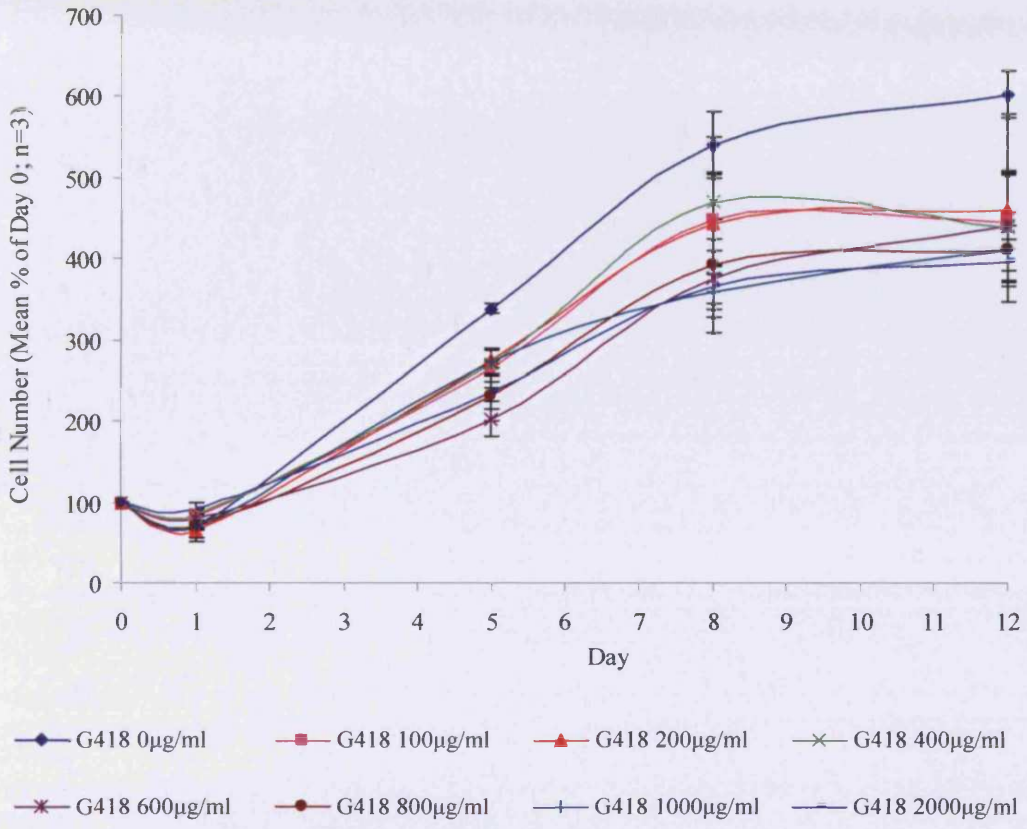

Figure 5.7 Effects of G418 (Geneticin) on MCF7-EV cell growth.

MCF7wt cells stably transfected with the pUSEamp empty vector plasmid (MCF7-EV) were seeded in W+5% into a 24-well plate at a density of 30,000 cells/well. After 24hrs, the medium was replaced with W+5% containing the selective antibiotic, G418 (Geneticin), at the stated concentrations (0-2000µg/ml). Cell number was then determined for each concentration on days 1, 5, 8 and 12 using a Beckman Coulter™ Multisizer II. Data is presented as Mean % of Day 0 ± S.D. (n=3).

Figure 5.8 (Overleaf) Effects of G418 (Geneticin) on MCF7-EV cell growth.

MCF7-EV cells were seeded in W+5% into a 24-well plate at a density of 30,000 cells/well. After 24hrs, the medium was replaced with W+5% containing the selective antibiotic, G418 (Geneticin), at the stated concentrations (0-2000µg/ml). Representative images of the cells were captured for each concentration on days 0, 1, 5, 8 and 12 using a Leica DM-IRE2 inverted microscope fitted with a Hoffman condenser (20x magnification).

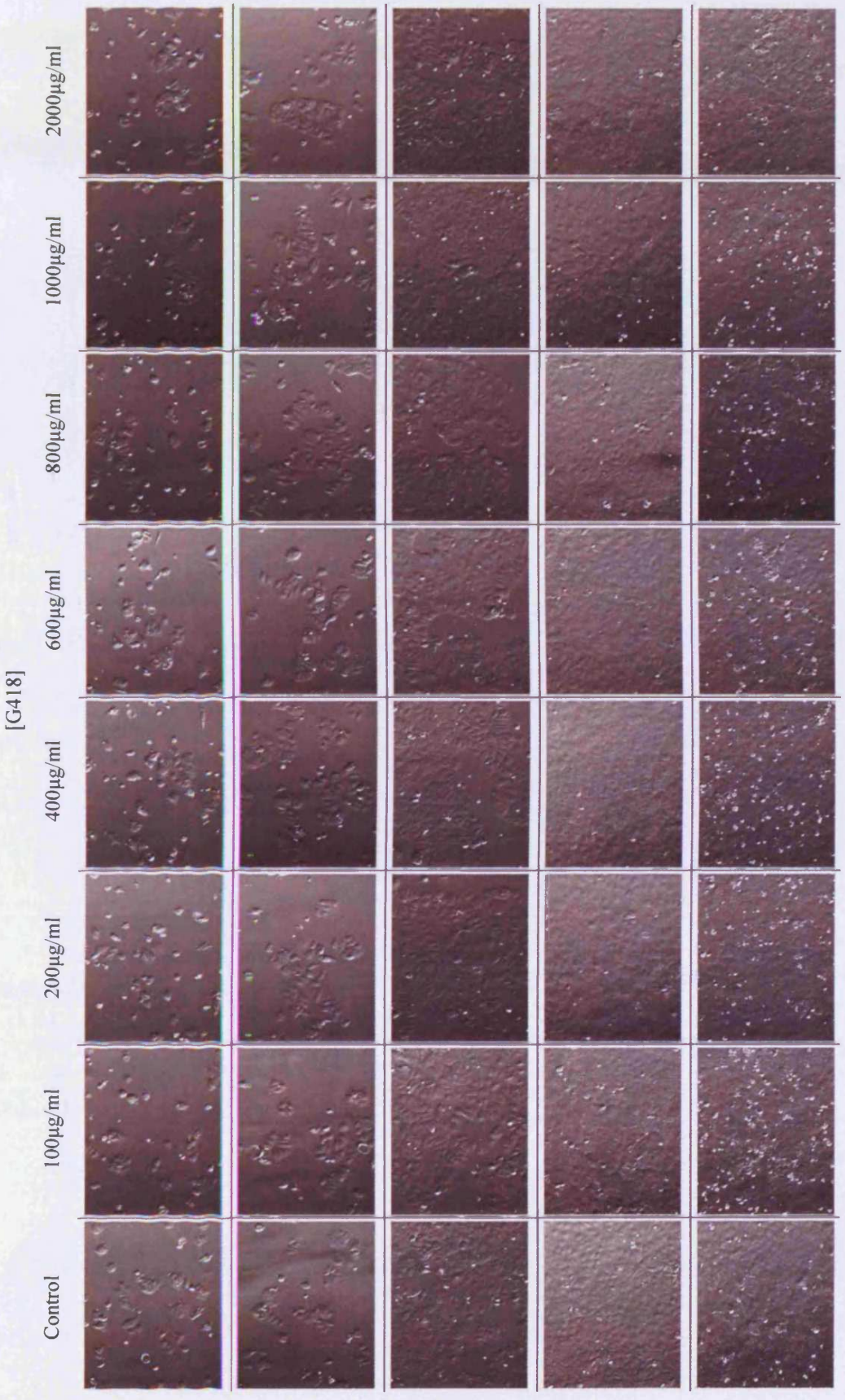
[G418]
Control
100µg/ml
200µg/ml
400µg/ml
600µg/ml
800µg/ml
1000µg/ml
2000µg/ml
Day 0
Day 1
Day 5
Day 8
Day 12

5.2.2.2 Characterisation of the stable MCF7-transfectants for Src expression and activation.

Next, the MCF7-S and MCF7-EV cell-lines were characterised for basal levels of activated and total Src protein. Cells were cultured to log phase growth, lysed for total proteins and then subjected to SDS-PAGE/Western blot analysis for Src pY419, Src pY530 and total Src protein. Figures 5.9A and 5.9B show that both Src activity (pY419) and total Src levels were significantly elevated in MCF7-S cells compared to MCF7-EV. Once again, levels of Src Y530 phosphorylation were unaltered, suggesting that the observed increases in Src pY419 and total Src protein were due to the expression of the Src Y529F gene, as opposed to changes in the expression of endogenous Src. For comparison, the levels of Src pY419 in all four cell-lines (MCF7wt, MCF7-EV, MCF7-S and Tam-R) are presented in figure 5.9C, with the data clearly showing the highest level of Src activation in the MCF7-S cells. Furthermore, this figure also confirms that the expression of Src Y529F in the MCF7-S cells was stable over a long period of time, with both early (P.4) and late (P.25) passages of MCF7-S cells exhibiting similar levels of Src activation.

Together, the data presented in sections 5.2.2.1 and 5.2.2.2 above confirm that the transfection of MCF7wt cells with the Src Y529F plasmid, and subsequent selection using the antibiotic, G418, successfully resulted in the generation of a stable, Src Y529F-expressing cell-line, designated MCF7-S.

5.2.2.3 Characterisation of the cell-phenotype displayed by the stable MCF7-transfectants.

Src possesses dual functionality within the cell in that it is able to act as both a tyrosine kinase and as an adapter molecule. The latter function of Src is independent of its kinase activity, and is mediated through direct protein-protein interactions via SH2 and SH3 protein-binding domains. These enable Src to activate other proteins by direct association and also, to act as a scaffold protein during the formation of protein complexes, such as focal adhesions.

To ensure that any phenotypic differences observed between MCF7-S and MCF7-EV cell-lines were a result of increased Src kinase activity, and not an

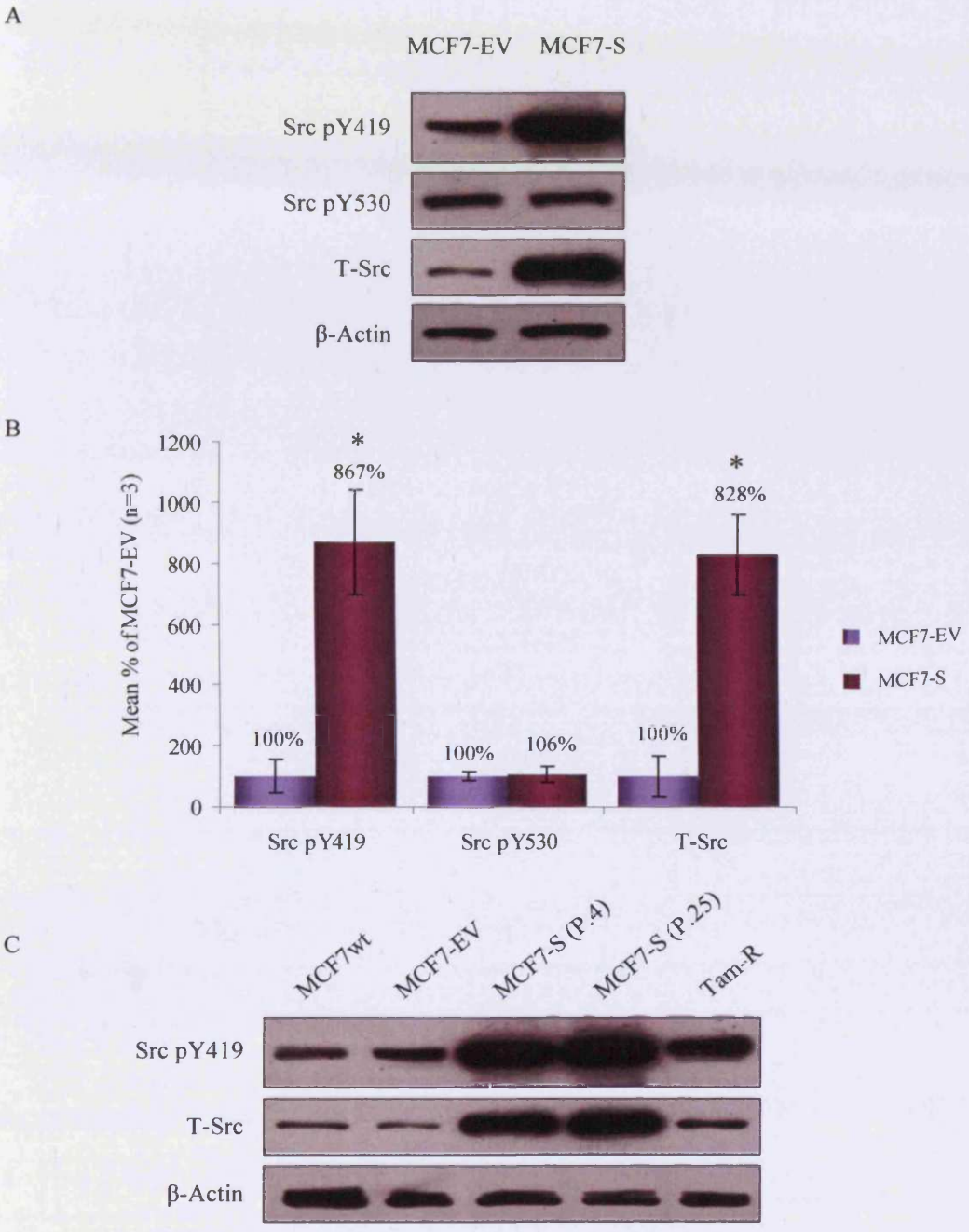

Figure 5.9 Levels of total and activated Src tyrosine kinase in MCF7-S versus MCF7-EV cells as determined by Western blotting.

MCF7-EV and MCF7-S cells were cultured to log-phase and lysed for proteins as described in materials and methods (section 2.4.1). Total soluble protein (40μg) was subjected to SDS-PAGE/Western blot analysis and the membranes probed with antibodies specific for Src pY419, pY530 and total Src (A). Densitometry was conducted on the bands obtained and the data, corrected for loading with β-actin, presented as Mean % of MCF7-EV ± S.D. (* $p<0.01$ vs. MCF7-EV; n=3) (B). For comparison of Src activity between the MCF7-S and Tam-R cell-lines, lysates from basal MCF7wt, MCF7-EV, MCF7-S and Tam-R cells were analysed for Src pY419 levels (C). To ensure the expression of the Src mutant was stable in the MCF7-S cells, lysates from both early (P.4) and late (P.25) passages were included in the analysis (C).

artefact of the increased levels of total Src protein in the cell (which would increase its availability for use as an adapter molecule), all characterisation experiments were conducted in the absence and presence of the AZM555130 Src inhibitor. To ascertain the efficacy of AZM555130 in the MCF7-S cell-line, cells treated with AZM555130 (0-5μM) for 24 hours were lysed and subjected to SDS-PAGE/Western blotting analysis for Src pY419 and total Src protein. Figure 5.10 shows that AZM555130 was effective at inhibiting Src activity in the MCF7-S cell-line (IC_{50}: 0.375μM); however, the MCF7-S cells were not as sensitive to the effects of AZM555130 as the Tam-R cell-line (IC_{50}: 0.02μM), and required concentrations of up to 5μM for maximal inhibition. Total Src protein levels were unaffected by AZM555130.

The morphologies of MCF7-EV and MCF7-S cells were assessed using phase contrast microscopy (figures 5.11C and 5.11D respectively). For comparison, MCF7wt and Tam-R cells are also presented (figures 5.11A and 5.11B respectively). MCF7-EV cells were very similar to MCF7wt cells in appearance and grew in dense, tightly-packed colonies, demonstrating a high degree of cell-cell contact. MCF7-S cells, on the other hand, had acquired a very different morphology and were now much more similar to the Tam-R cells in appearance. MCF7-S cells were seen to grow in loose colonies with very little evidence of cell-cell contacts between individual cells. Furthermore, these cells displayed a very angular appearance with markedly enhanced membrane activity (increased filopodia and lamellipodia formation). Interestingly, when basal MCF7-S cells were assayed for Src pY419 using ICC, the activated Src protein was found to be localised to these areas of increased membrane activity (figure 5.12 A-H). Treatment with AZM555130 (0-5μM) for 24 hours reduced membrane activity in the MCF7-S cells and re-established cell-cell contacts, resulting once more in the formation of dense, tightly-packed colonies as seen with the MCF7wt cells (figure 5.13).

The *in vitro* migratory and invasive capabilities of the MCF7-S and MCF7-EV cell-lines were measured in the absence and presence of AZM555130 (1μM) using the migration and invasion assays previously described (see sections

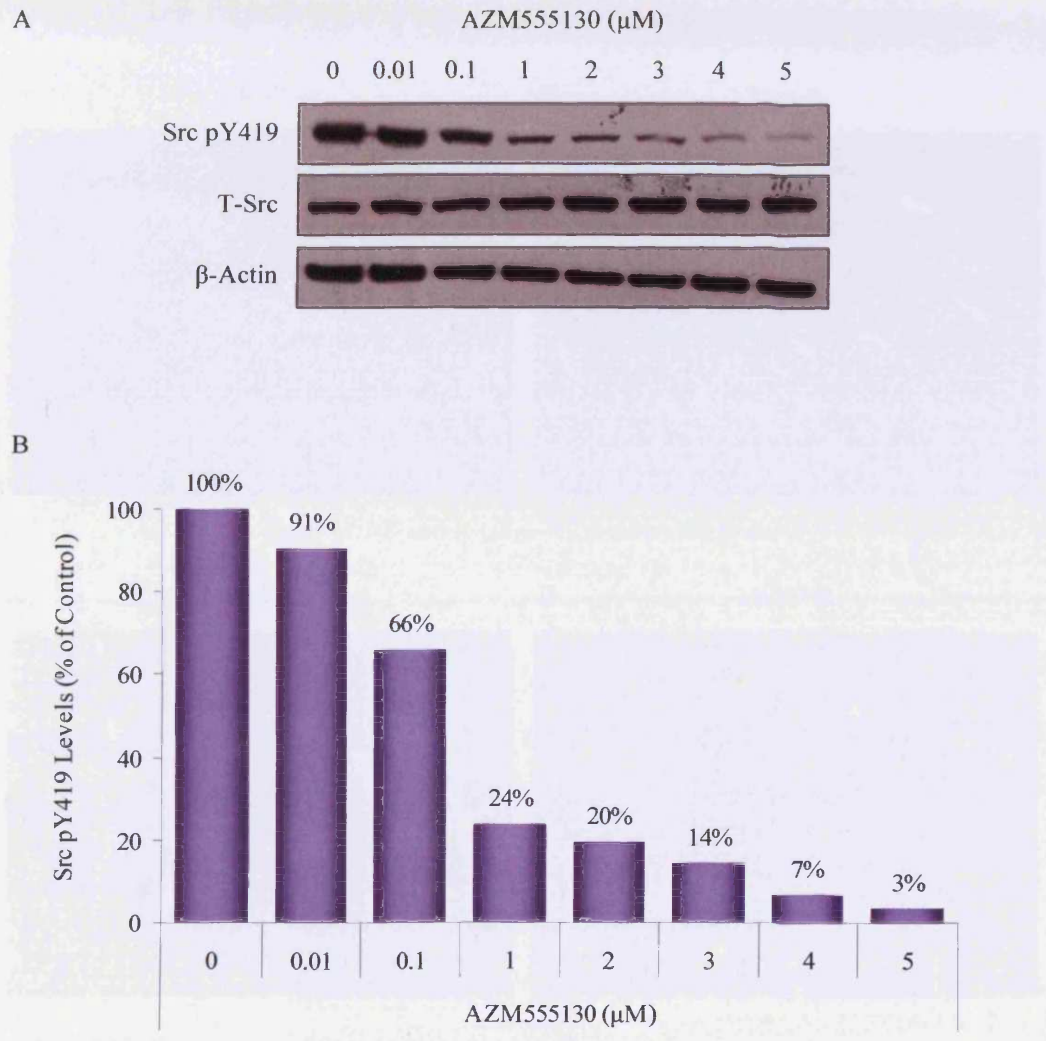

Figure 5.10 Dose-dependent effect of AZM555130 on Src activation in MCF7-S cells as determined by Western blotting.

MCF7-S cells were cultured to log-phase growth and then treated with AZM555130 at the stated concentrations for 24 hours. Control cells were treated with vehicle (DMSO) only for the same duration. Cells were then lysed for proteins as described in materials and methods (section 2.4.1). Total soluble protein (40μg) was subjected to SDS-PAGE/Western blot analysis and the membranes probed with antibodies specific for Src pY419 and total Src (A). Densitometry was conducted on the bands obtained and the data for Src pY419, corrected for loading with β-actin, presented as % of Control (B).

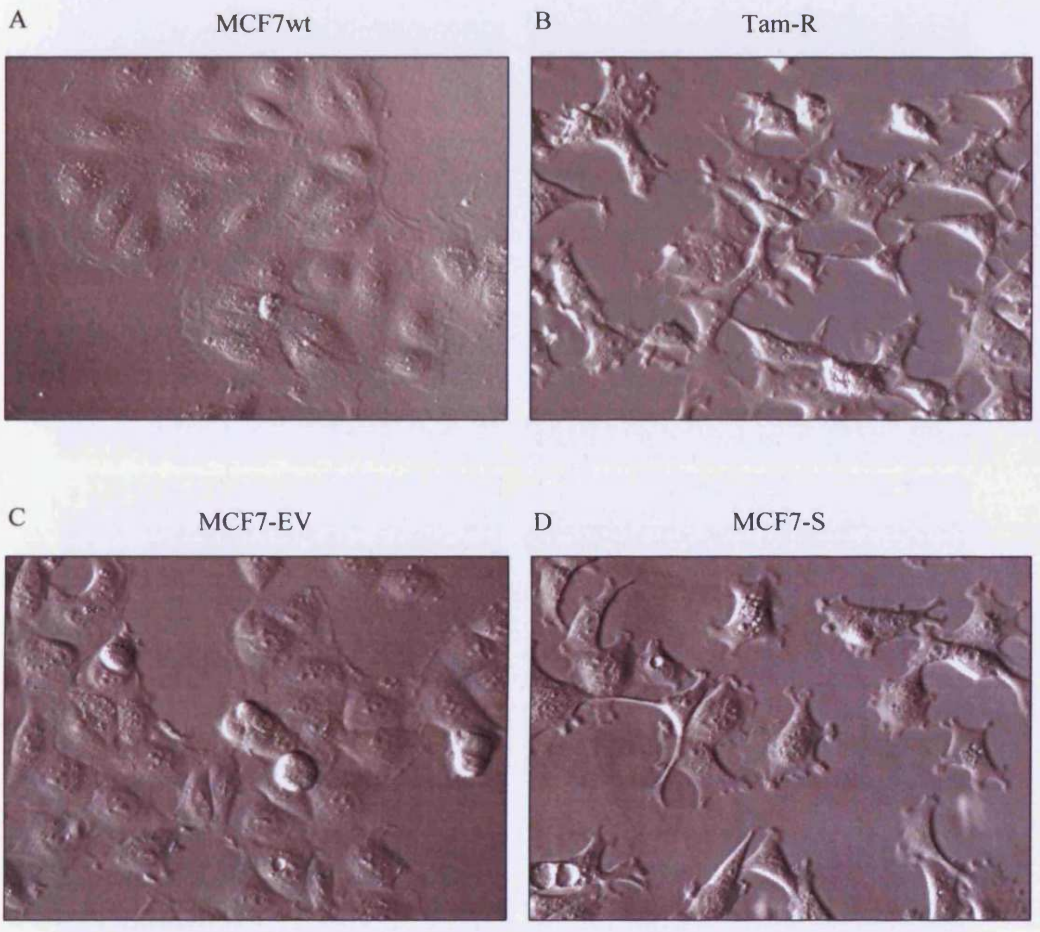

Figure 5.11 Morphology of MCF7-S and MCF7-EV cells.

MCF7wt (A), Tam-R (B), MCF7-EV (C) and MCF7-S (D) cells were grown in 100mm Petri-dishes under basal conditions (W+5% ± Tam [100nM]). When the cells had reached log-phase growth, representative images of the live cells were captured at 20x magnification using a Leica DM-IRE2 inverted microscope fitted with a Hoffman condenser.

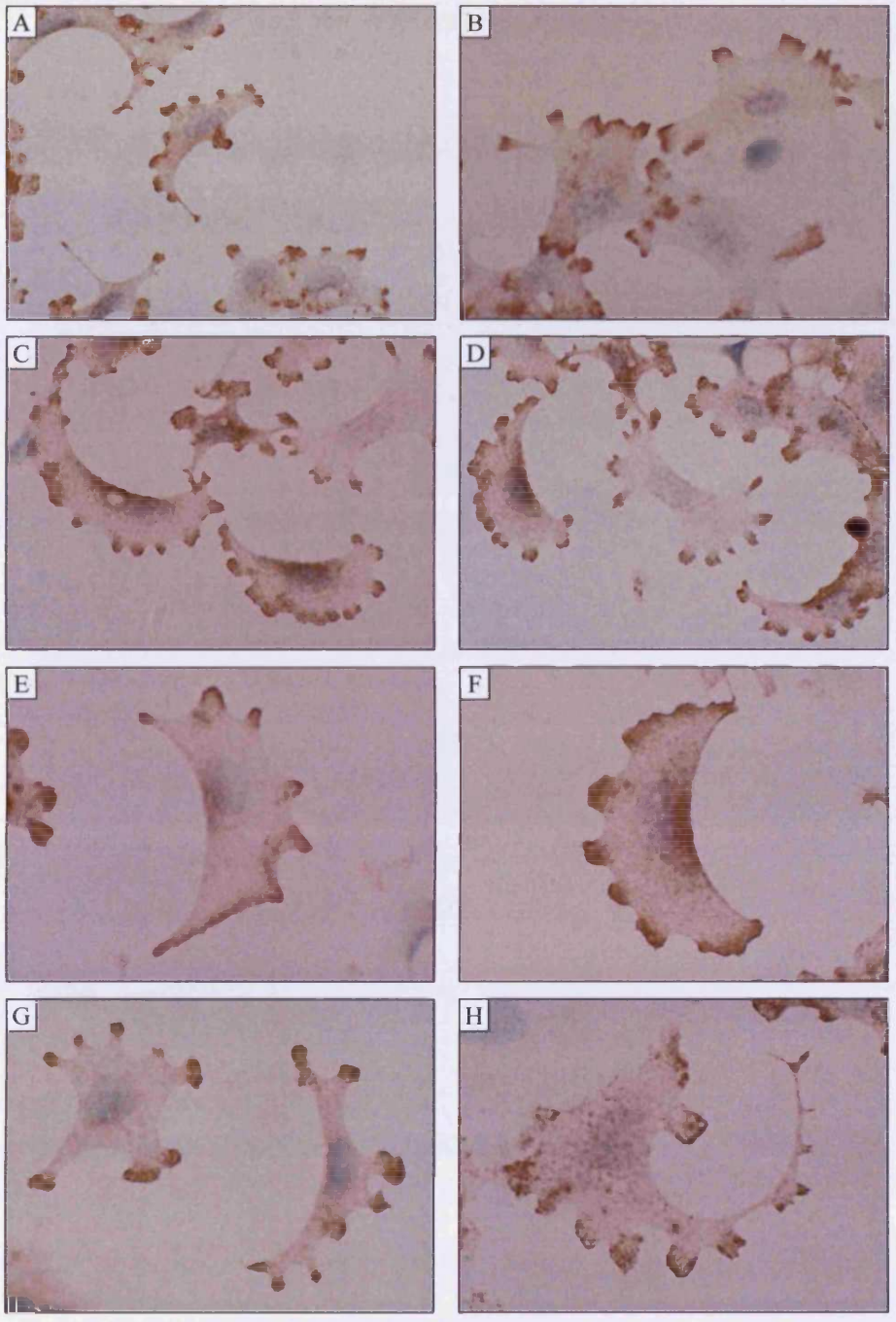

A-H: Src pY419

Figure 5.12 Localisation of activated Src tyrosine kinase in basal MCF7-S cells.

MCF7-S cells were cultured on coverslips until they reached log-phase growth and then fixed using the ERICA technique as described in materials and methods (section 2.5.1.1). The fixed cells were assayed for Src pY419 using a phospho-specific antibody, and the protein localisation was visualised using the DAKO EnVision™+ system peroxidase [DAB] kit as described in section 2.5.2. Representative images of the stained MCF7-S cells were captured at x20 (A-D) and x40 (E-H) magnification using an Olympus BH-2 phase contrast microscope.

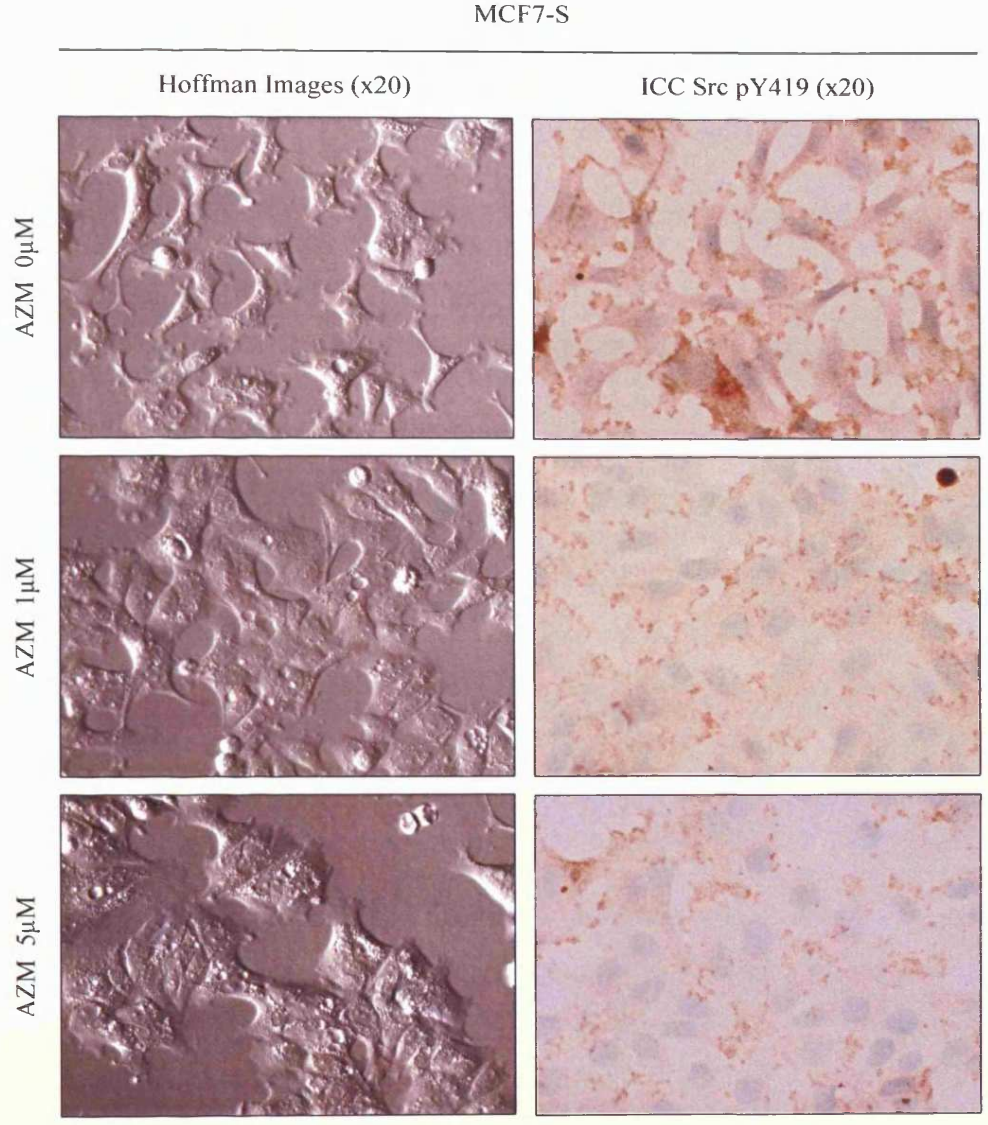

Figure 5.13 Effect of Src inhibition by AZM555130 on MCF7-S cell morphology.
For the Hoffman images, MCF7-S cells were seeded in W+5% onto 60mm Petri-dishes and cultured until they reached log-phase growth. The medium was then replaced with W+5% containing AZM555130 at the stated concentrations for 24 hours. Representative images of the live cells were captured at 20x magnification using a Leica DM-IRE2 inverted microscope fitted with a Hoffman condenser. For the ICC images, MCF7-S cells were cultured on coverslips until they reached log-phase growth and then treated with AZM555130 for 24 hours at the stated concentrations. The cells were then fixed using the ERICA technique and assayed for Src pY419 using a phospho-specific antibody as described in section 2.5. Representative images of the stained MCF7-S cells were captured at 20x magnification using an Olympus BH-2 phase contrast microscope.

2.10 and 2.11). Migration of MCF7-S cells over a fibronectin-coated surface was significantly increased (9.5-fold) compared to MCF7-EV (figure 5.14). Furthermore, migration of both MCF7-S and MCF7-EV cells was reduced by approximately 50% in the presence of AZM555130 at 1μM. Figure 5.15 presents similar results for the invasive capabilities of MCF7-S cells, with the data showing that invasion of MCF7-S cells through an artificial basement membrane (Matrigel™) was increased approximately 4.9-fold over that of MCF7-EV. Again, invasion, particularly in the MCF7-S cells, was significantly reduced in the presence of AZM555130 (1μM). The data presented in figures 5.14 and 5.15 suggests that the process of cell-invasion is more sensitive than that of cell-migration to AZM555130-induced Src inhibition. Interestingly, this was also previously noted following the treatment of Tam-R cells with AZM555130 at 0.1μM (section 4.2.2).

Enhanced motility and invasion in Tam-R cells were accompanied by altered cell-matrix attachment and an increased rate of cell-spreading, both of which may be due to elevated levels of Src activity in these cells (as discussed previously). As such, the affinity of MCF7-S cells for matrix-coated surfaces was examined to see whether this was true of this cell-line also.

MCF7-S and MCF7-EV cells were seeded into the wells of either an uncoated or fibronectin-coated 96-well plate and allowed to attach for 50 minutes. The number of attached cells was then assessed using the MTT assay (figure 5.16). Attachment to an uncoated plastic surface was significantly increased in MCF7-S cells compared to MCF7-EV, and was almost completely inhibited in both cell-lines by AZM555130 (1μM). Although there was no apparent difference in the attachment of these cell-lines to a fibronectin-coated surface, cell-attachment to this substrate was diminished by AZM555130 at 1μM, suggesting an as yet unclear role for Src and additional factors (e.g. integrins) in this process.

Tam-R cells were previously seen to possess a greater rate of attachment to a fibronectin-coated surface than MCF7wt cells (figure 3.15) and this may also be a result of the elevated Src activity exhibited by these cells. Therefore, the

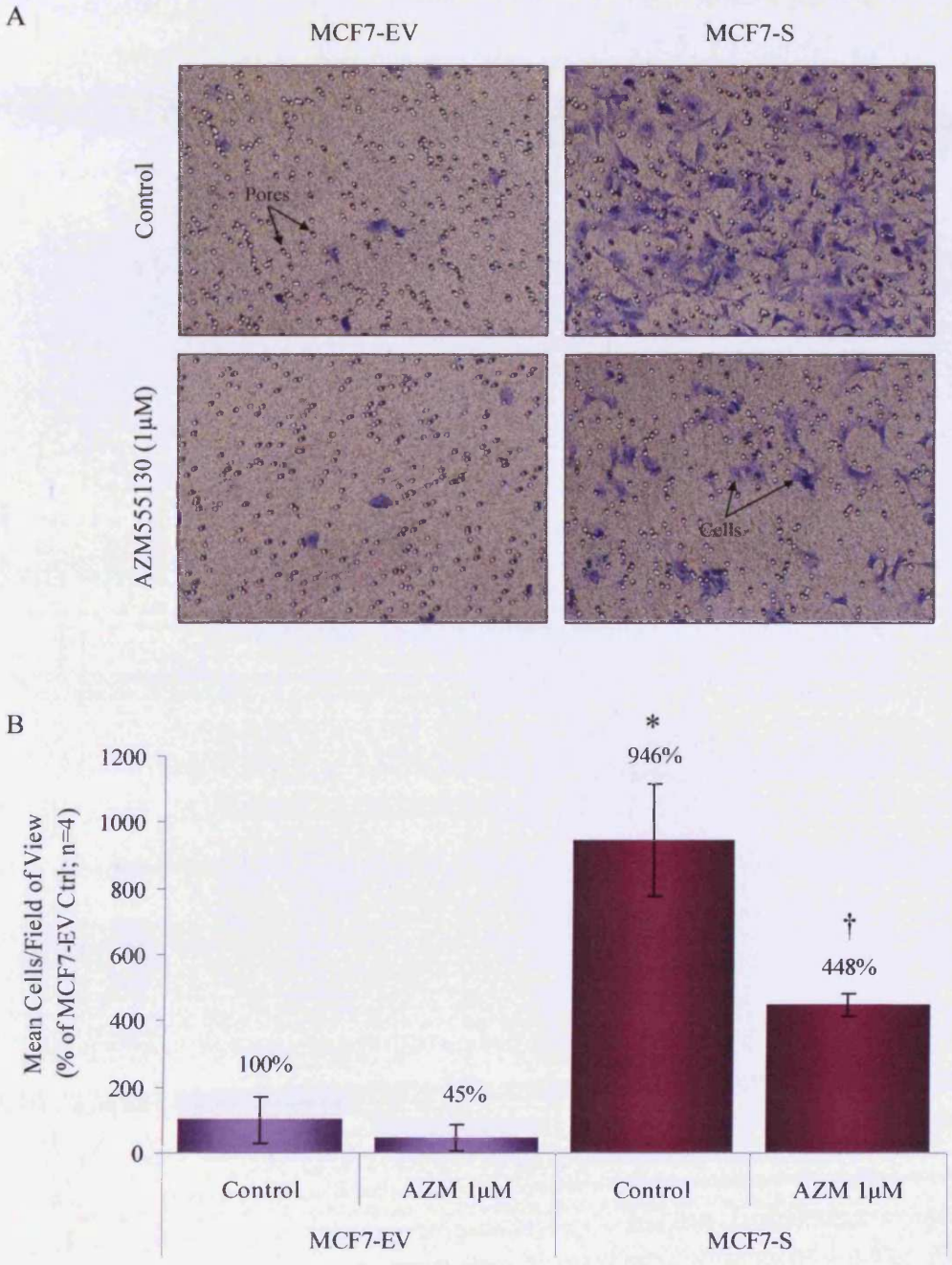

Figure 5.14 Migratory capacity of MCF7-S cells versus MCF7-EV.

The migratory capabilities of the MCF7-S and MCF7-EV cell-lines were assessed in the absence and presence of AZM555130 using *in vitro* migration assays as described in materials and methods (section 2.10). Representative images of the migratory cells (stained purple with crystal-violet) were captured using light microscopy at 20x magnification and are shown above (A). For quantification, the number of migratory cells in 5 random fields of view was counted using light microscopy and the data (mean cells/field of view) presented as % of MCF7-EV Control ± S.D. (* $p<0.001$ vs. MCF7-EV; † $p<0.05$ vs. Control; n=4) (B).

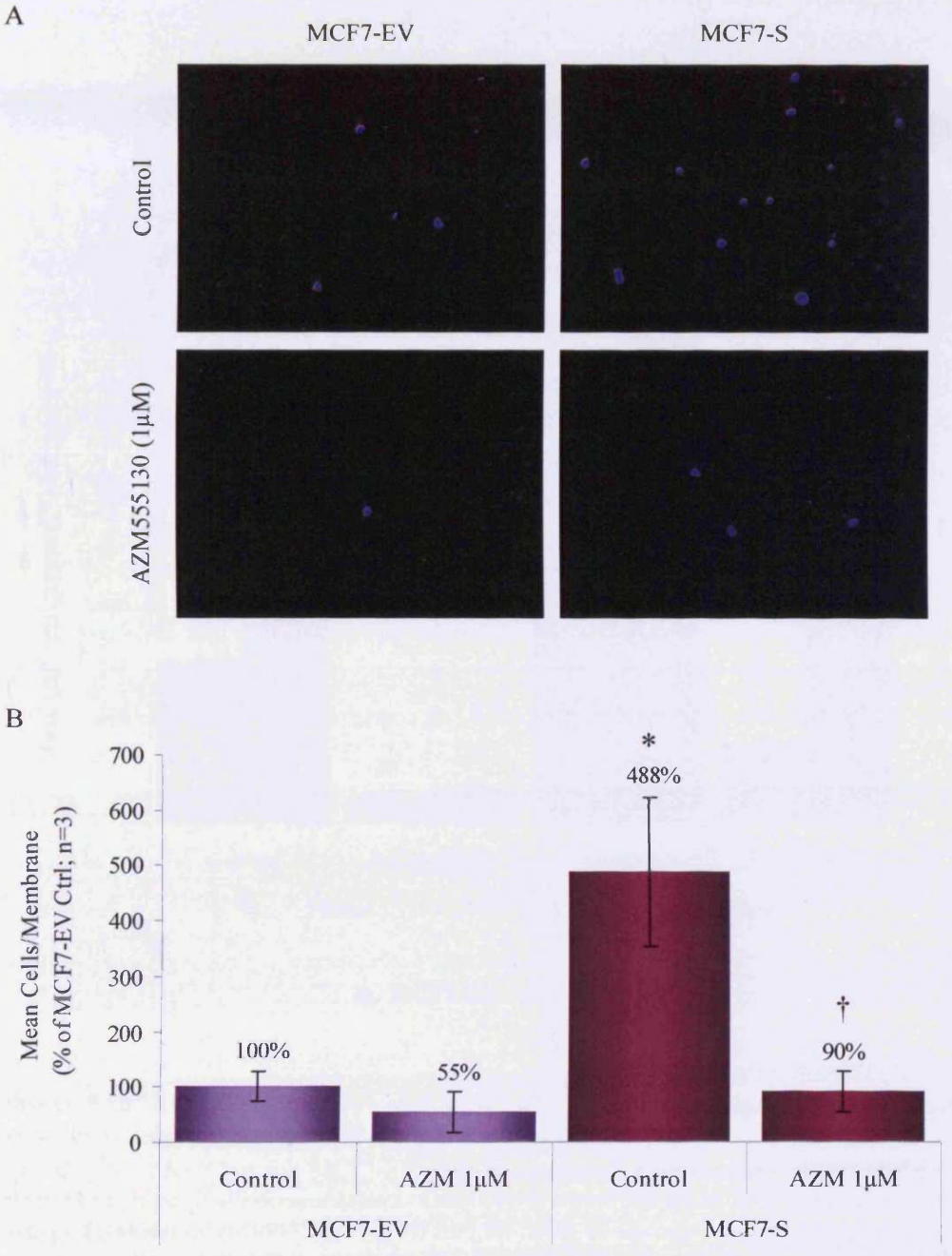

Figure 5.15 Invasive capacity of MCF7-S cells versus MCF7-EV.

The invasive capabilities of the MCF7-S and MCF7-EV cell-lines were assessed in the absence and presence of AZM555130 using *in vitro* invasion assays as described in materials and methods (section 2.11). Representative images of the invasive cells (stained blue with DAPI nuclear stain) were captured using fluorescence microscopy at 20x magnification (A). For quantification, the number of invasive cells per membrane was counted using fluorescence microscopy and the data (mean cells/membrane) presented as % of MCF7-EV Control ± S.D. (* $p<0.05$ vs. MCF7-EV; † $p<0.01$ vs. Control; n=3) (B).

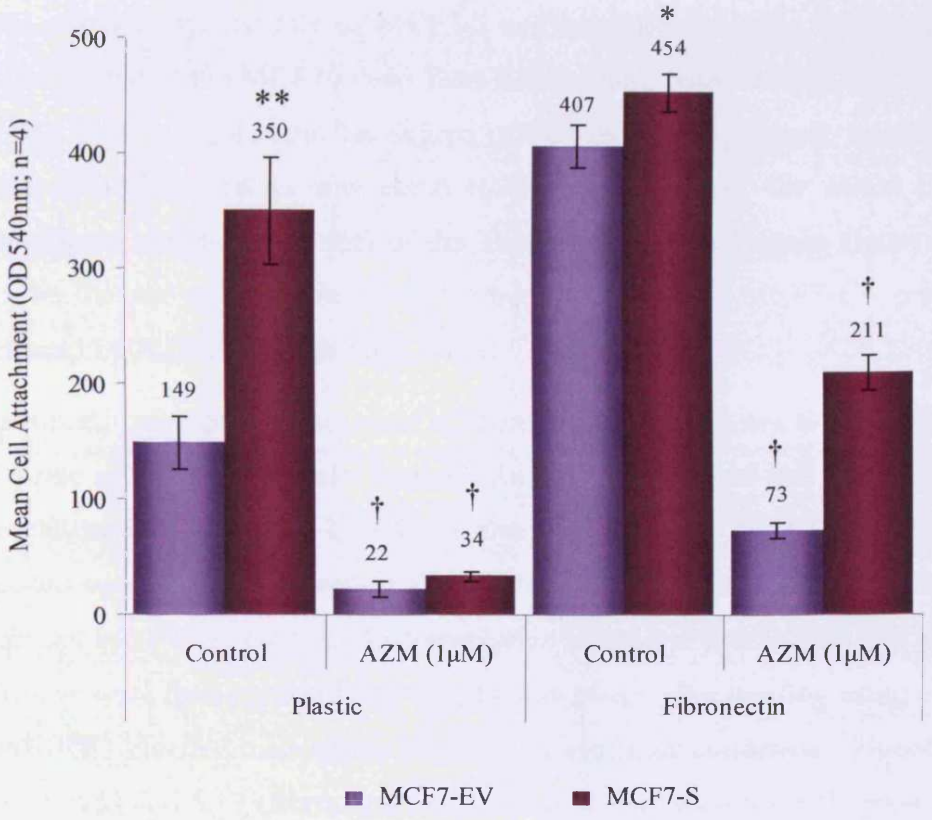

Figure 5.16 Affinity of MCF7-S and MCF7-EV cells for uncoated and matrix-coated surfaces as measured using a cell attachment assay.

The affinity of MCF7-S and MCF7-EV cells for uncoated or fibronectin-coated surfaces was measured using cell attachment assays. Cells ($4x10^4$) were seeded in W+5% containing either vehicle (DMSO) or AZM555130 (1μM) into the wells of uncoated or fibronectin-coated 96-well plates. Cells were left to attach for 50 minutes at 37°C after which the wells were washed with PBS and the number of attached cells assessed using the MTT assay. Data is presented as Mean Cell Attachment (OD_{540}) ± S.D. (* $p<0.01$ vs. MCF7-EV ** $p<0.001$ vs. MCF7-EV; † $p<0.001$ vs. Control; n=4) (B).

rate of cell-matrix attachment in MCF7-S and MCF7-EV cells was investigated next. Cell-attachment time course assays were performed with MCF7-S and MCF7-EV cells using the protocol previously described (see materials and methods section 2.9). Figure 5.17A shows that MCF7-S cells demonstrated a higher rate of attachment to a fibronectin matrix than MCF7-EV cells, and that the rate of attachment was greatest over the initial 20 minutes of the assay. Out of curiosity, the rate of MCF7-S cell-matrix attachment was then compared to that of the MCF7wt and Tam-R cell-lines. Interestingly, figure 5.17B shows that, even though the degree of cell-matrix attachment for MCF7-S cells after 50 minutes was equal to that of MCF7wt, the initial rate of attachment was closer to that of the Tam-R cells. Once again, figure 5.17A shows that the rate of attachment for both MCF7-S and MCF7-EV cells was reduced by AZM555130 at 1μM.

Enhanced cell-matrix attachment in Tam-R cells contributes to an increase in the rate at which these cells spread. As such, the rate of cell spreading was investigated in the MCF7-S cell-line also. MCF7-S and MCF7-EV cells were seeded onto either uncoated or fibronectin-coated 60mm Petri-dishes and incubated at 37°C as normal. Representative images of live cells at 20x magnification were then captured at 1-, 3-, 6- and 24-hrs after seeding using a Leica DM-IRE2 inverted microscope fitted with a Hoffman condenser. Figures 5.18 (uncoated) and 5.19 (fibronectin-coated) show that MCF7-S cells possessed a much greater rate of cell spreading than MCF7-EV cells on both surfaces. As was seen with MCF7wt and Tam-R cell-lines, cell spreading was more rapid in the presence of a fibronectin matrix for both MCF7-S and MCF7-EV cells.

Following the observations made regarding cell attachment, spreading, migration and invasion in the MCF7-S cell-line, these cells were then characterised for the phosphorylation of FAK and paxillin - two Src substrates known to be involved in the regulation of focal adhesion formation and turnover.

MCF7-S and MCF7-EV cells were cultured under basal conditions to log-phase growth, at which point they were lysed and subjected to SDS-PAGE/Western blotting. The membranes were then probed with antibodies

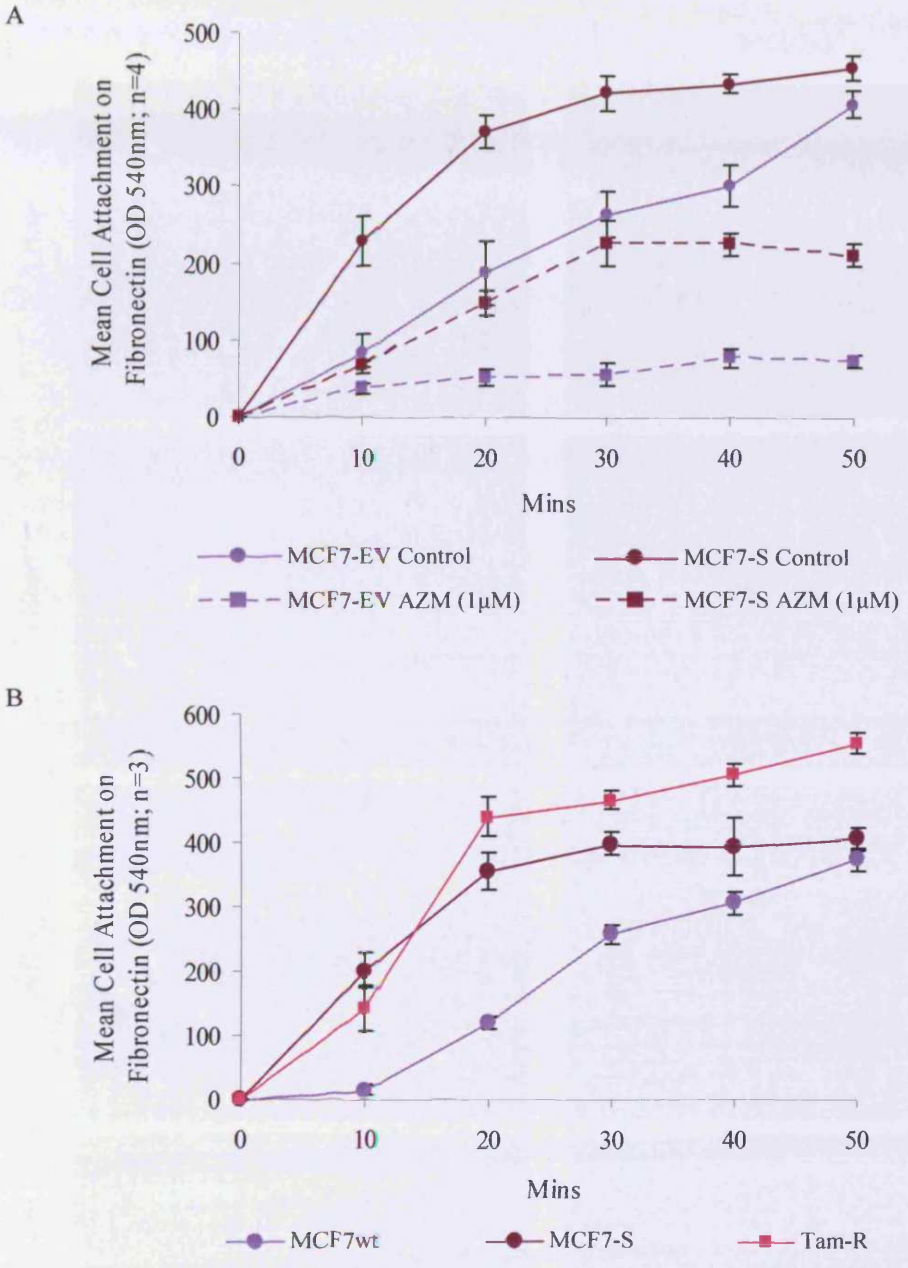

Figure 5.17 Rate of MCF7-S and MCF7-EV cell-attachment to a fibronectin-coated surface as measured using a cell attachment time-course assay.

The rate of MCF7-S and MCF7-EV attachment to a fibronectin-coated surface in the absence or presence of AZM555130 was measured using a cell attachment time-course assay. Cells ($4x10^4$) were seeded in W+5% containing either vehicle (DMSO) or AZM555130 (1μM) into the wells of a fibronectin-coated 96-well plate. Cells were left to attach for up to 50 minutes at 37°C. During the assay, medium containing unattached cells was removed at the given time points and replaced with PBS. The attached cells were kept in PBS until the end of the experiment and then measured using the MTT assay as normal. Data is presented as Mean Cell Attachment (OD_{540}) ± S.D. (n=4) (A). For comparison, the rate of MCF7-S cell attachment to a fibronectin-coated surface was also measured in relation to the rate of attachment of MCF7wt and Tam-R cells (B).

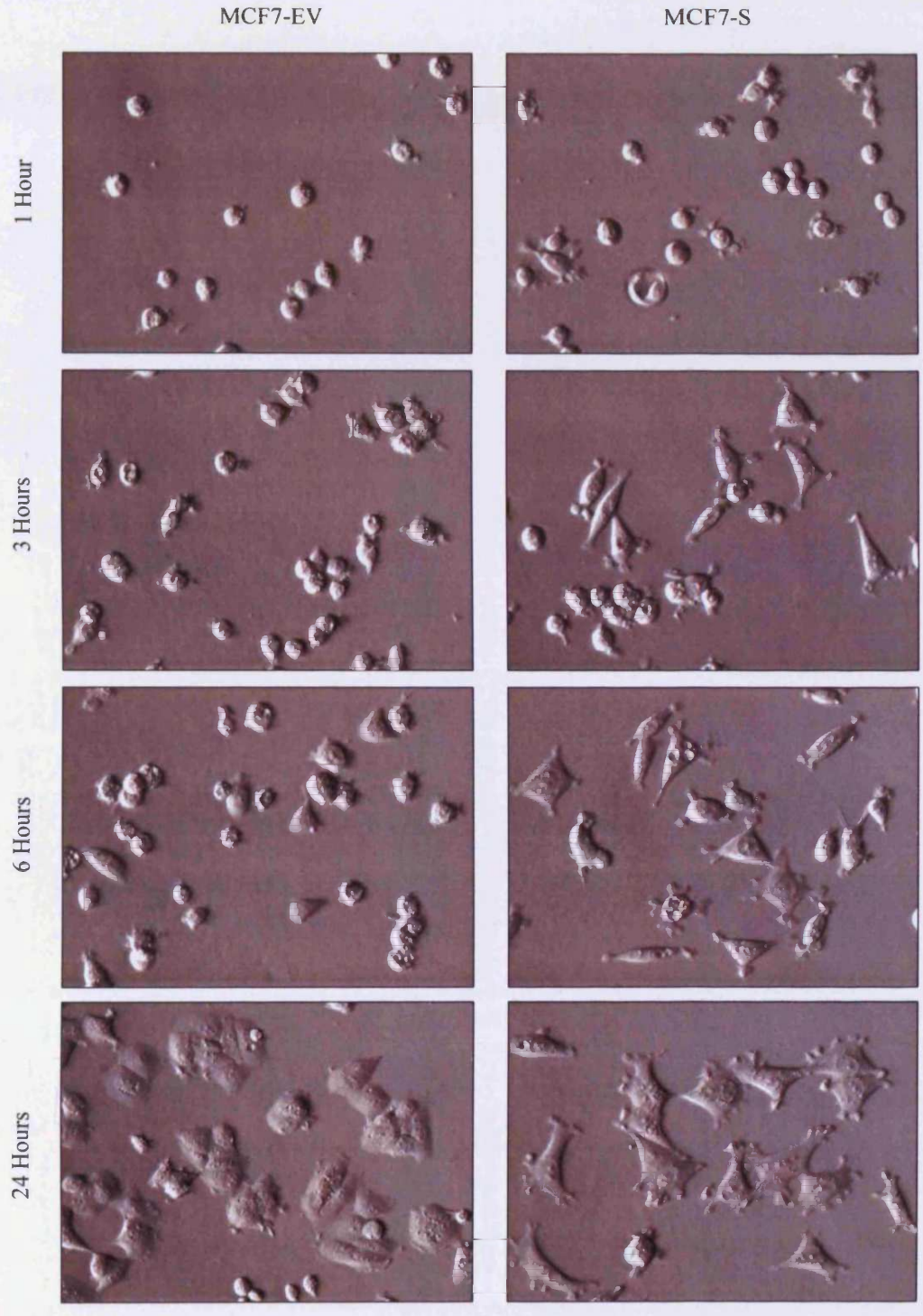

Figure 5.18 MCF7-EV and MCF7-S cell-spreading on an uncoated plastic surface.
MCF7-EV and MCF7-S cells ($1.5x10^6$) were seeded onto uncoated 60mm Petri-dishes and placed at 37°C. Representative images of the live cells at 20x magnification were captured 1-, 3-, 6- and 24-hours after seeding using a Leica DM-IRE2 inverted microscope fitted with a Hoffman condenser and a Hamamatsu C4742-96 digital camera.

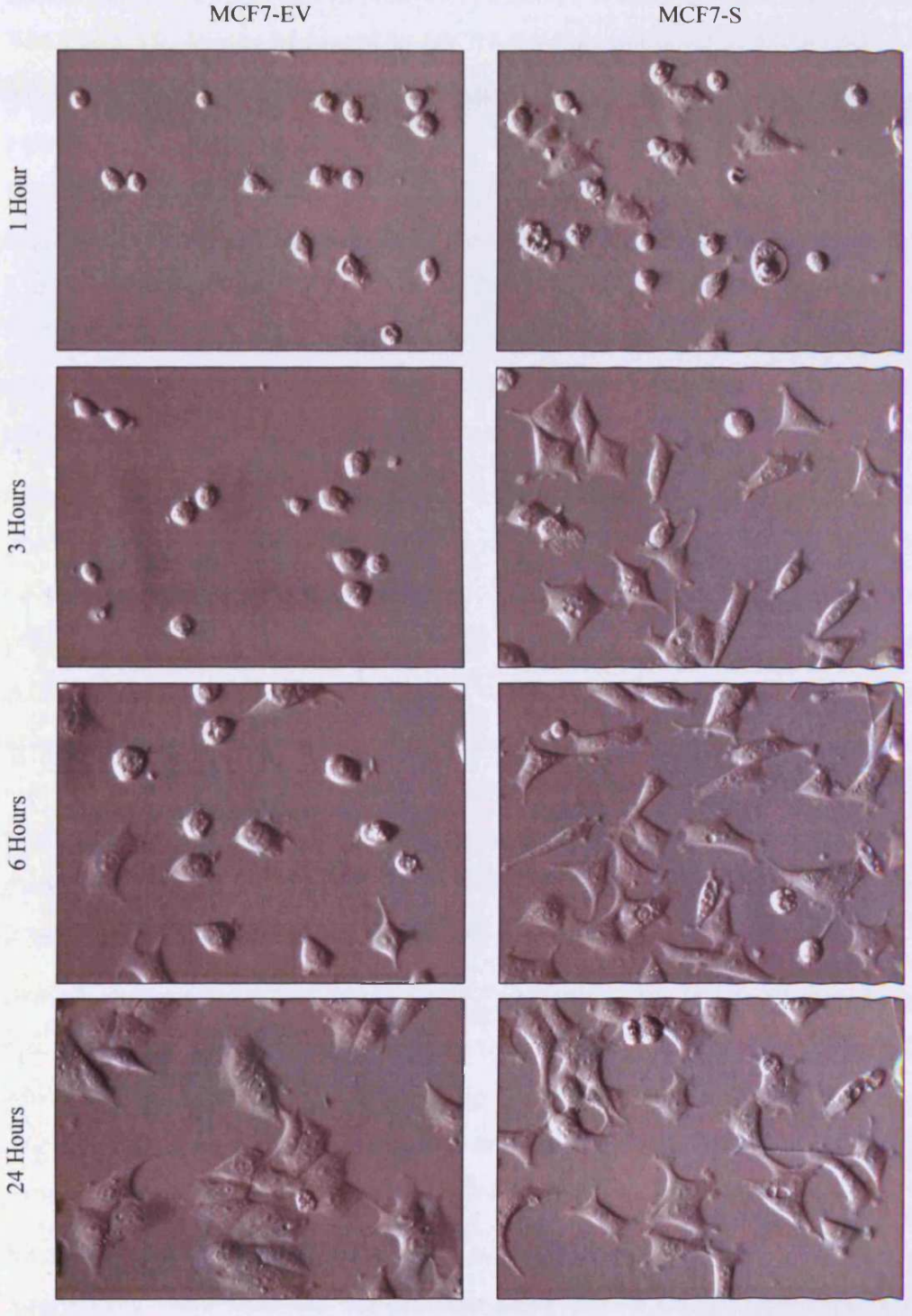

Figure 5.19 MCF7-EV and MCF7-S cell-spreading on a fibronectin-coated surface.
MCF7-EV and MCF7-S cells ($1.5x10^6$) were seeded onto fibronectin-coated 60mm Petri-dishes and placed at 37°C. Representative images of the live cells at 20x magnification were captured 1-, 3-, 6- and 24-hours after seeding using a Leica DM-IRE2 inverted microscope fitted with a Hoffman condenser and a Hamamatsu C4742-96 digital camera.

specific for FAK (pY397, pY861, pY925 and total) and paxillin (pY31 and total). Figure 5.20 shows that phosphorylation of FAK at all three sites (Y397, Y861 and Y925) was increased in MCF7-S cells compared to MCF7-EV, by 3.3-fold, 6.2-fold and 16.3-fold respectively. No differences in total FAK protein levels were seen. MCF7-S cells also displayed an 11-fold increase in the phosphorylation of paxillin at Y31 compared to MCF7-EV cells, in addition to a small (2-fold) increase in levels of total paxillin protein (figure 5.21). The phosphorylation of both FAK (pY397, pY861 and pY925) and paxillin (pY31) in MCF7-S cells was reduced by AZM555130 in a dose-dependent manner (figures 5.22 and 5.23 respectively), while levels of total FAK and paxillin protein were unaffected by the treatment.

Finally, cell counting experiments were used to assess the growth rates of both stably transfected cell-lines in comparison with those of MCF7wt and Tam-R cells over a period of 11 days. Figure 5.24 shows the growth rates of all four cell-lines, in addition to the growth rate of MCF7-S cells in the presence of AZM555130 at 1μM. The growth rate of MCF7-EV cells was indistinguishable from that of MCF7wt cells. However, MCF7-S cells grew at an enhanced rate that was initially comparable to that of Tam-R cells, and eventually reached 2127% of day 0 counts compared to 342% for MCF7-EV (a 6.2-fold increase). Even in the presence of AZM555130, growth of MCF7-S cells was 2.4-fold greater than basal MCF7-EV cell growth after 11 days.

Growth in Tam-R cells is driven by the aberrant activation of growth-factor receptor signalling pathways, primarily those initiated by EGFR and c-erbB2 which are members of the c-erbB receptor family [70]. Therefore, whether increased Src activity might augment c-erbB signalling in MCF7-S cells, thus providing a possible explanation for their enhanced growth, was examined.

Basal MCF7-EV and MCF7-S cells, in addition to basal Tam-R cells for comparison, were analysed for proteins using SDS-PAGE/Western blotting. Figure 5.25A shows that the phosphorylation of EGFR at Y845, a Src specific site, and Y1068 were both increased in MCF7-S cells, by 2-fold and 3.4-fold respectively compared to MCF7-EV. Furthermore, the level of total EGFR

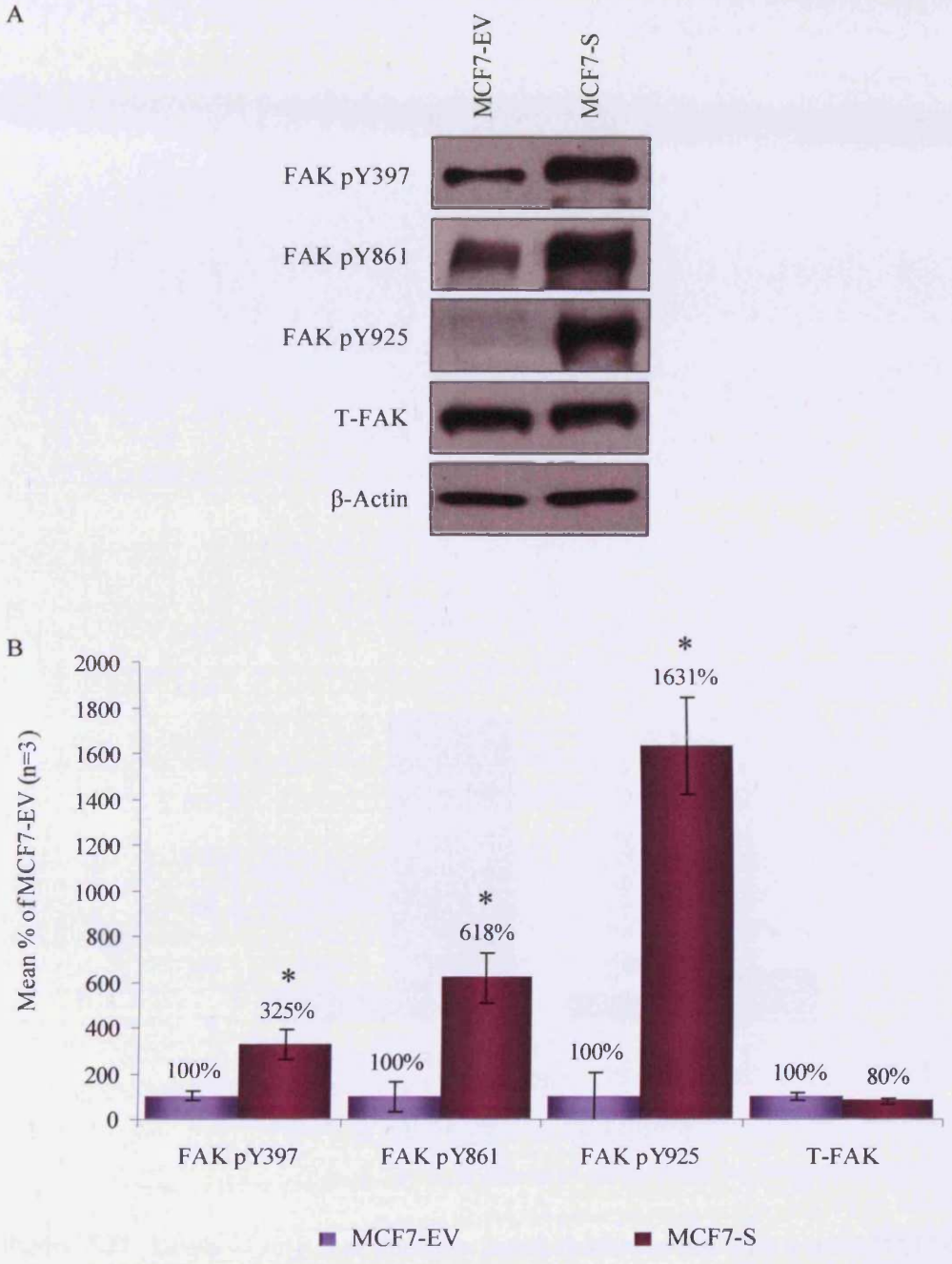

Figure 5.20 Levels of total and phosphorylated FAK in MCF7-S versus MCF7-EV cells as determined by Western blotting.

MCF7-EV and MCF7-S cells were cultured to log-phase growth and lysed for proteins as described in materials and methods (section 2.4.1). Total soluble protein (40μg) was subjected to SDS-PAGE/Western blot analysis and the membranes probed with antibodies specific for FAK pY397, pY861, pY925 and total FAK (A). Densitometry was conducted on the bands obtained and the data, corrected for loading with β-actin, is presented as Mean % of MCF7-EV ± S.D. (* $p<0.01$ vs. MCF7-EV; n=3) (B).

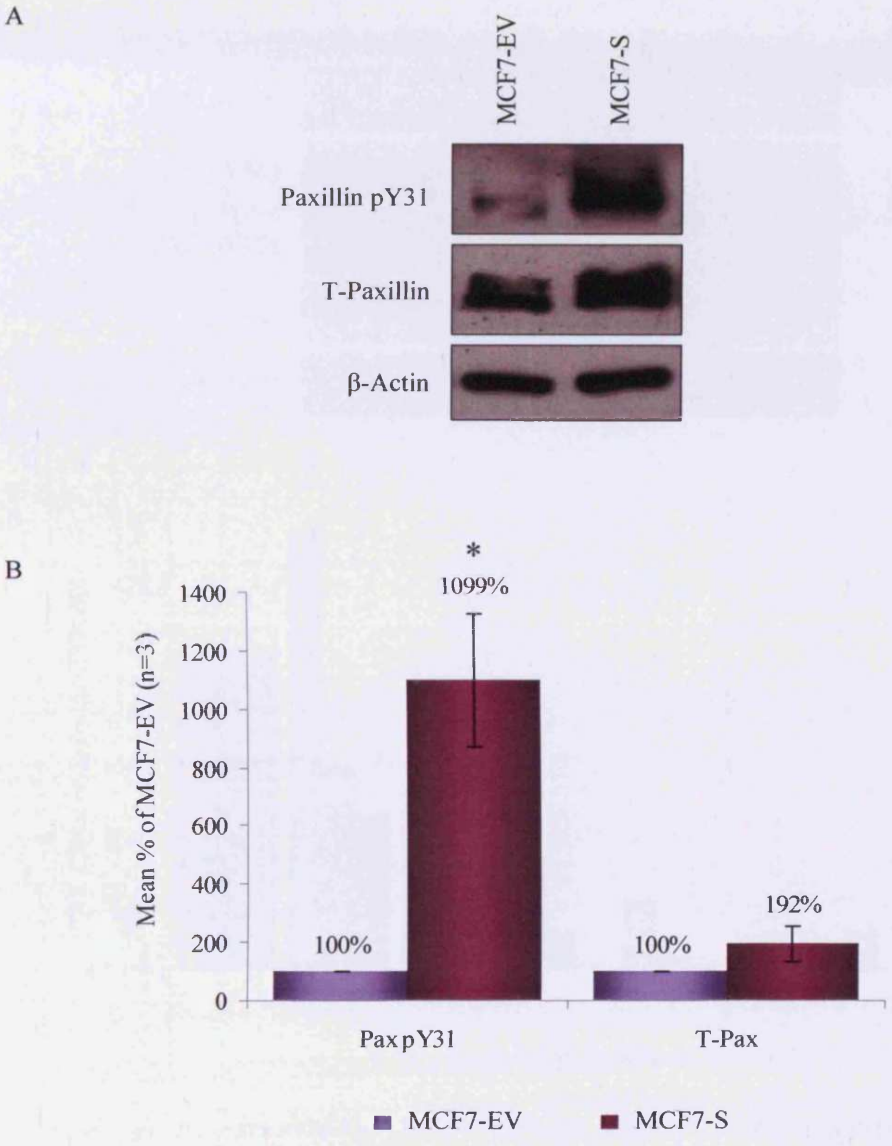

Figure 5.21 Levels of total and phosphorylated Paxillin in MCF7-S versus MCF7-EV cells as determined by Western blotting.

MCF7-EV and MCF7-S cells were cultured to log-phase growth and lysed for proteins as described in materials and methods (section 2.4.1). Total soluble protein (40μg) was subjected to SDS-PAGE/Western blot analysis and the membranes probed with antibodies specific for paxillin pY31 and total paxillin (A). Densitometry was conducted on the bands obtained and the data, corrected for loading with β-actin, is presented as Mean % of MCF7-EV ± S.D. (* $p<0.05$ vs. MCF7-EV; n=3) (B).

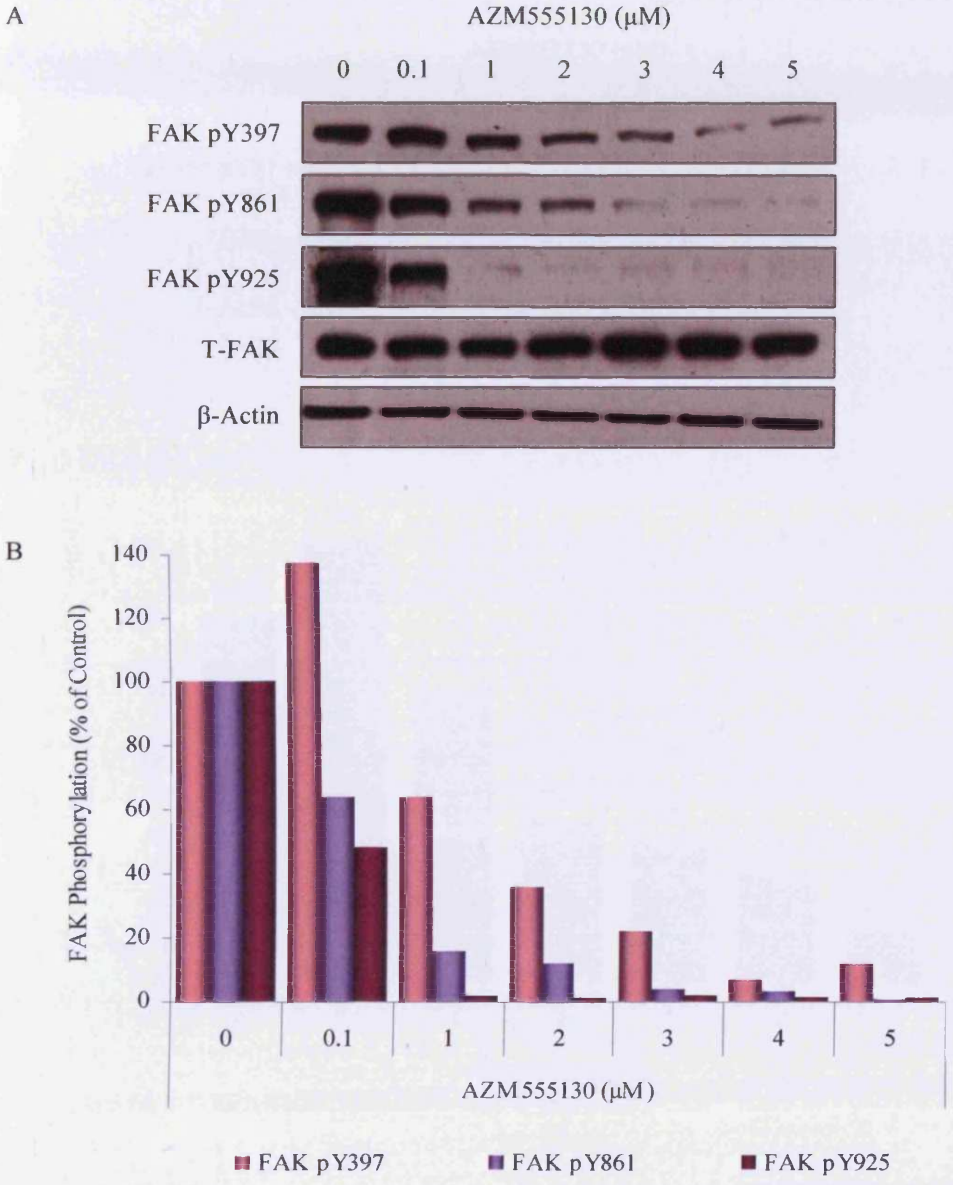

Figure 5.22 Dose-dependent effect of Src inhibition by AZM555130 on FAK phosphorylation in MCF7-S cells.

MCF7-S cells were cultured to log-phase growth and then treated with AZM555130 at the stated concentrations for 24 hours. Control cells were treated with vehicle (DMSO) only for the same duration. Cells were then lysed for proteins. Total soluble protein (40μg) was subjected to SDS-PAGE/Western blot analysis and the membranes probed with antibodies specific for FAK pY397, pY861, pY925 and total FAK (A). Densitometry was conducted on the bands obtained and the data for FAK pY397, pY861 and pY925, corrected for loading with β-actin, presented as % of Control (B).

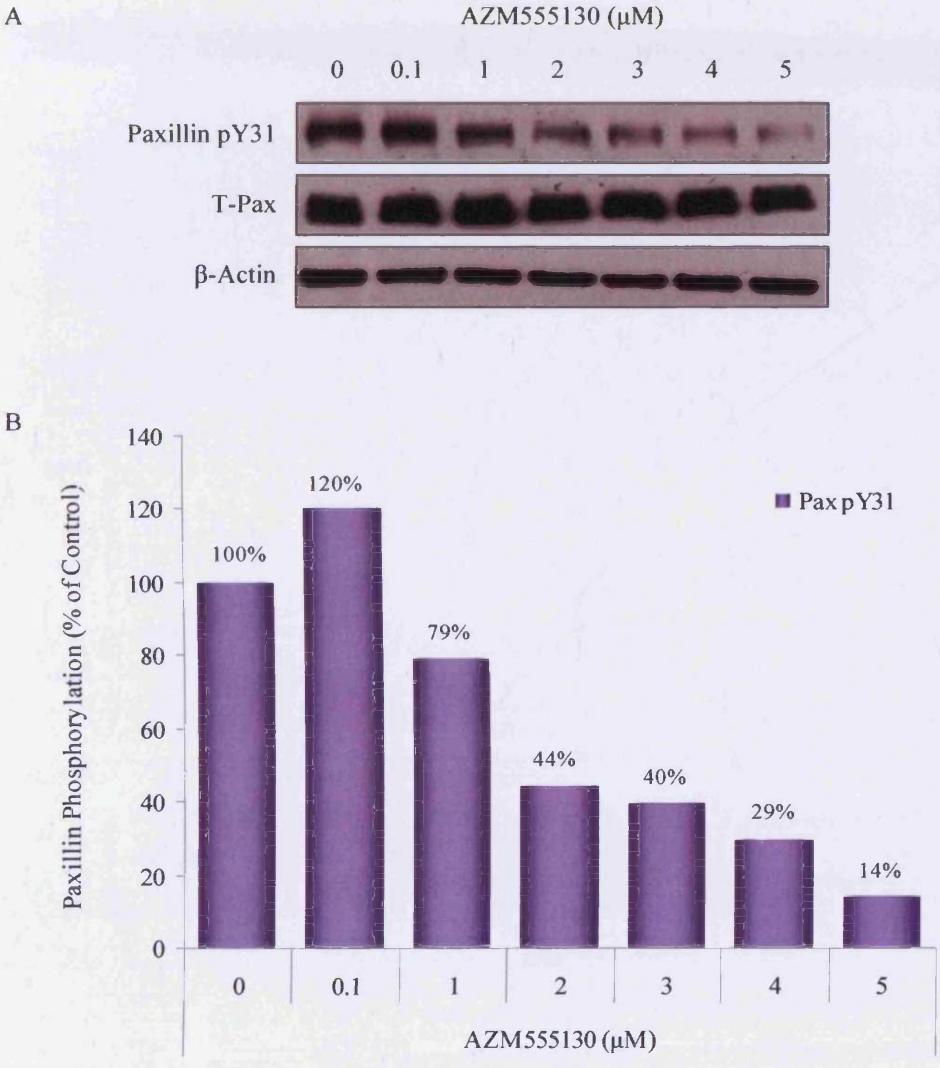

Figure 5.23 Dose-dependent effect of Src inhibition by AZM555130 on Paxillin phosphorylation in MCF7-S cells.

MCF7-S cells were cultured to log-phase growth and then treated with AZM555130 at the stated concentrations for 24 hours. Control cells were treated with vehicle (DMSO) only for the same duration. Cells were then lysed for proteins. Total soluble protein (40μg) was subjected to SDS-PAGE/Western blot analysis and the membranes probed with antibodies specific for paxillin pY31 and total paxillin (A). Densitometry was conducted on the bands obtained and the data for paxillin pY31, corrected for loading with β-actin, presented as % of Control (B).

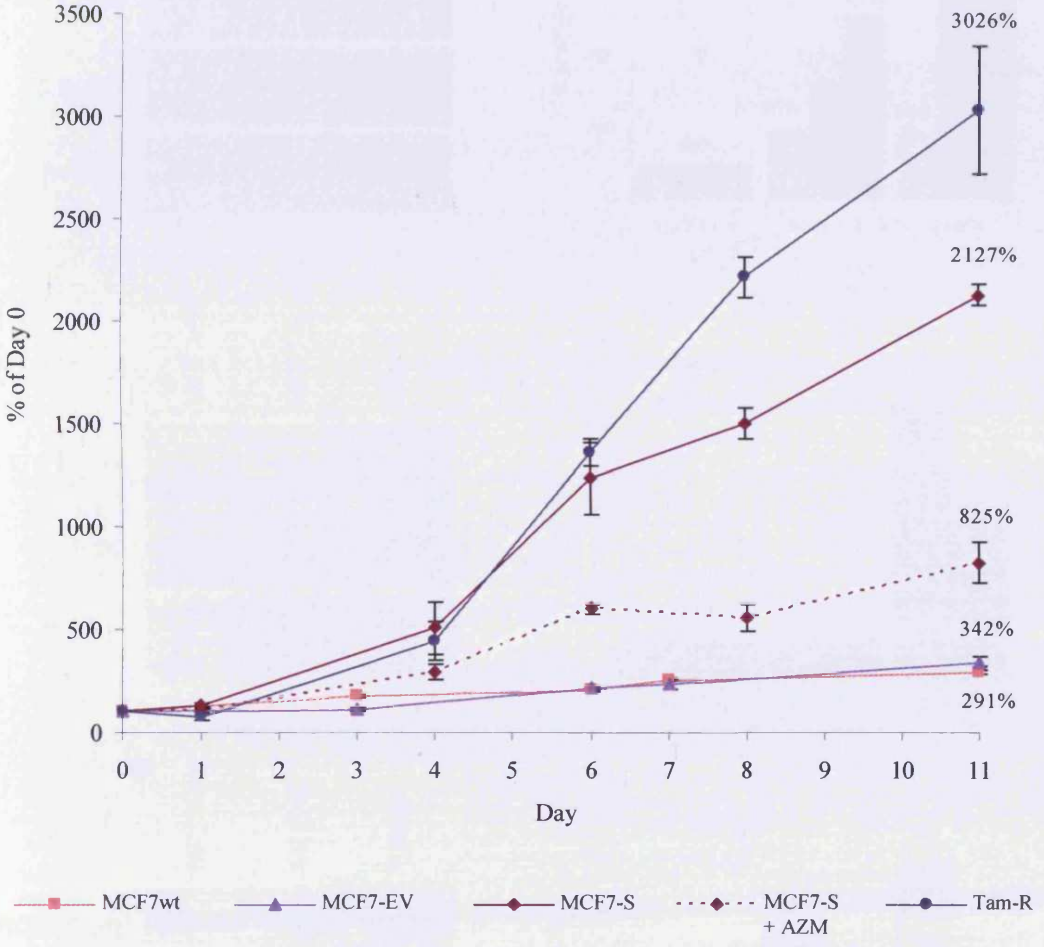

Figure 5.24 Basal growth rate of MCF7-S cells in comparison to growth of MCF7wt, MCF7-EV and Tam-R cell-lines.

MCF7wt, MCF7-EV, MCF7-S and Tam-R cells were seeded into a 24-well plate at a density of 30,000 cells/well. After 24 hours, the medium was replaced with W+5% ± Tam (100nM) ± AZM555130 (1μM) as appropriate. The cells were cultured as normal and cell number was determined on days 1, 3/4, 6, 7/8 and 11 using a Beckman Coulter™ Multisizer II. Data is presented as Mean % of Day 0 ± S.D. (n=3).

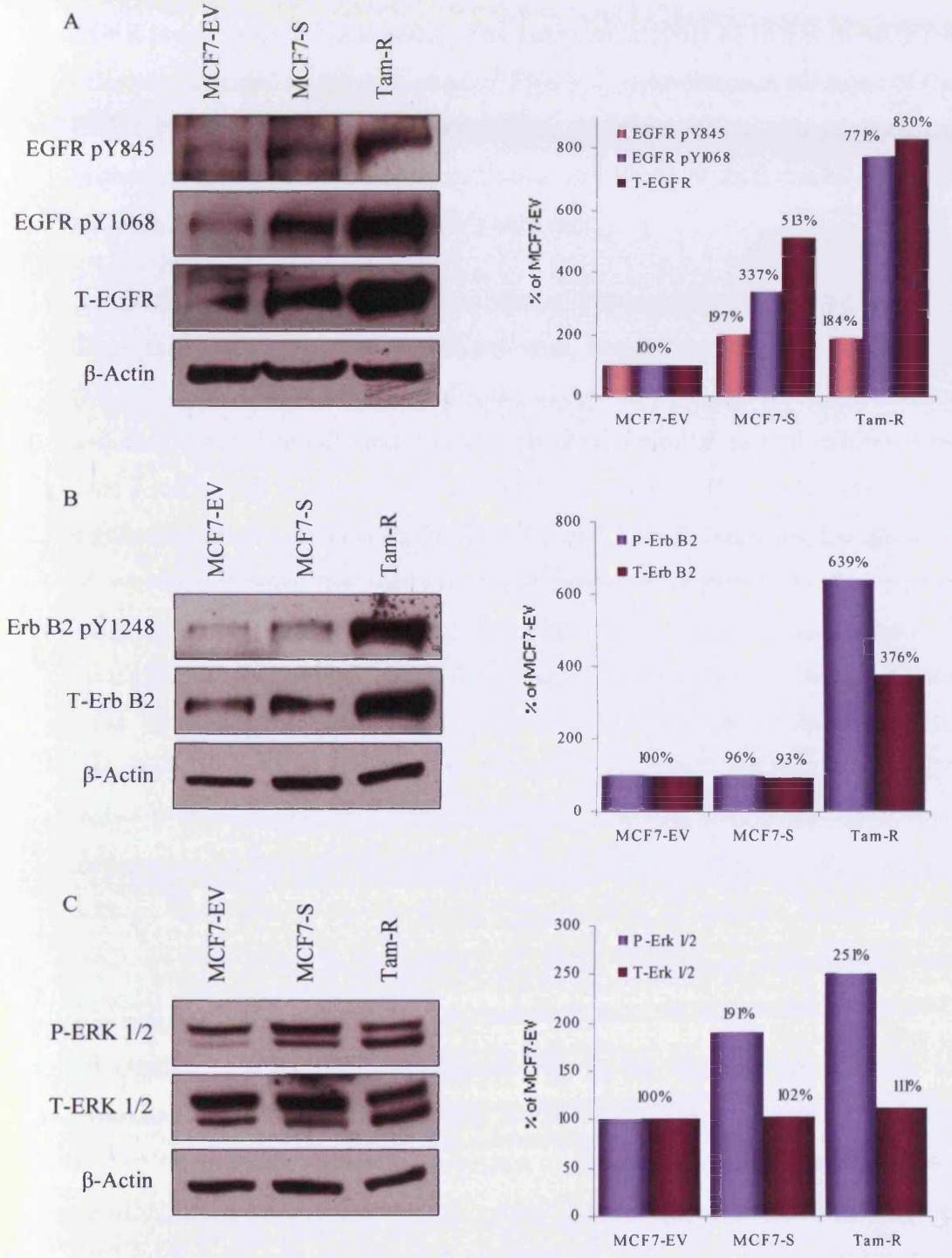

Figure 5.25 Preliminary studies into the activation of erb-receptor signalling pathways in MCF7-S cells.

MCF7-EV, MCF7-S and Tam-R cells were cultured to log-phase growth and lysed for proteins as described in materials and methods (section 2.4.1). Total soluble protein (40μg) was subjected to SDS-PAGE/Western blot analysis and the membranes probed with antibodies specific for EGFR (pY845, pY1068 and total; A), c-erb B2 (pY1248 and total; B) and ERK 1/2 (T202/Y204 and total; C). Densitometry was conducted on the bands obtained and the data, corrected for loading with β-actin, is presented as % of MCF7-EV ± S.D.

protein was also increased in MCF7-S cells (a 5-fold increase relative to total EGFR levels in MCF7-EV cells). The increased activity of EGFR in MCF7-S cells was reflected in the activation of ERK 1/2, a downstream substrate of the EGFR signalling pathway (figure 5.25C). However, there was no apparent difference in the levels of either activated (pY1248) or total c-erbB2 protein between the MCF7-EV and MCF7-S cell-lines.

5.2.3 Src: A potential mechanism of Tamoxifen-resistance?

Thus far, MCF7wt cells transfected with constitutively-active Src kinase (MCF7-S) have been shown to display altered morphological characteristics and an enhanced motile and invasive phenotype similar to that exhibited by Tam-R cells, which also possess elevated Src activity. Due to the phenotypic similarities observed between the MCF7-S and Tam-R cell-lines, the question of whether elevated Src activity could confer insensitivity to the growth inhibitory effects of tamoxifen, and thus be a potential mechanism of tamoxifen-resistance in the Tam-R cell-line, was considered. Growth studies were conducted on MCF7wt, MCF7-EV, MCF7-S and Tam-R cells in response to tamoxifen at increasing concentrations (10^{-9} - 10^{-6}M). Figure 5.26 shows that the growth of both MCF7wt and MCF7-EV cell-lines was significantly inhibited by tamoxifen at all concentrations used, with the efficacy of inhibition increasing as concentration increased. However, the effect of tamoxifen on the growth of either MCF7-S or Tam-R cells was minimal compared with control.

To confirm a role for Src kinase activity in the acquired insensitivity to tamoxifen treatment observed above, further tamoxifen dose-response growth studies were conducted in the presence of the specific Src kinase inhibitor, AZM555130 (1μM). Figure 5.27 shows, once again, that the growth of MCF7-EV cells was significantly inhibited by tamoxifen, while the MCF7-S cells were relatively unaffected by the treatment. However, in the presence of AZM555130 MCF7-S cells appear to regain their sensitivity to the growth inhibitory effects of tamoxifen, with the response of these cells to tamoxifen at increasing concentrations mirroring that seen with basal MCF7-EV cells.

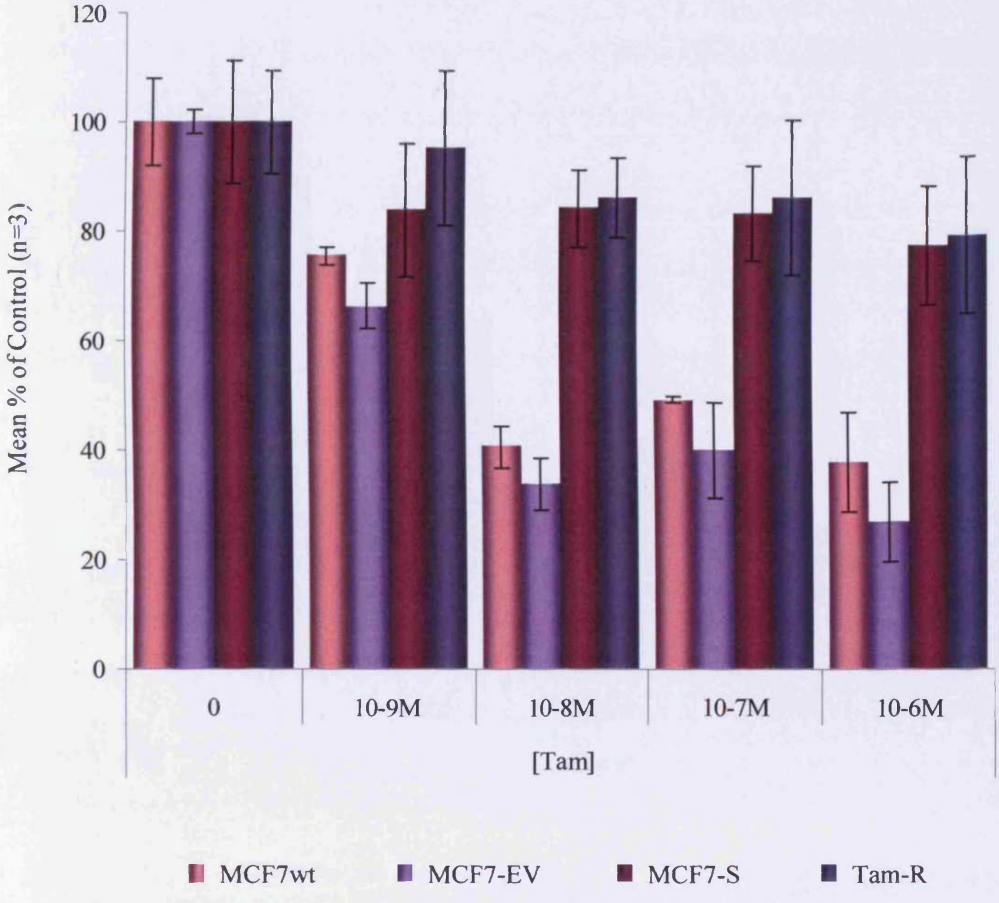

Figure 5.26 Dose-dependent effect of tamoxifen treatment on the growth of MCF7wt, MCF7-EV, MCF7-S and Tam-R cell-lines.

MCF7wt, MCF7-EV, MCF7-S and Tam-R cells were seeded in W+5% into a 24-well plate at a density of 40,000 cells/well. After 24hrs, the medium was replaced with W+5% containing 4-hydroxy-tamoxifen at the stated concentrations. Control cells were cultured in the presence of vehicle (ethanol) only. The cells were cultured as normal and cell number determined on day 12 using a Beckman Coulter™ Multisizer II. Data is presented as Mean % of Control ± S.D (n=3).

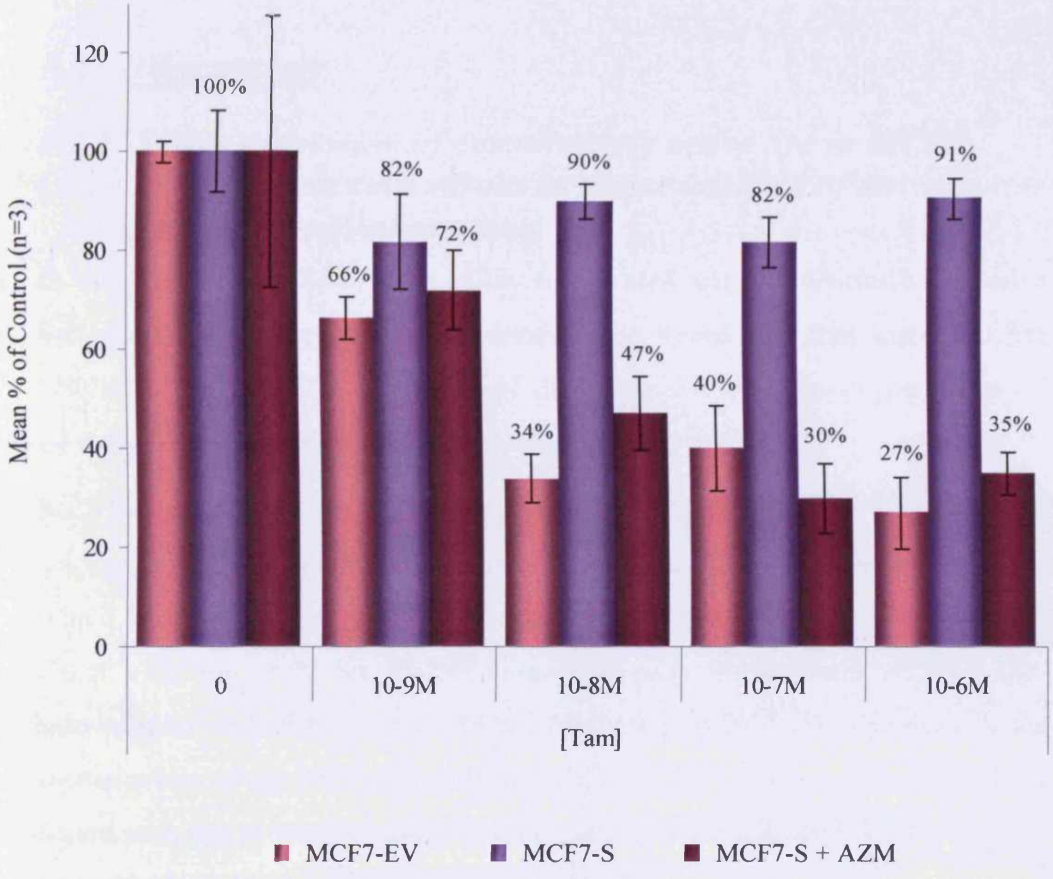

Figure 5.27 Dose-dependent effect of tamoxifen treatment on the growth of MCF7-S cells in the absence and presence of AZM555130.

MCF7-EV and MCF7-S cells were seeded in W+5% into a 24-well plate at a density of 40,000 cells/well. After 24hrs, the medium was replaced with W+5% containing 4-hydroxy-tamoxifen at the stated concentrations ± AZM555130 (1μM). Control cells were cultured in the presence of vehicle (ethanol/DMSO) only. The cells were cultured as normal and cell number determined on day 12 using a Beckman Coulter™ Multisizer II. Data is presented as Mean % of Control ± S.D (n=3).

More interesting, however, was that a similar result was observed when these experiments were repeated with MCF7wt and Tam-R cells. Figure 5.28 shows that, alone, tamoxifen elicited the expected effects on the growth of MCF7wt and Tam-R cells; however, in the presence of AZM555130 the growth of Tam-R cells was, once again, significantly inhibited by tamoxifen in a manner similar to that seen with hormone-sensitive MCF7wt cells.

5.3 Discussion

5.3.1 Stable expression of constitutively active Src in MCF7 breast cancer cells results in the acquisition of an aggressive cell-phenotype.

In this chapter, MCF7wt cells stably transfected with a constitutively active Src mutant were used to further confirm the hypothesis that increased Src activity is central to the regulation of the aggressive cell-phenotype displayed by tamoxifen-resistant breast cancer cells *in vitro*.

MCF7wt cells were transfected with the Src Y529F plasmid construct and selected out using G418 to generate a stable, Src Y529F-expressing cell-line, which has been called MCF7-S. Although time constraints did not permit clonal selection of the Src Y529F transfected cells, the resultant MCF7-S cell-line appears to exhibit a high degree of homogeneity. As a control in the investigation of the MCF7-S cell-phenotype, MCF7wt cells were stably transfected with the pUSEamp empty vector, giving rise to the MCF7-EV cell-line.

Characterisation of the MCF7-S cell-line for activated Src, as measured by Y419 phosphorylation [123], revealed an 8.7-fold increase compared to the MCF7-EV cells, with a corresponding rise in total Src protein also seen. Analysis of early (P.4) and late (P.25) passages of MCF7-S cells confirmed that the level of Src Y529F expression remained constant in these cells over time. Furthermore, MCF7-S cells demonstrated the highest level of activated Src of the four cell-lines used in this study, which may explain why they are less sensitive to the inhibitory effects of AZM555130 (for example, the IC_{50} of AZM555130 in MCF7-S cells is 0.375μM, compared to 0.02μM in Tam-R

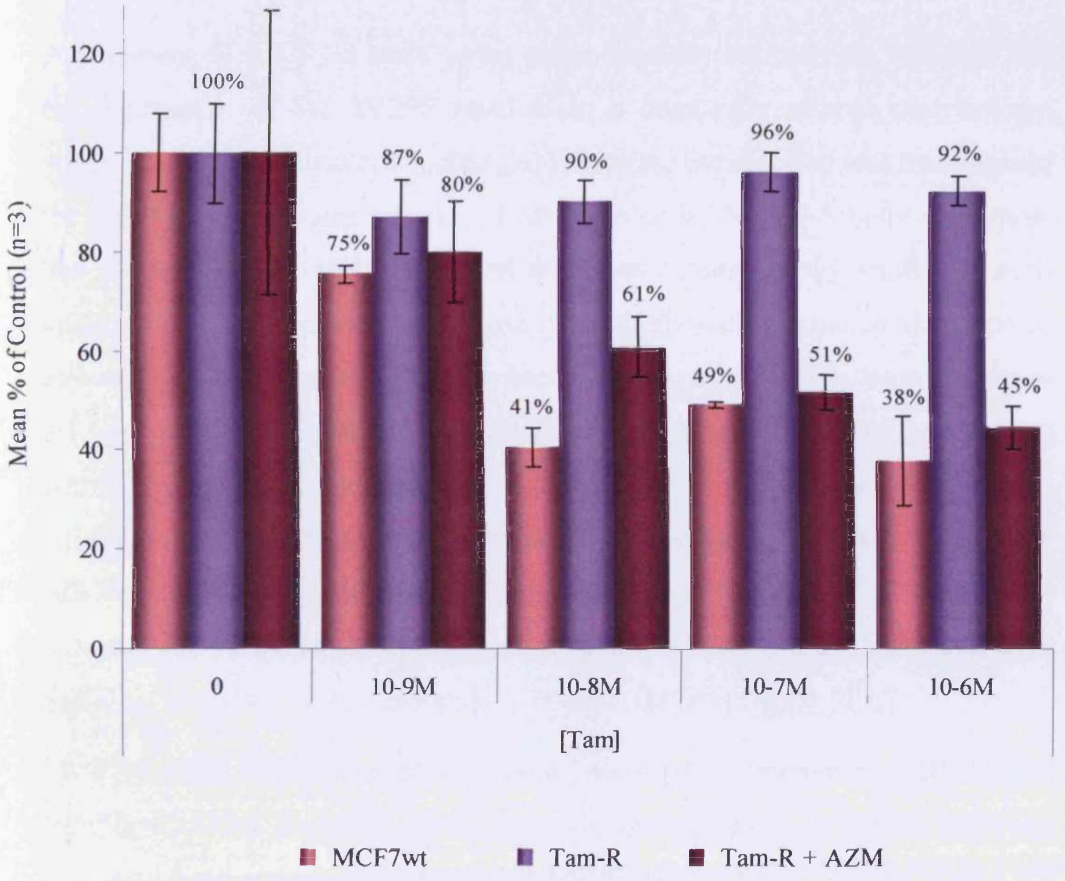

Figure 5.28 Dose-dependent effect of tamoxifen treatment on the growth of Tam-R cells in the absence and presence of AZM555130.

MCF7wt and Tam-R cells were seeded in W+5% into a 24-well plate at a density of 40,000 cells/well. After 24hrs, the medium was replaced with W+5% containing 4-hydroxy-tamoxifen at the stated concentrations ± AZM555130 (1μM). Control cells were cultured in the presence of vehicle (ethanol/DMSO) only. The cells were cultured as normal and cell number determined on day 12 using a Beckman Coulter™ Multisizer II. Data is presented as Mean % of Control ± S.D (n=3).

cells). Maximal inhibition of Src in MCF7-S cells required AZM555130 concentrations of 5μM or above; however, at such concentrations this compound was cytotoxic to the MCF7-EV cells. Thus, AZM555130 was used at 1μM in the majority of experiments conducted with these cells; in many cases, this resulted in the incomplete inhibition of the biological process being assessed, most likely due to the residual Src activity observed at this concentration.

Assessment of MCF7-S cells using phase-contrast microscopy revealed that the expression of Src Y529F resulted in a drastically altered morphology, while MCF7-EV cells were unchanged following transfection and had retained the morphological characteristics of MCF7wt cells. MCF7-S cells were more like Tam-R cells in appearance and exhibited a morphology similar to cells undergoing EMT, demonstrating loss of epithelial-cell characteristics such as cell-cell contact formation [255]. Increased Src activity has been shown to disrupt cell-cell adhesions by causing dissociation of E-cadherin/catenin complexes in a kinase-dependent manner [245, 256], and the loss of these adhesions has been associated with increased invasion in a number of cancer cell-lines *in vitro* [164]. Conversely, inhibition of Src with PP2 was seen to promote cell-cell contact formation in colon, liver and breast cancer cell-lines and also, to reduce liver metastasis in immunodeficient mice [237].

MCF7-S cells also demonstrated marked increases in membrane ruffling and lamellipodia and filopodia formation. Similar alterations in cell morphology have also been reported in epithelial KM12C colon cancer cells following the expression of Src Y529F [99]. Src plays a major role in the dynamic regulation of membrane activity through modulation of cell-matrix adhesions and reorganisation of the actin cytoskeleton [170]. Following binding to FAK and translocation to focal adhesions, Src recruits and phosphorylates Crk and $p130^{CAS}$. Src/FAK-$p130^{CAS}$ signalling ultimately results in the activation of a family of small GTPases (RhoA, Rac1 and cdc42) which are then able to remodel the cytoskeleton by initiating actin polymerisation, resulting in the appearance of membrane protrusions [257]. Further studies have revealed that cdc42 activation leads specifically to the formation of filopodia, while

activation of Rac1 gives rise to lamellipodia [170]; thus, investigation of the activities of these two proteins in the MCF7-S cells may provide further insight into the role of Src in the regulation of their morphology.

It has been suggested that Src, through the formation of Src/FAK signalling complexes, is able to act as a molecular switch that can alter the predominant cell-adhesion type from E-cadherin mediated cell-cell adhesions to integrin mediated cell-matrix adhesions [166]. This is reflected in the present study where the inhibition of Src activity in MCF7-S cells using AZM555130 (1-5μM) was seen to reduce cell-membrane activity and restore cell-cell contact formation, thus confirming that the morphological changes witnessed in these cells following transfection were a direct effect of elevated Src activity.

Interestingly, the constitutively active Src expressed in MCF7-S cells was detected almost exclusively at the areas of increased membrane activity discussed above. Fincham *et al.* have shown that the translocation of v-Src and activated c-Src from their site of synthesis to the cell membrane is mediated by interactions between the SH2/SH3 domains of Src and the actin cytoskeleton [118], and that this process is independent of Src's kinase activity [117]. Furthermore, Kaplan *et al.* demonstrated that mutation of c-Src at Y527 (Y-F substitution) was sufficient to cause the re-distribution of c-Src to focal adhesions at the cell periphery [258]. In addition, they reported that following co-expression of Src Y527F with wild-type c-Src in Src-deficient fibroblasts, wild-type Src remained in the perinuclear location while Src Y527F was still translocated to focal adhesions [258]. The images of Src pY419-stained MCF7-S cells in figure 5.12 show some evidence of perinuclear staining in addition to the strong membrane staining also seen, which, from Kaplan *et al.*'s observations, is likely to be Src that is endogenous to the parental MCF7 cell-line. Together, these data suggest that phosphorylated Y527 in wild-type Src can sequester the SH2/SH3 domains required for the translocation of Src to focal adhesions by maintaining a closed conformation. However, as the Src Y529F mutant is incapable of this, it is readily translocated to the cell membrane.

As mentioned previously, increased cell-membrane activity, accompanied by the acquisition of an EMT-like morphology, are both characteristic of a motile and invasive cell-phenotype [164, 166, 259]. Thus, the aggressive *in vitro* behaviour of the MCF7-S cell-line was investigated. Src Y529F-expressing MCF7-S cells demonstrated significantly enhanced migratory and invasive capacities, in addition to an increased rate of cell attachment and spreading on uncoated and matrix-coated surfaces. Elevated Src kinase activity has previously been implicated in the promotion of both cell motility and invasion [166]. For example, the transfection of fibroblasts and cancer cells with Src has been shown to increase their levels of migration and invasion [97], while the expression of a Src dominant-negative mutant or the use of siRNA to silence Src gene expression results in decreased motility, matrix-attachment and spreading in MCF7 cells [152]. Furthermore, expression of Src Y527F in MDA-MB-231 breast cancer cells has been associated with the increased formation of invadopodia [260], which are specialised actin-rich plasma membrane protrusions containing high levels of integrins, tyrosine kinases and proteolytic enzymes such as MMPs and are able to induce degradation of extracellular matrix components to facilitate invasion [261].

Treatment of MCF7-S cells with AZM555130 at 1μM resulted in a 50% and 80% reduction in motility and invasion respectively, suggesting that these two cellular processes might have differential sensitivities to Src inhibition. Interestingly, this was also noted with the Tam-R cell-line when AZM555130 was used at 0.1μM (section 4.2.2). It was hypothesized that this increased sensitivity to AZM555130 may be due to the greater number of Src-dependent events involved in the coordination of cellular invasion. In support of this, a recent study has shown that the expression of v-Src in $FAK^{-/-}$ fibroblasts was able to correct the defective cell motility exhibited by these cells; however, these cells retained their non-invasive phenotype despite the increased Src activity [177]. This suggests that motility and invasion are regulated by Src/FAK via distinct signalling pathways, and that, while FAK may be dispensable for cell motility in the presence of elevated Src activity, it would appear

to be crucial for the regulation of cellular invasion. Hsia *et al.* go on to suggest that this may be due to its role in the construction of invadopodia and in $p130^{CAS}$-Rac-JNK signalling which up-regulates the expression and activity of the MMP-2 and MMP-9 proteins required for the degradation of extracellular matrix components [177].

Elevated cell motility and invasion are often associated with altered cell-matrix attachment and so the affinity of MCF7-S cells for uncoated and matrix-coated surfaces were measured. The data show that MCF7-S cells demonstrated a greater degree of attachment to an uncoated surface after 50 minutes compared to the MCF7-EV cells, while no significant difference was seen in the attachment of these cells to a fibronectin-coated surface, initially suggesting that Src may not have a role to play in attachment to fibronectin. However, in the presence of the AZM555130 Src inhibitor, attachment of these cell-lines to both uncoated and fibronectin-coated surfaces was reduced. When the rate of MCF7-S cell-attachment to a fibronectin matrix was investigated the data revealed that it was increased compared to MCF7-EV. As with Tam-R cells, the rate of attachment of MCF7-S cells was greatest in the first 20 minutes. Interestingly, when MCF7-S cells were compared to the MCF7wt and Tam-R cell-lines, their initial rate of attachment was seen to be very similar to that of the Tam-R cells. However, after 20-30 minutes the level of attachment reached a plateau and the overall attachment of the MCF7-S cells at the end of the experiment was equal to that of MCF7wt cells. Together, these data confirm a role for Src in the regulation of cell-matrix attachment, but might also suggest the presence of a rate-limiting factor, such as low levels of integrin expression, which may be inherent to the MCF7wt cell-line from which the MCF7-S cells were derived and could be masking the true effect of elevated Src expression on cell-matrix attachment in these cells.

In addition to an increased rate of matrix-attachment MCF7-S cells also demonstrated enhanced cell spreading on both uncoated and fibronectin-coated surfaces. Src is thought to regulate cell-spreading via the formation of a Src/FAK signalling complex and the subsequent recruitment and phosphory-

lation of $p130^{CAS}$, which in turn leads to the activation of Rho-family GTPases to promote dynamic cyto-skeletal re-modelling [173, 174]. Src activity has previously been shown to regulate spreading of murine fibroblasts [246], while the expression of FAK correlates with the rate of cell-spreading in a number of different cancer cell-lines in culture [262]. Moreover, fibroblasts deficient in the expression of Src family members display significantly delayed cell-spreading on fibronectin and vitronectin matrices [246].

The Src-dependent activation of FAK and the subsequent initiation of its downstream signalling pathways are central to the regulation of cell migration, invasion, attachment and spreading [115, 176, 262, 263]. Western blot analysis of basal MCF7-S cells revealed increased phosphorylation of FAK at Y397, Y861 and Y925 compared to MCF7-EV cells, while total protein levels were unchanged. Furthermore, these cells also demonstrated elevated paxillin phosphorylation at Y31, in addition to a small increase in the levels of total paxillin protein. The phosphorylation of FAK at all three sites and of paxillin at Y31 were reduced by AZM555130 in a dose dependent manner.

The data show that the phosphorylation of FAK Y397 was increased in the Src Y529F-expressing MCF7-S cells, and that it was reduced following treatment with AZM555130 at higher concentrations (1-5μM). While this result was unexpected due to the established nature of Y397 as an auto-phosphorylation site, it does corroborate the data obtained in figure 4.13 where inhibition of Src activity in Tam-R cells resulted in a modest decrease in FAK Y397 phosphorylation. Expression of v-Src has previously been shown to phosphorylate FAK on Y397, while cells that lack expression of Src family kinases demonstrate decreased FAK Y397 phosphorylation [264]. Moreover, Brunton *et al.* report that FAK Y397 phosphorylation was increased 3.2-fold in KM12C colon cancer cells that were over-expressing activated Src [150].

While the mechanisms of FAK Y397 auto-phosphorylation are not yet fully understood, a supporting role is emerging for protein-protein interactions between FAK and cell-membrane proteins such as the EGF- and PDGF-receptors [205]. Like Src, FAK is normally maintained in an inactive form by

intra-molecular interactions [265]. In the case of FAK, these interactions involve the direct binding of the N-terminal FERM (band 4.1, ezrin, radixin, moesin homology) domain to the kinase domain, which blocks access to the active site of the kinase and prevents auto-phosphorylation of Y397. These interactions are disrupted following association with activated receptor proteins at the cell-membrane, which can displace the FERM domain from the kinase, thus releasing Y397 for auto-phosphorylation and the subsequent recruitment of Src for full kinase activation of FAK [265]. The proteins that can promote FAK Y397 auto-phosphorylation in this manner are not yet fully known, but of the ones that have been identified some are capable of being activated by Src, such as EGFR [145]. This may partially explain the effects of constitutive Src activity on the auto-phosphorylation site of FAK. Interestingly, Brunton *et al.* also demonstrated a 2-fold increase in FAK Y397 phosphorylation in KM12C cells expressing a kinase-inactive form of Src [150]. Furthermore, Gonzalez *et al.* have reported similar increases following the expression of Src dominant-negative in MCF7 breast cancer cells [152]. In both cases, this was explained by the protection of FAK Y397 from de-phosphorylation by phosphatases following binding of the kinase-defective Src due to its inability to dissociate from FAK and initiate focal adhesion turnover.

Phosphorylation of FAK at the Src-specific Y861 site was also increased in MCF7-S cells, as was the phosphorylation of paxillin Y31. The function of Y861 phosphorylation is not yet fully understood but it has been shown to be important in cell migration, invasion, anchorage independent growth and for the recruitment of $p130^{CAS}$ to focal adhesions which leads to JNK activation and MMP expression [225]. Moreover, the phosphorylation of FAK Y861 was necessary for the regulation of cell motility in a number of highly tumourigenic prostate cancer cell-lines [266]. Paxillin Y31 phosphorylation in bladder cancer cells has also been shown to regulate cell migration [224]. Furthermore, the recruitment of FAK and paxillin to β1-integrin following attachment to type IV collagen correlates with increased migration of SCC

cells on this matrix, while over-expression of paxillin in these cells also promoted migration and invasion [223].

MCF7-S cells also demonstrated an increase in the Src-specific phosphorylation of FAK Y925, which is thought to be important in the mediation of FAK degradation and focal adhesion turnover necessary for cell migration [150, 175]. Interestingly, phosphorylation of Y925 was the most sensitive of all three sites to the inhibition of Src with AZM555130 in MCF7-S cells, a phenomenon also witnessed in the Tam-R cell-line [211]. Y925 is located in the focal adhesion targeting (FAT) domain of FAK and, when phosphorylated, creates a high affinity Grb2 docking site. The binding of Grb2 to FAK Y925 initiates a signalling cascade that culminates in the activation of ERK 1/2, which in turn activates Calpain-2 to proteolytically degrade FAK and other focal adhesion proteins, leading to focal adhesion disassembly and increased migration [170, 176]. Thus, together, the data presented here suggest that the hyper-phosphorylation of FAK and paxillin by constitutively-active Src may be responsible for the increased cell attachment, spreading, migration and invasion exhibited by the MCF7-S cell-line.

In addition to an increased metastatic phenotype, MCF7-S cells also possessed an enhanced rate of growth under basal conditions, demonstrating a 6.2-fold increase in cell number at day 11 compared to MCF7-EV cells. Furthermore, the increased growth of these cells was inhibited by AZM555130 at 1μM. Interestingly, the observed growth rate of MCF7-S cells was comparable to that of Tam-R cells, which exhibit increased expression and activation of EGFR and c-erbB2 growth-factor receptors [70]; however, the growth of the MCF7-EV control cells was indistinguishable from that of MCF7wt. The role of Src in cell proliferation is subject to debate. For example, Brunton and colleagues showed that expression of kinase-defective Src in KM12C colon cancer cells had no effect on their proliferation [150]. Moreover, Welman *et al.* have reported that high levels of Src Y527F expression in HCT116 and SW480 colorectal cancer cell-lines actually appeared to inhibit cell growth [151]. Conversely, the expression of a Src dominant-negative mutant signifi-

cantly reduced the growth of MCF7 breast cancer cells in serum-free and serum-containing medium, as well as in medium containing EGF [152]. Furthermore, inhibition of Src using PP1 reduced anchorage-independent growth in MDA-MB-468, MCF7 and ZR-75-1 breast cancer cell-lines [153].

Src has been shown to interact with both EGFR and c-erbB2 growth-factor receptors [144, 267, 268]. In particular, Src possesses a well-established synergistic relationship with EGFR in which each protein is able to augment the activity of the other when both are over-expressed [145, 200], and this may contribute to tumour progression [228]. Src is able to potentiate EGFR signalling by phosphorylating tyrosine residues on its cytoplasmic domain, such as Y845, Y891, Y920 and Y1101, leading to enhanced EGFR signalling [201, 229, 269]. Moreover, in a cell-free system Src was also able to phosphorylate a recombinant EGFR auto-phosphorylation domain at sites corresponding to Y992, Y1068, Y1086, Y1101, Y1148 and Y1173 on EGFR [240].

Preliminary analysis of growth-factor receptor signalling in MCF7-S cells revealed elevated phosphorylation of EGFR at Y845 and Y1068. However, there was no change in the levels of c-erbB2 phosphorylation at Y1248. EGFR Y845 is a Src-specific phosphorylation site that promotes DNA synthesis, and may also promote the intrinsic tyrosine kinase activity of EGFR due to its location in the activation-loop of the kinase domain. Y1068, on the other hand, initiates a mitogenic signalling cascade resulting in the downstream activation of ERK 1/2. Correspondingly, an increase in the activation of ERK 1/2 was also observed in the MCF7-S cells, suggesting that this EGFR signalling pathway is active in these cells.

Surprisingly, increased levels of total EGFR protein were also seen in the MCF7-S cells compared to MCF7-EV. However, it is doubtful that this increase is a result of increased EGFR gene transcription as expression of Src Y529F has been shown to have no effect on EGFR mRNA levels [221]; rather, it is more likely to involve deregulation of the mechanisms responsible for the degradation of EGFR in the cell. Following ligand binding, activated EGFR is poly-ubiquitinated by c-Cbl. This action commits EGFR to degradation by the

26S proteosome, and results in decreased levels of EGFR protein and attenuation of the mitogenic signal [270]. However, in the presence of elevated Src activity c-Cbl itself is ubiquitinated and undergoes proteosomal degradation. Thus, sorting of the EGFR protein to the degradation pathway is compromised, leading to recycling of the receptor to the plasma membrane where it accumulates [221]. In support of this, Moro *et al.* have reported that integrin mediated signalling via Src not only increased the phosphorylation of EGFR on specific residues but also increased the amount of EGFR present at the cell surface, and that this increase was negated following inhibition of Src with PP1 [271]. If this mechanism is operational *in vivo* also, then it may have clinical implications, as enhanced EGFR signalling has been shown to confer a poor prognosis in many cancers [179].

The data presented here provide circumstantial evidence for a role for Src in the elevated growth of MCF7-S cells. However, further studies using specific inhibition of EGFR and c-erbB2 are required in order to determine whether growth-factor signalling is also involved.

5.3.2 Src: A potential mechanism of Tamoxifen-resistance?

The present study has demonstrated that Src activity is significantly elevated in the Tam-R cell-line, and this has since been witnessed by others in additional *in vitro* models of tamoxifen-resistance [160]. Importantly, the data presented here show that stable transfection of MCF7wt cells with constitutively-active Src enabled them to grow in the presence of tamoxifen. Furthermore, treatment of the MCF7-S and Tam-R cell-lines with AZM-555130 re-sensitised these cells to tamoxifen, restoring the significant growth-inhibition seen with MCF7-EV and MCF7wt cells.

Increased Src activity has been implicated in the development of resistance to a number of chemotherapeutic agents, including STI571 (chronic myelogenous leukaemia/acute lymphoblastic leukaemia), cisplatin and gefitinib (gallbladder adenocarcinoma), gemcitabine (pancreatic adenocarcinoma), paclitaxel (ovarian cancer) and oxaliplatin (colon cancer) (reviewed in [272]). Interestingly, Hiscox *et al.* [*Endocrine Related Cancer*, in press] and others

[273, 274] have demonstrated that the combined treatment of tamoxifen with a Src inhibitor enhances the growth-inhibitory effects of tamoxifen, with synergistic reductions in growth seen in MCF7 breast cancer cells. Together, these data provide compelling evidence for a role for Src in the acquisition and maintenance of an *in vitro* tamoxifen-resistant phenotype in ER-positive MCF7 breast cancer cells, and there are a number of mechanisms currently under investigation as to how Src might be able to achieve this.

Tam-R cells display increased expression and activation of EGFR [70] and the present study has shown that stimulation of these cells with EGF, TGFα or amphiregulin leads to an increase in Src activation. Furthermore, inhibition of Src in Tam-R cells results in a reduction in EGFR activity and downstream signalling via ERK 1/2. Together, these observations highlight the potential synergistic relationship that may exist between Src and EGFR in the Tam-R cell-line. Thus, as the Src Y529F-expressing MCF7-S cell-line also demonstrates elevated EGFR activity, increased EGFR signalling may present a possible explanation for the insensitivity of these cells to tamoxifen.

Cross-talk between EGFR and ER signalling pathways has been proposed as a mechanism of tamoxifen resistance [51, 74]. In such cases, the phosphorylation of EGFR at Y1068 initiates a signalling cascade that results in the downstream activation of ERK 1/2. Increased phosphorylation of ERK 1/2 is associated with poor response to anti-hormone therapies and decreased patient survival, and thus may be a useful prognostic indicator of the likely success of anti-hormone treatment in the clinic [71]. ERK 1/2 is able to promote ER signalling in the presence of tamoxifen by enhancing the phosphorylation of the ER AF-1 domain, thus facilitating the expression of AF-1-dependent genes (reviewed in [51]). In particular, Britton *et al.* have shown that ERK 1/2-dependent phosphorylation of ER on S118 in the AF-1 domain increases the expression of amphiregulin, which can then further stimulate EGFR dependent growth of Tam-R cells [73]. Thus, the inhibition of EGFR/ERK 1/2 signalling may be of therapeutic importance in tamoxifen-resistant breast cancer.

A further mechanism by which elevated Src activity might confer tamoxifen-resistance is through increased phosphorylation of ER and the promotion of ligand-independent gene transcription. While binding of tamoxifen inhibits the AF-2 domain of ER, the AF-1 domain is unaffected and is still able to regulate gene transcription [51]. In the presence of tamoxifen, Src can potentiate AF-1 activity, and hence AF-1-dependent gene transcription, through the promotion of ER phosphorylation at a number of sites (see figure 5.29). Interestingly, expression of v-Src in HeLa cells has been shown to confer a 2-fold increase in the transcriptional activity of ER under basal conditions or following stimulation with E_2; while in the presence of tamoxifen, v-Src was able to increase gene transcription 15-fold [275]. Three sites of Src-regulated ER phosphorylation have been identified - S118, S167 and Y527.

S118 phosphorylation, which is elevated in Tam-R cells, can be mediated by ERK 1/2 in response to ligand dependent growth-factor signalling [32]. However, Src is also able to increase ERK 1/2 activation and promote the phosphorylation of S118, either by potentiating EGFR activation or by promoting integrin-dependent FAK-Grb2-ERK 1/2 signalling [275]. S167, on the other hand, is phosphorylated following the activation of Akt, and is thought to be involved in the stabilisation of the ER/gene-promoter interactions necessary for AF-1-dependent gene transcription [33, 52]. Phosphorylation of S167 via Src-mediated signalling has been shown to promote the agonist activity of tamoxifen in tamoxifen-resistant Ishikawa endometrial adenocarcinoma cells, resulting in increased AF-1-dependent expression of genes such as c-myc and pS2. Furthermore, treatment of these cells with the SU6656 Src inhibitor reduced S167 phosphorylation and subsequent gene transcription, thus confirming the involvement of Src in this process [52]. Elevated Akt activation has been reported in the Tam-R cells [76], in addition to the expression of pS2 (R. Burmi, personal communication) and c-myc (C. Staka, personal communication) in the presence of tamoxifen. Thus, Akt activation may promote AF-1 mediated gene transcription in Tam-R cells; however, the importance of Src in this process is yet to be determined.

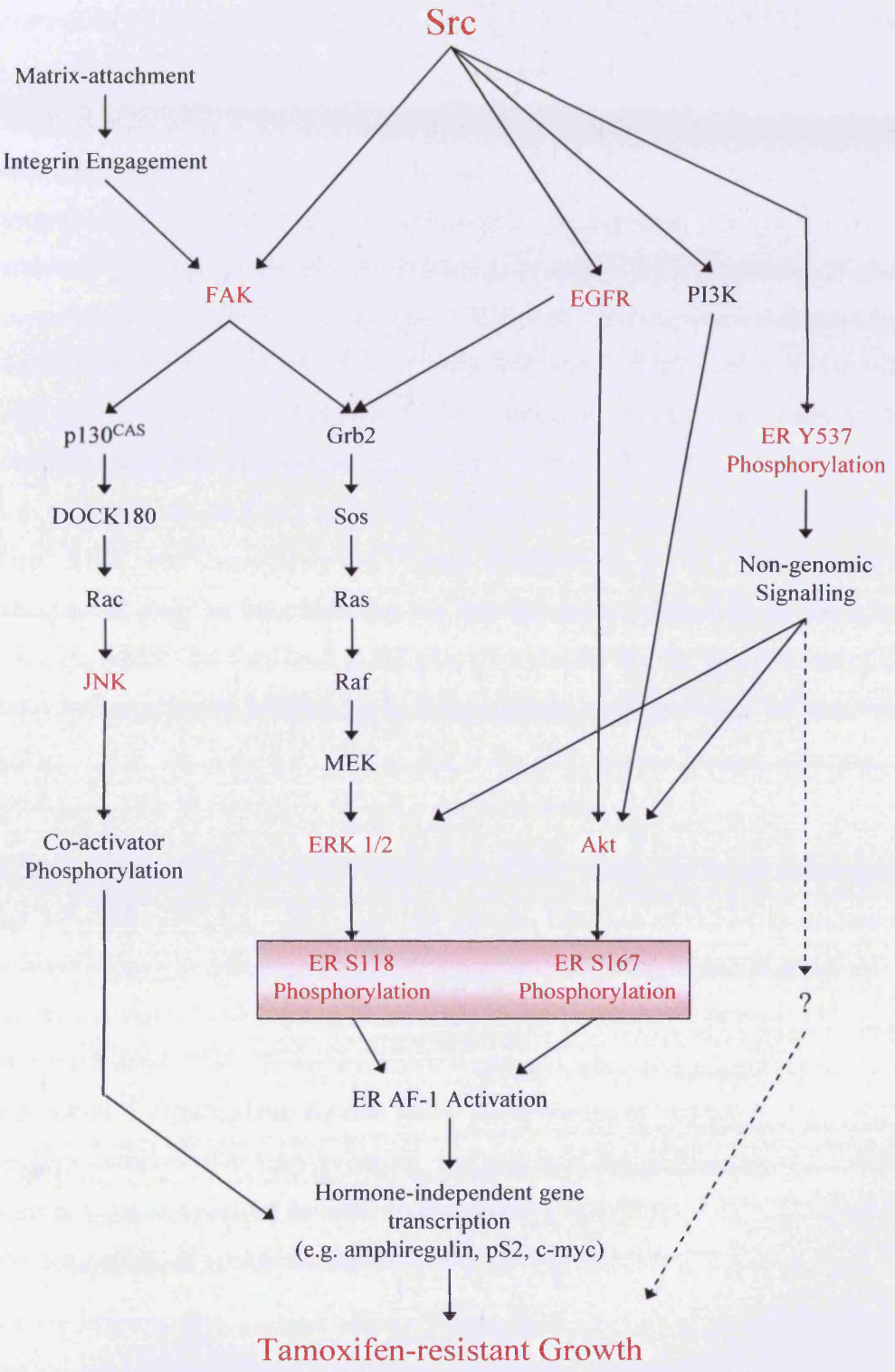

Figure 5.29 Proposed regulation of tamoxifen-resistant cell growth by Src.

Summary of the mechanisms reported in the literature by which Src may be able to promote ER phosphorylation and AF-1 activation in the presence of tamoxifen, leading to ligand-independent gene transcription and, potentially, hormone insensitivity. See text for Refs. Red indicates key component.

ER-dependent gene transcription is also regulated by the expression and activation of co-regulators, which are proteins that bind to the ER to either promote (co-activators) or inhibit (co-repressors) gene transcription [51]. Interestingly, Feng *et al.* [275] and Shah and Rowan [52] have demonstrated that Src, via the FAK-p130^{CAS}-dependent activation of JNK, can further promote AF-1-mediated gene transcription by activating the relevant co-activator proteins, such as CREB-binding-protein (CBP) or steroid receptor co-activator 1 (SRC-1). Furthermore, Sisci *et al.* have reported increased Src-dependent potentiation of AF-1 activity following attachment to fibronectin and type IV collagen matrices [253]. Integrin engagement leads to the activation of FAK and recruitment of Src to form a signalling complex which can then activate ERK 1/2 and JNK by distinct signalling pathways (Src/FAK-Grb2-MEK and Src/FAK-p130^{CAS}-Rac respectively [176]). Thus, matrix-attachment may be important for the Src-dependent activation of these two kinases, which can then lead to ER phosphorylation and the recruitment of co-activator proteins to promote gene transcription in the presence of tamoxifen [253]. This may explain why attempts to measure anchorage independent growth in Tam-R cells have failed in our laboratory.

The final site of ER phosphorylation is on Y537, which can be phosphorylated by Src directly [276]. Although the precise function of Y537 is unclear at present, it may be involved in ER dimerisation following ligand binding and in the facilitation of ER binding to an ERE in the promoter region of oestrogen-regulated genes [34]. However, more recent evidence also suggests that Y537 can act as a docking site for Src when phosphorylated, resulting in a Src/ER protein complex that may promote non-genomic ER signalling [43]. Thus, further work is required in order to determine if and how Y537 contributes to the acquisition of tamoxifen-resistance in ER-positive breast cancer.

In conclusion, this chapter showed that over-expression of constitutively-active Src was sufficient to confer tamoxifen insensitivity in ER-positive MCF7 breast cancer cells. Furthermore, it identified possible mechanisms of action by which this could occur. The data suggest that Src may play an

important role in the mediation of distinct signalling pathways that potentiate both growth-factor signalling and ligand-independent ER-mediated gene transcription, which together enable the cell to circumvent the growth inhibitory effects of tamoxifen therapy. Thus, as a common component in the mediation of these signalling pathways, Src may present a powerful therapeutic target in the treatment of tamoxifen-resistant disease. Further work is urgently required in order to fully understand the intricate relationship that may exist between Src and both EGFR and ER signalling in tamoxifen-resistant breast cancer.

5.4 Chapter Summary

- The MCF7-S cell-line was generated following the stable transfection of MCF7wt cells with a constitutively active Src mutant (Src Y529F). These cells displayed significantly elevated levels of Src activity in comparison to the vector-control cell-line (MCF7-EV).
- MCF7-S cells possess an extreme aggressive phenotype, demonstrating an altered morphology, an increased rate of cell-matrix attachment, and augmented migratory and invasive capabilities. Correspondingly, these cells displayed hyper-phosphorylation of FAK and paxillin at Src-specific sites.
- MCF7-S cells exhibited a higher rate of growth than MCF7-EV, in addition to increased activation of EGFR and ERK 1/2, but not c-erbB2.
- Importantly, MCF7-S cells displayed insensitivity to tamoxifen challenge at increasing concentrations. Further work is urgently required to elucidate the mechanism by which this occurs.
- In conclusion, this chapter demonstrates that expression of constitutively active Src in ER-positive MCF7 breast cancer cells was sufficient for the acquisition of an aggressive, tamoxifen-resistant cell-phenotype. As such, Src inhibition may be of therapeutic benefit in the treatment of tamoxifen-resistant breast cancer in the clinic.

Chapter Six

General Discussion & Conclusions

"The outcome of any serious research can only be to make two questions grow where only one grew before."

Thorsten Veblen (1857-1929.) US social scientist.
The Place of Science in Modern Civilization.

6 General Discussion and Conclusions

Acquired resistance to chemotherapeutic agents is a major problem in the clinical management of cancer. In breast cancer patients, many tumours that initially respond to tamoxifen may eventually acquire resistance to this anti-hormone, leading to disease relapse. Moreover, these tamoxifen-resistant tumours are frequently more aggressive in nature and are associated with a poor prognosis [197].

Using an *in vitro* cell model, our laboratory has previously demonstrated that elevated growth-factor receptor signalling may be a potential mechanism of acquired tamoxifen-resistance [70]. Furthermore, signalling cross-talk between growth-factor receptors and the ER in these cells may provide an additional growth stimulus [73]. These observations are evidenced by the fact that Tam-R cell growth can be inhibited with the EGFR inhibitor, gefitinib [70], or with the pure anti-oestrogen, fulvestrant [69]. Interestingly, Hiscox *et al.* have also reported that, in addition to EGFR-driven growth, Tam-R cells display a significantly elevated migratory and invasive capacity *in vitro*; however, this appears largely independent of EGFR signalling, since gefitinib has only a modest suppressive effect on these behaviours [180].

This thesis attempts to further characterise the aggressive phenotype of the Tam-R cells, and to investigate the possible cause(s) of these phenotypic changes which might lead to the enhanced metastatic potential of tamoxifen-resistant tumours *in vivo*. Src kinase activity was shown to be significantly elevated in Tam-R cells, where it plays a central role in the regulation of their aggressive cell-phenotype. Importantly, the data also suggest that elevated Src activity may contribute to the development of tamoxifen resistance, thereby highlighting its potential as a therapeutic target for the treatment of tamoxifen-resistant breast cancer in the clinic [277].

The over-expression and/or increased activation of Src has been widely reported in a number of cancers [101, 103], including breast, colorectal, pancreatic, ovarian and liver cancer [105-108, 219]; and thus, may represent a broad

spectrum therapeutic target in the fight against cancer. Src inhibition using either pharmacological or molecular techniques has been shown to be effective in a number of cancer models, both cell-line and animal based. For example, PP2 has been shown to reduce adhesion, cell spreading and migration in pancreatic endocrine tumour cell-lines [278], while pyrrolopyrimidine Src inhibitors reduced proliferation, adhesion, cell spreading, migration and invasion in the PC3 prostate carcinoma cell-line [279]. Furthermore, Src inhibition has also been shown to reduce the progression and metastasis of breast [162], pancreatic [155, 156, 161], and ovarian [157] tumours in nude mouse models.

A number of pharmacological inhibitors of Src activity are currently in development [243], with three front-runners emerging in the race to enter the clinic: AZD0530 (AstraZeneca) [236], BMS354825 (Dasatinib; Bristol Meyers Squibb Oncology) and SKI606 (Wyeth Research) [280]. Like AZM555130, these compounds are ATP analogues and work by competitively binding to the active site of the kinase domain of Src in a specific manner.

The efficacy of AZD0530 as an anti-proliferative and anti-invasive therapeutic agent has been extensively studied using *in vitro* cell models in our laboratory, demonstrating significant inhibition of cell-matrix attachment, migration and invasion, whilst showing only a modest effect on cell growth, [211, 247, 277]. Furthermore, AZD0530 has been shown to decrease proliferation and motility in a number of *in vitro* cell models; whilst pre-clinical *in vivo* experiments have demonstrated a reduction in tumour volume of over 95% and the prevention of metastasis in orthotopic mouse models [236]. BMS354825 (Dasatinib) has also been shown to suppress cell adhesion, migration and invasion and to inhibit Src signalling pathways involving FAK and $p130^{CAS}$ in prostate cancer cells [281]; whilst SKI-606 inhibited proliferation, migration and invasion in MDA-MB-231 breast cancer cells *in vitro*, and reduced tumour volume and metastasis in a xenograft mouse model of breast cancer *in vivo* [154].

The role of Src in proliferation is seemingly dependent on the tissue being studied, with some groups demonstrating no effect of Src on cellular growth

rates while others report varying degrees of growth inhibition following the reduction of Src activity [150-153]. Furthermore, Yezhelyev *et al.* have demonstrated anti-proliferative activity of the AZM475271 Src inhibitor on L3.6pl human pancreatic cells *in vivo* even though there was no effect on the proliferation of these cells *in vitro* [155], suggesting that the tumour micro-environment may influence the ability of Src to regulate cell growth. Data from the present study reports only a modest 50% reduction in the *in vitro* proliferation of the MCF7wt and Tam-R cell-lines.

Reasons for the inconsistencies observed when investigating the role of Src in proliferation are unknown, although clues may lie in the pattern of Src co-over-expression with steroid-hormone and/or growth-factor receptors in individual cell types; further work is required to determine this. Such complexities, however, imply that Src inhibitors are unlikely to be successful as mono-therapeutic agents in the treatment of cancer; more likely their role in the clinic will be as anti-invasive agents given in combination with a more effective anti-proliferative agent, such as tamoxifen or gefitinib, in order to reduce both tumour size and the risk of secondary disease. Indeed, current investigations in our laboratory have revealed that gefitinib and AZD0530 in combination work together to reduce cell growth, migration and invasion in Tam-R cells to a greater degree than when these compounds are used separately [247]. Furthermore, gemcitabine given in combination with a Src inhibitor in the treatment of pancreatic cancer growing orthotopically in nude mice is seen to synergistically reduce tumour volume and prevent lymph-node and liver metastasis in this model [155].

However, if Src inhibitors are going to complete phase II/III testing and enter the clinic as an anti-invasive therapy, then investigators must first be sure to select the relevant analytical end-points for this purpose. At present, the majority of clinical trials are designed to measure the effect of a compound on tumour shrinkage *in vivo* [233], whereas focussing on disease stabilisation and time to recurrence may be more suitable for these compounds [280].

Elvin and Garner [233] declare that:

> "The most relevant clinical end-point with which to demonstrate the impact of an anti-invasive therapy will be the long term reduction in the incidence and burden of metastatic disease and patient survival."

Therefore, the successful assessment of the efficacy of anti-invasive therapies will require the development of accurate and reliable methods of monitoring metastasis of tumours at the cellular level *in vivo*, and these new techniques should be non-invasive so as to allow their routine use in clinical trials. Current advances in technology are allowing researchers to closely follow the fate of tumour cells in animal models using novel imaging techniques such as bioluminescence imaging [282], intravital imaging [283-286], quantum dots [287] and activity-based probes [288, 289]. Thus, if these techniques can be scaled up to meet the demands of testing in human subjects, there may yet be hope for the future of Src inhibitors in the therapeutic arsenal against metastatic disease.

Importantly, the present study also reports that the expression of constitutively active Src was sufficient to confer tamoxifen-resistance in ER-positive MCF7 breast cancer cells *in vitro*. Challenge of the MCF7-S cell-line with tamoxifen at increasing concentrations demonstrated that these cells were insensitive to the growth-inhibitory effects of this anti-hormone, and that this insensitivity was negated in the presence of AZM555130. Furthermore, the data show that Tam-R cells were also re-sensitised to tamoxifen following co-treatment with AZM555130; while the most recent studies in our laboratory have revealed that the long-term treatment of MCF7wt cells with tamoxifen and AZD0530 in combination prevented the development of tamoxifen resistance in these cells [Hiscox *et al.* (2007) *Endocrine Related Cancer*, in press]. Together, these data suggest a role for Src in the acquisition and maintenance of the tamoxifen-resistant phenotype displayed by Tam-R cells.

In agreement with the present study, others have also suggested a role for Src in acquired resistance to tamoxifen. Planas-Silva and Hamilton have shown that Src promoted cell survival in MCF7 cells following the inhibition of ER

signalling with tamoxifen; whereas treatment with the AZD0530 Src inhibitor increased their sensitivity to tamoxifen-mediated growth inhibition, resulting in 95% inhibition when both compounds were used [273]. Herynk *et al.* have also demonstrated this synergistic inhibition of cell growth following blockade of both ER and Src activity [274]. Furthermore, inhibition of Src activity using PP2 was seen to restore the sensitivity of Tam-R cells to tamoxifen; although contrary to the observations made in the present study, these cells required prolonged treatment (~8 months) before these effects were seen [41].

Therefore, the data presented in this thesis, in addition to that of others in this field, strongly suggest a role for Src kinase activity in the development and maintenance of tamoxifen-resistance *in vitro*. While the precise mechanisms involved in this are not yet fully understood, Src may exert its effects on tamoxifen-resistant cell growth via interactions with the ER, either through the activation of the AF-1 domain or by the formation of 'signalsomes' following association with ER and other proteins, such as EGFR, to promote non-genomic ER signalling [35, 41]. Indeed, this may explain why Tam-R cells remain susceptible to treatment with fulvestrant, which works by promoting down-regulation of the ER protein to reduce cellular levels [69]. Thus, the use of Src inhibitors may be beneficial in the treatment of tamoxifen-resistant breast cancer in the clinic, while the combined use of Src inhibitors with tamoxifen during the anti-hormone responsive phase of the disease may prevent the development of resistance altogether [Hiscox *et al.* (2007) *Endocrine Related Cancer*, in press].

The therapeutic application of Src inhibitors to other forms of resistance may also be possible. For example, gefitinib (Iressa™; [242]) is a small-molecule tyrosine kinase inhibitor specific for EGFR which can improve the response to anti-hormone therapies *in vitro* [78]. However, as with tamoxifen, acquired resistance to gefitinib can also develop (as modelled in the tamoxifen-gefitinib double resistant cell-line, Tam/TKI-R [81, 290]), thus limiting the therapeutic value of this compound. Src has previously been implicated in the development of gefitinib resistance, with v-Src-expressing human gallbladder adeno-

carcinoma cells demonstrating a 200-fold increase in resistance to gefitinib compared to parental cells; an effect partially reversed following Src inhibition [291]. Furthermore, expression of the constitutively-active Src Y529F mutant in human pancreatic carcinoma cells has been shown to increase IGF-1R expression and accumulation on the plasma-membrane [292]. Interestingly, Jones *et al.* have shown IGF-1R signalling to be central in the gefitinib-resistant growth of Tam/TKI-R cells [81, 290]. Therefore, the role of Src in the development of gefitinib resistance in hormone-insensitive breast cancer should also be examined.

In addition to tamoxifen and gefitinib, Src has also been implicated in the development of resistance to a number of additional therapeutic agents (reviewed in [272]). For instance, Duxbury *et al.* showed that inhibition of Src with PP2 reduced both inherent and acquired resistance to gemcitabine in human pancreatic adenocarcinoma cells, and significantly reduced tumour growth and metastasis *in vivo* when these two compounds were given in combination [293]. Furthermore, expression of constitutively active Src or a dominant-negative Src mutant in these cells increased or decreased their resistance to gemcitabine respectively [293]. These findings have since been further reinforced following the use of siRNA to knockdown Src expression and activity in these cells [294]. Phase I/II clinical trials are currently under-way to assess co-treatment of gemcitabine with AZD0530 in patients with unresectable or metastatic pancreatic cancer [295]. Furthermore, the inhibition of Src has also been shown to not only increase the sensitivity of ovarian cancer cells to the cytotoxic effects of paclitaxel, but to re-sensitise paclitaxel-resistant ovarian cancer cells to this chemotherapeutic agent [296].

The role of additional Src-family-members in disease progression and drug resistance is also being investigated. Ongoing studies in our laboratory have highlighted a potential role for Lyn kinase in tamoxifen-resistant breast cancer, with both the expression and activity of this protein increased in our Tam-R cell model (R. Hendley and K.M. Taylor, personal communication). This is particularly interesting as the expression of Lyn was previously

thought to be restricted to haematopoietic cells [95]. In addition, the expression and activation of Hck and Lyn Src-family kinases is increased in Bcr/Abl-mediated chronic myelogenous leukaemia (CML) patients in blast-crisis, and correlates with disease progression and the development of imatinib resistance both *in vitro* and *in vivo* [297]. Therefore, dual-targeted Src-Bcr/Abl therapeutic agents such as AZD0530 and dasatinib may prove vital in combating imatinib-resistant CML in the clinic.

One concern that exists with the use of Src inhibitors is that the broad expression of Src and its role in the regulation of many critical cellular processes, even in normal tissues, may result in severe toxicity to the patient, and this line of thinking is most likely responsible for the delay in the development of Src inhibitors for use in the clinic. However, to date the only reported side-effect of Src inhibition in a mouse model is osteopetrosis – a bone disorder that results in the excessive accumulation of bone matrix due to impaired osteoclast function [298]. Indeed, this may actually be beneficial in the treatment of breast cancer as the use of anti-hormone therapies, particularly aromatase inhibitors, is often associated with osteoporosis and an increased risk of bone fractures [22]. Therefore, the inhibition of Src may have an additional therapeutic role in the treatment of osteoporosis [299]. Furthermore, phase I clinical trials using Src/Abl inhibitors in chronic myelogenous leukaemia have revealed only limited toxicity with these compounds [280]; while in additional trials, investigators report that these compounds are generally well-tolerated by patients [243, 280]. However, despite this, the effect of Src inhibition on immune cells and immune-system function has been closely monitored in phase I trials with AZD0530 due to the prevalence of Src and Src family members in haematopoietic cells [236].

In conclusion, the data presented in this thesis suggest that elevated Src kinase activity plays a key role in the acquisition and maintenance of the aggressive, tamoxifen-resistant phenotype exhibited by Tam-R cells *in vitro*. As such, the use of pharmacological Src inhibitors may be of therapeutic importance in the treatment of advanced tamoxifen-resistant breast cancer in the clinic,

particularly when given in combination with an anti-proliferative agent to specifically target tumour progression and metastasis, and increase patient survival. Furthermore, Src inhibitors may also have the potential to prevent the development of tamoxifen-resistance *in vivo*, in addition to the development of resistance to a number of additional chemotherapeutic agents, such as gefitinib. Thus, with a number of Src inhibitors now entering phase II clinical trials, a future where the clinical management of cancer is no longer complicated by metastatic progression or the development of drug resistance draws ever closer.

7 References

1. Parkin, D.M. and Fernandez, L.M. (2006). Use of statistics to assess the global burden of breast cancer. *Breast J* 12 Suppl 1, pp. S70-80.

2. Veronesi, U., Boyle, P., Goldhirsch, A., Orecchia, R. and Viale, G. (2005). Breast cancer. *Lancet* 365(9472), pp. 1727-1741.

3. Jemal, A., Siegel, R., Ward, E., Murray, T., Xu, J. and Thun, M.J. (2007). Cancer statistics, 2007. *CA Cancer J Clin* 57(1), pp. 43-66.

4. Quinn, M., Babb, P., Brock, A., Kirby, L. and Jones, J. (2001). In: *Cancer trends in England and Wales 1950–1999 (Studies on Medical and Population Subjects No. 66).* London: The Stationary Office, pp. 40-45.

5. Breast Cancer Care. (2007). *Breast Cancer Facts and Statistics.* [WWW]. Available at: <URL: http://www.breastcancercare.org.uk/content.php?page_id=1730> [Accessed: 14/07/07].

6. Cancer Research UK News and Resources web site. (2007). *CancerStats.* [WWW]. Available at: <URL: http://info.cancerresearchuk.org/cancerstats> [Accessed: 14/07/07].

7. Office for National Statistics. (2005). *Breast Cancer: Incidence rises while deaths continue to fall.* [WWW]. Available at: <URL: http://www.statistics.gov.uk/cci/nugget.asp?id=575> [Accessed: 14/07/07].

8. Office for National Statistics. (2007). *Cancer Survival: Rates improved during 1998-2001.* [WWW]. Available at: <URL: http://www.statistics.gov.uk/CCI/nugget.asp?ID=861&Pos=6&ColRank=2&Rank=448> [Accessed: 14/07/07].

9. McPherson, K., Steel, C.M. and Dixon, J.M. (2000). ABC of breast diseases. Breast cancer-epidemiology, risk factors, and genetics. *Bmj* 321(7261), pp. 624-628.

10. Beral, V. (2003). Breast cancer and hormone-replacement therapy in the Million Women Study. *Lancet* 362(9382), pp. 419-427.

11. Evans, D.G., Fentiman, I.S., McPherson, K., Asbury, D., Ponder, B.A. and Howell, A. (1994). Familial breast cancer. *Bmj* 308(6922), pp. 183-187.

12. Chang, J. and Elledge, R.M. (2001). Clinical management of women with genomic BRCA1 and BRCA2 mutations. *Breast Cancer Res Treat* 69(2), pp. 101-113.

13. Morton, M.S., Arisaka, O., Miyake, N., Morgan, L.D. and Evans, B.A.J. (2002). Phytoestrogen Concentrations in Serum from Japanese Men and Women over Forty Years of Age. *J. Nutr.* 132(10), pp. 3168-3171.

14. Quinn, M. and Allen, E. (1995). Changes in incidence of and mortality from breast cancer in England and Wales since introduction of screening. United Kingdom Association of Cancer Registries. *Bmj* 311(7017), pp. 1391-1395.

15. Blanks, R.G., Moss, S.M., McGahan, C.E., Quinn, M.J. and Babb, P.J. (2000). Effect of NHS breast screening programme on mortality from breast cancer in England and Wales, 1990-8: comparison of observed with predicted mortality. *Bmj* 321(7262), pp. 665-669.

16. Blanks, R.G., Moss, S.M. and Patnick, J. (2000). Results from the UK NHS breast screening programme 1994-1999. *J Med Screen* 7(4), pp. 195-198.

17. NHS Direct On-line. (2007). *NHS Direct Online Health Encyclopaedia: Cancer of the breast, female.* [WWW]. Available at: <URL: http://www.nhsdirect.nhs.uk/articles/article.aspx?articleId=76&sectionId=5&PrintPage=1> [Accessed: 14/07/07].

18. Breast Cancer Care. (2005). *Information Support: Treating Breast Cancer.* [WWW]. Available at: <URL: http://www.breastcancercare.org.uk/Publications/Booklets/8035/bcc_treating06_0.pdf> [Accessed: 17/07/07].

19. Bundred, N.J. (2001). Prognostic and predictive factors in breast cancer. *Cancer Treat Rev* 27(3), pp. 137-142.

20. Mansel, R.E., Fallowfield, L., Kissin, M., Goyal, A., Newcombe, R.G., Dixon, J.M., *et al.* (2006). Randomized Multicentre Trial of Sentinel Node Biopsy Versus Standard Axillary Treatment in Operable Breast Cancer: The ALMANAC Trial. *J Natl Cancer Inst* 98(9), pp. 599-609.

21. Breast Cancer Care. (2003). *Hormone Therapy.* [WWW]. Available at: <URL: http://www.breastcancercare.org.uk/Publications/Factsheets/3247/35-hormone%20therapies.pdf> [Accessed: 03/03/04].

22. Howell, A., Cuzick, J., Baum, M., Buzdar, A., Dowsett, M., Forbes, J.F., *et al.* (2005). Results of the ATAC (Arimidex, Tamoxifen, Alone or in Combination) trial after completion of 5 years' adjuvant treatment for breast cancer. *Lancet* 365(9453), pp. 60-62.

23. Nicholson, R.I., McClelland, R.A., Finlay, P., Eaton, C.L., Gullick, W.J., Dixon, A.R., *et al.* (1993). Relationship between EGF-R, c-erbB-2 protein expression and Ki67 immunostaining in breast cancer and hormone sensitivity. *Eur J Cancer* 29A(7), pp. 1018-1023.

24. Fisher, B., Costantino, J.P., Wickerham, D.L., Redmond, C.K., Kavanah, M., Cronin, W.M., *et al.* (1998). Tamoxifen for prevention of breast cancer: report of the National Surgical Adjuvant Breast and Bowel Project P-1 Study. *J Natl Cancer Inst* 90(18), pp. 1371-1388.

25. Hayes, D.F. and Robertson, J.F.R. (2002). Overview and concepts of endocrine therapy. In: *Endocrine Therapy of Breast Cancer.* (Robertson, J.F.R., Nicholson, R.I.and Hayes, D.F. eds). 1st ed. London: Martin Dunitz Ltd, pp. 127-153.

26. Jones, K.L. and Buzdar, A.U. (2004). A review of adjuvant hormonal therapy in breast cancer. *Endocr Relat Cancer* 11(3), pp. 391-406.

27. MacGregor, J.I. and Jordan, V.C. (1998). Basic guide to the mechanisms of antiestrogen action. *Pharmacol Rev* 50(2), pp. 151-196.

28. Kuiper, G.G., Enmark, E., Pelto-Huikko, M., Nilsson, S. and Gustafsson, J.A. (1996). Cloning of a novel receptor expressed in rat prostate and ovary. *Proc Natl Acad Sci U S A* 93(12), pp. 5925-5930.

29. Osborne, C.K. and Schiff, R. (2005). Estrogen-receptor biology: continuing progress and therapeutic implications. *J Clin Oncol* 23(8), pp. 1616-1622.

Chapter Seven

References

"Yet had Fleming not possessed immense knowledge and an unremitting gift of observation he might not have observed the effect of the hyssop mould. 'Fortune', remarked Pasteur, 'favours the prepared mind'."

André Maurois (Emile Herzog; 1885-1967). French Writer.
Life of Alexander Fleming.

30. Howell, A. (2006). Pure oestrogen antagonists for the treatment of advanced breast cancer. *Endocr Relat Cancer* 13(3), pp. 689-706.

31. Nicholson, R.I., Madden, T., Bryant, S. and Gee, J.M.W. (2002). Cellular and Molecular Actions of Estrogens and Antiestrogens in Breast Cancer. In: *Endocrine Therapy of Breast Cancer.* (Robertson, J.F.R., Nicholson, R.I.and Hayes, D.F. eds). 1st ed. London: Martin Dunitz Ltd, pp. 127-153.

32. Kato, S., Endoh, H., Masuhiro, Y., Kitamoto, T., Uchiyama, S., Sasaki, H., *et al.* (1995). Activation of the estrogen receptor through phosphorylation by mitogen-activated protein kinase. *Science* 270(5241), pp. 1491-1494.

33. Campbell, R.A., Bhat-Nakshatri, P., Patel, N.M., Constantinidou, D., Ali, S. and Nakshatri, H. (2001). Phosphatidylinositol 3-Kinase/AKT-Mediated Activation of Estrogen Receptor alpha. *J Biol Chem* 276(13), pp. 9817-9824.

34. Arnold, S.F., Vorojeikina, D.P. and Notides, A.C. (1995). Phosphorylation of tyrosine 537 on the human estrogen receptor is required for binding to an estrogen response element. *J Biol Chem* 270(50), pp. 30205-30212.

35. Song, R.X., Zhang, Z. and Santen, R.J. (2005). Estrogen rapid action via protein complex formation involving ERalpha and Src. *Trends Endocrinol Metab* 16(8), pp. 347-353.

36. Osborne, C.K., Zhao, H. and Fuqua, S.A. (2000). Selective estrogen receptor modulators: structure, function, and clinical use. *J Clin Oncol* 18(17), pp. 3172-3186.

37. Schiff, R., Massarweh, S., Shou, J. and Osborne, C.K. (2003). Breast cancer endocrine resistance: how growth factor signaling and estrogen receptor coregulators modulate response. *Clin Cancer Res* 9(1 Pt 2), pp. 447S-454S.

38. Osborne, C.K. (1999). Aromatase inhibitors in relation to other forms of endocrine therapy for breast cancer. *Endocr Relat Cancer* 6(2), pp. 271-276.

39. Massarweh, S. and Schiff, R. (2007). Unraveling the mechanisms of endocrine resistance in breast cancer: new therapeutic opportunities. *Clin Cancer Res* 13(7), pp. 1950-1954.

40. Shupnik, M.A. (2004). Crosstalk between steroid receptors and the c-Src-receptor tyrosine kinase pathways: implications for cell proliferation. *Oncogene* 23(48), pp. 7979-7989.

41. Fan, P., Wang, J., Santen, R.J. and Yue, W. (2007). Long-term Treatment with Tamoxifen Facilitates Translocation of Estrogen Receptor {alpha} out of the Nucleus and Enhances its Interaction with EGFR in MCF-7 Breast Cancer Cells 10.1158/0008-5472.CAN-06-1020. *Cancer Res* 67(3), pp. 1352-1360.

42. Yue, W., Fan, P., Wang, J., Li, Y. and Santen, R.J. (2007). Mechanisms of acquired resistance to endocrine therapy in hormone-dependent breast cancer cells. *J Steroid Biochem Mol Biol.*

43. Barletta, F., Wong, C.W., McNally, C., Komm, B.S., Katzenellenbogen, B. and Cheskis, B.J. (2004). Characterization of the interactions of estrogen receptor and MNAR in the activation of cSrc. *Mol Endocrinol* 18(5), pp. 1096-1108.

44. Green, S. and Furr, B. (1999). Prospects for the treatment of endocrine-responsive tumours. *Endocr Relat Cancer* 6(3), pp. 349-371.

45. Beatson, G.T. (1896). On the treatement of inoperable cases of carcinoma of the mamma: suggestions for a new method of treatment with illustrative cases. *Lancet* 2, pp. 105-107.

46. Jordan, V.C. (2006). Tamoxifen (ICI46,474) as a targeted therapy to treat and prevent breast cancer. *Br J Pharmacol* 147 Suppl 1, pp. S269-276.

47. Jordan, V.C. (2003). Tamoxifen: a most unlikely pioneering medicine. *Nat Rev Drug Discov* 2(3), pp. 205-213.

48. Jordan, V.C. (2003). Targeting antihormone resistance in breast cancer: a simple solution. *Ann Oncol* 14(7), pp. 969-970.

49. Lewis, J.S. and Jordan, V.C. (2005). Selective estrogen receptor modulators (SERMs): mechanisms of anticarcinogenesis and drug resistance. *Mutat Res* 591(1-2), pp. 247-263.

50. Osborne, C.K., Wakeling, A. and Nicholson, R.I. (2004). Fulvestrant: an oestrogen receptor antagonist with a novel mechanism of action. *Br J Cancer* 90 Suppl 1, pp. S2-6.

51. Ring, A. and Dowsett, M. (2004). Mechanisms of tamoxifen resistance. *Endocr Relat Cancer* 11(4), pp. 643-658.

52. Shah, Y.M. and Rowan, B.G. (2005). The Src kinase pathway promotes tamoxifen agonist action in Ishikawa endometrial cells through phosphorylation-dependent stabilization of estrogen receptor (alpha) promoter interaction and elevated steroid receptor coactivator 1 activity. *Mol Endocrinol* 19(3), pp. 732-748.

53. Morris, C. and Wakeling, A. (2002). Fulvestrant ('Faslodex')--a new treatment option for patients progressing on prior endocrine therapy. *Endocr Relat Cancer* 9(4), pp. 267-276.

54. Howell, A., Osborne, C.K., Morris, C. and Wakeling, A.E. (2000). ICI 182,780 (Faslodex): development of a novel, "pure" antiestrogen. *Cancer* 89(4), pp. 817-825.

55. Nicholson, R.I. and Johnston, S.R. (2005). Endocrine therapy--current benefits and limitations. *Breast Cancer Res Treat* 93 Suppl 1, pp. S3-10.

56. McClelland, R.A., Manning, D.L., Gee, J.M., Anderson, E., Clarke, R., Howell, A., *et al.* (1996). Effects of short-term antiestrogen treatment of primary breast cancer on estrogen receptor mRNA and protein expression and on estrogen-regulated genes. *Breast Cancer Res Treat* 41(1), pp. 31-41.

57. Gradishar, W.J. and Morrow, M. (2002). Advances in endocrine therapy of metastatic breast cancer. *Br J Surg* 89(12), pp. 1489-1492.

58. Gradishar, W.J. (2004). Tamoxifen--what next? *Oncologist* 9(4), pp. 378-384.

59. Baum, M. (1999). Use of aromatase inhibitors in the adjuvant treatment of breast cancer. *Endocr Relat Cancer* 6(2), pp. 231-234.

60. Osborne, C.K. and Schiff, R. (2005). Aromatase inhibitors: future directions. *J Steroid Biochem Mol Biol* 95(1-5), pp. 183-187.

61. Staka, C.M., Nicholson, R.I. and Gee, J.M. (2005). Acquired resistance to oestrogen deprivation: role for growth factor signalling kinases/oestrogen receptor cross-talk revealed in new MCF-7X model. *Endocr Relat Cancer* 12 Suppl 1, pp. S85-97.

62. Clarke, R., Liu, M.C., Bouker, K.B., Gu, Z., Lee, R.Y., Zhu, Y., *et al.* (2003). Antiestrogen resistance in breast cancer and the role of estrogen receptor signaling. *Oncogene* 22, pp. 7316-7339.

63. Early Breast Cancer Trialists' Collaborative Group (EBCTCG) (2005). Effects of chemotherapy and hormonal therapy for early breast cancer on recurrence and 15-year survival: an overview of the randomised trials. *Lancet* 365(9472), pp. 1687-1717.

64. Gee, J.M., Robertson, J.F., Gutteridge, E., Ellis, I.O., Pinder, S.E., Rubini, M., *et al.* (2005). Epidermal growth factor receptor/HER2/insulin-like growth factor receptor signalling and oestrogen receptor activity in clinical breast cancer. *Endocr Relat Cancer* 12 Suppl 1, pp. S99-S111.

65. Shou, J., Massarweh, S., Osborne, C.K., Wakeling, A.E., Ali, S., Weiss, H., *et al.* (2004). Mechanisms of tamoxifen resistance: increased estrogen receptor-HER2/neu cross-talk in ER/HER2-positive breast cancer. *J Natl Cancer Inst* 96(12), pp. 926-935.

66. Nicholson, R.I., Gee, J.M., Knowlden, J., McClelland, R., Madden, T.A., Barrow, D., *et al.* (2003). The biology of antihormone failure in breast cancer. *Breast Cancer Res Treat* 80 Suppl 1, pp. S29-34; discussion S35.

67. Gee, J.M.W., Giles, M. and Nicholson, R.I. (2004). Extreme growth factor signalling can promote oestrogen receptor-alpha loss: therapeutic implications in breast cancer. *Breast Cancer Res* 6(4), pp. 162-163.

68. Cheung, K.L., Willsher, P.C., Pinder, S.E., Ellis, I.O., Elston, C.W., Nicholson, R.I., *et al.* (1997). Predictors of response to second-line endocrine therapy for breast cancer. *Breast Cancer Res Treat* 45(3), pp. 219-224.

69. Hutcheson, I.R., Knowlden, J.M., Madden, T.A., Barrow, D., Gee, J.M., Wakeling, A.E., *et al.* (2003). Oestrogen receptor-mediated modulation of the EGFR/MAPK pathway in tamoxifen-resistant MCF-7 cells. *Breast Cancer Res Treat* 81(1), pp. 81-93.

70. Knowlden, J.M., Hutcheson, I.R., Jones, H.E., Madden, T., Gee, J.M., Harper, M.E., *et al.* (2003). Elevated levels of epidermal growth factor receptor/c-erbB2 heterodimers mediate an autocrine growth regulatory pathway in tamoxifen-resistant MCF-7 cells. *Endocrinology* 144(3), pp. 1032-1044.

71. Gee, J.M., Robertson, J.F., Ellis, I.O. and Nicholson, R.I. (2001). Phosphorylation of ERK1/2 mitogen-activated protein kinase is associated with poor response to anti-hormonal therapy and decreased patient survival in clinical breast cancer. *Int J Cancer* 95(4), pp. 247-254.

72. Nicholson, R.I., McClelland, R., Gee, J.M.W., Manning, D.L., Cannon, P., Robertson, J.F., *et al.* (1994). Transforming Growth Factor-alpha and Endocrine Sensitivity in Breast Cancer. *Cancer Res* 54, pp. 1684-1689.

73. Britton, D.J., Hutcheson, I.R., Knowlden, J.M., Barrow, D., Giles, M., McClelland, R.A., *et al.* (2006). Bidirectional cross talk between ERalpha and EGFR signalling pathways regulates tamoxifen-resistant growth. *Breast Cancer Res Treat* 96(2), pp. 131-146.

74. Nicholson, R.I., McClelland, R.A., Robertson, J.F. and Gee, J.M. (1999). Involvement of steroid hormone and growth factor cross-talk in endocrine response in breast cancer. *Endocr Relat Cancer* 6(3), pp. 373-387.

75. Nicholson, R.I., Hutcheson, I.R., Knowlden, J.M., Jones, H.E., Harper, M.E., Jordan, N., *et al.* (2004). Nonendocrine pathways and endocrine resistance: observations with antiestrogens and signal transduction inhibitors in combination. *Clin Cancer Res* 10(1 Pt 2), pp. 346S-354S.

76. Jordan, N.J., Gee, J.M., Barrow, D., Wakeling, A.E. and Nicholson, R.I. (2004). Increased constitutive activity of PKB/Akt in tamoxifen resistant breast cancer MCF-7 cells. *Breast Cancer Res Treat* 87(2), pp. 167-180.

77. Razandi, M., Pedram, A., Park, S.T. and Levin, E.R. (2003). Proximal events in signaling by plasma membrane estrogen receptors. *J Biol Chem* 278(4), pp. 2701-2712.

78. Gee, J.M., Harper, M.E., Hutcheson, I.R., Madden, T.A., Barrow, D., Knowlden, J.M., *et al.* (2003). The antiepidermal growth factor receptor agent gefitinib (ZD1839/Iressa) improves antihormone response and prevents development of resistance in breast cancer in vitro. *Endocrinology* 144(11), pp. 5105-5117.

79. Nicholson, R.I., Hutcheson, I.R., Hiscox, S.E., Knowlden, J.M., Giles, M., Barrow, D., *et al.* (2005). Growth factor signalling and resistance to selective oestrogen receptor modulators and pure anti-oestrogens: the use of anti-growth factor therapies to treat or delay endocrine resistance in breast cancer. *Endocr Relat Cancer* 12 Suppl 1, pp. S29-36.

80. Come, S.E., Buzdar, A.U., Ingle, J.N., Arteaga, C.L., Brodie, A.M., Colditz, G.A., *et al.* (2005). Proceedings of the Fourth International Conference on Recent Advances and Future Directions in Endocrine Manipulation of Breast Cancer: conference summary statement. *Clin Cancer Res* 11(2 Pt 2), pp. 861s-864s.

81. Jones, H.E., Gee, J.M., Taylor, K.M., Barrow, D., Williams, H.D., Rubini, M., *et al.* (2005). Development of strategies for the use of anti-growth factor treatments. *Endocr Relat Cancer* 12 Suppl 1, pp. S173-182.

82. Agrawal, A., Gutteridge, E., Gee, J.M., Nicholson, R.I. and Robertson, J.F. (2005). Overview of tyrosine kinase inhibitors in clinical breast cancer. *Endocr Relat Cancer* 12 Suppl 1, pp. S135-144.

83. Martin, G.S. (2004). The road to Src. *Oncogene* 23(48), pp. 7910-7917.

84. Brugge, J.S. and Erikson, R.L. (1977). Identification of a transformation-specific antigen induced by an avian sarcoma virus. *Nature* 269(5626), pp. 346-348.

85. Purchio, A.F., Erikson, E. and Erikson, R.L. (1977). Translation of 35S and of subgenomic regions of avian sarcoma virus RNA. *Proc Natl Acad Sci U S A* 74(10), pp. 4661-4665.

86. Purchio, A.F., Erikson, E., Brugge, J.S. and Erikson, R.L. (1978). Identification of a polypeptide encoded by the avian sarcoma virus src gene. *Proc Natl Acad Sci U S A* 75(3), pp. 1567-1571.

87. Collett, M.S., Brugge, J.S. and Erikson, R.L. (1978). Characterization of a normal avian cell protein related to the avian sarcoma virus transforming gene product. *Cell* 15(4), pp. 1363-1369.

88. Collett, M.S., Erikson, E., Purchio, A.F., Brugge, J.S. and Erikson, R.L. (1979). A normal cell protein similar in structure and function to the avian sarcoma virus transforming gene product. *Proc Natl Acad Sci U S A* 76(7), pp. 3159-3163.

89. Oppermann, H., Levinson, A.D., Varmus, H.E., Levintow, L. and Bishop, J.M. (1979). Uninfected vertebrate cells contain a protein that is closely related to the product of the avian sarcoma virus transforming gene (src). *Proc Natl Acad Sci U S A* 76(4), pp. 1804-1808.

90. Collett, M.S. and Erikson, R.L. (1978). Protein kinase activity associated with the avian sarcoma virus src gene product. *Proc Natl Acad Sci U S A* 75(4), pp. 2021-2024.

91. Erikson, R.L., Collett, M.S., Erikson, E. and Purchio, A.F. (1979). Evidence that the avian sarcoma virus transforming gene product is a cyclic AMP-independent protein kinase. *Proc Natl Acad Sci U S A* 76(12), pp. 6260-6264.

92. Hunter, T. and Sefton, B.M. (1980). Transforming gene product of Rous sarcoma virus phosphorylates tyrosine. *Proc Natl Acad Sci U S A* 77(3), pp. 1311-1315.

93. Collett, M.S., Purchio, A.F. and Erikson, R.L. (1980). Avian sarcoma virus-transforming protein, pp60src shows protein kinase activity specific for tyrosine. *Nature* 285(5761), pp. 167-169.

94. Levinson, A.D., Oppermann, H., Varmus, H.E. and Bishop, J.M. (1980). The purified product of the transforming gene of avian sarcoma virus phosphorylates tyrosine. *J Biol Chem* 255(24), pp. 11973-11980.

95. Thomas*, S.M. and Brugge**, J.S. (1997). Cellular functions regulated by Src family Kinases. *Annu. Rev. Cell Dev. Biol* 13, pp. 513-609.

96. Brown, M.T. and Cooper, J.A. (1996). Regulation, substrates and functions of src. *Biochimica et Biophysica Acta (BBA) - Reviews on Cancer* 1287(2-3 SU), pp. 121-149.

97. Yeatman, T.J. (2004). A Renaissance for Src. *Nature Reviews* 4, pp. 470-480.

98. Schwartzberg, P.L. (1998). The many faces of Src: multiple functions of a prototypical tyrosine kinase. *Oncogene* 17(11 Reviews), pp. 1463-1468.

99. Frame, M.C. (2004). Newest findings on the oldest oncogene; how activated src does it. *J Cell Sci* 117(7), pp. 989-998.

100. Bjorge, J.D., Jakymiw, A. and Fujita, D.J. (2000). Selected glimpses into the activation and function of Src kinase. *Oncogene* 19(49), pp. 5620-5635.

101. Irby, R.B. and Yeatman, T.J. (2000). Role of Src expression and activation in human cancer. *Oncogene* 19(49), pp. 5636-5642.

102. Rosen, N., Bolen, J.B., Schwartz, A.M., Cohen, P., DeSeau, V. and Israel, M.A. (1986). Analysis of pp60c-src protein kinase activity in human tumor cell lines and tissues. *J Biol Chem* 261(29), pp. 13754-13759.

103. Summy, J.M. and Gallick, G.E. (2003). Src family kinases in tumor progression and metastasis. *Cancer Metastasis Rev* 22(4), pp. 337-358.

104. Buhrow, S.A., Cohen, S. and Staros, J.V. (1982). Affinity labeling of the protein kinase associated with the epidermal growth factor receptor in membrane vesicles from A431 cells. *J Biol Chem* 257(8), pp. 4019-4022.

105. Verbeek, B.S., Vroom, T.M., Adriaansen-Slot, S.S., Ottenhoff-Kalff, A.E., Geertzema, J.G., Hennipman, A., *et al.* (1996). c-Src protein expression is increased in human breast cancer. An immunohistochemical and biochemical analysis. *J Pathol* 180(4), pp. 383-388.

106. Aligayer, H., Boyd, D.D., Heiss, M.M., Abdalla, E.K., Curley, S.A. and Gallick, G.E. (2002). Activation of Src kinase in primary colorectal carcinoma: an indicator of poor clinical prognosis. *Cancer* 94(2), pp. 344-351.

107. Lutz, M.P., Esser, I.B., Flossmann-Kast, B.B., Vogelmann, R., Luhrs, H., Friess, H., *et al.* (1998). Overexpression and activation of the tyrosine kinase Src in human pancreatic carcinoma. *Biochem Biophys Res Commun* 243(2), pp. 503-508.

108. Wiener, J.R., Windham, T.C., Estrella, V.C., Parikh, N.U., Thall, P.F., Deavers, M.T., *et al.* (2003). Activated SRC protein tyrosine kinase is overexpressed in late-stage human ovarian cancers. *Gynecol Oncol* 88(1), pp. 73-79.

109. Wilson, G.R., Cramer, A., Welman, A., Knox, F., Swindell, R., Kawakatsu, H., *et al.* (2006). Activated c-SRC in ductal carcinoma in situ correlates with high tumour grade, high proliferation and HER2 positivity. *Br J Cancer* 95(10), pp. 1410-1414.

110. Resh, M.D. (1994). Myristylation and palmitylation of Src family members: the fats of the matter. *Cell* 76(3), pp. 411-413.

111. Ducker, C.E., Upson, J.J., French, K.J. and Smith, C.D. (2005). Two N-myristoyltransferase isozymes play unique roles in protein myristoylation, proliferation, and apoptosis. *Mol Cancer Res* 3(8), pp. 463-476.

112. Roskoski, R., Jr. (2004). Src protein-tyrosine kinase structure and regulation. *Biochem Biophys Res Commun* 324(4), pp. 1155-1164.

113. Sandilands, E., Brunton, V.G. and Frame, M.C. (2007). The membrane targeting and spatial activation of Src, Yes and Fyn is influenced by palmitoylation and distinct RhoB/RhoD endosome requirements. *J Cell Sci.*

114. Boggon, T.J. and Eck, M.J. (2004). Structure and regulation of Src family kinases. *Oncogene* 23(48), pp. 7918-7927.

115. Yeo, M.G., Partridge, M.A., Ezratty, E.J., Shen, Q., Gundersen, G.G. and Marcantonio, E.E. (2006). Src SH2 arginine 175 is required for cell motility: specific focal adhesion kinase targeting and focal adhesion assembly function. *Mol Cell Biol* 26(12), pp. 4399-4409.

116. Fincham, V.J., Brunton, V.G. and Frame, M.C. (2000). The SH3 domain directs acto-myosin-dependent targeting of v-Src to focal adhesions via phosphatidylinositol 3-kinase. *Mol Cell Biol* 20(17), pp. 6518-6536.

117. Fincham, V.J. and Frame, M.C. (1998). The catalytic activity of Src is dispensable for translocation to focal adhesions but controls the turnover of these structures during cell motility. *Embo J* 17(1), pp. 81-92.

118. Fincham, V.J., Unlu, M., Brunton, V.G., Pitts, J.D., Wyke, J.A. and Frame, M.C. (1996). Translocation of Src kinase to the cell periphery is mediated by the actin cytoskeleton under the control of the Rho family of small G proteins. *J Cell Biol* 135(6 Pt 1), pp. 1551-1564.

119. Songyang, Z., Shoelson, S.E., Chaudhuri, M., Gish, G., Pawson, T., Haser, W.G., *et al.* (1993). SH2 domains recognize specific phosphopeptide sequences. *Cell* 72(5), pp. 767-778.

120. Stover, D.R., Furet, P. and Lydon, N.B. (1996). Modulation of the SH2 binding specificity and kinase activity of Src by tyrosine phosphorylation within its SH2 domain. *J Biol Chem* 271(21), pp. 12481-12487.

121. Pawson, T. and Gish, G.D. (1992). SH2 and SH3 domains: from structure to function. *Cell* 71(3), pp. 359-362.

122. Smart, J.E., Oppermann, H., Czernilofsky, A.P., Purchio, A.F., Erikson, R.L. and Bishop, J.M. (1981). Characterization of sites for tyrosine phosphorylation in the transforming protein of Rous sarcoma virus (pp60v-src) and its normal cellular homologue (pp60c-src). *Proc Natl Acad Sci U S A* 78(10), pp. 6013-6017.

123. Kmiecik, T.E. and Shalloway, D. (1987). Activation and suppression of pp60c-src transforming ability by mutation of its primary sites of tyrosine phosphorylation. *Cell* 49(1), pp. 65-73.

124. Roskoski, R., Jr. (2005). Src kinase regulation by phosphorylation and dephosphorylation. *Biochem Biophys Res Commun* 331(1), pp. 1-14.

125. Okada, M. and Nakagawa, H. (1989). A protein tyrosine kinase involved in regulation of pp60c-src function. *J Biol Chem* 264(35), pp. 20886-20893.

126. Bjorge, J.D., Pang, A. and Fujita, D.J. (2000). Identification of Protein-tyrosine Phosphatase 1B as the major tyrosine phosphatase activity capable of dephosphorylating and activating c-Src in several human breast cancer cell lines. *J. Biol. Chem.* 275(52), pp. 41439-41446.

127. Liang, F., Lee, S.Y., Liang, J., Lawrence, D.S. and Zhang, Z.Y. (2005). The role of protein-tyrosine phosphatase 1B in integrin signaling. *J Biol Chem* 280(26), pp. 24857-24863.

128. Sun, G., Sharma, A.K. and Budde, R.J. (1998). Autophosphorylation of Src and Yes blocks their inactivation by Csk phosphorylation. *Oncogene* 17(12), pp. 1587-1595.

129. Stover, D.R., Liebetanz, J. and Lydon, N.B. (1994). Cdc2-mediated modulation of pp60c-src activity. *J Biol Chem* 269(43), pp. 26885-26889.

130. Vadlamudi, R.K., Sahin, A.A., Adam, L., Wang, R.A. and Kumar, R. (2003). Heregulin and HER2 signaling selectively activates c-Src phosphorylation at tyrosine 215. *FEBS Lett* 543(1-3), pp. 76-80.

131. Ishizawar, R. and Parsons, S.J. (2004). c-Src and cooperating partners in human cancer. *Cancer Cell* 6(3), pp. 209-214.

132. Hanahan, D. and Weinberg, R.A. (2000). The hallmarks of cancer. *Cell* 100(1), pp. 57-70.

133. Irby, R.B., Mao, W., Coppola, D., Kang, J., Loubeau, J.M., Trudeau, W., *et al.* (1999). Activating SRC mutation in a subset of advanced human colon cancers. *Nat Genet* 21(2), pp. 187-190.

134. Daigo, Y., Furukawa, Y., Kawasoe, T., Ishiguro, H., Fujita, M., Sugai, S., *et al.* (1999). Absence of genetic alteration at codon 531 of the human c-src gene in 479 advanced colorectal cancers from Japanese and Caucasian patients. *Cancer Res* 59(17), pp. 4222-4224.

135. Wang, N.M., Yeh, K.T., Tsai, C.H., Chen, S.J. and Chang, J.G. (2000). No evidence of correlation between mutation at codon 531 of src and the risk of colon cancer in Chinese. *Cancer Lett* 150(2), pp. 201-204.

136. Nilbert, M. and Fernebro, E. (2000). Lack of activating c-SRC mutations at codon 531 in rectal cancer. *Cancer Genet Cytogenet* 121(1), pp. 94-95.

137. Tan, Y.X., Wang, H.T., Zhang, P., Yan, Z.H., Dai, G.L., Wu, M.C., *et al.* (2005). c-src activating mutation analysis in Chinese patients with colorectal cancer. *World J Gastroenterol* 11(15), pp. 2351-2353.

138. Taylor, K.M., Morgan, H.E., Smart, K., Zahari, N.M., Pumford, S., Ellis, I.O., *et al.* (2007). The emerging role of the LIV-1 subfamily of zinc transporters in breast cancer. *Mol Med.* 13(7-8), pp. 396-406.

139. Samet, J.M., Silbajoris, R., Wu, W. and Graves, L.M. (1999). Tyrosine Phosphatases as Targets in Metal-Induced Signaling in Human Airway Epithelial Cells. *Am. J. Respir. Cell Mol. Biol.* 21, pp. 357-364.

140. Wu, W., Graves, L.M., Gill, G.N., Parsons, S.J. and Samet, J.M. (2002). Src-dependent Phosphorylation of the Epidermal Growth Factor Receptor on Tyrosine 845 Is Required for Zinc-induced Ras Activation. *J. Biol. Chem.* 277(27), pp. 24252-24257.

141. Samet, J.M., Dewar, B.J., Wu, W. and Graves, L.M. (2003). Mechanisms of Zn(2+)-induced signal initiation through the epidermal growth factor receptor. *Toxicol Appl Pharmacol* 191(1), pp. 86-93.

142. Harris, K.F., Shoji, I., Cooper, E.M., Kumar, S., Oda, H. and Howley, P.M. (1999). Ubiquitin-mediated degradation of active Src tyrosine kinase. *Proc Natl Acad Sci U S A* 96(24), pp. 13738-13743.

143. Bromann, P.A., Korkaya, H. and Courtneidge, S.A. (2004). The interplay between Src family kinases and receptor tyrosine kinases. *Oncogene* 23(48), pp. 7957-7968.

144. Luttrell, D.K., Lee, A., Lansing, T.J., Crosby, R.M., Jung, K.D., Willard, D., *et al.* (1994). Involvement of pp60c-src with two major signaling pathways in human breast cancer. *Proc Natl Acad Sci U S A* 91(1), pp. 83-87.

145. Biscardi, J.S., Ishizawar, R.C., Silva, C.M., Parsons, S.J., Tice, D.A. and Belsches, A.P. (2000). Tyrosine kinase signalling in breast cancer: Epidermal growth factor receptor and c-Src interactions in breast cancer. *Breast Cancer Res* 2(3), pp. 203-210.

146. Migliaccio, A., Di Domenico, M., Castoria, G., Nanayakkara, M., Lombardi, M., de Falco, A., *et al.* (2005). Steroid receptor regulation of epidermal growth factor signaling through Src in breast and prostate cancer cells: steroid antagonist action. *Cancer Res* 65(22), pp. 10585-10593.

147. Riley, D., Carragher, N.O., Frame, M.C. and Wyke, J.A. (2001). The mechanism of cell cycle regulation by v-Src. *Oncogene* 20(42), pp. 5941-5950.

148. Chu, I., Sun, J., Arnaout, A., Kahn, H., Hanna, W., Narod, S., *et al.* (2007). p27 phosphorylation by Src regulates inhibition of cyclin E-Cdk2. *Cell* 128(2), pp. 281-294.

149. Moasser, M.M., Srethapakdi, M., Sachar, K.S., Kraker, A.J. and Rosen, N. (1999). Inhibition of Src kinases by a selective tyrosine kinase inhibitor causes mitotic arrest. *Cancer Res* 59(24), pp. 6145-6152.

150. Brunton, V.G., Avizienyte, E., Fincham, V.J., Serrels, B., Metcalf, C.A., 3rd, Sawyer, T.K., *et al.* (2005). Identification of Src-specific phosphorylation site on focal adhesion kinase: dissection of the role of Src SH2 and catalytic functions and their consequences for tumor cell behavior. *Cancer Res* 65(4), pp. 1335-1342.

151. Welman, A., Cawthorne, C., Ponce-Perez, L., Barraclough, J., Danson, S., Murray, S., *et al.* (2006). Increases in c-Src expression level and activity do not promote the growth of human colorectal carcinoma cells in vitro and in vivo. *Neoplasia* 8(11), pp. 905-916.

152. Gonzalez, L., Agullo-Ortuno, M.T., Garcia-Martinez, J.M., Calcabrini, A., Gamallo, C., Palacios, J., *et al.* (2006). Role of c-Src in human MCF7 breast cancer cell tumorigenesis. *J Biol Chem* 281(30), pp. 20851-20864.

153. Ishizawar, R.C., Tice, D.A., Karaoli, T. and Parsons, S.J. (2004). The C terminus of c-Src inhibits breast tumor cell growth by a kinase-independent mechanism. *J Biol Chem* 279(22), pp. 23773-23781.

154. Jallal, H., Valentino, M.L., Chen, G., Boschelli, F., Ali, S. and Rabbani, S.A. (2007). A Src/Abl kinase inhibitor, SKI-606, blocks breast cancer invasion, growth, and metastasis in vitro and in vivo. *Cancer Res* 67(4), pp. 1580-1588.

155. Yezhelyev, M.V., Koehl, G., Guba, M., Brabletz, T., Jauch, K.W., Ryan, A., *et al.* (2004). Inhibition of SRC tyrosine kinase as treatment for human pancreatic cancer growing orthotopically in nude mice. *Clin Cancer Res* 10(23), pp. 8028-8036.

156. Ischenko, I., Guba, M., Yezhelyev, M., Papyan, A., Schmid, G., Green, T., *et al.* (2007). Effect of Src kinase inhibition on metastasis and tumor angiogenesis in human pancreatic cancer. *Angiogenesis.*

157. Wiener, J.R., Nakano, K., Kruzelock, R.P., Bucana, C.D., Bast, R.C., Jr. and Gallick, G.E. (1999). Decreased Src tyrosine kinase activity inhibits malignant human ovarian cancer tumor growth in a nude mouse model. *Clin Cancer Res* 5(8), pp. 2164-2170.

158. Song, L., Morris, M., Bagui, T., Lee, F.Y., Jove, R. and Haura, E.B. (2006). Dasatinib (BMS-354825) selectively induces apoptosis in lung cancer cells dependent on epidermal growth factor receptor signaling for survival. *Cancer Res* 66(11), pp. 5542-5548.

159. Liu, Z., Falola, J., Zhu, X., Gu, Y., Kim, L.T., Sarosi, G.A., *et al.* (2004). Antiproliferative effects of Src inhibition on medullary thyroid cancer. *J Clin Endocrinol Metab* 89(7), pp. 3503-3509.

160. Planas-Silva, M.D., Bruggeman, R.D., Grenko, R.T. and Stanley Smith, J. (2006). Role of c-Src and focal adhesion kinase in progression and metastasis of estrogen receptor-positive breast cancer. *Biochem Biophys Res Commun* 341(1), pp. 73-81.

161. Trevino, J.G., Summy, J.M., Lesslie, D.P., Parikh, N.U., Hong, D.S., Lee, F.Y., *et al.* (2006). Inhibition of SRC expression and activity inhibits tumor progression and metastasis of human pancreatic adenocarcinoma cells in an orthotopic nude mouse model. *Am J Pathol* 168(3), pp. 962-972.

162. Rucci, N., Recchia, I., Angelucci, A., Alamanou, M., Del Fattore, A., Fortunati, D., *et al.* (2006). Inhibition of protein kinase c-Src reduces the incidence of breast cancer metastases and increases survival in mice: implications for therapy. *J Pharmacol Exp Ther* 318(1), pp. 161-172.

163. Sporn, M.B. (1996). The war on cancer. *Lancet* 347(9012), pp. 1377-1381.

164. Frixen, U.H., Behrens, J., Sachs, M., Eberle, G., Voss, B., Warda, A., *et al.* (1991). E-cadherin-mediated cell-cell adhesion prevents invasiveness of human carcinoma cells. *J Cell Biol* 113(1), pp. 173-185.

165. Hiscox, S., Jiang, W.G., Obermeier, K., Taylor, K., Morgan, L., Burmi, R., *et al.* (2006). Tamoxifen resistance in MCF7 cells promotes EMT-like behaviour and involves modulation of beta-catenin phosphorylation. *Int J Cancer* 118(2), pp. 290-301.

166. Avizienyte, E. and Frame, M.C. (2005). Src and FAK signalling controls adhesion fate and the epithelial-to-mesenchymal transition. *Curr Opin Cell Biol* 17(5), pp. 542-547.

167. Parsons, J.T., Martin, K.H., Slack, J.K., Taylor, J.M. and Weed, S.A. (2000). Focal Adhesion Kinase: a regulator of focal adhesion dynamics and cell movement. *Oncogene* 19, pp. 5606-5613.

168. McLean, G.W., Carragher, N.O., Avizienyte, E., Evans, J., Brunton, V.G. and Frame, M.C. (2005). The role of focal-adhesion kinase in cancer - a new therapeutic opportunity. *Nat Rev Cancer* 5(7), pp. 505-515.

169. Parsons, J.T. (2003). Focal adhesion kinase: the first ten years. *J Cell Sci* 116(8), pp. 1409-1416.

170. Frame, M.C., Fincham, V.J., Carragher, N.O. and Wyke, A.W. (2002). v-Src's Hold Over Actin and Cell Adhesions. *Nature Reviews* 3, pp. 233-245.

171. Schlaepfer, D.D., Mitra, S.K. and Ilic, D. (2004). Control of motile and invasive cell phenotypes by focal adhesion kinase. *Biochim Biophys Acta* 1692(2-3), pp. 77-102.

172. Wozniak, M.A., Modzelewska, K., Kwong, L. and Keely, P.J. (2004). Focal adhesion regulation of cell behavior. *Biochim Biophys Acta* 1692(2-3), pp. 103-119.

173. Titus, B., Schwartz, M.A. and Theodorescu, D. (2005). Rho proteins in cell migration and metastasis. *Crit Rev Eukaryot Gene Expr* 15(2), pp. 103-114.

174. Burbelo, P., Wellstein, A. and Pestell, R.G. (2004). Altered Rho GTPase signaling pathways in breast cancer cells. *Breast Cancer Res Treat* 84(1), pp. 43-48.

175. Katz, B.Z., Romer, L., Miyamoto, S., Volberg, T., Matsumoto, K., Cukierman, E., *et al.* (2003). Targeting membrane-localized focal adhesion kinase to focal adhesions: roles of tyrosine phosphorylation and SRC family kinases. *J Biol Chem* 278(31), pp. 29115-29120.

176. Schlaepfer, D.D. and Mitra, S.K. (2004). Multiple connections link FAK to cell motility and invasion. *Current Opinion in Genetics & Development* 14, pp. 1-10.

177. Hsia, D.A., Mitra, S.K., Hauck, C.R., Streblow, D.N., Nelson, J.A., Ilic, D., *et al.* (2003). Differential regulation of cell motility and invasion by FAK. *J Cell Biol* 160(5), pp. 753-767.

178. Wells, A., Kassis, J., Solava, J., Turner, T. and Lauffenburger, D.A. (2002). Growth factor-induced cell motility in tumor invasion. *Acta Oncol* 41(2), pp. 124-130.

179. Nicholson, R.I., Gee, J.M. and Harper, M.E. (2001). EGFR and cancer prognosis. *Eur J Cancer* 37 Suppl 4, pp. S9-15.

180. Hiscox, S., Morgan, L., Barrow, D., Dutkowski, C., Wakeling, A. and Nicholson, R. (2004). Tamoxifen resistance in breast cancer cells is accompanied by an enhanced motile and invasive phenotype: Inhibition by gefitinib ('Iressa', ZD1839). *Clinical & Experimental Metastasis* 21, pp. 201-212.

181. Saiki, R.K., Scharf, S., Faloona, F., Mullis, K.B., Horn, G.T., Erlich, H.A., *et al.* (1985). Enzymatic amplification of beta-globin genomic sequences and restriction site analysis for diagnosis of sickle cell anemia. *Science* 230(4732), pp. 1350-1354.

182. Saiki, R.K., Gelfand, D.H., Stoffel, S., Scharf, S.J., Higuchi, R., Horn, G.T., *et al.* (1988). Primer-directed enzymatic amplification of DNA with a thermostable DNA polymerase. *Science* 239(4839), pp. 487-491.

183. Giulietti, A., Overbergh, L., Valckx, D., Decallonne, B., Bouillon, R. and Mathieu, C. (2001). An overview of real-time quantitative PCR: applications to quantify cytokine gene expression. *Methods* 25(4), pp. 386-401.

184. Hiscox, S., Morgan, L., Green, T.P., Barrow, D., Gee, J. and Nicholson, R.I. (2005). Elevated Src activity promotes cellular invasion and motility in tamoxifen resistant breast cancer cells. *Breast Cancer Res Treat* 97(3), pp. 263-274.

185. Laemmli, U.K. (1970). Cleavage of structural proteins during the assembly of the head of bacteriophage T4. *Nature* 227(5259), pp. 680-685.

186. Towbin, H., Staehelin, T. and Gordon, J. (1979). Electrophoretic transfer of proteins from polyacrylamide gels to nitrocellulose sheets: procedure and some applications. *Proc Natl Acad Sci U S A* 76(9), pp. 4350-4354.

187. Kurien, B.T. and Scofield, R.H. (2003). Protein blotting: a review. *J Immunol Methods* 274(1-2), pp. 1-15.

188. Lowry, O.H., Rosebrough, N.J., Farr, A.L. and Randall, R.J. (1951). Protein Measurement with the Folin Phenol Reagent. *J. Biol. Chem.* 193(1), pp. 265-275.

189. Kricka, L.J. (1991). Chemiluminescent and bioluminescent techniques. *Clin Chem* 37(9), pp. 1472-1481.

190. Mattson, D.L. and Bellehumeur, T.G. (1996). Comparison of three chemiluminescent horseradish peroxidase substrates for immunoblotting. *Anal Biochem* 240(2), pp. 306-308.

191. Mosmann, T. (1983). Rapid colorimetric assay for cellular growth and survival: application to proliferation and cytotoxicity assays. *J Immunol Methods* 65(1-2), pp. 55-63.

192. Denizot, F. and Lang, R. (1986). Rapid colorimetric assay for cell growth and survival. Modifications to the tetrazolium dye procedure giving improved sensitivity and reliability. *J Immunol Methods* 89(2), pp. 271-277.

193. Hashemi, M., Ghavami, S., Eshraghi, M., Booy, E.P. and Los, M. (2007). Cytotoxic effects of intra and extracellular zinc chelation on human breast cancer cells. *European Journal of Pharmacology* 557(1), pp. 9-19.

194. ATCC-LGC. (2006). *LGC Promochem: Cell Biology Collection - ATCC® Number HTB-22™.* [WWW]. Available at: <URL: http://www.lgcpromochem-atcc.com/common/catalog/numSearch/numResults.cfm?collection=ce&atccNum=HTB-22> [Accessed: 20/02/07].

195. HyperCLDB. (2001). *MCF7 (human, Caucasian, breast, adenocarcinoma).* [WWW]. Available at: <URL: http://www.biotech.ist.unige.it/cldb/cl3371.html> [Accessed: 21/02/07].

196. Knowlden, J.M., Hutcheson, I.R., Barrow, D., Gee, J.M. and Nicholson, R.I. (2005). Insulin-like growth factor-I receptor signaling in tamoxifen-resistant breast cancer: a

supporting role to the epidermal growth factor receptor. *Endocrinology* 146(11), pp. 4609-4618.

197. Gee, J.M., Howell, A., Gullick, W.J., Benz, C.C., Sutherland, R.L., Santen, R.J., *et al.* (2005). Consensus statement. Workshop on therapeutic resistance in breast cancer: impact of growth factor signalling pathways and implications for future treatment. *Endocr Relat Cancer* 12 Suppl 1, pp. S1-7.

198. Osherov, N. and Levitzki, A. (1994). Epidermal-growth-factor-dependent activation of the src-family kinases. *Eur J Biochem* 225(3), pp. 1047-1053.

199. Mao, W., Irby, R., Coppola, D., Fu, L., Wloch, M., Turner, J., *et al.* (1997). Activation of c-Src by receptor tyrosine kinases in human colon cancer cells with high metastatic potential. *Oncogene* 15(25), pp. 3083-3090.

200. Maa, M., Leu, T., McCarley, D., Schatzman, R. and Parsons, S. (1995). Potentiation of Epidermal Growth Factor Receptor-Mediated Oncogenesis by c-Src: Implications for the Etiology of Multiple Human Cancers. *PNAS* 92(15), pp. 6981-6985.

201. Tice, D.A., Biscardi, J.S., Nickles, A.L. and Parsons, S.J. (1999). Mechanism of biological synergy between cellular Src and epidermal growth factor receptor. *PNAS* 96(4), pp. 1415-1420.

202. Wells, A., Gupta, K., Chang, P., Swindle, S., Glading, A. and Shiraha, H. (1998). Epidermal growth factor receptor-mediated motility in fibroblasts. *Microsc Res Tech* 43(5), pp. 395-411.

203. Huang, C., Jacobson, K. and Schaller, M.D. (2004). MAP Kinases and Cell Migration. *Journal of Cell Science* 117, pp. 4619-4628.

204. Reddy, K.B., Nabha, S.M. and Atanaskova, N. (2003). Role of MAP kinase in tumor progression and invasion. *Cancer Metastasis Rev* 22(4), pp. 395-403.

205. Sieg, D.J., Hauck, C.R., Ilic, D., Klingbeil, C.K., Schaefer, E., Damsky, C.H., *et al.* (2000). FAK integrates growth-factor and integrin signals to promote cell migration. *Nat Cell Biol* 2(5), pp. 249-256.

206. McClelland, R.A., Barrow, D., Madden, T.A., Dutkowski, C.M., Pamment, J., Knowlden, J.M., *et al.* (2001). Enhanced epidermal growth factor receptor signaling in MCF7 breast cancer cells after long-term culture in the presence of the pure antiestrogen ICI 182,780 (Faslodex). *Endocrinology* 142(7), pp. 2776-2788.

207. Nicholson, R.I., Hutcheson, I.R., Harper, M.E., Knowlden, J.M., Barrow, D., McClelland, R.A., *et al.* (2001). Modulation of epidermal growth factor receptor in endocrine-resistant, oestrogen receptor-positive breast cancer. *Endocr Relat Cancer* 8(3), pp. 175-182.

208. Rogers, S.J., Harrington, K.J., Rhys-Evans, P., P, O.C. and Eccles, S.A. (2005). Biological significance of c-erbB family oncogenes in head and neck cancer. *Cancer Metastasis Rev* 24(1), pp. 47-69.

209. Price, J.T., Wilson, H.M. and Haites, N.E. (1996). Epidermal growth factor (EGF) increases the in vitro invasion, motility and adhesion interactions of the primary renal carcinoma cell line, A704. *Eur J Cancer* 32A(11), pp. 1977-1982.

210. Price, D.J., Avraham, S., Feuerstein, J., Fu, Y. and Avraham, H.K. (2002). The invasive phenotype in HMT-3522 cells requires increased EGF receptor signaling through both PI 3-kinase and ERK 1,2 pathways. *Cell Commun Adhes* 9(2), pp. 87-102.

211. Hiscox, S., Jordan, N.J., Morgan, L., Green, T.P. and Nicholson, R.I. (2007). Src kinase promotes adhesion-independent activation of FAK and enhances cellular migration in tamoxifen-resistant breast cancer cells. *Clin Exp Metastasis* 24(3), pp. 157-167.

212. Maheshwari, G., Wiley, H.S. and Lauffenburger, D.A. (2001). Autocrine epidermal growth factor signaling stimulates directionally persistent mammary epithelial cell migration. *J Cell Biol* 155(7), pp. 1123-1128.

213. Kim, H. and Muller, W.J. (1999). The role of the epidermal growth factor receptor family in mammary tumorigenesis and metastasis. *Exp Cell Res* 253(1), pp. 78-87.

214. Lu, Z., Jiang, G., Blume-Jensen, P. and Hunter, T. (2001). Epidermal growth factor-induced tumor cell invasion and metastasis initiated by dephosphorylation and downregulation of focal adhesion kinase. *Mol Cell Biol* 21(12), pp. 4016-4031.

215. Frey, M.R., Golovin, A. and Polk, D.B. (2004). Epidermal growth factor-stimulated intestinal epithelial cell migration requires Src family kinase-dependent p38 MAPK signaling. *J Biol Chem* 279(43), pp. 44513-44521.

216. Frey, M.R., Dise, R.S., Edelblum, K.L. and Polk, D.B. (2006). p38 kinase regulates epidermal growth factor receptor downregulation and cellular migration. *Embo J* 25(24), pp. 5683-5692.

217. Hood, J.D. and Cheresh, D.A. (2002). Role of integrins in cell invasion and migration. *Nat Rev Cancer* 2(2), pp. 91-100.

218. Sloan, E.K., Pouliot, N., Stanley, K.L., Chia, J., Moseley, J.M., Hards, D.K., *et al.* (2006). Tumor-specific expression of alphavbeta3 integrin promotes spontaneous metastasis of breast cancer to bone. *Breast Cancer Res* 8(2), p. R20.

219. Masaki, T., Okada, M., Tokuda, M., Shiratori, Y., Hatase, O., Shirai, M., *et al.* (1999). Reduced C-terminal Src kinase (Csk) activities in hepatocellular carcinoma. *Hepatology* 29(2), pp. 379-384.

220. Parsons, S.J. and Parsons, J.T. (2004). Src family kinases, key regulators of signal transduction. *Oncogene* 23(48), pp. 7906-7909.

221. Bao, J., Gur, G. and Yarden, Y. (2003). Src promotes destruction of c-Cbl: implications for oncogenic synergy between Src and growth factor receptors. *Proc Natl Acad Sci U S A* 100(5), pp. 2438-2443.

222. Playford, M.P. and Schaller, M.D. (2004). The interplay between Src and integrins in normal and tumor biology. *Oncogene* 23(48), pp. 7928-7946.

223. Crowe, D. and Ohannessian, A. (2004). Recruitment of focal adhesion kinase and paxillin to beta1 integrin promotes cancer cell migration via mitogen activated protein kinase activation. *BMC Cancer* 4(1), p. 18.

224. Petit, V., Boyer, B., Lentz, D., Turner, C.E., Thiery, J.P. and Valles, A.M. (2000). Phosphorylation of tyrosine residues 31 and 118 on paxillin regulates cell migration through an association with CRK in NBT-II cells. *J Cell Biol* 148(5), pp. 957-970.

225. Lim, Y., Han, I., Jeon, J., Park, H., Bahk, Y.Y. and Oh, E.S. (2004). Phosphorylation of focal adhesion kinase at tyrosine 861 is crucial for Ras transformation of fibroblasts. *J Biol Chem* 279(28), pp. 29060-29065.

226. Hakak, Y. and Martin, G.S. (1999). Ubiquitin-dependent degradation of active Src. *Curr Biol* 9(18), pp. 1039-1042.

227. Bazley, L.A. and Gullick, W.J. (2005). The epidermal growth factor receptor family. *Endocr Relat Cancer* 12 Suppl 1, pp. S17-27.

228. Biscardi, J.S., Belsches, A.P. and Parsons, S.J. (1998). Characterization of human epidermal growth factor receptor and c-Src interactions in human breast tumor cells. *Mol Carcinog* 21(4), pp. 261-272.

229. Biscardi, J.S., Maa, M.C., Tice, D.A., Cox, M.E., Leu, T.H. and Parsons, S.J. (1999). c-Src-mediated phosphorylation of the epidermal growth factor receptor on Tyr845 and Tyr1101 is associated with modulation of receptor function. *J Biol Chem* 274(12), pp. 8335-8343.

230. Oude Weernink, P.A., Ottenhoff-Kalff, A.E., Vendrig, M.P., van Beurden, E.A., Staal, G.E. and Rijksen, G. (1994). Functional interaction between the epidermal growth factor receptor and c-Src kinase activity. *FEBS Lett* 352(3), pp. 296-300.

231. Ware, M.F., Tice, D.A., Parsons, S.J. and Lauffenburger, D.A. (1997). Overexpression of Cellular Src in Fibroblasts Enhances Endocytic Internalization of Epidermal Growth Factor Receptor. *J. Biol. Chem.* 272(48), pp. 30185-30190.

232. Wilde, A., Beattie, E.C., Lem, L., Riethof, D.A., Liu, S.-H., Mobley, W.C., *et al.* (1999). EGF Receptor Signaling Stimlates SRC Kinase Phosphorylation of Clathrin, Influencing Clathrin Redistribution and EGF Uptake. *Cell* 96, pp. 677-687.

233. Elvin, P. and Garner, A.P. (2005). Tumour invasion and metastasis: challenges facing drug discovery. *Curr Opin Pharmacol* 5(4), pp. 374-381.

234. Ple, P.A., Green, T.P., Hennequin, L.F., Curwen, J., Fennell, M., Allen, J., *et al.* (2004). Discovery of a new class of anilinoquinazoline inhibitors with high affinity and specificity for the tyrosine kinase domain of c-Src. *J Med Chem* 47(4), pp. 871-887.

235. Barlaam, B., Fennell, M., Germain, H., Green, T., Hennequin, L., Morgentin, R., *et al.* (2005). New heterocyclic analogues of 4-(2-chloro-5-methoxyanilino)quinazolines as potent and selective c-Src kinase inhibitors. *Bioorg Med Chem Lett* 15(24), pp. 5446-5449.

236. Hennequin, L.F., Allen, J., Breed, J., Curwen, J., Fennell, M., Green, T.P., *et al.* (2006). N-(5-chloro-1,3-benzodioxol-4-yl)-7-[2-(4-methylpiperazin-1-yl)ethoxy]-5- (tetrahydro-2H-pyran-4-yloxy)quinazolin-4-amine, a novel, highly selective, orally available, dual-specific c-Src/Abl kinase inhibitor. *J Med Chem* 49(22), pp. 6465-6488.

237. Nam, J.S., Ino, Y., Sakamoto, M. and Hirohashi, S. (2002). Src family kinase inhibitor PP2 restores the E-cadherin/catenin cell adhesion system in human cancer cells and reduces cancer metastasis. *Clin Cancer Res* 8(7), pp. 2430-2436.

238. Warren, S.L., Handel, L.M. and Nelson, W.J. (1988). Elevated expression of pp60c-src alters a selective morphogenetic property of epithelial cells in vitro without a mitogenic effect. *Mol Cell Biol* 8(2), pp. 632-646.

239. Gerdes, J., Lemke, H., Baisch, H., Wacker, H.H., Schwab, U. and Stein, H. (1984). Cell cycle analysis of a cell proliferation-associated human nuclear antigen defined by the monoclonal antibody Ki-67. *J Immunol* 133(4), pp. 1710-1715.

240. Lombardo, C.R., Consler, T.G. and Kassel, D.B. (1995). In vitro phosphorylation of the epidermal growth factor receptor autophosphorylation domain by c-src: identification of phosphorylation sites and c-src SH2 domain binding sites. *Biochemistry* 34(50), pp. 16456-16466.

241. Barker, A.J., Gibson, K.H., Grundy, W., Godfrey, A.A., Barlow, J.J., Healy, M.P., *et al.* (2001). Studies leading to the identification of ZD1839 (IRESSA): an orally active, selective epidermal growth factor receptor tyrosine kinase inhibitor targeted to the treatment of cancer. *Bioorg Med Chem Lett* 11(14), pp. 1911-1914.

242. Wakeling, A.E., Guy, S.P., Woodburn, J.R., Ashton, S.E., Curry, B.J., Barker, A.J., *et al.* (2002). ZD1839 (Iressa): an orally active inhibitor of epidermal growth factor signaling with potential for cancer therapy. *Cancer Res* 62(20), pp. 5749-5754.

243. Chen, T., George, J.A. and Taylor, C.C. (2006). Src tyrosine kinase as a chemotherapeutic target: is there a clinical case? *Anticancer Drugs* 17(2), pp. 123-131.

244. Ardern, H., Sandilands, E., Machesky, L.M., Timpson, P., Frame, M.C. and Brunton, V.G. (2006). Src-dependent phosphorylation of Scar1 promotes its association with the Arp2/3 complex. *Cell Motil Cytoskeleton* 63(1), pp. 6-13.

245. Owens, D.W., McLean, G.W., Wyke, A.W., Paraskeva, C., Parkinson, E.K., Frame, M.C., *et al.* (2000). The catalytic activity of the Src family kinases is required to disrupt cadherin-dependent cell-cell contacts. *Mol Biol Cell* 11(1), pp. 51-64.

246. Felsenfeld, D.P., Schwartzberg, P.L., Venegas, A., Tse, R. and Sheetz, M.P. (1999). Selective regulation of integrin--cytoskeleton interactions by the tyrosine kinase Src. *Nat Cell Biol* 1(4), pp. 200-206.

247. Hiscox, S., Morgan, L., Green, T.P., Barrow, D., Gee, J. and Nicholson, R.I. (2006). Elevated Src activity promotes cellular invasion and motility in tamoxifen resistant breast cancer cells. *Breast Cancer Res Treat* 97(3), pp. 263-274.

248. Ruest, P.J., Roy, S., Shi, E., Mernaugh, R.L. and Hanks, S.K. (2000). Phosphospecific antibodies reveal focal adhesion kinase activation loop phosphorylation in nascent and mature focal adhesions and requirement for the autophosphorylation site. *Cell Growth Differ* 11(1), pp. 41-48.

249. Leu, T.H. and Maa, M.C. (2002). Tyr-863 phosphorylation enhances focal adhesion kinase autophosphorylation at Tyr-397. *Oncogene* 21(46), pp. 6992-7000.

250. Lee, M., Kim, J.Y. and Koh, W.S. (2004). Apoptotic effect of PP2 a Src tyrosine kinase inhibitor, in murine B cell leukemia. *J Cell Biochem* 93(3), pp. 629-638.

251. Castoria, G., Migliaccio, A., Bilancio, A., Di Domenico, M., de Falco, A., Lombardi, M., *et al.* (2001). PI3-kinase in concert with Src promotes the S-phase entry of oestradiol-stimulated MCF-7 cells. *Embo J* 20(21), pp. 6050-6059.

252. Oktay, M., Wary, K.K., Dans, M., Birge, R.B. and Giancotti, F.G. (1999). Integrin-mediated activation of focal adhesion kinase is required for signaling to Jun NH2-terminal kinase and progression through the G1 phase of the cell cycle. *J Cell Biol* 145(7), pp. 1461-1469.

253. Sisci, D., Aquila, S., Middea, E., Gentile, M., Maggiolini, M., Mastroianni, F., *et al.* (2004). Fibronectin and type IV collagen activate ERalpha AF-1 by c-Src pathway: effect on breast cancer cell motility. *Oncogene* 23(55), pp. 8920-8930.

254. Planas-Silva, M.D. and Waltz, P.K. (2006). Estrogen promotes reversible epithelial-to-mesenchymal-like transition and collective motility in MCF-7 breast cancer cells. *The Journal of Steroid Biochemistry and Molecular Biology* In Press, Corrected Proof.

255. Thiery, J.P. (2002). Epithelial-mesenchymal transitions in tumour progression. *Nat Rev Cancer* 2(6), pp. 442-454.

256. Irby, R.B. and Yeatman, T.J. (2002). Increased Src activity disrupts cadherin/catenin-mediated homotypic adhesion in human colon cancer and transformed rodent cells. *Cancer Res* 62(9), pp. 2669-2674.

257. Cox, B.D., Natarajan, M., Stettner, M.R. and Gladson, C.L. (2006). New concepts regarding focal adhesion kinase promotion of cell migration and proliferation. *J Cell Biochem* 99(1), pp. 35-52.

258. Kaplan, K.B., Bibbins, K.B., Swedlow, J.R., Arnaud, M., Morgan, D.O. and Varmus, H.E. (1994). Association of the amino-terminal half of c-Src with focal adhesions alters their properties and is regulated by phosphorylation of tyrosine 527. *Embo J* 13(20), pp. 4745-4756.

259. Kijima, T., Maulik, G., Ma, P.C., Tibaldi, E.V., Turner, R.E., Rollins, B., *et al.* (2002). Regulation of cellular proliferation, cytoskeletal function, and signal transduction through CXCR4 and c-Kit in small cell lung cancer cells. *Cancer Res* 62(21), pp. 6304-6311.

260. Bowden, E.T., Onikoyi, E., Slack, R., Myoui, A., Yoneda, T., Yamada, K.M., *et al.* (2006). Co-localization of cortactin and phosphotyrosine identifies active invadopodia in human breast cancer cells. *Exp Cell Res* 312(8), pp. 1240-1253.

261. Ayala, I., Baldassarre, M., Caldieri, G. and Buccione, R. (2006). Invadopodia: a guided tour. *Eur J Cell Biol* 85(3-4), pp. 159-164.

262. Gabarra-Niecko, V., Schaller, M.D. and Dunty, J.M. (2003). FAK regulates biological processes important for the pathogenesis of cancer. *Cancer Metastasis Rev* 22(4), pp. 359-374.

263. McLean, G.W., Komiyama, N.H., Serrels, B., Asano, H., Reynolds, L., Conti, F., *et al.* (2004). Specific deletion of focal adhesion kinase suppresses tumor formation and blocks malignant progression. *Genes Dev* 18(24), pp. 2998-3003.

264. Hanks, S.K., Ryzhova, L., Shin, N.Y. and Brabek, J. (2003). Focal adhesion kinase signalling activities and their implications in the control of cell survival and motility. *Front Biosci* 8, pp. 982-996.

265. Lietha, D., Cai, X., Ceccarelli, D.F., Li, Y., Schaller, M.D. and Eck, M.J. (2007). Structural basis for the autoinhibition of focal adhesion kinase. *Cell* 129(6), pp. 1177-1187.

266. Slack, J.K., Adams, R.B., Rovin, J.D., Bissonette, E.A., Stoker, C.E. and Parsons, J.T. (2001). Alterations in the focal adhesion kinase/Src signal transduction pathway correlate with increased migratory capacity of prostate carcinoma cells. *Oncogene* 20(10), pp. 1152-1163.

267. Belsches, A.P., Haskell, M.D. and Parsons, S.J. (1997). Role of c-Src tyrosine kinase in EGF-induced mitogenesis. *Front Biosci* 2, pp. d501-518.

268. Belsches-Jablonski, A.P., Biscardi, J.S., Peavy, D.R., Tice, D.A., Romney, D.A. and Parsons, S.J. (2001). Src family kinases and HER2 interactions in human breast cancer cell growth and survival. *Oncogene* 20(12), pp. 1465-1475.

269. Stover, D.R., Becker, M., Liebetanz, J. and Lydon, N.B. (1995). Src phosphorylation of the epidermal growth factor receptor at novel sites mediates receptor interaction with Src and P85 alpha. *J Biol Chem* 270(26), pp. 15591-15597.

270. Alwan, H.A.J., van Zoelen, E.J.J. and van Leeuwen, J.E.M. (2003). Ligand-induced Lysosomal Epidermal Growth Factor Receptor (EGFR) Degradation is Preceeded by Proteasome-dependent EGFR De-ubiquitination. *J Biol Chem* 278(37), pp. 35781-35790.

271. Moro, L., Dolce, L., Cabodi, S., Bergatto, E., Erba, E.B., Smeriglio, M., *et al.* (2002). Integrin-induced epidermal growth factor (EGF) receptor activation requires c-Src and p130Cas and leads to phosphorylation of specific EGF receptor tyrosines. *J Biol Chem* 277(11), pp. 9405-9414.

272. Shah, A.N. and Gallick, G.E. (2007). Src, chemoresistance and epithelial to mesenchymal transition: are they related? *Anticancer Drugs* 18(4), pp. 371-375.

273. Planas-Silva, M.D. and Hamilton, K.N. (2006). Targeting c-Src kinase enhances tamoxifen's inhibitory effect on cell growth by modulating expression of cell cycle and survival proteins. *Cancer Chemother Pharmacol.*

274. Herynk, M.H., Beyer, A.R., Cui, Y., Weiss, H., Anderson, E., Green, T.P., *et al.* (2006). Cooperative action of tamoxifen and c-Src inhibition in preventing the growth of estrogen receptor-positive human breast cancer cells. *Mol Cancer Ther* 5(12), pp. 3023-3031.

275. Feng, W., Webb, P., Nguyen, P., Liu, X., Li, J., Karin, M., *et al.* (2001). Potentiation of estrogen receptor activation function 1 (AF-1) by Src/JNK through a serine 118-independent pathway. *Mol Endocrinol* 15(1), pp. 32-45.

276. Arnold, S.F., Obourn, J.D., Jaffe, H. and Notides, A.C. (1995). Phosphorylation of the human estrogen receptor on tyrosine 537 in vivo and by src family tyrosine kinases in vitro. *Mol Endocrinol* 9(1), pp. 24-33.

277. Hiscox, S., Morgan, L., Green, T. and Nicholson, R.I. (2006). Src as a therapeutic target in anti-hormone/anti-growth factor-resistant breast cancer. *Endocr Relat Cancer* 13(Supplement_1), pp. S53-59.

278. DiFlorio, A., Capurso, G., Milione, M., Panzuto, F., Geremia, R., Fave, G.D., *et al.* (2007). Src Family Kinase Activity Regulates Adhesion, Spreading and Migration of Pancreatic Endocrine Tumour Cells. *Endocr Relat Cancer* 14, pp. 111-124.

279. Recchia, I., Rucci, N., Festuccia, C., Bologna, M., MacKay, A.R., Migliaccio, S., *et al.* (2003). Pyrrolopyrimidine c-Src inhibitors reduce growth, adhesion, motility and invasion of prostate cancer cells in vitro. *Eur J Cancer* 39(13), pp. 1927-1935.

280. Summy, J.M. and Gallick, G.E. (2006). Treatment for advanced tumors: SRC reclaims center stage. *Clin Cancer Res* 12(5), pp. 1398-1401.

281. Nam, S., Kim, D., Cheng, J.Q., Zhang, S., Lee, J.H., Buettner, R., *et al.* (2005). Action of the Src family kinase inhibitor, dasatinib (BMS-354825), on human prostate cancer cells. *Cancer Res* 65(20), pp. 9185-9189.

282. Jenkins, D.E., Oei, Y., Hornig, Y.S., Yu, S.F., Dusich, J., Purchio, T., *et al.* (2003). Bioluminescent imaging (BLI) to improve and refine traditional murine models of tumor growth and metastasis. *Clin Exp Metastasis* 20(8), pp. 733-744.

283. Condeelis, J. and Segall, J.E. (2003). Intravital imaging of cell movement in tumours. *Nat Rev Cancer* 3(12), pp. 921-930.

284. Wang, W., Goswami, S., Sahai, E., Wyckoff, J.B., Segall, J.E. and Condeelis, J.S. (2005). Tumor cells caught in the act of invading: their strategy for enhanced cell motility. *Trends Cell Biol* 15(3), pp. 138-145.

285. Sidani, M., Wyckoff, J., Xue, C., Segall, J.E. and Condeelis, J. (2006). Probing the microenvironment of mammary tumors using multiphoton microscopy. *J Mammary Gland Biol Neoplasia* 11(2), pp. 151-163.

286. Wyckoff, J.B., Wang, Y., Lin, E.Y., Li, J.F., Goswami, S., Stanley, E.R., *et al.* (2007). Direct visualization of macrophage-assisted tumor cell intravasation in mammary tumors. *Cancer Res* 67(6), pp. 2649-2656.

287. Gao, X., Cui, Y., Levenson, R.M., Chung, L.W. and Nie, S. (2004). In vivo cancer targeting and imaging with semiconductor quantum dots. *Nat Biotechnol* 22(8), pp. 969-976.

288. Saghatelian, A., Jessani, N., Joseph, A., Humphrey, M. and Cravatt, B.F. (2004). Activity-based probes for the proteomic profiling of metalloproteases. *Proc Natl Acad Sci U S A* 101(27), pp. 10000-10005.

289. Jessani, N., Humphrey, M., McDonald, W.H., Niessen, S., Masuda, K., Gangadharan, B., *et al.* (2004). Carcinoma and stromal enzyme activity profiles associated with breast tumor growth in vivo. *Proc Natl Acad Sci U S A* 101(38), pp. 13756-13761.

290. Jones, H.E., Goddard, L., Gee, J.M.W., Hiscox, S., Rubini, M., Barrow, D., *et al.* (2004). Insulin-like growth factor-1 receptor signalling and acquired resistance to gefitinib (ZD1839; Iressa) in human breast and prostate cancer cells. *Endocr Relat Cancer* 11, pp. 1-22.

291. Qin, B., Ariyama, H., Baba, E., Tanaka, R., Kusaba, H., Harada, M., *et al.* (2006). Activated Src and Ras induce gefitinib resistance by activation of signaling pathways downstream of epidermal growth factor receptor in human gallbladder adenocarcinoma cells. *Cancer Chemother Pharmacol* 58(5), pp. 577-584.

292. Flossmann-Kast, B.B., Jehle, P.M., Hoeflich, A., Adler, G. and Lutz, M.P. (1998). Src stimulates insulin-like growth factor I (IGF-I)-dependent cell proliferation by increasing IGF-I receptor number in human pancreatic carcinoma cells. *Cancer Res* 58(16), pp. 3551-3554.

293. Duxbury, M.S., Ito, H., Zinner, M.J., Ashley, S.W. and Whang, E.E. (2004). Inhibition of SRC tyrosine kinase impairs inherent and acquired gemcitabine resistance in human pancreatic adenocarcinoma cells. *Clin Cancer Res* 10(7), pp. 2307-2318.

294. Duxbury, M.S., Ito, H., Zinner, M.J., Ashley, S.W. and Whang, E.E. (2004). siRNA directed against c-Src enhances pancreatic adenocarcinoma cell gemcitabine chemosensitivity. *J Am Coll Surg* 198(6), pp. 953-959.

295. Kleespies, A., Jauch, K.W. and Bruns, C.J. (2006). Tyrosine kinase inhibitors and gemcitabine: new treatment options in pancreatic cancer? *Drug Resist Updat* 9(1-2), pp. 1-18.

296. George, J.A., Chen, T. and Taylor, C.C. (2005). SRC tyrosine kinase and multidrug resistance protein-1 inhibitions act independently but cooperatively to restore paclitaxel sensitivity to paclitaxel-resistant ovarian cancer cells. *Cancer Res* 65(22), pp. 10381-10388.

297. Martinelli, G., Soverini, S., Rosti, G. and Baccarani, M. (2005). Dual tyrosine kinase inhibitors in chronic myeloid leukemia. *Leukemia* 19(11), pp. 1872-1879.

298. Lowe, C., Yoneda, T., Boyce, B.F., Chen, H., Mundy, G.R. and Soriano, P. (1993). Osteopetrosis in Src-deficient mice is due to an autonomous defect of osteoclasts. *Proc Natl Acad Sci U S A* 90(10), pp. 4485-4489.

299. Susa, M., Missbach, M. and Green, J. (2000). Src inhibitors: drugs for the treatment of osteoporosis, cancer or both? *Trends Pharmacol Sci* 21(12), pp. 489-495.

Chapter Eight

Appendices

8 Appendices

8.1 Appendix 1 – Cell Culture

8.1.1 Cell Culture Medium Recipes

rRPMI 1640 + 5% FCS (R+5%)	For 100ml	Final Concentration
RPMI 1640 (containing L-glutamine and phenol-red pH indicator)	93ml	-
FCS	5ml	5% (v/v)
Antibiotics (Penicillin 10,000units/ml; Streptomycin 10,000µg/ml)	1ml	Penicillin: 100 units/ml Streptomycin: 100µg/ml
Amphotericin B (250µg/ml)	1ml	2.5µg/ml

wRPMI 1640 + 5% SFCS (W+5%)	For 100ml	Final Concentration
Phenol-red-free RPMI 1640	91ml	-
SFCS	5ml	5% (v/v)
L-glutamine (10M)	2ml	200mM
Antibiotics (Penicillin 10,000units/ml; Streptomycin 10,000µg/ml)	1ml	Penicillin: 100 units/ml Streptomycin: 100µg/ml
Amphotericin B (250µg/ml)	1ml	2.5µg/ml

wDCCM (serum free)	For 100ml	Final Concentration
Phenol-red-free DCCM	96ml	-
L-glutamine	2ml	200mM
Antibiotics (Penicillin 10,000units/ml; Streptomycin 10,000µg/ml)	1ml	Penicillin: 100 units/ml Streptomycin: 100µg/ml
Amphotericin B (250µg/ml)	1ml	2.5µg/ml

8.1.2 Charcoal Stripping Procedure

Charcoal Solution:

2g Activated Charcoal

0.01g Dextran T70

18ml distilled H_2O

Stir vigorously for at least one hour

To strip 100ml Foetal Calf Serum:

Adjust serum pH to 4.2 using HCl (5M) and allow to equilibrate for 30 minutes at 4°C. Add charcoal solution (5ml) to serum and stir gently for 16 hours at 4°C. Remove charcoal by centrifugation (12,000g, 40 minutes) and coarse filter the supernatant through Whatman filter paper No. 4 (repeat filtration 2-3 times). Adjust serum pH to 7.2 with NaOH (5M) and sterilise serum by passing it through a Nalgene® Supor® Mach V bottle top filter (0.2μm). Stripped serum can then be aliquotted and stored at -20°C.

8.1.3 Trypsin/EDTA

Trypsin/EDTA is purchased from Invitrogen (Paisley, UK) as a 10x concentrated stock solution containing 5g trypsin, 2g EDTA-4NA and 8.5g NaCl per litre. The stock is diluted in PBS (1:10) before use to give a working solution of 0.05% (w/v) trypsin and 0.02% (w/v) EDTA.

8.1.4 Cryo-preservation of Cell-lines

8.1.4.1 Freezing Procedure

Place cells in suspension following trypsin/EDTA disruption of the cell mono-layer. Next, pellet cells by centrifugation (1000rpm, 5 minutes), re-suspend in medium (10ml) and count. Repeat centrifugation and re-suspend cells in medium* containing 7.5% DMSO (v/v) at a density of $1x10^6$ cells/ml. Aliquot cells (1ml) into labelled cryo-vials and place (in a lagged box) at -80°C for at least 24 hours. This is to ensure the freezing down process is gradual and, thus, minimises the risk of damage to the cells. Transfer cells to liquid nitrogen for long-term storage.

**Cell-lines are cryogenically preserved in 'home' medium (i.e. the medium in which they are routinely maintained) supplemented with 10% FCS or SFCS.*

8.1.4.2 Thawing Procedure

Remove cryo-vial from liquid nitrogen and thaw as quickly as possible to limit cell exposure to DMSO. In a sterile laminar-flow safety cabinet, spray vial with 70% EtOH and allow to evaporate completely prior to opening to prevent

microbial contamination. Remove cells to a sterile container, wash with medium (9ml) and pellet by centrifugation (1000rpm, 5 minutes). Aspirate supernatant and re-suspend cells in appropriate medium. Transfer cell suspension into a small flask (e.g. T-12.5) and place in an incubator (37°C, 5% CO_2) overnight. Change medium on the following day and then culture the cells as normal.

8.1.5 Cell Seeding Densities

Vessel	Surface Area	Volume of Medium	**Typical Cell Seeding Density***	Approximate Cell Number at Confluency*
35mm Petri-dish	9.6 cm^2	1.5 ml	**1 x 10^5**	1.2 x 10^6
60mm Petri-dish	28.3 cm^2	3 ml	**5 x 10^5**	3.2 x 10^6
100mm Petri-dish	78.5 cm^2	5 ml	**1 x 10^6**	8.8 x 10^6
T-25 Flask	25.0 cm^2	5 ml	**3 x 10^5**	2.8 x 10^6
T-75 Flask	75.0 cm^2	15 ml	**1 x 10^6**	8.4 x 10^6
24-well Plate	2.0 cm^2/well	1ml/well	**4 x 10^4 cells/well**	2 x 10^5 cells/well
96-well Plate	0.32 cm^2/well	100-150µl/well	**5 x 10^3 cells/well**	4 x 10^4 cells/well
Coverslips	As for 35mm Petri-dishes			

* Based on MCF7wt cells.

8.1.6 Constitution of Isoton® azide-free balanced electrolyte solution for use with Beckman Coulter™ Multisizer II

Component	g/L
NaCl	7.9
Na_2HPO_4	1.9
EDTA	0.4
NaH_2PO_4	0.2
NaF	0.3

8.2 Appendix 2 – Buffers and Solutions

8.2.1 Reverse Transcription and PCR

8.2.1.1 10x PCR Buffer

Component	Stock Concentration	For 20ml:	Final Concentration
Tris-HCl	0.5M (pH 8.3)	4ml	100mM
KCl	1M	10ml	500mM
$MgCl_2$	1M	0.3ml	15mM
Gelatine	2% (w/v)	0.1ml	0.01% (w/v)
Pure H_2O (Sigma)	-	5.6ml	-

- Tris-HCl and KCl solutions are made in-house and sterilised by autoclaving at 119°C.
- 10x PCR buffer is aliquotted and stored at -20°C.

8.2.1.2 Tris-Acetate-EDTA (TAE) Buffer (50x)

Component	For 1L:	Final Concentration
Tris (Base)	242g	2M
Glacial Acetic Acid	57.1ml	1M
EDTA (0.5M; pH 8.0)	100ml	0.05M

- pH to 8.3 and make up to 1L with distilled H_2O.
- Dilute 1:50 with distilled H_2O before use.

8.2.1.3 Sample Loading Buffer for Agarose Gel Electrophoresis

Component	For 10ml:	Final Concentration
Sucrose	6g	60% (w/v)
Bromophenol Blue	0.025g	0.25% (w/v)

- Make up to 10ml with RNase-free H_2O and filter using 0.2µm syringe filter to remove any un-dissolved bromophenol blue.

8.2.2 SDS-PAGE/Western Blotting

8.2.2.1 Cell Lysis Buffer for Total Soluble Protein

Component	For 100ml	Final Concentration
Tris base	0.61g	50mM
EGTA	0.19g	5mM
NaCl	0.87g	150mM
Triton X-100	1ml	1% (v/v)
H_2O	100ml	-

- Adjust pH to 7.5 with HCl (5M).
- Store at 4°C.
- Add phosphatase/protease inhibitors immediately before use.

8.2.2.2 Phosphatase/Protease Inhibitors

Inhibitor	Stock Concentration	Solvent	Volume added to 10ml Lysis Buffer	Final Concentration in Lysis Buffer
Sodium orthovanadate	100mM	H_2O	200µl	2mM
PMSF	100mM	Isopropanol	100µl	1mM
Sodium fluoride	2.5M	H_2O	100µl	25mM
Sodium molybdate	1M	H_2O	100µl	10mM
Phenylarsine	20mM	Chloroform	10µl	20µM
Leupeptin	5mg/ml	H_2O	20µl	10µg/ml
Aprotinin	2mg/ml	H_2O	40µl	8µg/ml

8.2.2.3 BSA Standard Curve for Bio-Rad D_C Protein Assay (50µl)

BSA Concentration (mg/ml)	BSA (µl) (1.45mg/ml stock)	Lysis Buffer (µl)
0.00	0.0	50.0
0.25	8.5	41.5
0.50	17.5	32.5
0.75	26.0	24.0
1.00	34.5	15.5
1.45	50.0	0.0

- BSA stock is 1.45mg/ml in H_2O.

8.2.2.4 SDS-PAGE Running Buffer

Component	For 1L:	Final Concentration
Tris base	3.03g	0.25M
Glycine	14.4g	1.92M
SDS	1g	0.1% (w/v)
H_2O	1L	-

- Adjust pH to 8.3 with HCl (5M).

8.2.2.5 Laemmli Sample Loading Buffer

Component	3x Stock (10ml)	5x Stock (10ml)	Final Concentration (when diluted as appropriate with cell lysate)
SDS	0.6g	1g	2% (w/v)
Glycerol	3ml	5ml	10% (v/v)
Tris base	3.6ml (0.5M stock)	3ml (1M stock)	60mM
H_2O	Make up to 10ml	Make up to 10ml	-
Bromophenol Blue	0.003g	0.005g	0.01% (w/v)

- Add 23.1mg (for 3x) or 38.5mg (for 5x) di-thiothreitol per ml Laemmli sample loading buffer immediately before use.
- Stock solutions of Tris base are pH 6.8.

8.2.2.6 Western Blot Transfer Buffer

Component	For 1L:	Final Concentration
Tris base	3.03g	0.25M
Glycine	14.4g	1.92M
Methanol	200ml	20% (v/v)
H_2O	800ml	-

8.2.2.7 Tris-buffered Saline (TBS)

Component	For 1L:	Final Concentration
Tris base	1.21g	10mM
NaCl	5.8g	100mM
H_2O	1L	-

- Adjust to pH 7.6 with HCl (5M).

8.2.2.8 TBS-Tween (TBS-T)

TBS (see section 8.2.2.7 above) containing 0.05% (v/v) Tween 20.

8.2.3 Immunocytochemistry

8.2.3.1 PBS

Component	For 5L:
NaCl	42.5g
K_2HPO_4	7.15g
KH_2PO_4	1.25g
Distilled H_2O	Make up to 5L

8.2.3.2 Fixatives

3.7% Formaldehyde Solution (used in ER-ICA fix):

- For 250ml, add formaldehyde (37% solution; 25ml) to PBS (225ml).

Formal-saline:

- For 500ml, add NaCl (4.5g) to formaldehyde (37% solution; 50ml) and tap water (450ml) and allow to dissolve.

8.2.3.3 Sucrose Storage Medium (SSM)

Component	For 500ml:
Sucrose	42.8g
$MgCl_2$	0.33g
PBS	250ml
Glycerol	250ml

- SSM is stored at -20°C.

8.3 Appendix 3 – Transfection Work

8.3.1 SOC Medium

SOC medium was purchased, pre-sterilized, from Sigma-Aldrich (Poole, Dorset, UK). The composition of SOC medium was as follows:

Component	Concentration
Tryptone	2% (w/v)
Yeast extract	0.5% (w/v)
NaCl	8.6mM
KCl	2.5mM
$MgSO_4$	20mM
Glucose	20mM

8.3.2 Luria-Bertani (LB) Agar Plates

Preparation of LB-agar plates was carried out under sterile conditions. A sachet of LB Agar EZMix™ powder (containing 5g Tryptone [a pancreatic digest of casein], 2.5g yeast extract, 2.5g NaCl and 7.5g agar) was added to 500ml distilled H_2O and mixed thoroughly. The agar solution was then autoclaved at 121°C and allowed to cool until the bottle could be held comfortably in the hand (~40°C). Ampicillin was added (final concentration of 100μg/ml) and the agar was poured into the required number of Petri-dishes (100mm). Plates were left to set for 1 hour before being wrapped in Saran wrap and stored at 4°C in the dark for up to 1 month.

8.3.3 Luria-Bertani (LB) Broth

LB-Broth was prepared under sterile conditions. A sachet of LB Broth EZMix™ powder (containing 5g Tryptone, 2.5g yeast extract and 2.5g NaCl) was added to 500ml distilled H_2O and mixed thoroughly. The broth was autoclaved at 121°C and stored at room temperature until use. LB-broth was supplemented with ampicillin (final concentration 100μg/ml) immediately before use.

8.3.4 Src Y529F in pUSEamp(-)

8.3.4.1 Nucleotide Sequence of Src Y529F Gene in pUSEamp(-) Vector

Vector/Intron (2348 – 2425) - Black
Mouse Src (948 – 2240) - Blue
Chicken Src (2241 – 2633) - Green
Mutation (TAC → TTC Substitution at 2611) - Red
EcoR1 Recognition Site - Purple

```
GACGGATCGGGAGATCTCCCGATCCCCTATGGTCGACTCTCAGTACAATCTGCTCTGATGCCGCATAGTTAAGCCAGTAT 80
CTGCTCCCTGCTTGTGTGTTGGAGGTCGCTGAGTAGTGCGCGAGCAAAATTTAAGCTACAACAAGGCAAGGCTTGACCGA 160
CAATTGCATGAAGAATCTGCTTAGGGTTAGGCGTTTTGCGCTGCTTCGCGATGTACGGGCCAGATATACGCGTTGACATT 240
GATTATTGACTAGTTATTAATAGTAATCAATTACGGGGTCATTAGTTCATAGCCCATATATGGAGTTCCGCGTTACATAA 320
CTTACGGTAAATGGCCCGCCTGGCTGACCGCCCAACGACCCCCGCCCATTGACGTCAATAATGACGTATGTTCCCATAGT 400
AACGCCAATAGGGACTTTCCATTGACGTCAATGGGTGGACTATTTACGGTAAACTGCCCACTTGGCAGTACATCAAGTGT 480
ATCATATGCCAAGTACGCCCCCTATTGACGTCAATGACGGTAAATGGCCCGCCTGGCATTATGCCCAGTACATGACCTTA 560
TGGGACTTTCCTACTTGGCAGTACATCTACGTATTAGTCATCGCTATTACCATGGTGATGCGGTTTTGGCAGTACATCAA 640
TGGGCGTGGATAGCGGTTTGACTCACGGGGATTTCCAAGTCTCCACCCCATTGACGTCAATGGGAGTTTGTTTTGGCACC 720
AAAATCAACGGGACTTTCCAAAATGTCGTAACAACTCCGCCCCATTGACGCAAATGGGCGGTAGGCGTGTACGGTGGGAG 800
GTCTATATAAGCAGAGCTCTCTGGCTAACTAGAGAACCCACTGCTTACTGGCTTATCGAAATTAATACGACTCACTATAG 880
GGAGACCCAAGCTGGCTAGCGTTTAAACGGGCCCTCTAGACTCGAGCGGCCGCCACTGTGCTGGATcATGGGCAGCAACA 960
AGAGCAAGCCCAAGGACGCCAGCCAGCGGCGCCGCAGCCTGGAGCCCTCGGAAAACGTGCACGGGGCAGGGGGCGCCTTC 1040
CCGGCCTCACAGACACCGAGCAAGCCCGCCTCCGCCGACGGCCACCGCGGGCCCAGCGCCGCCTTCGTGCCGCCCGCGGC 1120
CGAGCCCAAGCTCTTCGGAGGCTTCAACTCCTCGGACACCGTCACCTCCCCGCAGAGGGCGGGCGCTCTGGCAGGTGGGG 1200
TGACCACCTTTGTGGCCCTCTATGACTATGAGTCACGGACAGAGACTGACCTGTCCTTCAAGAAAGGGGAGCGGCTGCAG 1280
ATTGTCAATAACACGGAGGGAGACTGGTGGCTGGCACACTCGCTGAGCACGGGACAGACCGGTTACATCCCCAGCAACTA 1360
TGTGGCGCCCTCCGACTCCATCCAGGCTGAGGAGTGGTACTTTGGCAAGATCACTAGACGGGAATCAGAGCGGCTGCTGC 1440
TCAACGCCGAGAACCCGAGAGGGACCTTCCTCGTGAGGGAGAGTGAGACCACAAAAGGTGCCTACTGCCTCTCTGTATCC 1520
GACTTCGACAATGCCAAGGGCCTAAATGTGAAACACTACAAGATCCGCAAGCTGGACAGCGGCGGTTTCTACATCACCTC 1600
CCGCACCCAGTTCAACAGCCTGCAGCAGCTCGTGGCTTACTACTCCAAACATGCTGATGGCCTGTGTCACCGCCTCACTA 1680
CCGTATGTCCCACATCCAAGCCTCAGACCCAGGGATTGGCCAAGGATGCGTGGGAGATCCCCCGGGAGTCCCTGCGGCTG 1760
GAGGTCAAGCTGGGCCAGGGTTGCTTCGGAGAGGTGTGGATGGGGACCTGGAACGGCACCACGAGGGTTGCCATCAAAAC 1840
TCTGAAGCCAGGCACCATGTCCCCAGAGGCCTTCCTGCAGGAGGCCCAAGTCATGAAGAAACTGAGGCACGAGAAACTGG 1920
TGCAGCTGTATGCTGTGGTGTCGGAAGAACCCATTTACATTGTGACAGAGTACATGAACAAGGGGAGTCTGCTGGACTTT 2000
CTCAAGGGGGAAACGGGCAAATATTTGCGGCTACCCCAGCTGGTGGACATGTCTGCTCAGATCGCTTCAGGCATGGCCTA 2080
TGTGGAGCGGATGAACTATGTGCACCGGGACCTTCGAGCCGCCAATATCCTAGTAGGGGAGAACCTGGTGTGCAAAGTGG 2160
CCGACTTTGGGTTGGCCCGGCTCATAGAAGACAACGAATACACAGCCCGGCAAGGTGCCAAATTCCCCATCAAGTGGACA 2240
GCCCCCGAGGCAGCCCTCTATGGCCGGTTCACCATCAAGTCGGATGTCTGGTCCTTCGGCATCCTGCTGACTGAGCTGAC 2320
CACCAAGGGCCGGGTGCCATACCCAGGTGAGAGTTAGCATCACCCCCACACcCCGTGGGTTGGGCACAGCGTGTGACCCG 2400
GCCCCGCTGCCCTTCTTTCcACAGGGATGGTCAACAGGGAGGTGCTGGACCAGGTGGAGAGGGGCTACCGCATGCCCTGC 2480
CCGCCCGAGTGCCCCGAGTCGCTGCATGACCTCATGTGCCAGTGCTGGCGGAAGGACCCTGAGGAGCGGCCCACTTTTGA 2560
GTACCTGCAGGCCTTCCTGGAGGACTACTTCACCTCGACAGAGCCCCAGTTCCAGCCTGGAGAGAACCTATAGaTCTCTA 2640
GAAGCTTATCGATTAGTCCAATTTGTTAAAGACAGGATATCTGCAGAATTCCACCACACTGGACTAGTGGATCCGAGCTC 2720
GGTACCAAGCTTAAGTTTAAACCGCTGATCAGCCTCGACTGTGCCTTCTAGTTGCCAGCCATCTGTTGTTTGCCCCTCCC 2800
CCGTGCCTTCCTTGACCCTGGAAGGTGCCACTCCCACTGTCCTTTCCTAATAAAATGAGGAAATTGCATCGCATTGTCTG 2880
AGTAGGTGTCATTCTATTCTGGGGGGTGGGGTGGGGCAGGACAGCAAGGGGGAGGATTGGGAAGACAATAGCAGGCATGC 2960
TGGGGATGCGGTGGGCTCTATGGCTTCTGAGGCGGAAAGAACCAGCTGGGGCTCTAGGGGGTATCCCCACGCGCCCTGTA 3040
GCGGCGCATTAAGCGCGGCGGGTGTGGTGGTTACGCGCAGCGTGACCGCTACACTTGCCAGCGCCCTAGCGCCCGCTCCT 3120
TTCGCTTTCTTCCCTTCCTTTCTCGCCACGTTCGCCGGCTTTCCCCGTCAAGCTCTAAATCGGGGCATCCCTTTAGGGTT 3200
CCGATTTAGTGCTTTACGGCACCTCGACCCCAAAAAACTTGATTAGGGTGATGGTTCACGTAGTGGGCCATCGCCCTGAT 3280
AGACGGTTTTTCGCCCTTTGACGTTGGAGTCCACGTTCTTTAATAGTGGACTCTTGTTCCAAACTGGAACAACACTCAAC 3360
CCTATCTCGGTCTATTCTTTTGATTTATAAGGGATTTTGGGGATTTCGGCCTATTGGTTAAAAAATGAGCTGATTTAACA 3440
AAAATTTAACGCGAATTAATTCTGTGGAATGTGTGTCAGTTAGGGTGTGGAAAGTCCCCAGGCTCCCCAGGCAGGCAGAA 3520
GTATGCAAAGCATGCATCTCAATTAGTCAGCAACCAGGTGTGGAAAGTCCCCAGGCTCCCCAGCAGGCAGAAGTATGCAA 3600
AGCATGCATCTCAATTAGTCAGCAACCATAGTCCCGCCCCTAACTCCGCCCATCCCGCCCCTAACTCCGCCCAGTTCCGC 3680
CCATTCTCCGCCCCATGGCTGACTAATTTTTTTTATTTATGCAGAGGCCGAGGCCGCCTCTGCCTCTGAGCTATTCCAGA 3760
AGTAGTGAGGAGGCTTTTTTGGAGGCCTAGGCTTTTGCAAAAAGCTCCCGGGAGCTTGTATATCCATTTTCGGATCTGAT 3840
CAAGAGACAGGATGAGGATCGTTTCGCATGATTGAACAAGATGGATTGCACGCAGGTTCTCCGGCCGCTTGGGTGGAGAG 3920
GCTATTCGGCTATGACTGGGCACAACAGACAATCGGCTGCTCTGATGCCGCCGTGTTCCGGCTGTCAGCGCAGGGGCGCC 4000
CGGTTCTTTTTGTCAAGACCGACCTGTCCGGTGCCCTGAATGAACTGCAGGACGAGGCAGCGCGGCTATCGTGGCTGGCC 4080
ACGACGGGCGTTCCTTGCGCAGCTGTGCTCGACGTTGTCACTGAAGCGGGAAGGGACTGGCTGCTATTGGGCGAAGTGCC 4160
GGGGCAGGATCTCCTGTCATCTCACCTTGCTCCTGCCGAGAAAGTATCCATCATGGCTGATGCAATGCGGCGGCTGCATA 4240
CGCTTGATCCGGCTACCTGCCCATTCGACCACCAAGCGAAACATCGCATCGAGCGAGCACGTACTCGGATGGAAGCCGGT 4320
CTTGTCGATCAGGATGATCTGGACGAAGAGCATCAGGGGCTCGCGCCAGCCGAACTGTTCGCCAGGCTCAAGGCGCGCAT 4400
GCCCGACGGCGAGGATCTCGTCGTGACCCATGGCGATGCCTGCTTGCCGAATATCATGGTGGAAAATGGCCGCTTTTCTG 4480
GATTCATCGACTGTGGCCGGCTGGGTGTGGCGGACCGCTATCAGGACATAGCGTTGGCTACCCGTGATATTGCTGAAGAG 4560
CTTGGCGGCGAATGGGCTGACCGCTTCCTCGTGCTTTACGGTATCGCCGCTCCCGATTCGCAGCGCATCGCCTTCTATCG 4640
CCTTCTTGACGAGTTCTTCTGAGCGGGACTCTGGGGTTCGAAATGACCGACCAAGCGACGCCCAACCTGCCATCACGAGA 4720
TTTCGATTCCACCGCCGCCTTCTATGAAAGGTTGGGCTTCGGAATCGTTTTCCGGGACGCCGGCTGGATGATCCTCCAGC 4800
GCGGGGATCTCATGCTGGAGTTCTTCGCCCACCCCAACTTGTTTATTGCAGCTTATAATGGTTACAAATAAAGCAATAGC 4880
```

```
ATCACAAATTTCACAAATAAAGCATTTTTTTCACTGCATTCTAGTTGTGGTTTGTCCAAACTCATCAATGTATCTTATCA 4960
TGTCTGTATACCGTCGACCTCTAGCTAGAGCTTGGCGTAATCATGGTCATAGCTGTTTCCTGTGTGAAATTGTTATCCGC 5040
TCACAATTCCACACAACATACGAGCCGGAAGCATAAAGTGTAAAGCCTGGGGTGCCTAATGAGTGAGCTAACTCACATTA 5120
ATTGCGTTGCGCTCACTGCCCGCTTTCCAGTCGGGAAACCTGTCGTGCCAGCTGCATTAATGAATCGGCCAACGCGCGGG 5200
GAGAGGCGGTTTGCGTATTGGGCGCTCTTCCGCTTCCTCGCTCACTGACTCGCTGCGCTCGGTCGTTCGGCTGCGGCGAG 5280
CGGTATCAGCTCACTCAAAGGCGGTAATACGGTTATCCACAGAATCAGGGGATAACGCAGGAAAGAACATGTGAGCAAAA 5360
GGCCAGCAAAAGGCCAGGAACCGTAAAAAGGCCGCGTTGCTGGCGTTTTTCCATAGGCTCCGCCCCCCTGACGAGCATCA 5440
CAAAAATCGACGCTCAAGTCAGAGGTGGCGAAACCCGACAGGACTATAAAGATACCAGGCGTTTCCCCCTGGAAGCTCCC 5520
TCGTGCGCTCTCCTGTTCCGACCCTGCCGCTTACCGGATACCTGTCCGCCTTTCTCCCTTCGGGAAGCGTGGCGCTTTCT 5600
CAATGCTCACGCTGTAGGTATCTCAGTTCGGTGTAGGTCGTTCGCTCCAAGCTGGGCTGTGTGCACGAACCCCCCGTTCA 5680
GCCCGACCGCTGCGCCTTATCCGGTAACTATCGTCTTGAGTCCAACCCGGTAAGACACGACTTATCGCCACTGGCAGCAG 5760
CCACTGGTAACAGGATTAGCAGAGCGAGGTATGTAGGCGGTGCTACAGAGTTCTTGAAGTGGTGGCCTAACTACGGCTAC 5840
ACTAGAAGGACAGTATTTGGTATCTGCGCTCTGCTGAAGCCAGTTACCTTCGGAAAAAGAGTTGGTAGCTCTTGATCCGG 5920
CAAACAAACCACCGCTGGTAGCGGTGGTTTTTTTGTTTGCAAGCAGCAGATTACGCGCAGAAAAAAAGGATCTCAAGAAG 6000
ATCCTTTGATCTTTTCTACGGGGTCTGACGCTCAGTGGAACGAAAACTCACGTTAAGGGATTTTGGTCATGAGATTATCA 6080
AAAAGGATCTTCACCTAGATCCTTTTAAATTAAAAATGAAGTTTTAAATCAATCTAAAGTATATATGAGTAAACTTGGTC 6160
TGACAGTTACCAATGCTTAATCAGTGAGGCACCTATCTCAGCGATCTGTCTATTTCGTTCATCCATAGTTGCCTGACTCC 6240
CCGTCGTGTAGATAACTACGATACGGGAGGGCTTACCATCTGGCCCCAGTGCTGCAATGATACCGCGAGACCCACGCTCA 6320
CCGGCTCCAGATTTATCAGCAATAAACCAGCCAGCCGGAAGGGCCGAGCGCAGAAGTGGTCCTGCAACTTTATCCGCCTC 6400
CATCCAGTCTATTAATTGTTGCCGGGAAGCTAGAGTAAGTAGTTCGCCAGTTAATAGTTTGCGCAACGTTGTTGCCATTG 6480
CTACAGGCATCGTGGTGTCACGCTCGTCGTTTGGTATGGCTTCATTCAGCTCCGGTTCCCAACGATCAAGGCGAGTTACA 6560
TGATCCCCCATGTTGTGCAAAAAAGCGGTTAGCTCCTTCGGTCCTCCGATCGTTGTCAGAAGTAAGTTGGCCGCAGTGTT 6640
ATCACTCATGGTTATGGCAGCACTGCATAATTCTCTTACTGTCATGCCATCCGTAAGATGCTTTTCTGTGACTGGTGAGT 6720
ACTCAACCAAGTCATTCTGAGAATAGTGTATGCGGCGACCGAGTTGCTCTTGCCCGGCGTCAATACGGGATAATACCGCG 6800
CCACATAGCAGAACTTTAAAAGTGCTCATCATTGGAAAACGTTCTTCGGGGCGAAAACTCTCAAGGATCTTACCGCTGTT 6880
GAGATCCAGTTCGATGTAACCCACTCGTGCACCCAACTGATCTTCAGCATCTTTTACTTTCACCAGCGTTTCTGGGTGAG 6960
CAAAAACAGGAAGGCAAAATGCCGCAAAAAAGGGAATAAGGGCGACACGGAAATGTTGAATACTCATACTCTTCCTTTTT 7040
CAATATTATTGAAGCATTTATCAGGGTTATTGTCTCATGAGCGGATACATATTTGAATGTATTTAGAAAAATAAACAAAT 7120
AGGGGTTCCGCGCACATTTCCCCGAAAAGTGCCACCTGACGTC                                       7163
```

8.3.4.2 Amino Acid Sequence of Mutated Src Gene

Mutation (Y → F Substitution at 529) - Red

MGSNKSKPKDASQRRRSLEPSENVHGAGGAFPASQ
TPSKPASADGHRGPSAAFVPPAAEPKLFGGFNSSDT
VTSPQRAGALAGGVTTFVALYDYESRTETDLSFKK
GERLQIVNNTEGDWWLAHSLSTGQTGYIPSNYVAP
SDSIQAEEWYFGKITRRESERLLLNAENPRGTFLVR
ESETTKGAYCLSVSDFDNAKGLNVKHYKIRKLDSG
GFYITSRTQFNSLQQLVAYYSKHADGLCHRLTTVCP
TSKPQTQGLAKDAWEIPRESLRLEVKLGQGCFGEV
WMGTWNGTTRVAIKTLKPGTMSPEAFLQEAQVMK
KLRHEKLVQLYAVVSEEPIYIVTEYMNKGSLLDFLK
GETGKYLRLPQLVDMSAQIASGMAYVERMNYVHR
DLRAANILVGENLVCKVADFGLARLIEDNEYTARQ
GAKFPIKWTAPEAALYGRFTIKSDVWSFGILLTELT
TKGRVPYPGMVNREVLDQVERGYRMPCPPECPESL
HDLMCQCWRKDPEERPTFEYLQAFLEDYFTSTEPQ
FQPGENL

8.3.4.3 Restriction Enzyme Recognition Sites for Src Y529F Plasmid

A schematic diagram and a table listing the recognition sites of single-cutting restriction enzymes for the Src Y529F plasmid is shown below. The diagram and table were compiled using the NEBcutter V2.0 tool available on the New England BioLabs Inc. web-site (http://tools.neb.com/NEBcutter2/index.php).

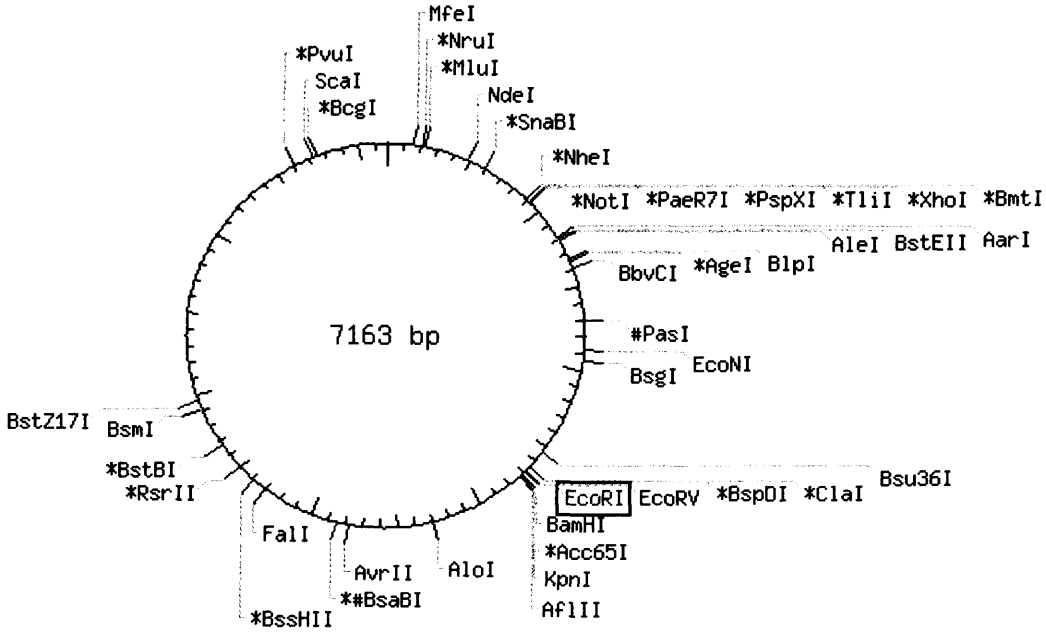

Enzyme	*Specificity*	*Cut positions (blunt - 5' ext. - 3' ext.)*
AarI	CACCTGCNNNN$^{\blacktriangledown}$NNNN$_{\blacktriangle}$	1182/1186
Acc65I	G$^{\blacktriangledown}$GTAC$_{\blacktriangle}$C	2721/2725
AflII	C$^{\blacktriangledown}$TTAA$_{\blacktriangle}$G	2730/2734
AgeI	A$^{\blacktriangledown}$CCGG$_{\blacktriangle}$T	1338/1342
AleI	CACNN$^{\blacktriangledown}$$_{\blacktriangle}$NNGTG	1209
AloI	$_{\blacktriangle}$(N)$_5^{\blacktriangledown}$(N)$_7$GAAC(N)$_6$TCC(N)$_7$$_{\blacktriangle}(N)_5^{\blacktriangledown}$	3298/3293 and 3330/3325
AvrII	C$^{\blacktriangledown}$CTAG$_{\blacktriangle}$G	3786/3790
BamHI	G$^{\blacktriangledown}$GATC$_{\blacktriangle}$C	2709/2713
BbvCI	CC$^{\blacktriangledown}$TCA$_{\blacktriangle}$GC	1387/1390
BcgI	$_{\blacktriangle}$NN$^{\blacktriangledown}$(N)$_{10}$CGA(N)$_6$TGC(N)$_{10}$$_{\blacktriangle}NN^{\blacktriangledown}$	6745/6743 and 6779/6777
BlpI	GC$^{\blacktriangledown}$TNA$_{\blacktriangle}$GC	1323/1326

BmtI	G▴CTAG▾C	899/895
BsaBI	GATNN▾NNATC	3855
BsgI	GTGCAG$(N)_{14}$▴NN▾	1941/1939
BsmI	GAATG▴CN▾	4916/4914
BspDI	AT▾CG▴AT	2649/2651
BssHII	G▾CGCG▴C	4393/4397
BstBI	TT▾CG▴AA	4678/4680
BstEII	G▾GTNAC▴C	1199/1204
BstZ17I	GTA▾TAC	4968
Bsu36I	CC▾TNA▴GG	2539/2542
ClaI	AT▾CG▴AT	2649/2651
EcoNI	CCTNN▾N▴NNAGG	1878/1879
EcoRI	**G▾AATT▴C**	2686/2690
EcoRV	GAT▾ATC	2678
FalI	▴$(N)_5$▾$(N)_8$AAG$(N)_5$CTT$(N)_8$▴$(N)_5$▾	4304/4299 and 4336/4331
KpnI	G▴GTAC▾C	2725/2721
MfeI	C▾AATT▴G	161/165
MluI	A▾CGCG▴T	228/232
NdeI	CA▾TA▴TG	484/486
NheI	G▾CTAG▴C	895/899
NotI	GC▾GGCC▴GC	927/931
NruI	TCG▾CGA	208
PaeR7I	C▾TCGA▴G	921/925
PasI	CC▾CWG▴GG	1709/1712
PspXI	VC▾TCGA▴GB	921/925
PvuI	CG▴AT▾CG	6610/6608
RsrII	CG▾GWC▴CG	4512/4515
ScaI	AGT▾ACT	6720
SnaBI	TAC▾GTA	590
TliI	C▾TCGA▴G	921/925
XhoI	C▾TCGA▴G	921/925

8.3.5 pUSEamp(-) Vector

8.3.5.1 Nucleotide Sequence of pUSEamp(-) Empty Vector

CMV Promoter (209 – 863) - Blue
Multiple Cloning Site (895 – 1010) - Green
Neomycin Resistance Gene (2137 - 2931) - Red
Ampicillin Resistance Gene (4436 – 5297) - Grey
EcoR1 Recognition Site (954) - Purple

```
GACGGATCGGGAGATCTCCCGATCCCCTATGGTCGACTCTCAGTACAATCTGCTCTGATGCCGCATAGTTAAGCCAGTAT 80
CTGCTCCCTGCTTGTGTGTTGGAGGTCGCTGAGTAGTGCGCGAGCAAAATTTAAGCTACAACAAGGCAAGGCTTGACCGA 160
CAATTGCATGAAGAATCTGCTTAGGGTTAGGCGTTTTGCGCTGCTTCGCGATGTACGGGCCAGATATACGCGTTGACATT 240
GATTATTGACTAGTTATTAATAGTAATCAATTACGGGGTCATTAGTTCATAGCCCATATATGGAGTTCCGCGTTACATAA 320
CTTACGGTAAATGGCCCGCCTGGCTGACCGCCCAACGACCCCCGCCCATTGACGTCAATAATGACGTATGTTCCCATAGT 400
AACGCCAATAGGGACTTTCCATTGACGTCAATGGGTGGACTATTTACGGTAAACTGCCCACTTGGCAGTACATCAAGTGT 480
ATCATATGCCAAGTACGCCCCCTATTGACGTCAATGACGGTAAATGGCCCGCCTGGCATTATGCCCAGTACATGACCTTA 560
TGGGACTTTCCTACTTGGCAGTACATCTACGTATTAGTCATCGCTATTACCATGGTGATGCGGTTTTGGCAGTACATCAA 640
TGGGCGTGGATAGCGGTTTGACTCACGGGGATTTCCAAGTCTCCACCCCATTGACGTCAATGGGAGTTTGTTTTGGCACC 720
AAAATCAACGGGACTTTCCAAAATGTCGTAACAACTCCGCCCCATTGACGCAAATGGGCGGTAGGCGTGTACGGTGGGAG 800
GTCTATATAAGCAGAGCTCTCTGGCTAACTAGAGAACCCACTGCTTACTGGCTTATCGAAATTAATACGACTCACTATAG 880
GGAGACCCAAGCTGGCTAGCGTTTAAACGGGCCCTCTAGACTCGAGCGGCCGCCACTGTGCTGGATATCTGCAGAATTCC 960
ACCACACTGGACTAGTGGATCCGAGCTCGGTACCAAGCTTAAGTTTAAACCGCTGATCAGCCTCGACTGTGCCTTCTAGT 1040
TGCCAGCCATCTGTTGTTTGCCCCTCCCCCGTGCCTTCCTTGACCCTGGAAGGTGCCACTCCCACTGTCCTTTCCTAATA 1120
AAATGAGGAAATTGCATCGCATTGTCTGAGTAGGTGTCATTCTATTCTGGGGGGTGGGGTGGGGCAGGACAGCAAGGGGG 1200
AGGATTGGGAAGACAATAGCAGGCATGCTGGGGATGCGGTGGGCTCTATGGCTTCTGAGGCGGAAAGAACCAGCTGGGGC 1280
TCTAGGGGGTATCCCCACGCGCCCTGTAGCGGCGCATTAAGCGCGGCGGGTGTGGTGGTTACGCGCAGCGTGACCGCTAC 1360
ACTTGCCAGCGCCCTAGCGCCCGCTCCTTTCGCTTTCTTCCCTTCCTTTCTCGCCACGTTCGCCGGCTTTCCCCGTCAAG 1440
CTCTAAATCGGGGCATCCCTTTAGGGTTCCGATTTAGTGCTTTACGGCACCTCGACCCCAAAAAACTTGATTAGGGTGAT 1520
GGTTCACGTAGTGGGCCATCGCCCTGATAGACGGTTTTTCGCCCTTTGACGTTGGAGTCCACGTTCTTTAATAGTGGACT 1600
CTTGTTCCAAACTGGAACAACACTCAACCCTATCTCGGTCTATTCTTTTGATTTATAAGGGATTTTGGGGATTTCGGCCT 1680
ATTGGTTAAAAAATGAGCTGATTTAACAAAAATTTAACGCGAATTAATTCTGTGGAATGTGTGTCAGTTAGGGTGTGGAA 1760
AGTCCCCAGGCTCCCCAGGCAGGCAGAAGTATGCAAAGCATGCATCTCAATTAGTCAGCAACCAGGTGTGGAAAGTCCCC 1840
AGGCTCCCCAGCAGGCAGAAGTATGCAAAGCATGCATCTCAATTAGTCAGCAACCATAGTCCCGCCCCTAACTCCGCCCA 1920
TCCCGCCCCTAACTCCGCCCAGTTCCGCCCATTCTCCGCCCCATGGCTGACTAATTTTTTTTATTTATGCAGAGGCCGAG 2000
GCCGCCTCTGCCTCTGAGCTATTCCAGAAGTAGTGAGGAGGCTTTTTTGGAGGCCTAGGCTTTTGCAAAAAGCTCCCGGG 2080
AGCTTGTATATCCATTTTCGGATCTGATCAAGAGACAGGATGAGGATCGTTTCGCATGATTGAACAAGATGGATTGCACG 2160
CAGGTTCTCCGGCCGCTTGGGTGGAGAGGCTATTCGGCTATGACTGGGCACAACAGACAATCGGCTGCTCTGATGCCGCC 2240
GTGTTCCGGCTGTCAGCGCAGGGGCGCCCGGTTCTTTTTGTCAAGACCGACCTGTCCGGTGCCCTGAATGAACTGCAGGA 2320
CGAGGCAGCGCGGCTATCGTGGCTGGCCACGACGGGCGTTCCTTGCGCAGCTGTGCTCGACGTTGTCACTGAAGCGGGAA 2400
GGGACTGGCTGCTATTGGGCGAAGTGCCGGGGCAGGATCTCCTGTCATCTCACCTTGCTCCTGCCGAGAAAGTATCCATC 2480
ATGGCTGATGCAATGCGGCGGCTGCATACGCTTGATCCGGCTACCTGCCCATTCGACCACCAAGCGAAACATCGCATCGA 2560
GCGAGCACGTACTCGGATGGAAGCCGGTCTTGTCGATCAGGATGATCTGGACGAAGAGCATCAGGGGCTCGCGCCAGCCG 2640
AACTGTTCGCCAGGCTCAAGGCGCGCATGCCCGACGGCGAGGATCTCGTCGTGACCCATGGCGATGCCTGCTTGCCGAAT 2720
ATCATGGTGGAAAATGGCCGCTTTTCTGGATTCATCGACTGTGGCCGGCTGGGTGTGGCGGACCGCTATCAGGACATAGC 2800
GTTGGCTACCCGTGATATTGCTGAAGAGCTTGGCGGCGAATGGGCTGACCGCTTCCTCGTGCTTTACGGTATCGCCGCTC 2880
CCGATTCGCAGCGCATCGCCTTCTATCGCCTTCTTGACGAGTTCTTCTGAGCGGGACTCTGGGGTTCGAAATGACCGACC 2960
AAGCGACGCCCAACCTGCCATCACGAGATTTCGATTCCACCGCCGCCTTCTATGAAAGGTTGGGCTTCGGAATCGTTTTC 3040
CGGGACGCCGGCTGGATGATCCTCCAGCGCGGGGATCTCATGCTGGAGTTCTTCGCCCACCCCAACTTGTTTATTGCAGC 3120
TTATAATGGTTACAAATAAAGCAATAGCATCACAAATTTCACAAATAAAGCATTTTTTTCACTGCATTCTAGTTGTGGTT 3200
TGTCCAAACTCATCAATGTATCTTATCATGTCTGTATACCGTCGACCTCTAGCTAGAGCTTGGCGTAATCATGGTCATAG 3280
CTGTTTCCTGTGTGAAATTGTTATCCGCTCACAATTCCACACAACATACGAGCCGGAAGCATAAAGTGTAAAGCCTGGGG 3360
TGCCTAATGAGTGAGCTAACTCACATTAATTGCGTTGCGCTCACTGCCCGCTTTCCAGTCGGGAAACCTGTCGTGCCAGC 3440
TGCATTAATGAATCGGCCAACGCGCGGGGAGAGGCGGTTTGCGTATTGGGCGCTCTTCCGCTTCCTCGCTCACTGACTCG 3520
CTGCGCTCGGTCGTTCGGCTGCGGCGAGCGGTATCAGCTCACTCAAAGGCGGTAATACGGTTATCCACAGAATCAGGGGA 3600
TAACGCAGGAAAGAACATGTGAGCAAAAGGCCAGCAAAAGGCCAGGAACCGTAAAAAGGCCGCGTTGCTGGCGTTTTTCC 3680
ATAGGCTCCGCCCCCCTGACGAGCATCACAAAAATCGACGCTCAAGTCAGAGGTGGCGAAACCCGACAGGACTATAAAGA 3760
TACCAGGCGTTTCCCCCTGGAAGCTCCCTCGTGCGCTCTCCTGTTCCGACCCTGCCGCTTACCGGATACCTGTCCGCCTT 3840
TCTCCCTTCGGGAAGCGTGGCGCTTTCTCAATGCTCACGCTGTAGGTATCTCAGTTCGGTGTAGGTCGTTCGCTCCAAGC 3920
TGGGCTGTGTGCACGAACCCCCCGTTCAGCCCGACCGCTGCGCCTTATCCGGTAACTATCGTCTTGAGTCCAACCCGGTA 4000
AGACACGACTTATCGCCACTGGCAGCAGCCACTGGTAACAGGATTAGCAGAGCGAGGTATGTAGGCGGTGCTACAGAGTT 4080
CTTGAAGTGGTGGCCTAACTACGGCTACACTAGAAGGACAGTATTTGGTATCTGCGCTCTGCTGAAGCCAGTTACCTTCG 4160
GAAAAAGAGTTGGTAGCTCTTGATCCGGCAAACAAACCACCGCTGGTAGCGGTGGTTTTTTTGTTTGCAAGCAGCAGATT 4240
ACGCGCAGAAAAAAAGGATCTCAAGAAGATCCTTTGATCTTTTCTACGGGGTCTGACGCTCAGTGGAACGAAAACTCACG 4320
TTAAGGGATTTTGGTCATGAGATTATCAAAAAGGATCTTCACCTAGATCCTTTTAAATTAAAAATGAAGTTTTAAATCAA 4400
TCTAAAGTATATATGAGTAAACTTGGTCTGACAGTTACCAATGCTTAATCAGTGAGGCACCTATCTCAGCGATCTGTCTA 4480
TTTCGTTCATCCATAGTTGCCTGACTCCCCGTCGTGTAGATAACTACGATACGGGAGGGCTTACCATCTGGCCCCAGTGC 4560
TGCAATGATACCGCGAGACCCACGCTCACCGGCTCCAGATTTATCAGCAATAAACCAGCCAGCCGGAAGGGCCGAGCGCA 4640
GAAGTGGTCCTGCAACTTTATCCGCCTCCATCCAGTCTATTAATTGTTGCCGGGAAGCTAGAGTAAGTAGTTCGCCAGTT 4720
AATAGTTTGCGCAACGTTGTTGCCATTGCTACAGGCATCGTGGTGTCACGCTCGTCGTTTGGTATGGCTTCATTCAGCTC 4800
```

```
CGGTTCCCAACGATCAAGGCGAGTTACATGATCCCCCATGTTGTGCAAAAAAGCGGTTAGCTCCTTCGGTCCTCCGATCG 4880
TTGTCAGAAGTAAGTTGGCCGCAGTGTTATCACTCATGGTTATGGCAGCACTGCATAATTCTCTTACTGTCATGCCATCC 4960
GTAAGATGCTTTTCTGTGACTGGTGAGTACTCAACCAAGTCATTCTGAGAATAGTGTATGCGGCGACCGAGTTGCTCTTG 5040
CCCGGCGTCAATACGGGATAATACCGCGCCACATAGCAGAACTTTAAAAGTGCTCATCATTGGAAAACGTTCTTCGGGGC 5120
GAAAACTCTCAAGGATCTTACCGCTGTTGAGATCCAGTTCGATGTAACCCACTCGTGCACCCAACTGATCTTCAGCATCT 5200
TTTACTTTCACCAGCGTTTCTGGGTGAGCAAAAACAGGAAGGCAAAATGCCGCAAAAAAGGGAATAAGGGCGACACGGAA 5280
ATGTTGAATACTCATACTCTTCCTTTTTCAATATTATTGAAGCATTTATCAGGGTTATTGTCTCATGAGCGGATACATAT 5360
TTGAATGTATTTAGAAAAATAAACAAATAGGGGTTCCGCGCACATTTCCCCGAAAAGTGCCACCTGACGTC          5431
```

8.3.5.2 *Restriction Enzyme Recognition Sites for pUSEamp Empty Vector*

A schematic diagram and a table listing the recognition sites of single-cutting restriction enzyme for the pUSEamp empty vector plasmid is shown below. The diagram and table were compiled using the NEBcutter V2.0 tool available on the New England BioLabs Inc. web-site (http://tools.neb.com/NEBcutter2/index.php).

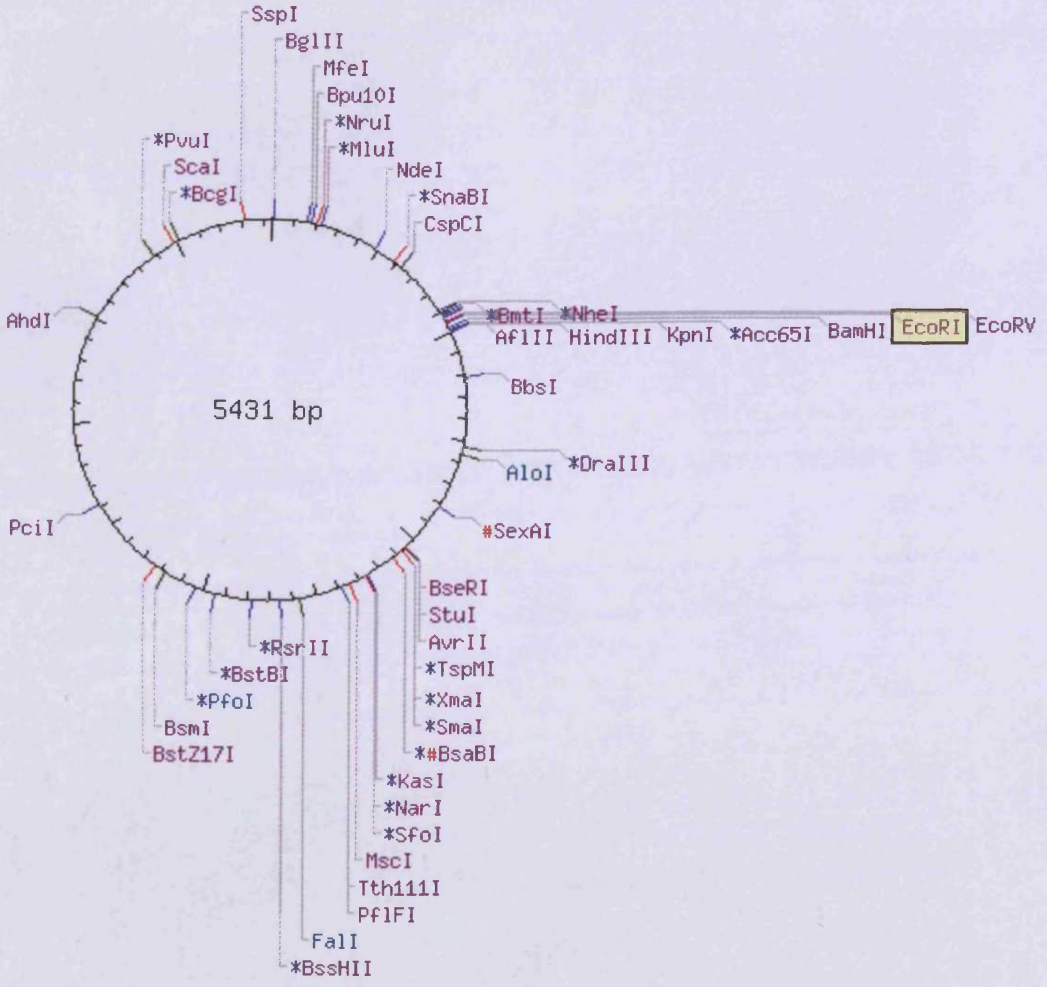

Enzyme	*Specificity*	*Cut positions* (blunt - 5' ext. - 3' ext.)
Acc65I	G▼GTAC▲C	989/993
AflII	C▼TTAA▲G	998/1002
AhdI	GACNN▲N▼NNGTC	4508/4507
AloI	▲(N)5▼(N)7GAAC(N)6TCC(N)7▲(N)5▼	1566/1561 and 1598/1593
ApaI	G▲GGCC▼C	913/909
AvrII	C▼CTAG▲G	2054/2058
BamHI	G▼GATC▲C	977/981
BbsI	GAAGACNN▼NNNN▲	1216/1220
BcgI	▲NN▼(N)10CGA(N)6TGC(N)10▲NN▼	5013/5011 and 5047/5045
BglII	A▼GATC▲T	12/16
BmtI	G▲CTAG▼C	899/895
Bpu10I	CC▼TNA▲GC	180/183
BsaBI	GATNN▲NNATC	2123
BseRI	GAGGAG(N)8▲NN▼	2050/2048
BsmI	GAATG▲CN▼	3184/3182
BssHII	G▼CGCG▲C	2661/2665
BstBI	TT▼CG▲AA	2946/2948
BstZ17I	GTA▼TAC	3236
CspCI	▲NN▼(N)11CAA(N)5GTGG(N)10▲NN▼	626/624 and 661/659
DraIII	CAC▲NNN▼GTG	1530/1527
EcoO109I	RG▼GNC▲CY	910/913
EcoRI	**G▼AATT▲C**	954/958
EcoRV	GAT▼ATC	946
FalI	▲(N)5▼(N)8AAG(N)5CTT(N)8▲(N)5▼	2572/2567 and 2604/2599
HindIII	A▼AGCT▲T	995/999
KasI	G▼GCGC▲C	2263/2267
KpnI	G▲GTAC▼C	993/989
MfeI	C▼AATT▲G	161/165
MluI	A▼CGCG▲T	228/232
MscI	TGG▼CCA	2346

NarI	GG▾CG▴CC	2264/2266
NdeI	CA▾TA▴TG	484/486
NheI	G▾CTAG▴C	895/899
NotI	GC▾GGCC▴GC	927/931
NruI	TCG▾CGA	208
PaeR7I	C▾TCGA▴G	921/925
PciI	A▾CATG▴T	3615/3619
PflFI	GACN▾N▴NGTC	2382/2383
PfoI	T▾CCNGG▴A	3039/3044
PspOMI	G▾GGCC▴C	909/913
PspXI	VC▾TCGA▴GB	921/925
PvuI	CG▴AT▾CG	4878/4876
RsrII	CG▾GWC▴CG	2780/2783
ScaI	AGT▾ACT	4988
SexAI	A▾CCWGG▴T	1821/1826
SfoI	GGC▾GCC	2265
SmaI	CCC▾GGG	2077
SnaBI	TAC▾GTA	590
SspI	AAT▾ATT	5312
StuI	AGG▾CCT	2053
TliI	C▾TCGA▴G	921/925
TspMI	C▾CCGG▴G	2075/2079
Tth111I	GACN▾N▴NGTC	2382/2383
XbaI	T▾CTAG▴A	915/919
XhoI	C▾TCGA▴G	921/925
XmaI	C▾CCGG▴G	2075/2079

8.4 Appendix 4 - Abstracts of Published Journal Articles

Tamoxifen Resistance in Breast Cancer Cells Is Accompanied by an Enhanced Motile and Invasive Phenotype: Inhibition by Gefitinib ('Iressa', ZD1839)

Hiscox, S., Morgan, L., Barrow, D., Dutkowski, C., Wakeling, A. and Nicholson, R.I.

Despite an initial response to anti-hormonal therapies, the development of resistance will occur in a significant number of breast cancer patients. The mechanisms that underlie acquired resistance are not yet clear. Using a previously established *in vitro* cell model of tamoxifen resistance in MCF7 cells, shown to display autocrine epidermal growth factor receptor (EGFR) signalling, we assessed how resistance might modulate their metastatic phenotype *in vitro*, as metastatic disease is the single most important factor affecting the mortality of cancer patients. Furthermore, we investigated the effect of the EGFR tyrosine kinase inhibitor (EGFR-TKI), gefitinib ('Iressa', ZD1839; AstraZeneca), on this behaviour.

The acquisition of tamoxifen resistance in MCF7 cells was accompanied by a dramatic and significant increase in their invasive and motile nature. The affinity of these cells for matrix components was also enhanced. Inhibition of EGFR signalling with gefitinib reduced both basal and TGFα-stimulated invasion and motility and reduced cell-matrix adhesion. In conclusion, we demonstrate here that resistance to tamoxifen in breast cancer cells is accompanied by a significant increase in their basal motile and invasive activity, properties associated with increased metastatic potential. Inhibition of EGFR signalling by gefitinib significantly inhibited cell motility and invasion thus suggesting a role for the EGF receptor in the aggressive phenotype of tamoxifen-resistant breast cancer cells.

2004. *Clin Exp Metastasis* 21(3), pp. 201-212.

Tamoxifen Resistance in MCF7 Cells Promotes EMT-Like Behaviour and Involves Modulation of Beta-Catenin Phosphorylation.

Hiscox, S., Jiang, W.G., Obermeier, K., Taylor, K., Morgan, L., Burmi, R., Barrow, D. and Nicholson, R. I.

We have previously demonstrated that, following acquisition of endocrine resistance, breast cancer cells display an altered growth rate together with increased aggressive behaviour *in vitro*. Since dysfunctional cell-cell adhesive interactions can promote an aggressive phenotype, we investigated the integrity of this protein complex in our breast cancer model of tamoxifen resistance.

In culture, tamoxifen-resistant MCF7 (Tam-R) cells grew as loosely packed colonies with loss of cell-cell junctions and demonstrated altered morphology characteristic of cells undergoing epithelial-to-mesenchymal transition (EMT). Neutralising E-cadherin function promoted the invasion and inhibited the aggregation of endocrine-sensitive MCF7 cells, whilst having little effect on the behaviour of Tam-R cells. Additionally, Tam-R cells had increased levels of tyrosine-phosphorylated beta-catenin, whilst serine/threonine-phosphorylated beta-catenin was decreased. These cells also displayed loss of association between beta-catenin and E-cadherin, increased cytoplasmic and nuclear beta-catenin and elevated transcription of beta-catenin target genes known to be involved in tumour progression and EMT. Inhibition of EGFR kinase activity in Tam-R cells reduced beta-catenin tyrosine phosphorylation, increased beta-catenin-E-cadherin association and promoted cell-cell adhesion. In such treated cells, the association of beta-catenin with Lef-1 and the transcription of c-myc, cyclin-D1, CD44 and COX-2 were also reduced.

These results suggest that homotypic adhesion in tamoxifen-resistant breast cancer cells is dysfunctional due to EGFR-driven modulation of the phosphorylation status of beta-catenin and may contribute to an enhanced aggressive phenotype and transition towards a mesenchymal phenotype *in vitro*.

2006. *Int J Cancer* 118(2), pp. 290-301.

Elevated Src Activity Promotes Cellular Invasion and Motility in Tamoxifen Resistant Breast Cancer Cells.

Hiscox, S., Morgan, L., Green, T.P., Barrow, D., Gee, J. and Nicholson, R.I.

Src kinase plays a central role in growth factor signalling, regulating a diverse array of cellular functions including proliferation, migration and invasion. Recent studies have demonstrated that Src activity is frequently elevated in human tumours and correlates with disease stage. We have previously demonstrated that, upon acquisition of tamoxifen resistance, MCF7 cells display increased epidermal growth factor receptor (EGFR) activation and a more aggressive phenotype *in vitro*. Since tumours exhibiting elevated EGFR signalling may possess elevated levels of Src activity, we wished to investigate the role of Src in our MCF7 model of endocrine resistance.

Src kinase activity was significantly elevated in tamoxifen-resistant (Tam-R) cells in comparison to wild type MCF7 cells. This increase was not due to elevated Src protein or gene expression. Treatment of Tam-R cells with the novel Src inhibitor, AZD0530, significantly reduced the amount of activated Src detectable in both cell types whilst having no effect on total Src levels. AZD0530 significantly suppressed the motile and invasive nature of Tam-R cells *in vitro*, reduced basal levels of activated focal adhesion kinase (FAK) and paxillin and promoted elongation of focal adhesions. Furthermore, the use of this compound in conjunction with the EGFR inhibitor, gefitinib, was markedly additive towards inhibition of Tam-R cell motility and invasion.

These observations suggest that Src plays a pivotal role in mediating the motile and invasive phenotype observed in endocrine-resistant breast cancer cells. The use of Src inhibitors in conjunction with EGFR inhibitors such as gefitinib may provide an effective method with which to prevent cancer progression and metastasis.

2006. *Breast Cancer Res Treat* 97(3), pp. 263-274.

Src as a Therapeutic Target in Anti-Hormone/Anti-Growth-Factor Resistant Breast Cancer.

Hiscox, S., Morgan, L., Green, T. and Nicholson, R.I.

Endocrine therapy is the treatment of choice in hormone receptor-positive breast cancer. However, the effectiveness of anti-hormone drugs, such as tamoxifen, is limited because of the development of resistance, ultimately leading to disease progression and patient mortality. Using *in vitro* cell models of anti-hormone resistance, we have previously demonstrated that altered growth factor signalling contributes to an endocrine insensitive phenotype.

Significantly, our recent studies have revealed that the acquisition of endocrine resistance in breast cancer is accompanied by a greatly enhanced migratory and invasive phenotype. Furthermore, therapeutic intervention using anti-growth factor mono-therapies, despite an initial growth suppressive phase, again results in the development of a resistant state and a further augmentation of their invasive phenotype. Using the dual specific Src/Abl kinase inhibitor, AZD0530, we have highlighted a central role for Src kinase in promoting the invasive phenotype that accompanies both anti-hormone and anti-growth factor resistance. Importantly, the use of Src inhibitors in combination with anti-growth factor therapies appears to be additive, producing a marked inhibitory effect on cell growth, migration and invasion and ultimately prevents the emergence of a resistant phenotype.

These observations suggest that the inhibition of Src activity may present a novel therapeutic intervention strategy, particularly when used as an adjuvant in endocrine-resistant breast disease, with the potential to delay or prevent the acquisition of subsequent resistance to anti-growth factor therapies.

2006. *Endocr Relat Cancer* 13(S1), pp. S53-59.

Src Kinase Promotes Adhesion-Independent Activation of FAK and Enhances Cellular Migration in Tamoxifen-Resistant Breast Cancer Cells.

Hiscox, S., Jordan, N.J., Morgan, L., Green, T.P. and Nicholson, R.I.

Src kinase is intimately involved in the control of matrix adhesion and cell migration through its ability to modulate the activity of focal adhesion kinase (FAK). In light of our previous observations that acquisition of tamoxifen resistance in breast cancer cells is accompanied by elevated Src kinase activity, we wish to investigate whether FAK function is also altered in these cells and if this leads to an enhanced migratory phenotype.

In *in vitro* adhesion assays, tamoxifen-resistant (Tam-R) MCF7 cells had a greater affinity for the matrix proteins fibronectin, laminin, vitronectin and collagen and subsequently demonstrated a much greater migratory capacity across these substrates compared to their weakly-migratory, endocrine-sensitive counterparts. Additionally, elevated levels of activated Src in Tam-R cells promoted an increase in FAK phosphorylation at Y861 and Y925 and uncoupled FAK activation from an adhesion-dependent process. Inhibition of Src activity using the Src/Abl inhibitor AZD0530 reduced FAK activity, suppressed cell spreading on matrix-coated surfaces and significantly inhibited cell migration.

Our data thus suggest that Src kinase plays a central role in the enhanced migratory phenotype that accompanies endocrine resistance through its modulation of FAK signalling and demonstrates the potential use of Src inhibitors as potent suppressors of tumour cell migration.

2007. *Clin Exp Metastasis* 24(3), pp. 157-167.

"Maybe it's all just a bunch of stuff that happened."

Homer Simpson (1989-). Safety Inspector, Springfield Nuclear Power Plant. The Simpsons, Episode 7F22 'Blood Feud'.